

X-ray Scattering Principal Investigators' Meeting

Zoom Meeting

January 18–19, 2023

This document was produced under contract number DE-SC0014664 between the U.S. Department of Energy and Oak Ridge Associated Universities.

The research grants and contracts described in this document are supported by the U.S. DOE Office of Science, Office of Basic Energy Sciences, Materials Sciences and Engineering Division.

Foreword

This abstract book summarizes the scientific content of the 2023 X-ray Scattering Principal Investigators' (PI) Meeting sponsored by the Division of Materials Sciences and Engineering (DMSE) of the Office of Basic Energy Sciences (BES) of the U.S. Department of Energy. The meeting, held via Zoom on January 18–19, 2023, was the seventh in a series covering the projects funded by the BES DMSE X-ray Scattering Program. In addition to x-ray scattering, the program and meeting included PIs involved in ultrafast techniques and instrumentation as applied to materials science research. BES DMSE has a long tradition of supporting a comprehensive scattering program in recognition of the high impact these tools have in discovery and use-inspired research. Ultrafast sources have entered the x-ray regime, and time-resolved experiments on the femto-second time scale, involving radiation across a broad energy spectrum, have become an important part of the program.

The DMSE X-ray Scattering Program supports basic research using x-ray scattering, spectroscopy, and imaging for materials research, primarily at major BES-supported user facilities. X-ray scattering serves as one of the primary tools for characterizing the atomic, electronic and magnetic structures and excitations of materials. Information on structure and dynamics becomes the basis for identifying new materials and describing mechanisms underlying their unique behavior. Other key aspects of this activity are the development and improvement of next-generation instrumentation and data analysis tools, including the development of ultrafast techniques involving pulsed radiation sources.

The purpose of the PI meeting was to bring together researchers funded by BES in the x-ray scattering and ultrafast materials research area, to facilitate the exchange of new results and research highlights, to foster new ideas and collaborations among the participants, and to identify the needs of the research community. The meetings also help DMSE to assess the state of the program and chart future directions.

Table of Contents

Agenda	vi
--------------	----

Abstracts

Laboratory Abstracts

Dynamics and Control of Magnetic and Charge Order in Complex Oxides

<i>Mark P. M. Dean, Matteo Mitrano, and Robert M. Konik</i>	2
---	---

Time-Resolved Soft X-Ray Materials Science at the LCLS and ALS

<i>T. P. Devereaux, T. F. Heinz, H.-C. Jiang, W.-S. Lee, A. R. Lindenberg, B. Moritz, Z.-X. Shen, and T. Cuk</i>	8
--	---

Synchrotron Radiation Studies

<i>Stephan O. Hruszkewycz, Yue Cao, Matthew J. Highland, Haidan Wen, and Hoydoo You</i>	12
---	----

Spin Chain Bootstrap

<i>Robert Konik, Mark Dean, Igor Zaliznyak, Jonathan Pelliciari, Genda Gu, Abhay Pasupathy, Andreas Weichselbaum, Layla Hormozi, Ning Bao, Tzu-Chieh Wei, and Ananda Roy</i>	18
--	----

Ultrafast Materials Science

<i>Alessandra Lanzara, Aaron Bostwick, and Chris Jozwiak</i>	23
--	----

Structural Dynamics in Functional Materials

<i>Aaron Lindenberg, Mariano Trigo, David Reis, and William Chueh</i>	29
---	----

X-ray studies of complex materials at high pressure

<i>Wendy L. Mao, Hemamala Karunadasa, and Yu Lin</i>	34
--	----

Structural Signatures of Hidden Order in Spin-Orbit Coupled Systems

<i>Raymond Osborn, Stephan Rosenkranz, Charlotte Haley, and Mihai Anitescu</i>	39
--	----

X-ray Scattering

<i>Ian Robinson and Emil Bozin</i>	45
--	----

Nanoscale Structure and Motion of Non-collinear Spin Phases

<i>Sujoy Roy</i>	54
------------------------	----

Tracking intergranular strain dynamics with near-atomic scale coherent x-ray imaging at next generation light sources

<i>Richard L. Sandberg, Robert M. Suter, Anthony D Rollett, Anastasios Pateras, Stephan Hruszkewycz, Wonsuk Cha, and Ross J. Harder</i>	59
---	----

Electronic and Magnetic Properties of Quantum Materials <i>Zhi-xun Shen, T.P. Devereaux, B. Moritz, P.S. Kirchman, J.A. Sobota, M. Hashimoto, and D.H. Lu</i>	63
Ultrafast Bursts of Coherent X-rays to Unveil Fluctuations in Quantum Matter <i>J. J. Turner</i>	69
Automated sorting of coherent diffraction data from XFELs <i>Longlong Wu, Ian Robinson, Shinjae Yoo, and Yuewei Lin</i>	75
University Abstracts	
Emergent and Tunable Properties in Ultrathin Film Structures <i>Tai Chang Chiang</i>	82
Optical models and sample environments for resonant soft X-ray scattering of carbon nanostructured materials <i>Brian A. Collins</i>	88
Resonant coherent diffractive imaging of complex materials <i>Riccardo Comin</i>	93
Elucidating structural changes and nonradiative pathways of semiconductor nanocrystals under photoexcitation <i>Benjamin Cotts and Jihong Ma</i>	98
Multidimensional Coherent Spectroscopy of van der Waals materials and heterostructures <i>Steven T. Cundiff</i>	101
Detecting Indistinguishable Photons at an X-ray Synchrotron Source <i>Stephen M. Durbin</i>	105
Dynamics of Complex Magnetic and Ferroelectric Polarization Configurations <i>Paul G. Evans</i>	107
Helical Dichroism and Coherent Diffractive Imaging With Twisted X-Ray Beams <i>Edwin Fohtung and Jian Shi</i>	113
Electronic and Structural Dynamics in Quantum Materials <i>Nuh Gedik</i>	119
Elucidating Emergence in Strongly Coupled Hierarchical Functional Materials <i>Naomi Ginsberg, David Limmer, Dmitri Talapin, and Samuel Teitelbaum</i>	124

Transient and Metastable Order Created by Ultrafast Light <i>V. Gopalan, Y. Cao, L.Q. Chen, J.W. Freeland, A.M. Lindberg, L.W. Martin, Vladimir Stoica, and H. Wen</i>	129
Emergent Phenomena at Mott Interfaces – a Time- and Depth-Resolved Approach <i>Alexander Gray</i>	138
Novel topological and superconducting materials and their excitation properties <i>M. Zahid Hasan</i>	143
Ultrafast enhancement of antiferromagnetic second-harmonic generation in BiFeO₃ <i>Wanzheng Hu</i>	150
Probing Twisted 2D Heterostructures using Focused Photoemission Spectroscopy <i>Jyoti Katoch</i>	154
Ultrafast Coherent X-Ray Studies of Quantum Materials <i>Roopali Kukreja</i>	159
Ultrafast control of spin fluctuations in light-driven quantum materials <i>Matteo Mitrano</i>	163
Ultrafast Probing and Manipulation of Magnetic Materials using Polarization-Shaped Laser and Coherent Soft X-Ray Beams <i>Margaret Murnane and Henry Kapteyn</i>	166
Multimodal Quantum Material Control Monitored with Ultrafast Coherent X-rays <i>Keith A. Nelson, Riccardo Comin, James Freericks, David Reis, Mariano Trigo, and Nicholas Sirica</i>	170
Lattice instabilities, emergent electronic phases and collective behavior rooted in the quantum world <i>V. Petkov</i>	180
Coherent x-ray scattering investigations of nanoscale magnetic fluctuations in frustrated magnets <i>Kemp Plumb</i>	185
Creating New Quantum States of Matter in Time and Space Through Engineering Artificial Interfaces and Structures <i>Andrej Singer, Nicole Benedek, Ankit Disa, Darrell Schlom, and Kyle Shen</i>	189
Layer-By-Layer Disentanglement of Electronic States in Quantum Materials <i>Shuolong Yang</i>	207

Author Index	212
Participant List.....	215

Agenda

2023 BES X-Ray Scattering PI Virtual Meeting

January 18-19, 2023

All times are Eastern Time

Wednesday, January 18

9:45 – 10:00 AM *Zoom Log in*

10:00 Morning greet and warm-up

11:00 Ultrafast at XFELs: facilities, new end stations, productivity, high rep rate strategies

12:00 Correlation spectroscopy, time domain strategies, FT analysis

13:00 Break, breakout rooms

14:00 Coherent X-ray Imaging

15:00 Ultrafast without x-rays: optical spectroscopy, photoluminescence, electron diffraction

16:00 Break, breakout rooms

17:00 Excitation sources – THz tuning, above gap pulse, polarization, time sequences.

18:00 Daily wrap-up, happy hour

Thursday, January 19

10:00 Morning greet and warm-up

11:00 Theory in support of experiments: computational analysis, hypothesis driven science

12:00 Synthesis in support of experiments: right sample, in-place synthesis, environmental control

13:00 Break, breakout rooms

14:00 ARPES: time, space, and spin filtering

15:00 Magnetism and spin structure sensitivity

16:00 Break, breakout rooms

17:00 Special topics: entanglement, multi-modal, wave mixing

18:00 Daily wrap-up, happy hour

*Laboratory
Abstracts*

Dynamics and Control of Magnetic and Charge Order in Complex Oxides

Mark P. M. Dean ¹, Matteo Mitrano², Robert M. Konik ¹

¹Brookhaven National Laboratory, ²Harvard University

Keywords Resonant inelastic x-ray scattering (RIXS); quantum materials; strong electronic correlations; ultrafast physics; x-ray free electron laser (XFEL)

Research Scope

The identification and control of novel electronic phases in quantum materials is a major theme of modern science. Central to this challenge is that novel phases often involve multiple charge, spin, orbital, and lattice degrees of freedom interacting in a complex manner at the atomic length scale. Resonant inelastic x-ray scattering (RIXS) offers unique advantages for probing quantum materials as it is sensitive to all these degrees of freedom. Being an x-ray scattering technique, it furthermore encodes the spatial dependence of these interactions, through the momentum-dependence of the scattering cross-section.

The main goal of the Dynamics and Control in Complex Oxides field work proposal is to study charge, spin, lattice, and orbital dynamics using advanced x-ray techniques in order to better understand the electronic properties of complex oxides and their manipulation via external stimuli. We have particular strengths in time resolved RIXS and ultrafast physics and are working to extend the state of the art in these techniques and to apply them to several prototypical quantum materials. Our current areas of focus are excitonic and dimerized materials and the manipulation of charge-transfer energy scales in complex oxides. These materials offer a richer set of active degrees of freedom than the simpler magnets studied previously within this field work proposal. We plan to study means to directly photo-excite magnetic and orbital degrees of freedom to switch between electronic states in quantum materials and to investigate the role of hybridization in the manipulation of electronic states in correlated oxides.

Recent Progress

- We have been studying the model easy-axis gapped antiferromagnetic insulator $\text{Sr}_3\text{Ir}_2\text{O}_7$ and have measured the ultrafast magnon behavior of this material after photo-doping across its Mott gap with 2 micron laser excitation [P6]. This allowed us to compare directly with our prior measurements on

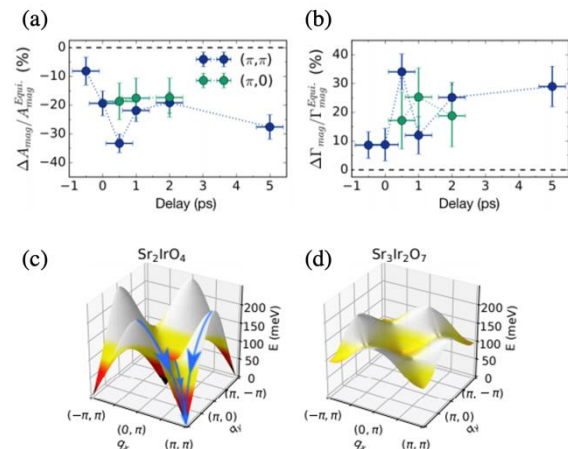


Figure 1: Ultrafast RIXS measurements of easy axis gapped antiferromagnet $\text{Sr}_3\text{Ir}_2\text{O}_7$. [R1]. (a)&(b) show the reduce magnon intensity and increased magnon linewidth at both high symmetry reciprocal space locations after photoexcitation. (c)&(d) Illustrate the magnon “bottleneck” effect .

essentially gapless magnet Sr_2IrO_4 [R1]. The results obtained, shown in Figure 1(a)&(b), reveal that transient magnetic fluctuations are trapped throughout the entire Brillouin zone, opposite to the behavior in nearly gapless Sr_2IrO_4 [11]. The result was interpreted with a spin-bottleneck scenario, in which the full recovery of magnetism is delayed by the existence of a large magnon gap as illustrated in Figure 1(c)&(d). Our results suggest that materials featuring isotropic magnetic interactions are preferred to achieve rapid manipulation of magnetic order. Spin-wave theory modelling proved that magnetic order in $\text{Sr}_3\text{Ir}_2\text{O}_7$ is strongly influenced by the bilayer structure of this material. To understand this phenomenology more deeply, we re-examined the nature of magnetism in $\text{Sr}_3\text{Ir}_2\text{O}_7$. We found that the material is a realization of a long-predicted antiferromagnetic excitonic insulator, which we illustrate in Figure 2 [P1]. This state

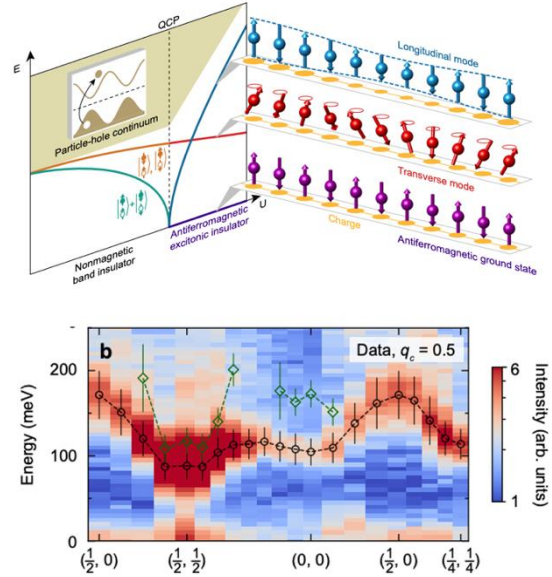


Figure 2: Top: Phase diagram showing the longitudinal magnetic exciton mode in cyan, which is of mixed magnetic and charge character. Bottom: Resonant inelastic x-ray scattering (RIXS) measurement of $\text{Sr}_3\text{Ir}_2\text{O}_7$. Points corresponding to the excitonic longitudinal modes are colored in green [1].

forms when the magnetic binding energy between electrons and holes exceeds the energy cost of creating the electron-hole pair by exciting the particles across a narrow band-gap. Its key signature is the appearance of a low-energy longitudinal magnetic excitation that is involved in the formation of the ordered state below the magnetic transition temperature of 285 K, which we detected using Ir L-edge RIXS. We also explained the quantum spin liquid magnetic properties of $\text{Ba}_4\text{Ir}_3\text{O}_{10}$. A cancelation of magnetic interactions was found to break up the apparently two-dimensional magnetic lattice to yield spinon excitations, which are characteristic of quasi-one-dimensional magnetic lattices [P2].

- We have succeeded in demonstrating the feasibility of ultrafast X-ray pair distribution function (ufPDF) measurements by examining the dimer excitations of CuIr_2S_4 . The very local structure (first 10 Å in PDF) has a predominantly subpicosecond response, presumably immediately following an induced change of electronic state of the dimers. Further distance neighbors (intermediate length-scale) respond with a ~ 35 ps decay which is the same time constant measured in optical reflectivity studies. PDF structure refinement shows a progressive Ir-Ir dimer reconfiguration with an intermediate relaxation time. This demonstrates how uf-PDF, in contrast to single crystal diffuse scattering, which is restricted to a segment of Brillouin zone, can track the full sequence of events as i) electronic structure changes, followed by ii) rapid response of the dimers, then finally iii) development of long-range structural correlations.

Seeing this progression demonstrates the unique potential of the uf-PDF method, mapping out the combination of time and distance within a structure undergoing a transition.

Future Plans

- *Excitonic and dimerized materials*: Looking forwards we are aiming to extend our ultrafast RIXS studies to materials with a more complex manifold of electronic and magnetic transitions. We have identified dimerized [R2] and double perovskite iridates [R3] for this purpose and have characterized them with synchrotron RIXS. These materials host low and high-spin electronic states, which offer a new route toward intrinsically switching magnetic states via photoexcitation. XFEL beamtime has been secured for this project and schemes to perform the photoexcitation are currently being finalized. Theoretical calculations supporting these efforts are underway.
- *Charge transfer physics*: Controlling the charge-transfer energy scale in quantum materials is an important potential means to tune the electronic properties of quantum materials. We recently measured the charge-transfer energy of low-valence nickelate material $\text{La}_4\text{Ni}_3\text{O}_8$ [P4]. This parameter describes the energy difference between the nickel and oxygen states and is key to understanding the electronic properties of this class of materials. This parameter is also key to the relatively strong magnetic exchange in this material, which we also measured in a separate study [P8]. A study of the charge dynamics of this material has been performed recently at the SACLA XFEL, which is currently being analyzed. We also plan to study how the charge transfer energy scale can be modified transiently via photoexcitation using ultrafast RIXS and have an upcoming experiment on this topic at SACLA.
- *Technique development*. We have constructed a new hard x-ray RIXS spectrometer that has been commissioned at the SACLA XFEL. This system uses a novel configuration in which the detector position is actuated via linear translation stages, rather than a rotation centered around the analyzer. We have also commissioned a new bent analyzer system at the Stanford Synchrotron Radiation Lightsource. The initially constructed analyzer is of worse quality than anticipated, so a new analyzer is being procured and will be tested in the coming months.

References – referenced with

1. M.P.M. Dean, Yue Cao, X. Liu, S. Wall, D. Zhu, Roman Mankowsky, V. Thampy, X.M. Chen, J.G. Vale, D. Casa, Jungho Kim, A. H. Said, P. Juhas, R. Alonso-Mori, J. M. Glownia, A. Robert, J. Robinson, M. Sikorski, S. Song, M. Kozina, H. Lemke, L. Patthey, S. Owada, T. Katayama, M. Yabashi, Yoshikazu Tanaka, T. Togashi, J. Liu, C. Rayan Serrao, B. J. Kim, L. Huber, C.-L. Chang, D. F. McMorrow, M. Först, and J. P. Hill, *Ultrafast energy and momentum resolved dynamics of magnetic correlations in photo-doped Mott insulator Sr_2IrO_4* , Nature Materials **15**, 601–605 (2016)
2. Y Wang, Ruitang Wang, Jungho Kim, MH Upton, D Casa, T Gog, G Cao, G Kotliar, MPM Dean, and X Liu, *Direct Detection of Dimer Orbitals in $\text{Ba}_5\text{AlIr}_2\text{O}_{11}$* , Phys. Rev. Lett. **122**, 106401 (2019)

3. Bo Yuan, J. P. Clancy, A. M. Cook, C. M. Thompson, J. Greedan, G. Cao, B. C. Jeon, T. W. Noh, M. H. Upton, D. Casa, T. Gog, A. Paramekanti, and Young-June Kim, *Determination of Hund's coupling in 5d oxides using resonant inelastic x-ray scattering*, Phys. Rev. B **95**, 235114 (2017)
4. Nuh Gedik, Ding-Shyue Yang, Gennady Logvenov, Ivan Bozovic, Ahmed H. Zewail, *Nonequilibrium Phase Transitions in Cuprates Observed by Ultrafast Electron Crystallography*, Science 316, 425 (2007)

Publications

These a referenced by

Publications intellectually led by this FWP

1. D. G. Mazzone, Y. Shen, H. Suwa, G. Fabbri, J. Yang, S.-S. Zhang, H. Miao, J. Sears, Ke Jia, Y. G. Shi, M. H. Upton, D. M. Casa, X. Liu, Jian Liu, C. D. Batista, and M. P. M. Dean, *Antiferromagnetic excitonic insulator state in Sr₃Ir₂O₇*, Nature Communications **13**, 913 (2022)
2. Y. Shen, J. Sears, G. Fabbri, A. Weichselbaum, W. Yin, H. Zhao, D. G. Mazzone, H. Miao, M. H. Upton, D. Casa, R. Acevedo-Esteves, C. Nelson, A. M. Barbour, C. Mazzoli, G. Cao, and M. P. M. Dean, *Emergence of Spinons in Layered Trimer Iridate Ba₄Ir₃O₁₀*, Phys. Rev. Lett. **129**, 207201 (2022)
3. Wei Wang, Junjie Li, Lijun Wu, Jennifer Sears, Fuhao Ji, Xiaozhe Shen, Alex H. Reid, Jing Tao, Ian K. Robinson, Yimei Zhu, and Mark P. M. Dean, *Dual-stage structural response to quenching charge order in magnetite*, Phys. Rev. B **106**, 195131 (2022)
4. Y. Shen, J. Sears, G. Fabbri, J. Li, J. Pelliciari, I. Jarrige, Xi He, I. Bozovic, M. Mitrano, Junjie Zhang, J. F. Mitchell, A. S. Botana, V. Bisogni, M. R. Norman, S. Johnston, and M. P. M. Dean, *Role of Oxygen States in the Low Valence Nickelate La₄Ni₃O₈*, Phys. Rev. X **12**, 011055 (2022)
5. Mark P. M. Dean, *Waves divide the Fermi sea*, Nature Physics **18**, 379–380 (2022)
6. Daniel G. Mazzone, Derek Meyers, Yue Cao, James G. Vale, Cameron D. Dashwood, Youguo Shi, Andrew J. A. James, Neil J. Robinson, Jiaqi Lin, Vivek Thampy, Yoshikazu Tanaka, Allan S. Johnson, Hu Miao, Ruitang Wang, Tadesse A. Assefa, Jungho Kimm, Diego Casa, Roman Mankowsky, Diling Zhu, Roberto Alonso-Mori, Sanghoon Song, Hasan Yavas, Tetsuo Katayama, Makina Yabashi, Yuya Kubota, Shigeki Owada, Jian Liu, Junji Yang, Robert M. Konik, Ian K. Robinson, John P. Hill, Desmond F. McMorrow, Michael Först, Simon Wall, Xuerong Liu, Mark P. M. Dean, *Laser-Induced Transient Magnons in Sr₃Ir₂O₇ Throughout the Brillouin Zone*, Proceedings of the National Academy of Sciences of the United States of America **118**, e2103696118 (2021)
7. H. Miao, G. Fabbri, R. J. Koch, D. G. Mazzone, C. S. Nelson, R. Acevedo-Esteves, G. D. Gu, Y. Li, T. Yilimaz, K. Kaznatcheev, E. Vescovo, M. Oda, T. Kurosawa, N. Momono, T. Assefa, I. K. Robinson, E. S. Bozin, J. M. Tranquada, P. D. Johnson, and M. P. M. Dean, *Charge*

- density waves in cuprate superconductors beyond the critical doping*, npj Quantum Materials **6**, 31 (2021)
8. J. Q. Lin, P. Villar Arribi, G. Fabbris, A. S. Botana, D. Meyers, H. Miao, Y. Shen, D. G. Mazzone, J. Feng, S. G. Chiuzbăian, A. Nag, A. C. Walters, M. García-Fernández, Ke-Jin Zhou, J. Pelliciani, I. Jarrige, J. W. Freeland, Junjie Zhang, J. F. Mitchell, V. Bisogni, X. Liu, M. R. Norman, and M. P. M. Dean, *Strong Superexchange in a $d^{9-\delta}$ Nickelate Revealed by Resonant Inelastic X-Ray Scattering*, Phys. Rev. Lett. **126**, 087001 (2021)
 9. L.L. Wu, P. Juhas, S. Yoo, and I. Robinson, *Complex imaging of phase domains by deep neural networks*, IUCRJ **8** 12-21 (2021)
 10. Longlong Wu, Shinjae Yoo, Ana F. Suzana, Tadesse A. Assefa, Jiecheng Diao, Ross J. Harder, Wonsuk Cha and Ian K. Robinson, *3D Coherent X-ray Imaging via Deep Convolutional Neural Networks*, npj Computational Materials **7** 175 (2021)
 11. Y. Shen, G. Fabbris, H. Miao, Y. Cao, D. Meyers, D. G. Mazzone, T. Assefa, X. M. Chen, K. Kisslinger, D. Prabhakaran, A. T. Boothroyd, J. M. Tranquada, W. Hu, A. M. Barbour, S. B. Wilkins, C. Mazzoli, I. K. Robinson and M. P. M. Dean, *Charge Condensation and Lattice Coupling Drives Stripe Formation in Nickelates*, Physical Review Letters **126**, 177601 (2021)
 12. Longlong Wu, Yao Shen, Andi M. Barbour, Wei Wang, Dharmalingam Prabhakaran, Andrew T. Boothroyd, Claudio Mazzoli, John M. Tranquada, Mark P. M. Dean, and Ian K. Robinson, *Real Space Imaging of Spin Stripe Domain Fluctuations in a Complex Oxide*, Phys. Rev. Lett. **127**, 275301 (2021)
 13. Wei Wang, Lijun Wu, Junjie Li, Niraj Aryal, Xilian Jin, Yu Liu, Mikhail Fedurin, Marcus Babzien, Rotem Kupfer, Mark Palmer, Cedimir Petrovic, Weiguo Yin, Mark P. M. Dean, Ian K. Robinson, Jing Tao, and Yimei Zhu, *Photoinduced anisotropic lattice dynamic response and domain formation in thermoelectric SnSe*, npj Quantum Materials **6**, 97 (2021)
 14. C. D. Dashwood, A. Geondzhian, J. G. Vale, A. C. Pakpour-Tabrizi, C. A. Howard, Q. Faure, L. S. I. Veiga, D. Meyers, S. G. Chiuzbaian, A. Nicolaou, N. Jaouen, R. B. Jackman, A. Nag, M. Garcia-Fernandez, Ke-Jin Zhou, A. C. Walters, K. Gilmore, D. F. McMorrow, and M. P. M. Dean, *Probing electron-phonon interactions away from the Fermi level with resonant inelastic x-ray scattering*, Phys. Rev. X **11**, 041052 (2021)

Collaborative publications

15. Ernest Pastor, David Moreno-Mencía, Maurizio Monti, Allan S. Johnson, Nina Fleischmann, Cuixiang Wang, Youguo Shi, Xuerong Liu, Daniel G. Mazzone, Mark P. M. Dean, and Simon Wall, *Nonthermal breaking of magnetic order via photogenerated spin defects in the spin-orbit coupled insulator $Sr_3Ir_2O_7$* , Phys. Rev. B **105**, 064409 (2022)
16. Min Gyu Kim, Andi Barbour, Wen Hu, Stuart B. Wilkins, Ian K. Robinson, Mark P. M. Dean, Junjie Yang, Choongjae Won, Sang-Wook Cheong, Claudio Mazzoli, and Valery Kiryukhin, *Real-space observation of fluctuating antiferromagnetic domains*, Science Advances **8**, eabj9493 (2022)

17. Junyi Yang, Hidemaro Suwa, Derek Meyers, Han Zhang, Lukas Horak, Zhaosheng Wang, Gilberto Fabbris, Yongseong Choi, Jenia Karapetrova, Jong-Woo Kim, Daniel Haskel, Philip J. Ryan, M. P. M. Dean, Lin Hao, and Jian Liu, *Quasi-Two-Dimensional Anomalous Hall Mott Insulator of Topologically Engineered $J_{eff}=1/2$ Electrons*, Phys. Rev. X **12**, 031015 (2022)
18. L. Chaix, B. Lebert, H. Miao, A. Nicolaou, F. Yakhou, H. Cercellier, S. Grenier, N. B. Brookes, A. Sulpice, S. Tsutsui, A. Bosak, L. Paolasini, D. Santos-Cottin, H. Yamamoto, I. Yamada, M. Azuma, T. Nishikubo, T. Yamamoto, M. Katsumata, M. P. M. Dean, and M. d'Astuto, *Bulk charge density wave and electron-phonon coupling in superconducting copper oxychlorides*, Phys. Rev. Research **4**, 033004 (2022)
19. Yanhong Gu, Yilin Wang, Jiaqi Lin, Jonathan Pellicciari, Jiemin Li, Myung-Geun Han, Marcus Schmidt, Gabriel Kotliar, Claudio Mazzoli, Mark P. M. Dean, and Valentina Bisogni, *Site-specific electronic and magnetic excitations of the skyrmion material Cu_2OSeO_3* , Communications Physics **5**, 156 (2022)
20. R. Wang, J. Sun, D. Meyers, J. Q. Lin, J. Yang, G. Li, H. Ding, Anthony D. DiChiara, Y. Cao, J. Liu, M. P. M. Dean, Haidan Wen, and X. Liu, *Single-Laser-Pulse-Driven Thermal Limit of the Quasi-Two-Dimensional Magnetic Ordering in Sr_2IrO_4* , Phys. Rev. X **11**, 041023 (2021)
21. Haoxiang Li, T. T. Zhang, A. Said, G. Fabbris, D. G. Mazzone, J. Q. Yan, D. Mandrus, Gábor B. Halász, S. Okamoto, S. Murakami, M. P. M. Dean, H. N. Lee, and H. Miao, *Giant phonon anomalies in the proximate Kitaev quantum spin liquid α - $RuCl_3$* , Nature Communications **12**, 3513 (2021)
22. Haoxiang Li, Tiantian Zhang, A. Said, Y. Fu, G. Fabbris, D. G. Mazzone, J. Zhang, J. Lapano, H. N. Lee, H. C. Lei, M. P. M. Dean, S. Murakami, and H. Miao, *Observation of a chiral wave function in the twofold-degenerate quadruple Weyl system $BaPtGe$* , Phys. Rev. B **103**, 184301 (2021)
23. M. Hepting, M. P. M. Dean, and W. S. Lee, *Soft X-ray Spectroscopy of Low-Valence Nickelates*, Front. Phys. **9**, 808683 (2021)
24. John M. Tranquada, Mark P. M. Dean, and Qiang Li, *Superconductivity from Charge Order in Cuprates*, Journal of the Physical Society of Japan **90**, 111002 (2021)

Time-Resolved Soft X-Ray Materials Science at the LCLS and ALS

T.P. Devereaux^{1,2}, T. F. Heinz^{1,3}, H.-C. Jiang¹, W.-S. Lee¹, A. R. Lindenberg^{1,2}, B. Moritz¹, Z.-X. Shen^{1,3,4}, T. Cuk^{1,5}

1. Stanford Institute for Materials and Energy Sciences, SLAC, Menlo Park, CA94025
2. Department of Materials Science and Engineering, Stanford University, Stanford, CA 94305
3. Department of Applied Physics, Stanford University, Stanford, CA 94305
4. Department of Physics, Stanford University, Stanford, CA 94305
5. Department of Chemistry, University of Colorado at Boulder, Boulder, CO 80309

Self-identify keywords to describe your project: Quantum Materials, resonant inelastic x-ray scattering, time domain spectroscopy, theory/simulation, and x-ray free electron lasers

Research Scope

This program connects concepts of ultrafast time-domain science with those for momentum- and energy-domain x-ray spectroscopy. The combined activities bring a synergy to explore how materials behave under extreme conditions, driving lattice and charge conformational changes by applying short pulses or high fields. The purpose of this research is to develop a world-class program on the dynamics of complex materials using the x-ray beamlines available at LCLS and other state-of-the-art synchrotrons to address the grand challenge problems of emergence, non-equilibrium dynamics, and to probe model systems for deep insights on materials for energy conversion, transport, and efficiency.

Theoretical calculations and simulations conducted in parallel with experimental progress will establish a formalism for describing non-equilibrium physics of strongly correlated and related materials and provide additional guidance to experiments. This activity requires the development of novel theoretical and computational tools and as well as the deployment of standard techniques designed to uncover the nature of the many-body state both in and out of equilibrium.

Recent Progress

- **RIXS study of charge order in the high-T_c cuprate superconductors** - We have conducted temperature dependent study of charge order (CO) and its influence on charge and phonon degrees of freedom in the nearly-optimally doped Bi2212 cuprate. The CO order parameter and the associated RIXS phonon anomaly exhibits a paradoxical temperature dependent behavior. Namely, the anomalies enhance despite the reduction of the CO order parameter in the superconducting state at low temperatures. We have attributed this paradoxical behavior as a spectroscopic fingerprint of CO quantum fluctuation near a critical point. We have also constructed a model to mimic the behavior via the damping of the fluctuations. [W.-S. Lee *et al.*, *Nature Physics* **17**, 53 (2021)].

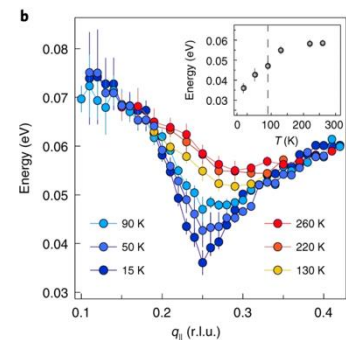


Figure 3: RIXS phonon dispersions for different temperatures. Inset: Phonon energy at $q=0.25$ r.l.u. Dashed line indicates T_c.

- **Magnetic excitations in new nickelate superconductors** -We have investigated magnetic

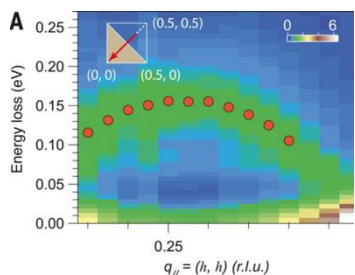


Figure 2: RIXS intensity maps versus energy loss and projected in-plane momentum transfer along three high-symmetry directions, as indicated with red arrows in the insets, which show a Brillouin zone with the first AFM zone shaded. Measurements were taken at 20 K. The red circles indicate peak positions of the magnetic excitation spectra.

excitations in the infinite-layer nickelate superconductors $\text{Nd}_{1-x}\text{Ni}_x\text{O}_2$, using RIXS at the Ni L -edge. We found the first evidence of magnetic excitations with high energy scales (~ 200 meV) in the parent compound of the nickelate superconductor. Upon doping, the magnetic excitations become overdamped with slight softening of their energy scale. This suggest that strongly correlated Mott physics should also play an important role in sculpting the properties of the nickelate superconductors. [H. Lu *et al. Science* 373, 213 (2021)]

- **Ultrafast charge and energy transport across two-dimensional atomic junctions** - Following selective excitation of WSe₂, we measure unexpectedly concurrent heating of both WSe₂ and WS₂ on a

1 picosecond timescale, an observation that is not explained by phonon transport across the interface. Using first-principles calculations, we identify a fast channel, involving an electronic state hybridized across the heterostructure, enabling phonon-assisted interlayer transfer of photoexcited electrons. Phonons are emitted in both layers on femtosecond timescales via this channel, consistent with the simultaneous lattice heating observed experimentally. Taken together, our work indicates strong electron-phonon coupling via layer-hybridized electronic states – a novel route to control energy transport across atomic junctions. [A. Sood *et al., Nature Nano.* (2022). <https://doi.org/10.1038/s41565-022-01253-7>]

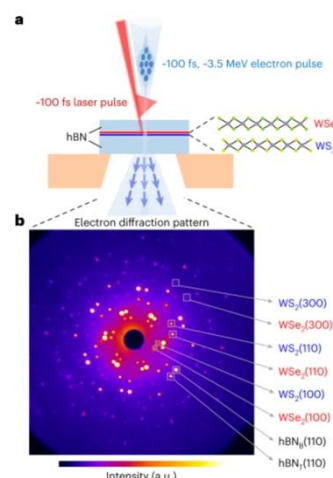


Figure 3: Top: Experimental setup probing dynamic response of 2D van der Waals heterostructures. Bottom: Electron diffraction pattern of heterostructure showing how selective probing of each atomic layer is enabled.

Future Plans

- **Infrastructure and Equipment Development**
 - We will work closely with staff scientists at LCLS-II for commissioning the new qRIXS instrument at NEH 2.2, LCLS-II, as well as the planned early science experiments. These activities are expected to ramp up in FY23 when the superconducting LINAC at LCLS-II starts commissioning, and the initial construction of qRIXS endstation at NEH 2.2 finishes. In addition, to gain first-hand experience of time-resolved RIXS at high repetition rate, we have actively participated the user-assisted scientific commissioning beamtime at the hRIXS instrument/European XFEL, as well as requesting user beamtime. These activities will directly benefit the commissioning and early science experiment at qRIXS, LCLS-II.
- **RIXS Studies of Quantum Materials**
 - We will continue to use RIXS to investigate the elementary excitations in representative quantum materials. We will continue to explore novel transition metal oxides, such as infinite-layer transition metal oxides, whose synthesis and characterizations are currently broadly explored in Hwang’s FWP. In addition, we also plan to explore RIXS measurements

for excitonic behaviors in van der Waal materials and collective excitations in topological materials, such as the Kagome metal CsV_3Sb_5 and the layered antiferromagnet NiPS_3 . These activities not only provide new fundamental information on these materials of current interest, but also provide scientific cases for the upcoming time-resolved RIXS experiment at LCLS-II.

- **Ultrafast THz Emission Spectroscopy and Ultrafast Electron Diffraction**

- The capabilities for probing ultrafast charge transfer dynamics and ultrafast phonon dynamics in heterostructures of 2D materials using, respectively THz emission spectroscopy and ultrafast electron diffraction (UED), will be applied to gain a full understanding of the role of twist angle on these fundamental dynamical processes. The regime in which moiré effects and strong electron correlations emerge will be a subject of particular attention.

- **Synthesis of Quantum Materials**

- We have synthesized and characterized 1D cuprates, using MBE combined with x-ray diffraction and ARPES, covering a wide range of doping for systematic soft x-ray RIXS investigations. The goal moving forward is to further test Hubbard-like and extended model descriptions for cuprate physics. Initial measurements are planned at APS and NSLS-II. We have prepared several target oxide thin films with a diversity of properties for upcoming RIXS experiments at LCLS-II, with flat samples of large areas that make these experiments much easier to perform.
- We have synthesized single crystals of electron-doped cuprates and will perform synchrotron RIXS experiments, in synergy with ARPES and tr-ARPES experiments in FWP10027. Such activities will help set stage for future time resolved experiments at LCLS-II.

- **Theory Activities**

- We will study the lightly doped Hubbard model on the six-leg square ladders to search for superconductivity and its interplay with second-neighbor electron hopping t' . We will calculate its ground state phase and compare it with that of the 4-leg square cylinder and look for possible guidance for the phase diagram in two dimensions.

Publications

Publications that were primarily driven by this FWP

1. H. Lu, M. Rossi, A. Nag, M. Osada, D. F. Li, K. Lee, B. Y. Wang, M. Garcia-Fernandez, S. Agrestini, Z. X. Shen, E. M. Been, B. Moritz, T. P. Devereaux, J. Zaanen, H. Y. Hwang, Ke-Jin Zhou, W. S. Lee, *Magnetic excitations in infinite-layer nickelates*, Science **373**, 213 (2021).
2. Wei-Sheng Lee, *X-ray Studies of the CDW Ground State and Excitations in High-Tc Cuprates*, J. Phys. Soc. Jap. **90**, 111004 (2021).
3. W. S. Lee, K. J. Zhou, M. Hepting, J. Li, A. Nag, A. C. Walters, M. Garcia-Fernandez, H. Robarts, M. Hashimoto, H. Lu, B. Nosarzewski, D. Song, H. Eisaki, Z. X. Shen, B. Moritz, J. Zaanen, T. P. Devereaux, *Spectroscopic Fingerprint of Charge Order Melting via Quantum Fluctuations in a Superconducting Cuprate*, Nature Physics **17**, 53 (2021).
4. Hong-Chen Jiang, *Superconductivity in the doped quantum spin liquid on the triangular lattice*, npj Quantum Mater. **6**, 71 (2021).
5. Zengqing Zhuo, Kehua Dai, Ruimin Qiao, Rui Wang, Jinpeng Wu, Yali Liu, Jiayue Peng, Liquan Chen, Y.-D. Chuang, Feng Pan, Z.-X. Shen, Gao Liu, Hong Li, T. P. Devereaux,

- Wanli Yang, *Cycling mechanism of Li_2MnO_3 : Li-CO₂ batteries and commonality on oxygen redox in cathode materials*, *Joule* **5**, 975-997 (2021).
6. Yuan Chen, Yao Wang, Martin Claassen, Brian Moritz, T. P. Devereaux, *Observing photo-induced chiral edge states of graphene nanoribbons in pump-probe spectroscopies*, *npj Quantum Mater.* **5**, 84 (2020).
 7. Haiyu Lu, Makoto Hashimoto, Su-Di Chen, Shigeyuki Ishida, Dongjoon Song, Hiroshi Eisaki, Abhishek Nag, Mirian Garcia-Fernandez, Riccardo Arpaia, Giacomo Ghiringhelli, Lucio Braicovich, Jan Zaanen, Brian Moritz, Kurt Kummer, Nicholas B. Brookes, Ke-Jin Zhou, Zhi-Xun Shen, Thomas P. Devereaux, and Wei-Sheng Lee, *Identification of a characteristic doping for charge order phenomena in Bi-2212 cuprates via RIXS*, *Phys. Rev. B* **106**, 155109 (2022).
 8. Ta Tang, Brian Moritz, and Thomas P. Devereaux, *Spectra of a gapped quantum spin liquid with a strong chiral excitation on the triangular lattice*, *Physical Review B* **106**, 064428 (2022).
 9. Hong-Chen Jiang, Steven A. Kivelson, *Stripe order enhanced superconductivity in the Hubbard model*, *PNAS* **119**, e2109406119 (2021).
 10. M. Hepting, M. P. Dean, W. S. Lee, *Soft X-Ray Spectroscopy of Low-Valence Nickelates*, *Frontiers in Physics* **9**, 808683 (2021)
 11. Ta Tang, Yao Wang, Brian Moritz, and Thomas P. Devereaux, *Orbitally selective resonant photodoping to enhance superconductivity*, *Physical Review B* **104**, 174516 (2021)
 12. A. Sood, J. B. Haber, J. Carlstrom, E. A. Peterson, E. Barre, J. D. Georganas, A. H. M. Reid, X. Shen, M. R. Zajac, E. C. Regan, J. Yang, T. Taniguchi, K. Watanabe, F. Wang, X. Wang, J. B. Neaton, T. F. Heinz, A. M. Lindenberg, F. D. da Jornada, & A. Raja, *Bidirectional phonon emission in two-dimensional heterostructures triggered by ultrafast charge transfer*, *Nat. Nanotechnol.* (2022). <https://doi.org/10.1038/s41565-022-01253-7>.

Synchrotron Radiation Studies

Stephan O. Hruszkewycz, Yue Cao, Matthew J. Highland, Haidan Wen, and Hoydoo You, Materials Science Division, Argonne National Laboratory

Keywords

Coherent diffraction, time-resolved measurements, in-situ materials studies, XFEL, synchrotron

Program Scope

The long-term goal of this program is to make novel use of x-ray light sources worldwide to solve prominent problems in materials science and condensed matter physics through in-situ and time-resolved measurements. This research promises to reveal fundamental processes central to the nation's needs in strategic areas such as energy, infrastructure, and information. Our approach is to overcome critical challenges that can be addressed at x-ray light source facilities through in-situ microscopic, spectroscopic, and time-resolved measurements of materials that reveal fundamental connections between structural heterogeneity, their dynamics, and materials properties. The current focus is to take advantage of coherent and ultrafast x-rays to provide insight into fundamental mechanisms of structural evolution in quantum materials, materials for energy, and structural materials under controlled conditions. These insights will be enabled through pioneering development of in-situ and time-resolved x-ray methods that take full advantage of transformative improvements in x-ray light source characteristics, with a special emphasis on designing impactful experiment campaigns at the coming upgraded APS.

Recent Progress

Coherent diffraction analysis methods: Developing new methods and approaches is integral to harnessing the full potential of state-of-the-art light sources for materials science. We developed new algorithms and measurement methods for image reconstruction from coherent x-ray diffraction patterns. These developments will enable improvements in the robustness of in-situ ptychography experiments through better image convergence [1] and will enable the use of high x-ray energies for BCDI, which affords greater penetrating power and better access to in-situ environments [2, 3]. We have also developed new XPCS analysis that allows improved determination of the g_2 function given broad distributions of per-frame incident x-ray intensities via appropriate weighting [4], and we recently were able to implement this method for real-time analysis during an experiment at the MID instrument at the EU-XFEL.

Imaging nanoscale crystal structure and evolution in-situ: Establishing the governing structure/property relationships and defect dynamics of nanoscale crystals under real-world conditions requires methods that can access environments relevant to functioning and that can resolve crystal defects in real time. We have made significant progress in enabling such studies with x-rays and gained fundamental insights by utilizing in-situ BCDI to reveal strain dynamics in

metallic grains and particles under local electrochemical control [5] and conditions relevant to catalysis [6], as we highlight below.

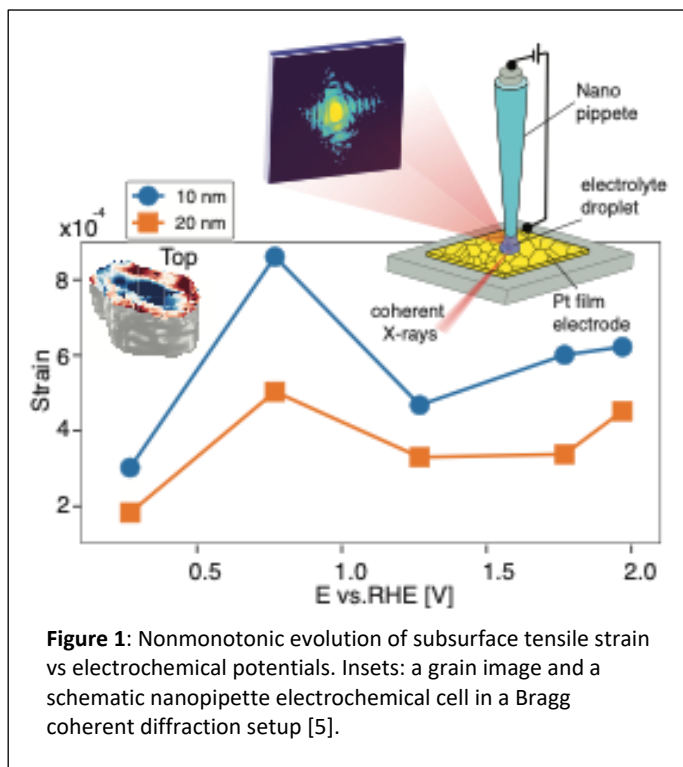
In-situ Bragg coherent diffraction imaging (BCDI) combined with a nanopipette electrochemical cell (NEC) [5] revealed previously unknown details of how the strain in a single Pt grain changes in response to electrochemical polarization. The imaging studies were performed under conditions relevant to place-exchange-oxidation and oxygen-evolution reactions. It was found that the top 10 nm of Pt at the electrode/electrolyte interface responded sensitively to applied potentials, but, surprisingly, this response was not fully reversible. These observations were afforded by the high strain sensitivity of BCDI combined with the near-zero X-ray scattering background of the submicron scale NEC setup (Figure 1).

In-situ BCDI was also used to monitor circumferential compressive strain and concomitant radial tensile strain on the surfaces of Pt-Ni nanoparticles of various compositions during Ni dissolutions in successive electrochemical cycles [6]. The initial compositional strain was determined, and the elastic strain was

monitored during successive voltametric cycles as a function of Ni dissolution, as deduced from three-dimensional images from BCDI and from measurements of the average lattice constants. The results show that higher levels of initial Ni composition resulted in the more dissolution and higher levels of compressive strain at the surface, forming a core-shell structure with a Pt-rich shell which displayed improved oxygen reduction reaction activity. These studies complement our understanding of electrochemically active surfaces of single crystals [7, 8].

Measuring local dynamics during thin film phase transitions and at interfaces: Hard x-rays provide the ability to interrogate crystal films and interfaces under conditions that induce structural dynamics and phase transformations. In order to observe the local variations of these dynamic processes evoked by driving forces such as optical excitation, elevated temperature, or gas-phase chemical potential, we utilized focused hard x-ray beams that provide local structural information and yield insights not accessible by ensemble measurements, as highlighted here.

When driven by ultrashort excitation, nanoscale phase regions evolve rapidly during first-order phase transformations, posing a significant characterization challenge. We utilized a newly



developed laser-pumped x-ray nanodiffraction imaging technique with 100-ps temporal and 25-nm spatial resolutions to reveal new pathways of nanoscale structural rearrangement upon ultrafast optical excitation which differ from those occurring during quasi-equilibrium transitions [9]. Using the magnetostructural transition in FeRh as a prototypical first-order phase transition, we found that the pre-existing nanoscale variation in phase composition results in spatially inhomogeneous changes of phase fraction after ultrafast optical excitation. The spatial inhomogeneity leads to nanoscale temperature variations and subsequent in-plane heat transport, which are responsible for spatially distinct relaxation pathways on nanometer length scales.

We also developed a new spatially and temporally resolved method to study mesoscale energy transport in materials with 100 ps and 300 nm resolution via optical transient grating pump and focused x-ray diffraction probe (TGXD) measurements [10]. This was achieved by using a spatially modulated optical excitation (i.e., transient grating pump) probed by time-resolved hard x-ray microdiffraction to resolve the resultant crystal structural changes in real space. The technique's application was demonstrated in a comparative study of the multiferroic oxide BiFeO₃, which exhibits a photoinduced strain (structural grating) with an amplitude proportional to the optical fluence, and FeRh, which undergoes a magnetostructural phase transformation found to have a non-linear location-dependent relaxation

We also utilized in-situ microbeam studies to study surface step dynamics on crystal surfaces [11, 12, 13]. The $\alpha\beta\alpha\beta$ stacking sequence of hexagonal close-packed and related crystals typically results in steps on vicinal {0001} surfaces that have alternating A and B structures with different growth kinetics. However, because it is difficult to experimentally identify which step has the A or B structure, it has not been possible to determine which has faster adatom attachment kinetics. We showed that *in situ* microbeam surface X-ray scattering can determine whether A or B steps have faster kinetics under specific growth conditions. We demonstrated this for organo-metallic vapor phase epitaxy (OMVPE) of (0001) GaN. X-ray measurements performed during growth find that the average width of terraces above A steps increases with growth rate, indicating that attachment rate constants are higher for A steps, in contrast to most predictions. Our results have direct implications for understanding the atomic-scale mechanisms of GaN growth and can be applied to a wide variety of related crystals, including wide bandgap host materials for quantum information science [14].

Future Plans

The future plan of the program is to continue to provide insight into fundamental mechanisms, dynamics, and local ordering that control materials properties, phase transformations, and interfaces via novel in-situ and time-resolved x-ray measurements at forefront light sources. Immediate program goals center on studying quantum materials, materials for energy, and structural materials that reveal these connections with a special emphasis on developing and demonstrating impactful experiments that capitalize on the improved brightness of the APS after its upgrade. We plan to pursue area of study outlined here:

Manipulation of quantum materials: Harnessing the potential of quantum phenomena within materials offers tremendous opportunities but requires understanding and control of the complex atomic and nanoscale structure and dynamics over wide time scales that dictate properties. We plan experiments that will provide such insights by targeting several exemplar systems in which delicate manipulation and balancing of energetically similar states in a material provide opportunities for control of state and properties. Using pump-probe scanning Bragg nanodiffraction and ptychography, newly discovered optically induced ordered phases in ferroelectric / paraelectric superlattice structures will be studied to reveal the mechanisms of their formation and their dynamic properties. We will also study connections between electrical properties and local order and dynamics in canonical charge-density wave materials and relaxor ferroelectrics with advances in XPCS and scanning nanodiffraction data analysis and interpretation. We will also pursue in-situ experiments aimed at developing optimal routes for processing single crystal SiC for quantum information technologies where control of near-surface lattice structure, phase, defect content, and step dynamics are critical for functioning. These research thrusts will all establish and demonstrate capabilities for exploiting coherence combined with wide-angle Bragg diffraction at APS-U and at MHz XFEL sources.

Materials for energy and infrastructure: We will focus on studies aimed at control of nanoscale materials structure and dynamics at and near interfaces in materials relevant to energy and infrastructure where in-situ measurements are necessary to gain new fundamental insights. We will perform studies of lattice response in nanoscale crystals of oxides such as ceria with BCDI under cyclic electrochemical and gas-phase environments for energy conversion materials with the aim of revealing the connection between internal strain and oxygen ion transport across the nanoparticle interface. We will also develop methods that build on our recent successful demonstrations of combined BCDI and SECCM to enable multi-Bragg peak measurements accessible by varying x-ray energy to conclusively determine surface strain in individual grains undergoing electrochemical cycling. We will also perform multiscale measurements of grains within bulk polycrystalline high-performance structural alloys by leveraging the significant increase in coherent flux at high x-ray energies at 4th generation light sources to gain insight into strain fields at grain boundaries in embedded grains up to 10 microns in size. First measurements at the ERSR-EBS will focus on tackling prominent method development challenges associated with this new regime of BCDI and the challenges of integration of the resulting images with coarse-resolution diffraction microscopy measurements of the bulk sample. This research thrust will pave the way for early in-situ BCDI experiments at several feature beamlines of the upgraded APS.

Method development areas: Integrated within these research directions is a focus on developing enabling methods to make maximal use of coherent and ultrafast x-ray. Specific areas of development include ultrafast Bragg ptychography, variable wavelength multi-Bragg-peak in-situ BCDI with SECCM, serial XPCS at MHz XFELs, high energy BCDI extending to 10-micron-scale grains, multi-Bragg-peak image reconstruction algorithm advances, and in-situ capabilities.

Publications

1. “A matrix-free Levenberg-Marquardt algorithm for efficient ptychographic phase retrieval.” S. Kandel, S. Maddali, Y. S. G. Nashed, S. O. Hruszkewycz, C. Jacobsen, M. Allain. *Optics Express* 29, 23019 (2021). <https://doi.org/10.1364/OE.422768> published July 7, 2021.
2. “Sub-pixel high-resolution imaging of high-energy x-rays inspired by sub-wavelength optical imaging.” N. Bertaux, M. Allain, J. Weizeorick, J.-S. Park, P. Kenesei, S. D. Shastri, J. Almer, M. J. Highland, S. Maddali, S. O. Hruszkewycz. *Optics Express* 29, 35003 (2021). <https://doi.org/10.1364/OE.438945> published October 11, 2021.
3. “Detector tilt considerations in Bragg coherent diffraction imaging: A simulation study,” S. Maddali, M. Allain, P. Li, V. Chamard, S. O. Hruszkewycz. *Crystals* 10, 1150 (2020). <https://doi.org/10.3390/cryst10121150> published December 17, 2020.
4. “The effect of intensity fluctuations on sequential x-ray photon correlation spectroscopy at the x-ray free electron laser facilities.” Y. Cao, D. Sheyfer, Z. Jiang, S. Maddali, H. You, B. X. Wang, Z. G. Ye, E. M. Dufresne, H. Zhou, G. B. Stephenson, S. O. Hruszkewycz. *Crystals* 10, 1109 (2020). <https://doi.org/10.3390/cryst10121109> published December 4, 2020.
5. “Operando nanoscale imaging of electrochemically induced strain in a locally polarized Pt Grain.” D. Sheyfer, R. G. Mariano, T. Kawaguchi, W. Cha, R. Harder, M. W. Kanan, S. O. Hruszkewycz, H. You, M. J. Highland. *Nano Letters*. <https://doi.org/10.1021/acs.nanolett.2c01015> Published Dec 21, 2022.
6. “Electrochemically Induced Strain Evolution in Pt-Ni Alloy Nanoparticles Observed by Bragg Coherent Diffraction Imaging.” T. Kawaguchi, V. Komanicky, V. Latyshev, W. Cha, E. R. Maxey, R. Harder, T. Ichitsubo, H. You. *Nano Letters* 21, 5945 (2021). <https://doi.org/10.1021/acs.nanolett.1c00778> published July 12, 2021.
7. “In-situ to ex-situ in-plane structure evolution of stern layers on Pt(111) surface: Surface X-ray scattering studies.” T. Kawaguchi, Y. Liu, E. A. Karapetrova, V. Komanicky, H. You. *Journal of Electroanalytical Chemistry* 875, 11495 (2020). <https://doi.org/10.1016/j.jelechem.2020.114495> published October 15, 2020.
8. “Stern layers on RuO₂ (100) and (110) in electrolyte: Surface x-ray scattering studies.” T. Kawaguchi, R. R. Rao, J. R. Lunger, Y. Liu, D. Walko, E. A. Karapetrova, V. Komanicky, Y. Shao-Horn, H. You. *Journal of Electroanalytical Chemistry* 875, 114228 (2020). <https://doi.org/10.1016/j.jelechem.2020.114228> published October 15, 2020.
9. “X-ray nanodiffraction imaging reveals distinct nanoscopic dynamics of an ultrafast phase transition,” Y. Ahn, M. J. Cherukara, Z. Cai, M. Bartlein, T. Zhou, A. DiChiara,

- D. A. Walko, M. V. Holt, E. E. Fullerton, P. G. Evans, H. Wen. PNAS 119, e2118597119 (2022). <https://doi.org/10.1073/pnas.2118597119> published May 6, 2022.
10. “Optical transient grating pumped x-ray diffraction microscopy for studying mesoscale structural dynamics,” T. D. Frazer, Y. Zhu, Z. Cai, D. A. Walko, C. Adamo, D. G. Schlom, E. Fullerton, P. G. Evans, S. O. Hruszkewycz, Y. Cao, H. Wen, Scientific Reports 11, 19322 (2021). Published Sept 27, 2021.
 11. “In-situ microbeam surface x-ray scattering reveals alternating step kinetics during crystal growth.” G. Ju, D. Xu, C. Thompson, M. J. Highland, J. A. Eastman, W. Walkosz, P. Zapol, G. B. Stephenson. Nature Communications 12, 1721 (2021). <https://doi.org/10.1038/s41467-021-21927-5> published March 19, 2021.
 12. “Crystal truncation rods from miscut surfaces with alternating terminations.” G. Ju, D. Xu, C. Thompson, M. J. Highland, J. A. Eastman, W. Walkosz, P. Zapol, G. B. Stephenson. Physical Review B 103, 125402 (2021). <https://doi.org/10.1103/PhysRevB.103.125402> published March 2, 2021.
 13. “Burton-Cabrera-Frank theory for surfaces with alternating step types.” G. Ju, D. Xu, C. Thompson, M. J. Highland, J. A. Eastman, W. Walkosz, P. Zapol, G. B. Stephenson. Physical Review B 105, 054312 (2022). <https://doi.org/10.1103/PhysRevB.105.054312> published February 22, 2022.
 14. “Designing silicon carbide heterostructures for quantum information science: challenges and opportunities.” K. J. Harmon, N. Deegan, M. J. Highland, H. He, P. Zapol, F. J. Heremans, S. O. Hruszkewycz. Materials for Quantum Technology 2, 023001 (2022). <https://doi.org/10.1088/2633-4356/ac6b76> published May 23, 2022.

Spin Chain Bootstrap

Principal Investigators:

Brookhaven National Lab: Robert Konik, Mark Dean, Igor Zaliznyak, Jonathan Pelliciari, Genda Gu, Abhay Pasupathy, Andreas Weichselbaum, Layla Hormozi

Northeastern University: Ning Bao

Stony Brook University: Tzu-Chieh Wei

Rutgers University: Ananda Roy

Keywords: Laser pump-probe experiments; Measuring entanglement in quantum materials; Quantum algorithms for low-dimensional systems

Research Scope: This proposal aims to improve our understanding of the coherence and entanglement properties of low energy spin excitations in many-body magnetic solid-state systems based on rare earths. To accomplish this, our research has two thrusts. In the first, we will develop pulsed laser experimental modalities to probe the non-equilibrium properties of rare-earth based magnetic chain systems. These modalities will exploit the unusually long lifetimes present in such materials. Inelastic neutron scattering, magnetic force microscopy, and resonant inelastic x-ray scattering and absorption will be used to probe the spatial and temporal evolution of the spin correlations and their electronic multiplet structure. Long coherence times are inherent to rare earth systems but may be enhanced in these materials by the presence of so-called quantum scars, eigenstates of the system with athermal properties that violate the eigenstate thermalization hypothesis. In this thrust, we will also develop the ability to determine quantum information measures in non-equilibrium material systems. In the second thrust, we will develop quantum algorithms informed by quantum information theoretic approaches to describe the non-equilibrium dynamics of such rare-earth materials. In particular, we will apply lessons obtained from the structure of tensor networks to develop efficient quantum algorithms able to compute both their ground state and non-equilibrium behavior.

Recent Progress:

Preparations for Ultrafast Laser Studies at the SIX Beamline at NSLS II

We are planning ultrafast laser studies of Yb-doped Yttrium aluminum perovskite and Yttrium aluminum garnet samples at NSLS II's SIX beamline. The ultrafast laser that will power these experiments is expected to be delivered in January 2023. To prepare for this delivery, we have performed design construction and testing of the optics of the laser system compatible with the constraint of the SIX experimental setup.

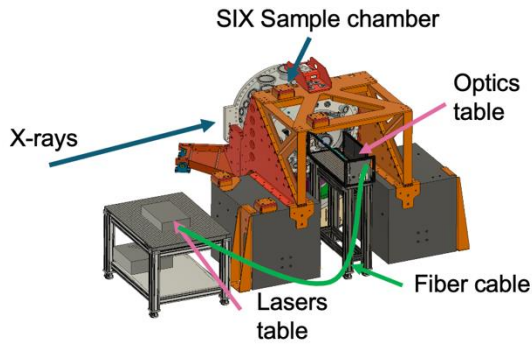


Fig. 4: Experimental design of the laser setup at SIX.

The design is given in Fig. 1. Due to the physical space available, the laser system will be placed on two specifically sized optical tables connected through a fiber cable transporting the laser beam from the “laser table” to the “optics table”. The first table accommodates the multiple laser sources while the second one is dedicated to collimating, focusing, and directing the beam inside the SIX sample chamber and onto the sample. This second table also contains the beam diagnostics and will be used for testing our neutron pump-probe setup.

To prepare for our ultrafast studies, in the past year we have worked on performing experiments on the Yb-based materials of interest in equilibrium conditions. The preliminary results are important as currently no RIXS data is available on the response of these materials due to the uncommon edge used (Yb M edge) and the relatively young field of high resolution RIXS. To this end, we have prepared Yb-doped yttrium aluminum perovskite (Yb:YAP) and yttrium aluminum garnet (Yb:YAG) samples with optically polished surfaces suitable for our planned experiments. Preliminary measurements of Yb M₄-edge resonant inelastic x-ray scattering (RIXS) have been conducted at SIX – see Fig. 2. As expected, a clear enhancement of intensity is seen at the Yb M₄ resonance corresponding to exciting electrons from the Yb 3d_{3/2} core states to the Yb 4f valence states. Zooming in on these transitions, we see the fine structure of the spectra, which vary between Yb:YAP and Yb:YAG.

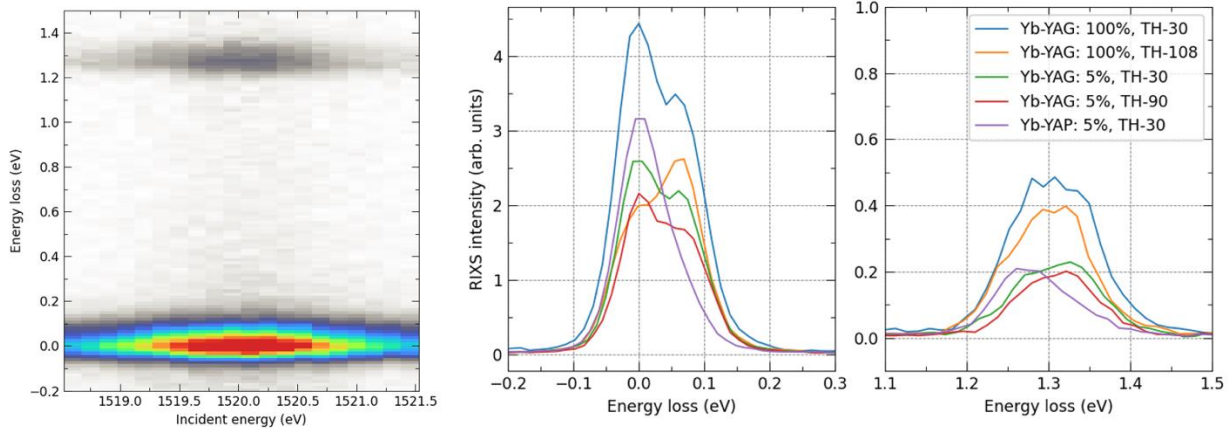


Fig. 2: Equilibrium resonant inelastic x-ray scattering (RIXS) measurements of Yb doped materials. Left: RIXS intensity of the 5% doped Yb:YAP sample as a function of incident energy showing that the signal resonates at the Yb M₄ edge of 1520 eV. The central and right panels show the fine structure of the low energy and 1.3 eV manifolds, respectively, for the different samples of 100% Yb-YAG, 5% Yb YAG, and 5% Yb-YAP, in which differences arising from changes in crystal field configurations are visible.

Developing Laser-Pump Neutron Spectroscopy Capability at ORNL's SNS

A collaborative development proposal, “Optical control of Yb-based qubit candidates using laser-pump neutron spectroscopy” for the HYSPEC and CNCS instruments was submitted to Oak Ridge National Laboratory in the 2022B proposal round and received an alternate status, allowing us to initiate a collaborative development with the ORNL team. The possible technological routes of how to setup an optical pump-probe sample environment for neutron scattering experiments were identified and conceptual design work has begun. Regular meetings of the BNL and the ORNL teams are being held. The collaborative development proposal has been resubmitted in the 2023A proposal round with the goal of carrying out prototyping and testing measurements.

In preparation for our laser-pump studies, we are planning equilibrium neutron studies of the relevant rare earth materials. High optical quality crystals of 100% and 5% substituted Yb:YAG were obtained through collaboration with the Scintillation Materials Research Center at the University of Tennessee; similar Yb:YAP crystals were made available for this work by the collaborator Podlesnyak at ORNL. Proposals to measure the crystal field splitting of the lowest, $J=7/2$ Yb spin-orbit multiplet in these crystals on SEQUOIA spectrometer at the SNS were submitted in the 2023A proposal call. Proposals to quantify the ground state and the effective spin Hamiltonian in these materials were submitted in the same proposal round to the CNCS spectrometer. While we expect that some of our proposals will receive beam time, in view of the reduced neutron availability due to the upcoming SNS shutdown to upgrade the power, we have also submitted proposals to the LET spectrometer at ISIS, UK and are considering conducting measurements at J-PARC in Japan.

Measuring Entanglement in Quantum Materials

We have developed [P1] a theoretical framework by which the time dependence of entanglement measures such as the Renyi entropies were able to be computed after a quantum quench in any system that can be described by a 1+1d bosonic field theory (i.e. spin chains, 1d Hubbard models, 1d cold atomic systems).

Quantum Algorithms for Low-Dimensional Systems

We benchmarked [P2] the use of deep multi-scale entanglement renormalization (DMERA) circuits as means to prepare ground states of spin chains on a quantum computer. As a model system we considered quantum Ising spin chains. We found that DMERA circuits strongly outperform a standard Quantum Alternating Operator Ansatz for ground state preparation.

Future Plans:

Ultrafast Laser Studies at the SIX Beamline at NSLS II

We expect delivery of the ultrafast laser system this January. We have been awarded beamtime through the NSLS-II user program to perform full experiments once the laser is delivered. We thus plan to characterize the changes in the RIXS spectra as a function of laser fluence, time delay, and sample temperature and build up a detailed spectroscopic picture of the physical principles underlying the functioning of these materials.

Developing Laser-Pump Neutron Spectroscopy Capability at ORNL's SNS

As discussed above, we have submitted/are in the process of submitting a number of beamtime proposals both in order to develop the pump-probe capability at the SNS and to characterize the equilibrium properties of our rare earth samples.

Measuring Entanglement in Quantum Materials using Scanning Tunneling Microscopy

We are planning to measure entanglement in rare earth spin chains using scanning tunneling microscopy techniques. In order to perform the measurements, it is necessary that the substrate is at least minimally conductive. At the same time, to preserve coherence, it is essential that the spin chain should not be too strongly coupled to a metal. We will therefore use as a sample an ultrathin layer (1-3 atomic layers) of aluminum oxide which is doped during growth with the rare earth of choice. This aluminum oxide will be deposited on conducting Nb-doped SrTiO₃ substrates which will serve both as a flat substrate and as a counter electrode for STM measurements.

Two methods for measuring entanglement will be explored. In the first technique, we will use the Electron Spin Resonance techniques developed by the IBM group (C. Lutz, A. Heinrich) to probe the quantum dynamics of a spin chain. In a very recent work, the group demonstrated that it is possible to measure entanglement between two spins separated by a short distance on a substrate by performing spin-polarized STM measurements on one of the spins [R1]. In the second technique, we will use measurements of the STM LDOS spectrum to place bounds on the multipartite entanglement in a spin chain. This spectrum can be connected to the quantum Fisher information for a witness operator based on a single-particle fermionic operator. This will extend previous work on using the QFI to estimate the multi-partite entanglement in bosonic spin systems [R2].

Quantum Algorithms for Low-Dimensional Systems

We give here two elements of our work on quantum algorithms. In the first, we plan to follow up on our previous work [P2] on the modular design of state preparation algorithms for spin chains. To this end, we plan to implement the algorithms on current generation quantum hardware to enable accurate error benchmarking for algorithms of this type. We also plan further study of the

incidental symmetry-driven error mitigation strategy discovered in [P2]. We will determine whether it can be applied generically to near-term quantum algorithms.

In the second, we will explore algorithms for the preparation of long-range entangled (LRE) states. Such states are also essential for applications to quantum metrology, robust quantum memories, and measurement-based and fault-tolerant quantum computation. It has been shown recently that the introduction of non-unitary operations can lead to efficient, finite-depth circuits for preparing certain LRE states [R3]. Inspired by these recent results, we aim to develop tools to allow the design of efficient quantum algorithms for the preparation of certain string-net models that are universal for quantum computation. String-nets are a class of lattice models that can realize all two-dimensional topological phases of matter.

References

R1. S.Phark et al., *Utilizing a single atom magnet and oscillating electric fields to coherently drive magnetic resonance in single atoms*, arXiv:2212.13380.

R2. A. Scheie, P. Laurell, A. M. Samarakoon, B. Lake, S. E. Nagler, G. E. Granroth, S. Okamoto, G. Alvarez, and D. A. Tennant, *Phys. Rev. B* 103, 224434 (2021).

R3. N. Tantivasadakarn, R. Thorngren, A. Vishwanath, and R. Verresen. Long-range entanglement from measuring symmetry-protected topological phases. <https://arXiv.2112.01519>, 2021.

Publications

P1. Postquantum Quench Growth of Renyi Entropies in Low-Dimensional Continuum Bosonic Systems, Sara Murciano, Pasquale Calabrese, and Robert M. Konik, *Phys. Rev. Lett.* 129, 106802 (2022).

P2. Variational quantum simulation of critical Ising model with symmetry averaging, Troy J. Sewell, Ning Bao, Stephen P. Jordan, arXiv: 2210.15053

P3. *Measurement-based quantum simulation of Abelian lattice gauge theories*, Hiroki Sukeno, Takuya Okuda, arXiv: 2210.10909.

P4. He Zhao, Raymond Blackwell, Shigeyuki Ishida, Akira Iyo, Hiroshi Eisaki, Abhay N. Pasupathy, Kazuhiro Fujita, “Smectic Pair Density Wave Order in $\text{EuRbFe}_4\text{As}_4$ ”, Under review in *Nature* (2022).

Ultrafast Materials Science

Alessandra Lanzara

University California, Berkeley and Materials Sciences Division - Lawrence Berkeley National Laboratory

Aaron Bostwick and Chris Jozwiak

Advanced Light Source, Lawrence Berkeley National Laboratory

Keywords: time resolved ARPES and spin-ARPES, excitons, topological excitonic states, charge density wave and photoinduced phase transitions.

Research Scope

The use of external knobs such as light and strain to control quantum materials is allowing us to access on demand new quantum phases and collective excitations that often exist only far away from equilibrium. However, our lack of understanding of how and why these properties emerge is limiting our ability to fully exploit this control. The main challenges lie in the access to how microscopic processes drive macroscopic changes, and under which regimes new states appear.

Our goal is to tackle these challenges by providing the first holistic approach to studying quantum phase transitions and collective excitations with momentum resolution, by accessing several orders of magnitude in space and time, across which emergence develops. This will be possible by advancing and coupling a portfolio of state-of-the-art angle resolved photoemission spectroscopy (ARPES) tools, that span across many orders of magnitude in spatial resolution (from mm-nm), and in time resolution (from steady-state to femtoseconds), and across the unexplored ranges of the combined capabilities.

To address the current needs and challenges in the field, our main line of research will cover the exploration of non-thermal phases such as excitonic states, photoinduced phase transitions through manipulation of electron - boson interactions and exploration of heterogeneity down to its mesoscopic length scale at the onset of a phase transition.

These works have benefitted uniquely from the combination of the state-of-the-art spectroscopic tools developed in the PI's laboratories, together with the unique Laser-X platform, with micron- and sub-micron resolution, simultaneous capability of applying in operando fields and currents, tunable ultrafast pump laser with variable repetition rate and probe energy.

Recent Progress

Our work in the past year has focused on a) driving spin orbit coupling and Rashba splitting on ultrafast time scale; b) investigation of momentum resolved formation of excitonic states in quantum materials; c)

a) Electric field gating is one of the most fundamental tuning knobs for all modern solid state technology and is the foundation for many solid-state devices such as transistors. Current methods

for in-situ back-gated devices are difficult to fabricate, introduce unwanted contaminants, and, most importantly, cannot reveal dynamics induced by the onset of the field, and are unsuited for picosecond time-resolved electric field studies. In our work we have discovered a new way to generate ultrafast back-gating, by leveraging the surface band bending inherent to many semiconductor's materials. Our new architecture consists of a standard bulk semiconductor material and a layered material on the surface. Optical pulses generate picosecond time varying electric field on the surface material driving an ultrafast switching. We have successfully applied this method to a quantum well Rashba system, among the most promising candidates for spin-based devices, to modulate spin orbit coupling and Rashba, followed by the creation of long lived states through a Lifshitz transition¹. The power of this method, is in the generation of ultrafast electric field that allows switching capabilities faster than 10GHz, much faster than anything that can be achieved today. The other benefit of this approach, is that it doesn't need any fabrication or lithography and will enable light-driven electronic and spintronics devices such as transistors, spin-transistors and photo- controlled Rashba circuitry. This method can be applied with minimal effort to any two-dimensional material, for both exfoliated and molecular beam epitaxy grown samples. In the near future we plan to adopt this methodology to modify electron-boson interaction through a phase transition.

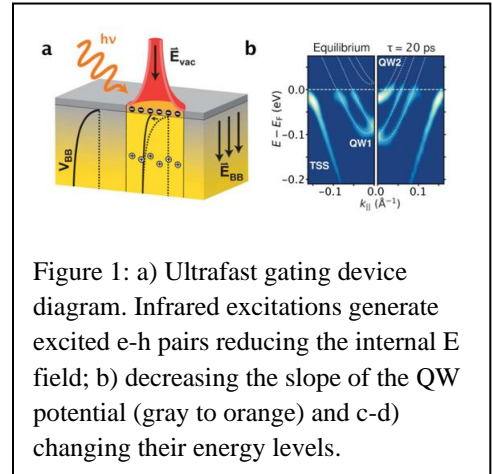


Figure 1: a) Ultrafast gating device diagram. Infrared excitations generate excited e-h pairs reducing the internal E field; b) decreasing the slope of the QW potential (gray to orange) and c-d) changing their energy levels.

b) Excitons have played significant roles in functionality of optoelectrical and energy-harvesting devices and in realization of exotic quantum phases involving Mott physics, charge density wave formations and Bose-Einstein condensations. Leveraging our in-house high-resolution extreme-ultraviolet (XUV) time- resolved angle-resolved photoemission spectroscopy (trARPES) with high energy, momentum, and time resolution we have studied the effect of exciton formation on the band structure of a monolayer MoS₂. We revealed exciton-driven renormalization of the

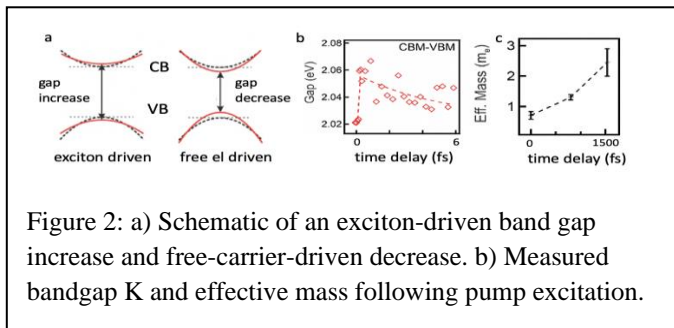


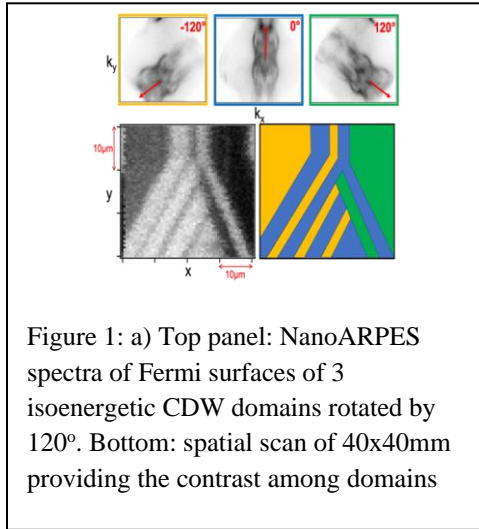
Figure 2: a) Schematic of an exciton-driven band gap increase and free-carrier-driven decrease. b) Measured bandgap K and effective mass following pump excitation.

electronic structure in a similar fashion as in the case of other many body interactions². Specifically, we saw a surprising exciton-driven bandgap increase, by as much as 40 meV, in contrast to the typical bandgap decrease previously reported and associated to screening (see figure 2), and a simultaneous enhancement of the effective

mass GW calculations explained these findings in terms of screened vs unscreened interactions.

In the future we plan to expand these studies to other excitonic states and specifically to topological excitonic states.

c) In recent years attention has been given to a class of TMD that exhibit peculiar CDW order due their “mixed dimensionality”. TaTe2 is one of such examples, where the material appears structurally close to 2D, but electronically similar to a quasi-1D material. The interest in these materials stems from the similarity with the nematic phase and stripe order phase observed in a variety of correlated materials, with the most famous example being the stripe phase in cuprates.



In a recent work we have shown that within the CDW state a decoupling between the structural and electronic periodicity occurs. The crystal has threefold symmetry in the plane and therefore the question arises of what direction will be chosen at the electronic level to set the charge order among three structurally equivalent and energy degenerate ones. By using nanoARPES we succeeded in imaging three separate domains coexisting on the same sample, offset by 120 degrees.

In the future we plan to look into the physics of the phase separation, and namely whether the boundaries between different domains are randomly directed and stem from impurities/defects, or if instead they follow a specific crystallographic direction and how we can externally control of the electronic anisotropy with light.

Future Plans

In the next year we plan to build upon on our recent work on excitonic states in topological insulators and 2D materials to search for condensation and other exciton driven renormalization phenomena. We also plan to investigate how microscopic inhomogeneities trigger one competing order to emerge during a phase transition by a combination of ARPES studies down to heterogeneity’s own mesoscopic length scale (from few nm to few mm) and by photo-inducing the phase transitions.

a) Excitonic landscape in momentum space: By leveraging the recent discovery that excitonic states carry unique signatures in the single particle spectral function measured we plan to uncover the complex landscape of short-lived excitons (ps-sub ns) in van der Waals heterostructures and topological materials. We will focus on the evolution of the excitonic state, and its signature in the single particle spectral function across the exciton Mott transition with the main focus on exciton dynamics, exciton-driven band structure and gap renormalization, and exciton condensation³. Along the same line, we will expand our preliminary studies to the case of indirect excitonic topological states. These states are appealing as they could host excitonic condensation at high temperature and with topological protection. tr-ARPES is ideal to probe condensation given its specific signatures on the band structure, such as bandgap opening in the

topological surface state at the Fermi level and renormalization of the bulk valence band in the form of a camel like dispersion.

b) Creation of transient non thermal phases far from equilibrium: Our objective is to use ultrashort and intense pulses of light, tailored to vibrational excitations, to create new collective states and to disentangle degenerate competing orders hidden in static conditions and then study the electronic response via tr ARPES. This study follows the proposal from mid-IR optical spectroscopy of transient induced superconductivity⁴. Our focus will be on the study of doped C_{60}/STO and $/Bi_2Se_3$ and $FeSe/STO$, through mode-selective tr-ARPES experiments. For both systems experiments will be conducted by coupling mid IR light pulses to excite the Raman active phonons of the substrate. The benefit of this method is that these excitations should act as an indirect perturbation of the lattice. The ability of tr-ARPES to directly access order parameter dynamics and coherence, provides a unique means to solve the long-standing debate on the real origin of these light driven states.

c) Coexisting structural and electronic orders in TaS_2 : TaS_2 is probably one of the first examples where multiple first order phase transitions between four different CDW states were observed as a function of temperature, thickness and external pressure, resulting in spatial inhomogeneity and spatially varying domains of different structural and electronic order⁵. Studies at the mesoscopic scales are sparse and mostly limited to the structural degrees of freedom. Here we propose to fill this gap by studying the electronic structure of the thermally induced transition(s) in 1T- TaS_2 both in its bulk form and for the monolayer case, grown by chemical vapor transport. Temperature and uniaxial strain, up to 2%, will be used to trigger the collapse from the Mott gap state to metallic state, and to induce and control different orders and new non thermal electronic and lattice states.

d) Mixed dimensionality in $TaTe_2$: In addition to TaS_2 , the less investigated $TaTe_2$ is an interesting compound due to its “mixed dimensionality”: structurally close to 2D but electronically similar to a quasi-1D material. Given its threefold symmetry with three structurally equivalent and energy degenerate states the question is whether charge ordering favors a specific direction among the three structurally equivalent and energy degenerate ones. Specifically, the next immediate goal is to look into the physics of the phase separation, and namely whether the boundaries between different domains are randomly directed and stem from impurities/defects, or if instead they follow a specific crystallographic direction. This in turn will lead to the external control of the electronic anisotropy.

References

1. S. Ciocys, N. Maksimovic, J. G. Analytis, A. Lanzara, “Driving ultrafast spin and energy modulation in quantum well states via photo-induced electric fields” npj quantum Materials **7**, 1-10 (2022)

2. Y. Lin, Y. Chan, W. Lee, L. S. Lu, Z. Li, W. H. Chang, C. K. Shih, R. Kaindl, S. G. Louie, A. Lanzara, *Exciton Driven Renormalization of quasiparticle band structure in monolayer MoS₂*, Phys. Rev. B **106**, L081117 (2022)
3. B. Seradjeh, J. E. Moore, M. Franz, *Exciton condensation and charge fractionalization in a topological insulator film*, Phys. Rev. Lett. **103**, 066402 (2009).
4. M. Budden, et al., *Evidence for metastable photo-induced superconductivity in K₃C₆₀*, Nature Physics **17**, 611 (2021)
5. L. Stojchevska, I. Vaskivskiy T. Mertly, P. Ksar, D. Svetin, S. Brazovskii, D. Mihailovic, *Ultrafast switching to a stable hidden quantum state in an electronic crystal*, Science **344**, 177 (2014).

Publications

2. T. R. Xu, T. Scaffidi and X. Y. Cao. “Does scrambling equal chaos?,” Physical Review Letters **124** (14) (2020).
3. V. B. Bulchandani, C. Karrasch and J. E. Moore, “Superdiffusive transport of energy in one-dimensional metals”, Proceedings of the National Academy of Sciences **117** (23), 12713 (2020).
4. C. Stansbury and A. Lanzara, “PyARPES: An analysis framework for multimodal angle-resolved photoemission spectroscopies”, SoftwareX **11**, 100472 (2020).
5. S. Ciocys, T. Morimoto, R. Mori, K. Gotlieb, Z. Hussain, J. G. Analytis, J. E. Moore and A. Lanzara, “Manipulating long-lived topological surface photovoltage in bulk-insulating topological insulators Bi₂Se₃ and Bi₂Te₃”, npj Quantum Materials **5** (1), 16 (2020).
6. C.-Y. Lin, L. Moreschini and A. Lanzara, “Present and future trends in spin ARPES”, EPL (Europhysics Letters) **134** (5), 57001 (2021).
7. S. C. Furuya, K. Takasan and M. Sato, “Control of superexchange interactions with DC electric fields”, Physical Review Research **3** (3) (2021).
8. Y. Tanikawa, K. Takasan and H. Katsura, “Exact results for nonlinear Drude weights in the spin-1/2 XXZ chain”, Physical Review B **103** (20) (2021).
9. C. H. Stansbury, M. I. B. Utama, C. G. Fatuzzo, E. C. Regan, D. Q. Wang, Z. Y. Xiang, M. C. Ding, K. Watanabe, T. Taniguchi, M. Blei, Y. X. Shen, S. Lorcy, A. Bostwick, C. Jozwiak, R. Koch, S. Tongay, J. Avila, E. Rotenberg, F. Wang and A. Lanzara, “Visualizing electron localization of WS₂/WSe₂ moire superlattices in momentum space”, Science Advances **7** (37) (2021).
10. N. Dale, R. Mori, M. I. B. Utama, J. D. Denlinger, C. Stansbury, C. G. Fatuzzo, S. Zhao, K. Lee, T. Taniguchi, K. Watanabe, C. Jozwiak, A. Bostwick, E. Rotenberg, R. J. Koch, F. Wang and A. Lanzara, “Correlation-driven electron-hole asymmetry in graphene field effect devices”, npj Quantum Materials **7** (1), 9 (2022).
11. Y. Lin, M. Huber, S. Rajpurohit, Y. Zhu, K. M. Siddiqui, D. H. Eilbott, L. Moreschini, P. Ai, J. D. Denlinger, Z. Mao, L. Z. Tan and A. Lanzara, “Evidence of nested quasi-one-dimensional Fermi surface and decoupled charge-lattice orders in layered TaTe₂”, Physical Review Research **4** (2), L022009 (2022).
12. W. Lee, Y. Lin, L.S. Lu, W. C. Chueh, M. K. Liu, X. Q. Li, W. H. Chang, R. A. Kaindl, C. K. Shih, “Time-resolved ARPES Determination of a Quasi-Particle Band Gap and Hot Electron Dynamics in Monolayer MoS₂”, Nano Letters **21** (17), 7363-7370 (2021).

13. R. Mori, K. Wang, T. Morimoto, S. Ciocys, J. D. Denlinger, J. Paglione and A. Lanzara, "*Observation of a Flat and Extended Surface State in a Topological Semimetal*", *Materials* **15** (8) (2022).
14. Y. Lin, Y. Chan, W. Lee, L. S. Lu, Z. Li, W. H. Chang, C. K. Shih, R. Kaindl, S. G. Louie, A. Lanzara, *Exciton Driven Renormalization of quasiparticle band structure in monolayer MoS₂*, *Phys. Rev. B* **106**, L081117 (2022)
15. S. Ciocys, N. Maksimovic, J. G. Analytis, A. Lanzara, "*Driving ultrafast spin and energy modulation in quantum well states via photo-induced electric fields*" *npj quantum Materials* **7**, 1-10 (2022)
16. R. Mori, S. Ciocys, K. Takasan, p. Ai, k. currier, T. Morimoto, J. E. Moore, A. Lanzara. "*Spin polarized spatially indirect excitons in a topological insulator*", To be published – *Nature* (2022)

Structural Dynamics in Functional Materials

Aaron Lindenberg^{1,2}, Mariano Trigo¹, David Reis^{1,3}, William Chueh^{1,2}

¹Stanford Institute for Materials and Energy Sciences, SLAC, Menlo Park, CA 94025

²Department of Materials Science and Engineering, Stanford University, Stanford, CA 94035

³Department of Applied Physics, Stanford University, Stanford, CA 94035

Keywords: Ultrafast science, x-ray free electron lasers, ultrafast electron diffraction, quantum materials, operando studies

Research Scope

Our program is focused on understanding the role structure and dynamics play in the functionality of materials. It is organized into two main interconnected areas: (1) Probing switching dynamics, intermediate states, and metastable phases, involving short range, atomic-scale distortions and (2) Probing nanoscale and mesoscale distortions and dynamic heterogeneity. Combined with unique tools at SLAC and close theoretical collaborations, these represent a new means for understanding and manipulating the functional properties of materials and devices which in turn arise from atomic and meso-scale motions, processes typically blurred in time and in space by prior experimental approaches. In this FWP we make central use of the user facilities at SLAC including the Linac Coherent Light Source as well as the Stanford Synchrotron Radiation Laboratory and the Advanced Light Source at Lawrence Berkeley National Laboratory. Our team and the associated scientific efforts have played a key role in the development of new facilities at SLAC, including LCLS-II, LCLS-II-HE, and UED, and at ALS, including COSMIC. Experiments within this FWP involve in-situ studies of non-equilibrium metastable phases and materials at phase boundaries, dynamic transition states, and the role of heterogeneity. Measurements of the first atomic/ionic steps associated with how these transformations occur are key to understanding these intrinsically dynamic processes, and are uniquely made possible by the facilities at SLAC/Stanford and this collaborative team.

Recent Progress

1. We carried out LCLS experiments probing the dynamic response of the layered IV-VI material SnSe under above gap excitation, showing a new type of non-thermal lattice instability and the formation of a new Immm structural phase not found in equilibrium. This structure is identified by measurements of the dynamic response of many Bragg peaks enabling reconstruction of the unit cell. These results suggest new strategies for using ultrafast lasers to induce normally inaccessible non-equilibrium structures. Y. Huang et al., “Observation of a novel lattice instability in ultrafast photoexcited SnSe”, *Phys. Rev. X* **12**, 011029 (2022).

2. Operando ultrafast electron diffraction studies investigated the pulsed E-field-induced pathway underlying the insulator-to-metal transition in VO₂ within an operating device. We demonstrate that pulsed electrical excitation induces a transient isostructural phase which mediates the transition between the structurally-distinct equilibrium phases. Our measurements also reveal a universal transition pathway (comparing photoexcitation to electrical excitation) across eight orders of magnitude in timescale. A. Sood et al., “Universal phase dynamics in VO₂ switches revealed by ultrafast operando diffraction,” *Science* **373**, 352 (2021).

3. Experiments at the LCLS defined a new approach for visualizing the dynamic polaronic distortions that occur in the hybrid perovskites. This work used time-domain diffuse x-ray scattering as a momentum-resolved phonon spectroscopy of the locally distorted structure to probe charge-induced local heterogeneous distortions and quantify the elastic strain fields associated with these electron-phonon coupling process, proposed to underlie the unique optoelectronic functionality of these materials. We observe a radially expanding nanometre-scale strain field associated with the formation and relaxation of polarons in photoexcited perovskites. Estimates of the magnitude and shape of the polaronic distortion are obtained, providing direct insights into the dynamic structural distortions that occur in these materials. B. Guzelturk et

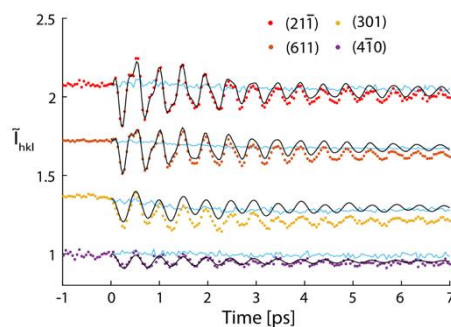


Fig. 1. Time-resolved diffraction intensity for various peaks from which transient structure is reconstructed.

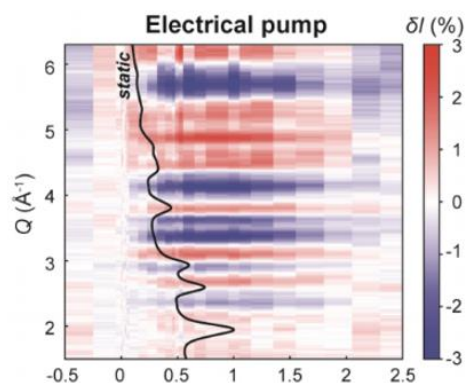


Fig. 2. Transient changes as a function of time and momentum transfer during the field-driven insulator-to-metal transition in VO₂. Static diffraction pattern shown by solid black curve.

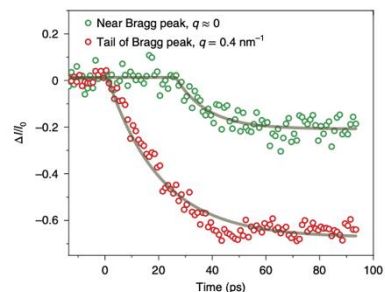


Fig. 3. Time-resolved diffraction changes at selected momentum transfers.

al., “Visualization of dynamic polaronic strain fields in hybrid lead halide perovskites”, *Nature Materials*, **20**, 618 (2021).

4. We investigated intercalation-driven transformations in 2D materials using a combination of in-situ x-ray scattering, cyclic voltammetry, and in-situ UED. This work reports on the discovery of a new metastable phase of lithium-intercalated WTe_2 featuring the largest in-plane chemical expansion coefficient ever observed in a single-phase material. The unusual actuation of Li_xWTe_2 is linked to the formation of a newly-discovered metastable crystallographic phase. Further we show that this response can be potentially used as a new type of straintronic device allowing for modulation of strain at high frequencies. P. Muscher et al., “Highly-efficient uniaxial in-plane stretching of a 2D material via ion insertion” *Advanced Materials* **33**, 2101875 (2021); see also: A. Sood et al., “Electrochemical ion insertion from the atomic to the device scale” *Nature Reviews Materials*, **6**, 847 (2021).

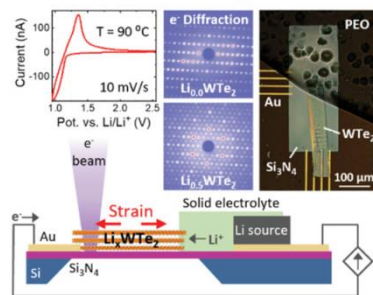


Fig. 4. All-solid electron-transparent setup for in-situ ion intercalation.

5. Solid-state ionic conduction is a key enabler of electrochemical energy storage and conversion but the mechanistic, atomic scale properties that underlie this functionality remain poorly understood. In this work, inspired by studies of fluids and biophysical systems, we carried out purely theoretical efforts to re-examine anomalous diffusion in the iconic two-dimensional fast-ion conductors, the β - and β'' -aluminas. We provide a fundamental understanding of the AC ionic conductivity and investigate the origins of persistent sub-diffusive ionic transport. Our characterization of memory effects in transport connects atomistic defect chemistry to macroscopic performance with minimal assumptions and enables mechanism-driven ‘atoms-to-device’ optimization of fast-ion conductors. “Defect-Driven Anomalous Transport in Fast-Ion Conducting Solid Electrolytes”, A. Poletayev et al. *Nature Materials*, **21**, 1066 (2022). Ongoing efforts use strong-field THz pulses to manipulate ions in these materials and probe time-dependent correlations and memory loss effects (A. Poletayev et al., arXiv: 2110.06522 (2022)).

Future Plans

1. Facility development: We continue to be active users at LCLS and other free electron lasers around the world, as well as at synchrotrons such as the Advanced Photon Source and Advanced Light Source, and at the SLAC Ultrafast Electron Diffraction Facility. At UED, operando studies building on the work described above are now in analysis stage probing ultrafast dynamics in ion-intercalated 2D materials driven by optical and THz fields. A number of new efforts involving in-situ device-scale E-field-driven switching responses in ferroelectrics are also in progress, building on the VO_2 work described above. At the LCLS, in collaboration with SLAC accelerator scientists, we are working to enable electron-beam-based THz pump / x-ray probe measurements. This setup, now installed downstream of the LCLS undulators, uses the Coulomb field of the LCLS electron bunch in conjunction with co-timed femtosecond x-ray pulses to probe subsequent structural dynamics with elemental specificity using soft x-ray spectroscopy.

2. Building on the work described above on the monochalcogenides, we are exploring new types of optical control of materials using sub-gap excitation. Combining table-top femtosecond stimulated Raman scattering in conjunction with time-domain x-ray scattering at the Advanced Photon Source, this defines new opportunities for opto-mechanical control of materials and the induction of new metastable phases with unique functional properties.

3. Ongoing efforts probing dynamics in charge density wave (CDW) systems reveal exquisite details of the formation of topological defects (dislocations) of the CDW thanks to the extremely high wavevector resolution of the x-ray FEL. Topological defects are observed as distinctive power-law scaling of the structure factor $S(k)$ vs k . These topological defects are controlled by light pulses, and these measurements demonstrate that ultrafast excitation can create non-equilibrium states that are inaccessible by other means. In LaTe_3 , we have shown that the transient CDW order is associated with these defects and the competing a -order of LaTe_3 exists in the dislocation cores.

4. We are collaborating with groups at the ALS to employ ultrafast scanning transmission X-ray microscopy to investigate ion transport and intercalation-induced phase transformation in 2D materials such as Li-WTe_2 . We have recently secured an Approved Program at ALS to carry out this development effort.

Publications

13. P. Muscher, D. Rehn, A. Sood, K. Lim, D. Luo, X. Shen, M. Zajac, F. Lu, A. Mehta, Y. Li, X. Wang, E. Reed, W.C. Chueh, A.M. Lindenberg. “Highly efficient uniaxial in-plane stretching of a 2D material via ion insertion,” *Advanced Materials*, **33**, 2101875 (2021).
14. A. Sood, X. Shen, Y. Shi, S. Kumar, S. Park, M. Zajac, Y. Sun, L-Q. Chen, S. Ramanathan, X. Wang, W. C. Chueh, A. M. Lindenberg, “Universal phase dynamics in VO_2 switches revealed by ultrafast operando diffraction,” *Science*, **373**, 352 (2021).
15. A. Sood, A. Poletayev, D. A. Cogswell, P. M. Csernica, J. T. Mefford, D. Fraggadakis, M. F. Toney, A. M. Lindenberg, M. Z. Bazant, and W. C. Chueh, “Electrochemical ion insertion from the atom to device scale,” *Nature Reviews Materials* **6**, 847 (2021).
16. B. Guzelturk, T. Winkler, T. Van de Goor, M. D. Smith, S. A. Bourelle, S. Feldmann, Mariano Trigo, S. Teitelbaum, H-G. Steinrück, G. A. de la Pena, R. Alonso-Mori, D. Zhu, T. Sato, H. I. Karunadasa, M. F. Toney, F. Deschler, Aaron M. Lindenberg, “Visualization of Dynamic Polaronic Strain Fields in Hybrid Lead Halide Perovskites,” *Nature Materials* **20**, 618 (2021).
17. J.T. Mefford, A.R. Akbashev, M. Kang, C. L. Bentley, W.E. Gent, H. D. Deng, D. H. Alsem, Y.-S. Yu, N. J. Salmon, D. A. Shapiro, P. R. Unwin, William C. Chueh. “Correlative operando microscopy of oxygen evolution electrocatalysts” *Nature* **593**, 67 (2021).
18. S. W. Teitelbaum, T. C. Henighan, H. Liu, M. P. Jiang, D. Zhu, M. Chollet, T. Sato, E. D. Murray, S. Fahy, S. O'Mahony, T.P. Bailey, C. Uher, M. Trigo, D. Reis, “Measurements of nonequilibrium interatomic forces using time-domain x-ray scattering,” *Phys. Rev. B* **103**, L180101 (2021).

19. M. Trigo, P. Giraldo-Gallo, J. N. Clark, M.E. Kozina, T. Henighan, M.P. Jiang, M. Chollet, I. R. Fisher, J. M. Glowonia, T. Katayama, P. S. Kirchmann, D. Leuenberger, H. Liu, D. Reis, Z. X. Shen, and D. Zhu, “Ultrafast formation of domain walls of a charge density wave in SmTe_3 ,” *Phys. Rev. B* **103**, 054109 (2021)
20. P.M. Csernica, S. S. Kalirai, W. E. Gent, K. Lim, Y.-S. Yu, Y. Liu, S.-J. Ahn, E. Kaeli, X. Xu, K. H. Stone, A. F. Marshall, R. Sinclair, D. A. Shapiro, M. F. Toney, William C. Chueh, “Persistent and Partially Mobile Oxygen Vacancies in Li-Rich Layered Oxides,” *Nature Energy*, **6**, 642 (2021).
21. C. Baumer, J. Li, Q. Lu, A.Y.-L. Liang, L. Jin, H. P. Martins, T. Duchon, M. Glöß, S. M. Gericke, M. A. Wohlgemuth, M. Giesen, E. E. Penn, R. Dittmann, F. Gunkel, R. Waser, M. Bajdich, S. Nemsak, J. T. Mefford, W.C. Chueh, “Tuning electrochemically-driven surface transformation in atomically-flat LaNiO_3 thin films for enhanced water electrolysis,” *Nature Materials* **20**, 674–682 (2021).
22. B. Guzelturk, M. Trigo, O. Delaire, D. A. Reis, and A. M. Lindenberg. “Dynamically tunable terahertz emission enabled by anomalous optical phonon responses in lead telluride”. *ACS Photonics*, 8(12):3633– 3640, 12 2021.
23. I. Abate, S. Y. Kim, C.D. Pemmaraju, M. F. Toney, W. Yang, T.P. Devereaux, W.C. Chueh, L. F. Nazar, “The role of metal substitution in tuning anion redox in sodium metal layered oxides revealed by X-ray spectroscopy and theory “, *Angew. Chem. Int. Ed.* **60**, 10880 (2021)
24. D. Luo, J. Tang, X. Shen, F. Ji, J. Yang, S. Weathersby, M. Kozina, Z. Chen, J. Xiao, Y. Ye, T. Cao, G. Zhang, X. Wang, A.M. Lindenberg, “Twist-angle-dependent ultrafast charge transfer in MoS_2 -graphene van der Waals heterostructures,” *Nano Lett.* **21**, 8051 (2021).
25. Y. Huang, S. Yang, S. Teitelbaum, G. de la Pena, T. Sato, M. Chollet, D. Zhu, J. L. Niedziela, D. Bansal, A. F. May, A.M. Lindenberg, O. Delaire, D.A. Reis, and M. Trigo, "Observation of a novel lattice instability in ultrafast photoexcited SnSe ", *Phys. Rev. X* **12**, 011029, (2022).
26. M.P. Jiang, S. Fahy, A. Hauber, É.D. Murray, I. Savić, C. Bray, J. N. Clark, T. Henighan, M. Kozina, Aaron M. Lindenberg, P. Zalden, M. Chollet, J.M. Glowonia, M.C. Hoffmann, T. Sato, D. Zhu, O. Delaire, A.F. May, B.C. Sales, R. Merlin, Mariano Trigo, and David A. Reis, "Observation of photo-induced plasmon-phonon coupling in PbTe via ultrafast x-ray scattering", *Structural Dynamics* **9**, 024301, (2022).
27. A. Poletayev, J. Dawson, S. Islam, A.M. Lindenberg, “Defect-driven anomalous transport in fast-ion conducting solid electrolytes,” *Nature Materials* **21**, 1066 (2022).
28. A. Y.-L. Liang, W. C. Chueh, “Impedance Modeling for Mixed Conductors with Simultaneous Insertion & Electrocatalytic Reactions: A Case Study of Transition-Metal Hydroxides in Aqueous Electrolyte”, *J. Electrochem. Soc.* **169**, 056502 (2022).
29. F. Murphy-Armando, É. D. Murray, I. Savić, M. Trigo, D. A. Reis, and S. Fahy, “Electronic heat generation in semiconductors: non-equilibrium excitation and evolution of zone-edge phonons via electron-phonon scattering in photo-excited germanium”, *Appl. Phys. Lett.* **122**, 012202 (2023).
30. A. R. Akbashev, V. Roddatis, C. Baeumer, T. Liu, J. T. Mefford, W. C. Chueh. Probing the stability of SrIrO_3 during active water electrolysis via operando atomic force microscopy. *Energy & Environ. Sci.* 2023. (in press).

X-ray studies of complex materials at high pressure

Wendy L. Mao, Stanford University & SLAC National Accelerator Laboratory

Hemamala Karunadasa, Stanford University & SLAC National Accelerator Laboratory

Yu Lin, SLAC National Accelerator Laboratory

Self-identify keywords to describe your project:

diamond anvil cell

lattice compression

X-ray scattering

halide perovskites and analogs

Program Scope

The theme of our FWP is manipulating the ground and excited states of complex materials by understanding their atomic and electronic structures at high pressure. Here, high pressure studies inform synthetic design towards improved materials and novel lattice architectures enable the realization of unprecedented high-pressure phenomena. The overarching goal of this research program is to disentangle the local and long-range structural response to pressure and understand how their cooperative interactions contribute to the macroscopic behavior of complex materials. Our proposed research program relies on our ability to characterize materials using a suite of *in situ* techniques – in particular X-ray probes – at the relevant energy, spatial, and temporal scales. As an archetypal materials family to pursue these fundamental studies, halide perovskites are an ideal platform of crystalline semiconductors to demonstrate how both thermodynamic properties and excited-state dynamics can be systematically tuned through mechanical compression. Our activities will be closely tied to SLAC facilities, and we will leverage expertise at SLAC through existing and new collaborations with the many groups within the Division of Materials Science working in condensed matter physics, ultrafast science, and theory.

Our research portfolio is organized under three main research thrusts: 1) Controlling lattice heterogeneity and electronic dimensionality – to understand how lattice compression affects the local structural heterogeneity (i.e. defects, disorder, and dynamics) and orbital interactions across ordered lattice vacancies; 2) Creating emergent electronic states – to generate itinerant electrons at high pressure, which can lead to interactions that yield novel electronic phenomena; 3) Accessing metastability and beyond equilibrium matter – to characterize and control matter away from equilibrium and find pathways to novel phases not accessible otherwise. For all three research thrusts, it is crucial that we continue to develop and enhance *in situ* and *in operando* X-ray diagnostics along with extreme environment capabilities for the characterization and study of these complex materials.

Recent Progress

- *Electron-electron interaction and a Fermi-liquid-like metal in δ -CsPbI₃*: We observed rare electron-electron interaction induced by Cs-mediated electron redistribution in compressed δ -

CsPbI₃. Insulating δ -CsPbI₃ transforms to a Fermi-liquid-like metal at high pressure, concomitant with a structural transition from a 1D chain to a 3D phase. Pressure increases the 5d state occupation in Cs and I, which results in the electron-electron interaction and renders a Fermi-liquid-like state (Ke et al., Nat. Commun. 2022).

- *One-dimensional (1D) metallicity in δ -CsSnI₃*: We demonstrated pressure-induced 1D metallicity in δ -CsSnI₃. XRD and Raman spectroscopy indicate that the 1D chain structure of δ -CsSnI₃ is maintained in the high-pressure metallic phase while the SnI₆ octahedral chains are distorted. Experiments and first-principles DFT calculations show that pressure induces Sn-Sn hybridization and enhances Sn-I coupling within the chains that broaden the Sn-5p and I-5p bands and close the bandgap (Ke et al, J. Am. Chem. Soc. in press).
- *Charge reservoirs in an expanded halide perovskite analog (dmpz)[Sn₂X₆] (X = Br⁻ and I⁻) and pressure-enhanced conductivity*: We described a novel strategy of using redox-active organic molecules as stoichiometric electron acceptors in metal-halide semiconductors. Pressure enables the redox-active organic cations to dope the material through internal charge-transfer, enhancing the conductivity (Matheu et al., Angew. Chem. Int. Ed. 2022).
- *Tuning defects in a halide double perovskite with pressure*: We report the first experimental investigation on the effect of pressure on defects in halide perovskites. Modest compression first increases the conductivity of Cs₂AgTlBr₆ by an order of magnitude and decreases its bandgap from 0.94 eV to 0.7 eV. Subsequent compression yields complex optoelectronic behavior, wherein the conductivity ranges across at least four orders of magnitude. These conductivity changes cannot be explained by the evolving bandgap. Instead, they can be understood as tuning of the bromine vacancy defect with pressure—varying between a delocalized shallow defect state with a small ionization energy and a spatially localized deep defect state with a large ionization energy (Wolf et al, J. Am. Chem. Soc. 2022).
- *Superconductivity in compressed transition metal perovskite chalcogenides*: We observed intriguing insulating-to-metallic, and to-superconducting transitions in BaTiS₃ and BaTiSe₃ at high pressure. Both materials become superconducting at ~60 GPa with a T_c of ~3 K. T_c increases with pressure and reaches above 9 K at 120 GPa for BaTiS₃ and 6 K at 80 GPa for BaTiSe₃. Structural displacements in the quasi-1D network could be the origin of the change in the electronic structures.
- *Mixed-valence 2D perovskites*: We studied high-pressure structures and optical and electronic properties of a layered halide perovskite with three different metal ions in the octahedral sites: (BA)₄[Cu^{II}(Cu^IIn^{III})_{0.5}]Cl₈ (1_{BA}; BA⁺ = butylammonium). Compressing 1_{BA} reduces the onset energy of intervalence charge transfer between the Cu(I) and Cu(II) centers from 1.2 eV at ambient pressure to 0.2 eV at 21 GPa, while the electronic conductivity of 1_{BA} increases by 4 orders of magnitude upon compression to 20 GPa. Encouraged by the newly emerged properties, we demonstrated an efficient mechanochemical synthesis to expand this family of mixed-valence halide perovskites with complex compositions.
- *Data-driven approaches for high-pressure halide perovskite studies*: We have introduced data-driven approaches, complementary to the experiments and simulations, for understanding the behavior of halide perovskites at high pressure and predicting new materials. Our results from studying an all-inorganic CsPbI₃ perovskite phase validated the use of crystal graph convolutional neural network (CGCNN) for predicting materials properties. The best CGCNN model predicts the bandgap and enthalpy with high fidelity when the system undergoes uniaxial strain or hydrostatic compression.

- *XFEL-DAC opportunities:* We are continuing to make significant efforts in developing high-pressure ultrafast X-ray characterization. We will have an X-ray pump, X-ray probe experiment on DAC samples at HED, EuXFEL in June 2023. Another major effort is to enable the optical-pump, X-ray probe experiments in a DAC at LCLS-II.

Future Plans

- *Exploring exotic electronic states in the perovskite and non-perovskite metal halides:* We plan to extend the successful structural and electronic studies on CsPbI₃ to analogous systems. For example, the ability to access a reliable perovskite phase of 10% Cs@(FA)PbI₃ at ambient conditions along with the thermodynamically stable non-perovskite phase of δ -(FA)PbI₃ allows us to perform parallel measurements and analyses to search for states such as a strange metal. The results can guide our efforts for studying halide perovskite-based superconductors.
- *Controlling the phase stability and accessing metastability:* We will study the competing effects between octahedral tilting and octahedral volume shrinkage in perovskite chalcogenides at high pressure and find design principles for the phase control. Structural transitions resulting from these two factors alone or in combination are present across many perovskite materials. We plan to study a series of perovskite chalcogenides with a goal of obtaining a unified scheme to explain their structural evolution trends at high pressure. This could offer fundamental insight into accessing and stabilizing perovskite structures and drive the search for novel perovskite materials.
- *Understanding the superconductivity in transition metal perovskite chalcogenides and continuing the search for exotic electronic states in halide perovskites:* The novel superconducting transitions observed in both BaTiS₃ and BaTiSe₃ motivate us to uncover the underlying structural origins and carrier scattering mechanisms. The exciting electronic structures observed in these quasi-1D networks in both halide perovskites and perovskite chalcogenides at high pressure provide insight in achieving diverse electronic platforms in the board family of low-dimensional perovskite systems. The unusual electron-electron interaction and abnormal electronic transport behavior found in compressed CsPbI₃ motivate the continued search for novel phases and states in halide perovskites and related lattice architectures. We plan to conduct ultralow-temperature (down to 50 mK) electrical transport measurements on CsPbI₃ at high pressure.
- *Probing local disorder in single and double perovskites:* Static and dynamic (local) structural disorder have significant influence on the optoelectronic properties of halide perovskites. We will continue to utilize X-ray total scattering measurements for understanding the local structural deviations that could be ubiquitous in halide perovskites, particularly at high pressure. We will use advanced atom-based modeling, e.g., reverse Monte-Carlo simulations, to understand pressure-induced, partially amorphous phases of (FA)PbI₃, (MA)PbBr₃, and CsPbBr₃. The nature of the partial amorphization in these 3D halide perovskites will shed light on their structural and electronic origins at high pressure.
- *The high-pressure properties of perovskites containing three or more octahedral metals:* We have recently devised synthetic methods to access complex metal compositions in halide perovskites, including mixed-valence compositions with low-energy intervalence charge

transfer transitions. The effects of compression on these materials are expected to yield rich electronic and magnetic properties that will be studied in detail.

- *The high-pressure properties of gold perovskites:* We have recently synthesized gold-halide perovskites featuring unusual architectures and we also expanded the number of “gold cage” perovskite compositions that we reported in 2021. We plan on tracking their structural, optical, and transport properties at high pressures to study the effects of compressing two inorganic sublattices of different dimensionality.
- *The high-pressure properties of perovskites with vacancies:* We are continuing to study the effect of compressing vacancies in halide double perovskites to understand the extent of electronic communication in these 0D materials with band structures that are reminiscent of 3D materials.
- *LCLS-II and XFEL developments:* LCLS-II HE is planned for 2027-2028, but with an initial high energy upgrade to >20 keV using the Cu-Linac (120 Hz) and the new LCLS-II undulators available, and we are in discussion with beamline scientists at LCLS to propose experiments at the XPP and XCS instruments. The process of enabling DAC measurements at LCLS-II will likely require a number of steps that can include modification of DAC designs, feasibility tests with model materials at lower pressures, additional experiments with more complex materials, pushing to higher pressures, etc. Our X-ray pump, X-ray probe XFEL-DAC experiments in EuXFEL in June 2023 will provide significant guidance for implementing and extending the capability at LCLS.

Publications 2021-2022

Type 1:

1. F. Ke, J. J. Yan, R. Matheu, S. Y. Niu, N. R. Wolf, H. Yang, K. Yin, J. Wen, Y. S. Lee, H. I. Karunadasa, W. L. Mao, Y. Lin, *Quasi-one-dimensional metallicity in compressed CsSnI₃*, J. Am. Chem. Soc., DOI:10.1021/jacs.2c10884 (2022).
2. K. P. Lindquist, J. A. Vigil, A. Su, H. I. Karunadasa, *A practical guide to 3D halide perovskites: Structure, synthesis, and measurement*, Comprehensive Inorganic Chemistry III, DOI: 10.1016/B978-0-12-823144-9.00137-0 (2022).
3. F. Ke, J. J. Yan, S. Y. Niu, J. J. Wen, K. T. Yin, H. Yang, N. R. Wolf, H. I. Karunadasa, Y. S. Lee, W. L. Mao, and Y. Lin, *Cesium-mediated electron redistribution and electron-electron interaction in high-pressure metallic CsPbI₃*, Nat. Commun. **13**, 7067 (2022).
4. N. Wolf, A. Jaffe, A. Slavney, W. L. Mao, L. Leppert, and H. I. Karunadasa, *Tuning Defects in a Halide Double Perovskite with Pressure*, J. Am. Chem. Soc. **144**, 20763 (2022).
5. W. L. Mao and Y. Lin, *Making the most of metastability*, Science **377**, 814 (2022).
6. R. Matheu, F. Ke, A. Breidenbach, N. Wolf, Y. Lee, Z. Liu, L. Leppert, Y. Lin, H. I. Karunadasa, *Charge Reservoirs in an Expanded Halide Perovskite Analog: Enhancing High-Pressure Conductivity through Redox-Active Molecules*, Angew. Chem. Int. Ed. e202202911 (2022).
7. R. Matheu, J. A. Vigil, E. J. Crace, H. I. Karunadasa, *The halogen chemistry of halide perovskites*, Trends Chem. **4**, 206 (2022).

8. M. L. Aubrey, A. Saldivar Valdes, M. R. Filip, B. A. Connor, K. P. Lindquist, J. B. Neaton, H. I. Karunadasa, *Directed assembly of layered perovskite heterostructures as single crystals*, Nature **597**, 355 (2021).
9. C. Chen, Y. Lin, W. Zhou, M. Gong, J. Z. Wu, J. N. Wang, F. Yang, K. T. Lam, Q. S. Zeng, W. Gao, J-m. Zuo, J. Liu, G. Hong, A. L. Antaris, M-C. Lin, J. Guo, W. L. Mao, H. Dai, *Sub-10-nm graphene nanoribbons with atomically smooth edges and high mobility from squashed carbon nanotubes*, Nat. Electron. **4**, 653 (2021).
10. F. Ke, C. Wang, C. Jia, N. R. Wolf, J. Yan, S. Niu, T. P. Devereaux, H. I. Karunadasa, W. L. Mao, Y. Lin, *Preserving a robust CsPbI₃ perovskite phase via pressure-directed octahedral tilt*, Nat. Commun. **12**, 461 (2021).
11. Y. Dai, H. Liu, T. Geng, F. Ke, S. Niu, K. Wang, Y. Qi, B. Zou, B. Yang, W. L. Mao and Y. Lin, *Pressure-Induced Excimer Formation and Fluorescence Enhancement of an Anthracene Derivative*, J. Mater. Chem. C **9**, 934 (2021).
12. N. R. Wolf, B. A. Connor, A. H. Slavney, H. I. Karunadasa, *Doubling the stakes: The promise of halide double perovskites*, Angew. Chem. Int. Ed. **60**, 2 (2021).
13. K. Lindquist, M. Boles, S. Mack, J. B. Neaton, H. I. Karunadasa, *Gold-cage perovskites: A three-dimensional Au^{III}-X framework encasing isolated MX₆³⁻ octahedra (M^{III} = In, Sb, Bi; X = Cl⁻, Br⁻, I⁻)*, J. Am. Chem. Soc. **143**, 7440 (2021).
14. B. A. Connor, R. Smaha, J. Li, A. Gold-Parker, A. J. Heyer, M. F. Toney, Y. Lee, H. I. Karunadasa, *Alloying a single and a double perovskite: A Cu⁺²⁺ mixed-valence layered halide perovskite with strong optical absorption*, Chem. Sci. **12**, 8689 (2021).

Type 2: (collaborative publications)

15. J. Yan, L. Zhang, J. Liu, N. Li, N. Tamura, B. Chen, Y. Lin, W. L. Mao, H. Zhang, *Pressure induced suppression of Jahn-Teller distortions and enhanced electronic properties in high-entropy oxide (Mg_{0.2}Ni_{0.2}Co_{0.2}Zn_{0.2}Cu_{0.2})O*, Appl. Phys. Lett. **119**, 151901 (2021).
16. B. Guzelturk, T. Winkler, T. Van de Goor, M. D. Smith, S. A. Bourelle, S. Feldmann, M. Trigo, S. Teitelbaum, H-G. Steinrück, G. A. de la Pena, R. Alonso-Mori, D. Zhu, T. Sato, H. I. Karunadasa, M. F. Toney, F. Deschler, A. M. Lindenberg, *Visualization of dynamic polaronic strain field in hybrid lead halide perovskites*, Nat. Mater. **20**, 618 (2021).

Structural Signatures of Hidden Order in Spin-Orbit Coupled Systems

Raymond Osborn, Stephan Rosenkranz, Charlotte Haley, Mihai Anitescu

Argonne National Laboratory

Eun-Ah Kim, Kilian Weinberger

Cornell University

Keywords: Diffuse X-ray Scattering, Hidden Order, 3D- Δ PDF, Machine Learning

Research Scope

This project investigates structural correlations in a number of materials that have strong spin-orbit coupling, which undergo anomalous phase transitions. The goal is to determine the origin of those transitions and to resolve controversies in the existing literature about the underlying physics. The focus on systems with spin-orbit coupling is motivated by the theoretical work by Liang Fu and others [1,2], who predict the existence of novel electronic phases due to multipolar nematicity or metallic ferroelectricity, and the lack of experimental verification of those theories in structural studies [3], with different experimental techniques coming to contradictory conclusions regarding the nature of the primary order parameter [4, 5].

Our group has been developing methods of measuring both long and short-range structural correlations by collecting large reciprocal space volumes of data, comprising several terabytes per day, using high-energy x-rays at the Advanced Photon Source (APS) [6] (Fig. 1), which allow the detailed temperature dependence of structural correlations to be determined in a few hours. This has required the development of automated workflows, which reduce 100GB data sets into reciprocal space coordinates as fast as it is collected. We have formed a team that combines materials science and x-ray scattering expertise within Materials Science Division with expertise in two computational domains, machine learning and spectral analysis, in order both to accelerate the identification of different contributions to $S(\mathbf{Q})$ as a function of temperature and to provide robust and easily interpretable maps of structural distortions using 3D- Δ PDF methods.

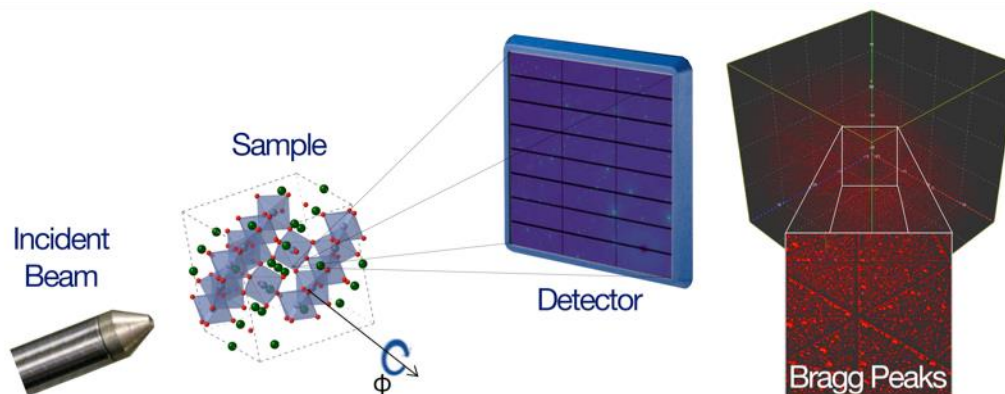


Fig. 1: Schematic diagram of the experimental setup. The sample is rotated around the ϕ -axis continuously through 360° in a monochromatic x-ray beam while frames are collected in the fast area detector every 0.1° . This sweeps a section of the Ewald sphere through a reciprocal space volume that can contain hundreds, thousands, or even tens of thousands of Brillouin Zones. In the right-hand figure, every dot represents a measured Bragg peak.

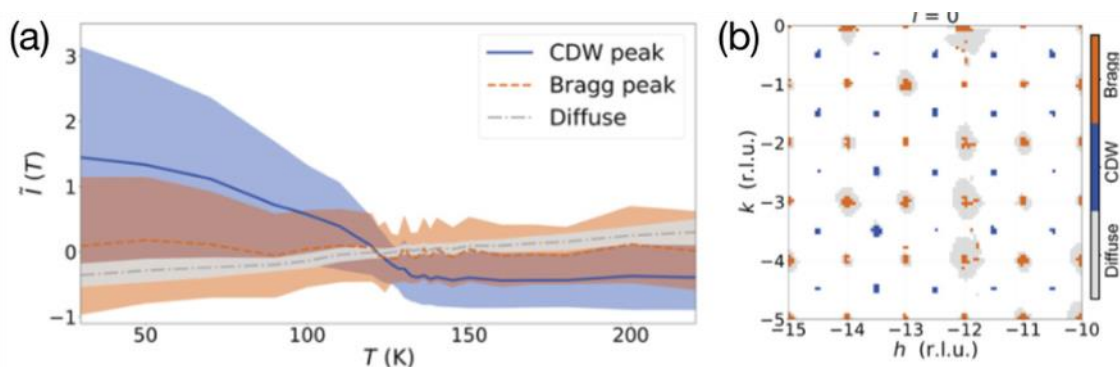


Fig. 2: (a) Temperature trajectories of three clusters with intensities above the threshold produced by *X-TEC*. (b) \mathbf{Q} -dependence of the three clusters showing the locations of the superlattice peaks (blue).

Recent Progress

Unsupervised Machine Learning

In order to analyze large volumes of $S(\mathbf{Q})$ without significant selection bias, we have developed algorithms based on unsupervised machine learning [7]. The raw data from a single sample at each temperature setting is over 100GB in size, collected in ~ 20 minutes, generating a fine reciprocal space mesh of $\sim 5 \times 10^8$ \mathbf{Q} bins from several thousand Brillouin zones (BZ) (Fig. 1). Our approach is to exploit the fact that our measurements are typically made at a large number of temperatures (20 to 30 or more). Contributions to the scattering in each \mathbf{Q} bin will have a different temperature dependence depending on its physical origin. If there is a phase transition, for example, superlattice peaks will appear at the same relative \mathbf{Q} in many BZs at the critical temperature and will increase in intensity with common critical exponents as the temperature is lowered, whereas thermal diffuse scattering will monotonically decrease in intensity (Fig. 2). Unsupervised machine learning can be used to group all the bins into a few clusters that represent these different contributions to the scattering, providing a reciprocal space map of the \mathbf{Q} -dependence of each one.

The algorithms have been implemented in a Python package, known as *X-Ray-Diffraction Temperature Clustering (X-TEC)* (<https://github.com/KimGroup/XTEC>). *X-TEC* handles the wide dynamic range in $S(\mathbf{Q})$ by normalizing to either the mean or the variance of each bin as a function of temperature. It also accounts for correlations between neighboring bins to reduce random cluster assignments using a method called label-smoothing. With these enhancements, we are able to identify both superlattice peaks and the surrounding diffuse scattering even though they differ in intensity by factors of 10^3 or more. This is accomplished using two modes of operation. *X-TEC smoothed* mode (*X-TEC-s*) is best suited for detecting order parameters reflected in the peak centers, while *X-TEC detailed* mode (*X-TEC-d*) can probe finer details in the diffuse scattering and reveal the nature of fluctuations in high-resolution data (See Ref. 7).

Multidimensional Spectral Analysis

Until recently, diffuse scattering was usually simulated by atomistic models, which take a long time to develop and refine with large 3D volumes of data. However, the recent development of the 3D- Δ PDF method, a three-dimensional version of pair-distribution-function (PDF) analysis, provides an alternative approach that requires no prior modeling [8]. In 3D, it is possible to remove the Bragg peaks before performing the real-space transform, a technique known as “punch-and-fill,” thereby generating maps of interatomic vector probabilities that only include

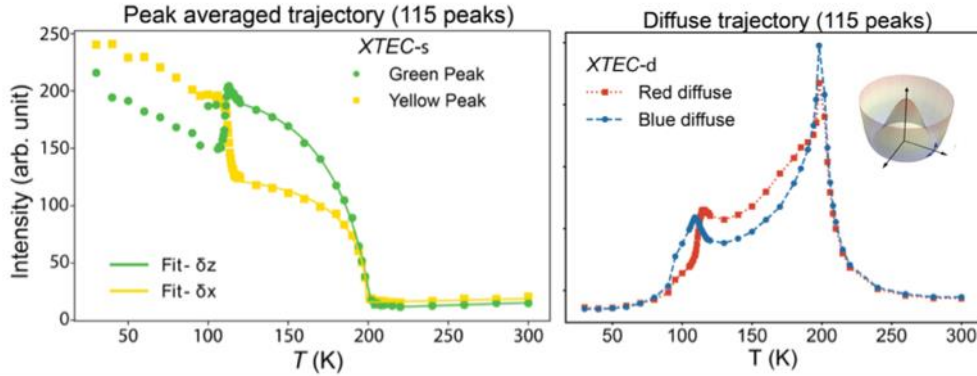


Fig. 3: (left) *X-TEC* Clusters identifying two sets of superlattice peaks that are forbidden in the cubic pyrochlore structure of $\text{Cd}_2\text{Re}_2\text{O}_7$, but emerge below the structural phase transition at 200K. The peak intensities grow with a 2D-XY critical exponent, consistent with a two-component E_u order parameter. (Right) *X-TEC* clusters of diffuse scattering clusters around the two sets of superlattice peaks reveal Goldstone mode fluctuations that are consistent with a Mexican hat potential connecting the two nearly-degenerate E_u modes [7].

those whose probabilities differ from the average structure. This allows the disorder to be directly visualized and vastly simplifies interpretation.

Our project contains expertise in 3D spectral analysis, which is not as well developed as in 1D and 2D because of a relative lack of applications in other fields. As examples, we have developed new methods of optimizing Fourier transform taper functions using the Nyström method and Gauss Legendre integration [9], in order to remove an important source of leakage artifacts caused by the asymmetry in measured data volumes, and ways of concentrating spectral information on specific scattering features, using tiled Gaussian filters [10]. We have implemented many of these spectral analysis methods in our data reduction software, *NXRefine* (<https://github.com/axmas-anl/nxrefine>), now used regularly on Sector 6-ID-D at the APS and available on QM2 at CHESS.

Machine Learning Analysis of Structural Order and Goldstone Modes in $\text{Cd}_2\text{Re}_2\text{O}_7$

$\text{Cd}_2\text{Re}_2\text{O}_7$, which is a compound that undergoes two structural phase transitions at 112K and 200K, was one of the materials identified by Liang Fu as possibly displaying multipolar nematic order because the distortions were too small for the transitions to be structurally driven [1,4]. We have performed measurements as a function of temperature and used *X-TEC* to reveal both the critical behavior of the primary order parameter and the Goldstone mode fluctuations that drive symmetry breaking at a lower temperature (Fig. 3) [7]. Both the critical exponents of the Bragg peaks and the temperature dependence of diffuse scattering around them are consistent with the condensation of a two-component E_u order parameter at 200K and Goldstone mode fluctuations between the two nearly degenerate E_u modes below the transition. Furthermore, an analysis of the order parameter behavior using the *X-TEC*-derived selection rules revealed an anti-phase distortion of the Cd and Re sublattices, not seen before, and suggests that an additional first-order phase transition at 112K is due to the competition between these two distortions.

Order-disorder transitions in $(\text{Ca},\text{Sr})_3\text{Rh}_4\text{Sn}_{13}$

For over 60 years, structural phase transitions have usually been discussed in terms of two limiting categories [11], depending on the nature of the anharmonic potential driving the transition. In the first category, “displacive” transitions result from the condensation of soft

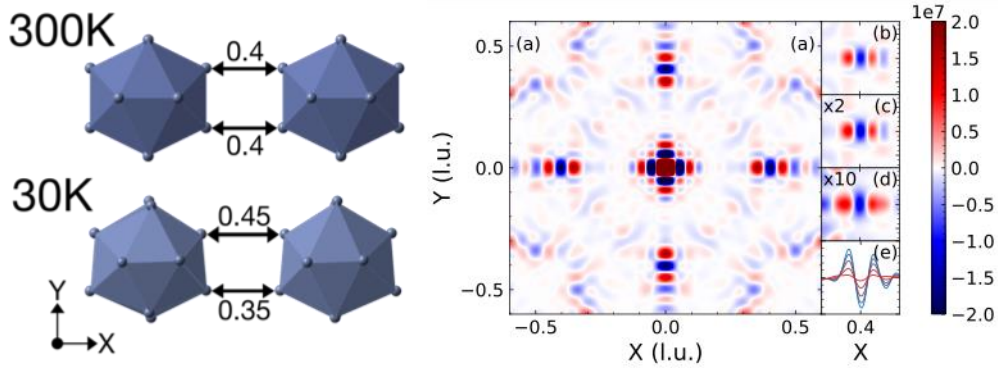


Fig. 4: (left) Neighboring tin icosahedra in $\text{Sr}_3\text{Rh}_4\text{Sn}_{13}$, showing the local distortions below T_c . These distortions are evident in the 3D- Δ PDF maps (right) in the peak splitting at $X=0.4$. The amplitude of the splitting is temperature independent both below *and* above $T_c = 130\text{K}$ at (b) 30K (c) 100K, (d) 150K (e) 30-150K [10].

phonon modes, whereas the distorted ions in “order-disorder” transitions occupy sites located at the minima of deep multi-well potentials. In the past, classifications into these two categories have proved ambiguous because they were based on properties *above* the structural phase transition where the distinction becomes blurred. Our improvements to the 3D- Δ PDF method have allowed a determination of the local distortions both above *and* below the transitions, because it incorporates both the superlattice peak and diffuse scattering intensities [10]. We demonstrated this new capability in the quasi-skutterudite compound, $(\text{Ca}_x\text{Sr}_{1-x})_3\text{Rh}_4\text{Sn}_{13}$, in which structural phase transitions are suppressed to a quantum critical point with either pressure or chemical substitution, *e.g.*, by calcium [12]. It has been suggested that these are charge-density-wave (CDW) transitions, which are rare in 3D materials, but the nature of the charge disproportionation has never been established. Our results conclusively show that the transitions in these quasi-skutterudites are order-disorder in character, because the distortion amplitude is independent of temperature (Fig. 4). This calls into question whether these compounds are really CDWs driven by an electronic instability. We suggest that the loss of structural coherence at T_c makes the electronic excitations incoherent, producing pseudogap fluctuations above T_c , similar to those seen in “bad” metals such as the cuprates.

Future Plans

The project depends on the close interaction of materials scientists at Argonne with experts in machine learning and spectral analysis, three fields that are usually only weakly connected. The next step is to fully integrate all three. For example, the Gaussian tiling method described above is a form of spectral concentration, *i.e.*, focusing on specific features of interest in \mathbf{Q} -space before applying the transform to real space. The results of X -TEC can be used to generalize this approach, by selectively transforming specific clusters that represent different contributions to the disorder. We also plan to explore the use of advanced statistical techniques, such as compressed sensing, to improve the quality of 3D- Δ PDF maps, and machine learning to identify disorder models that are consistent with the constraints of the space groups of the undistorted structures. We are now in the process of shifting our data reduction/analysis platform to the Argonne Leadership Computing Facility, where performance would be sufficient for more computationally intensive approaches. We believe that in the future, such comprehensive methods for studying structural disorder will become an increasingly vital tool for the materials science community.

Publications

1. J. Venderley, M. Matty, M. Krogstad, J. Ruff, G. Pleiss, V. Kishore, D. Mandrus, D. Phelan, L. Poudel, A. G. Wilson, K. Weinberger, P. Upreti, S. Rosenkranz, R. Osborn, E.-A. Kim, *Harnessing Interpretable and Unsupervised Machine Learning to Address Big Data from Modern X-Ray Diffraction*, Proceedings of the National Academy of Sciences **119**, e2109665119 (2022).
2. P. Upreti, M. Krogstad, C. Haley, M. Anitescu, V. Rao, L. Poudel, O. Chmaissem, S. Rosenkranz, and R. Osborn, *Order-Disorder Transitions in $(Ca_xSr_{1-x})_3Rh_4Sn_{13}$* , Physical Review Letters **128**, 095701 (2022).
3. K. Mallayya, J. Straquadine, M. Krogstad, M. Bachmann, A. Singh, R. Osborn, S. Rosenkranz, I. R. Fisher, E.-A. Kim, *Bragg glass signatures in Pd_xErTe_3 with X-ray diffraction Temperature Clustering (X-TEC)*, arXiv 2207.14795 (submitted to Nature Physics).
4. C. Haley, M. Anitescu, V. Rao, M. Krogstad, R. Osborn, and S. Rosenkranz, *Estimation of 3D Pair Distribution Function from censored observations of x-ray scattering intensity*, Computer Physics Communications (in preparation).

References

1. L. Fu, *Parity-Breaking Phases of Spin-Orbit-Coupled Metals with Gyrotropic, Ferroelectric, and Multipolar Orders*, Physical Review Letters **115**, 026401 (2015).
2. W. Witczak-Krempa, G. Chen, Y. B. Kim, and L. Balents, *Correlated Quantum Phenomena in the Strong Spin-Orbit Regime*, Annual Review of Condensed Matter Physics **5**, 57 (2014).
3. G. Cao and P. Schlottmann, *The Challenge of Spin-Orbit-Tuned Ground States in Iridates: A Key Issues Review*, Reports on Progress in Physics **81**, 042502 (2018).
4. J. W. Harter, Z. Y. Zhao, J.-Q. Yan, D. G. Mandrus, and D. Hsieh, *A Parity-Breaking Electronic Nematic Phase Transition in the Spin-Orbit Coupled Metal $Cd_2Re_2O_7$* , Science **356**, 295 (2017).
5. L. Zhao, D. H. Torchinsky, H. Chu, V. Ivanov, R. Lifshitz, R. Flint, T. Qi, G. Cao, and D. Hsieh, *Evidence of an Odd-Parity Hidden Order in a Spin-Orbit Coupled Correlated Iridate*, Nature Physics **12**, 32 (2016).
6. M. J. Krogstad, S. Rosenkranz, J. M. Wozniak, G. Jennings, J. P. C. Ruff, J. T. Vaughey, and R. Osborn, *Reciprocal Space Imaging of Ionic Correlations in Intercalation Compounds*, Nature Materials **19**, 63 (2020).
7. J. Venderley, M. Matty, M. Krogstad, J. Ruff, G. Pleiss, V. Kishore, D. Mandrus, D. Phelan, L. Poudel, A. G. Wilson, K. Weinberger, P. Upreti, S. Rosenkranz, R. Osborn, E.-A. Kim, *Harnessing Interpretable and Unsupervised Machine Learning to Address Big Data from Modern X-Ray Diffraction*, Proceedings of the National Academy of Sciences **119**, e2109665119 (2022).
8. T. Weber and A. Simonov, *The Three-Dimensional Pair Distribution Function Analysis of Disordered Single Crystals: Basic Concepts*, Zeitschrift für Kristallographie **227**, 238 (2012).

9. C. Haley, M. Anitescu, V. Rao, M. Krogstad, R. Osborn, and S. Rosenkranz, *Estimation of 3D Pair Distribution Function from censored observations of x-ray scattering intensity*, Computer Physics Communications (in preparation).
10. P. Upreti, M. Krogstad, C. Haley, M. Anitescu, V. Rao, L. Poudel, O. Chmaissem, S. Rosenkranz, and R. Osborn, *Order-Disorder Transitions in $(Ca_xSr_{1-x})_3Rh_4Sn_{13}$* , Physical Review Letters **128**, 095701 (2022).
11. A. Bruce and R. A. Cowley, *Structural Phase Transitions III. Critical Dynamics and Quasi-Elastic Scattering*, Advances in Physics **29**, 219 (1980).
12. L. E. Klintberg, S. K. Goh, P. L. Alireza, P. J. Saines, D. A. Tompsett, P. W. Logg, J. Yang, B. Chen, K. Yoshimura, and F. M. Grosche, *Pressure- and Composition-Induced Structural Quantum Phase Transition in the Cubic Superconductor $Sr_3Ir_4Sn_{13}$* , Physical Review Letters **109**, 237008 (2012).

X-ray Scattering

Ian Robinson, Condensed Matter Physics and Materials Science Division, BNL

Emil Bozin, Condensed Matter Physics and Materials Science Division, BNL

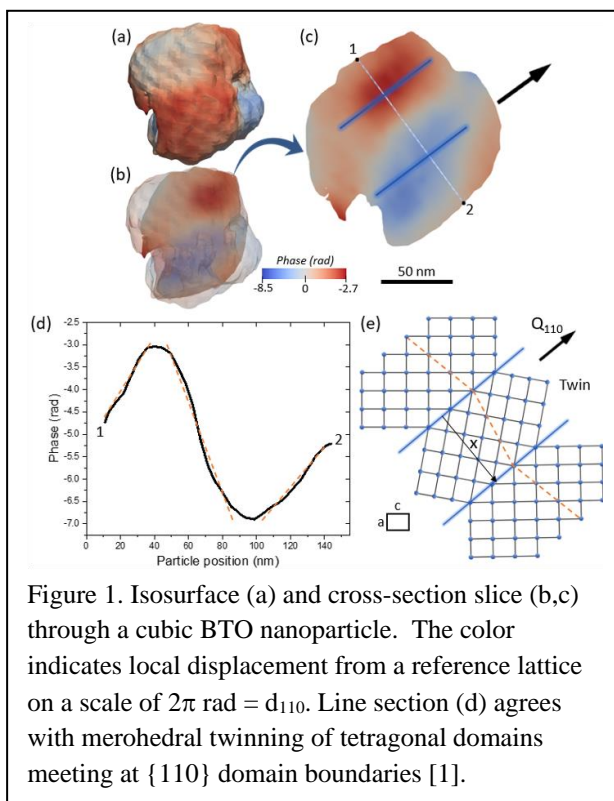
Keywords: Quantum materials, Phase transitions, Nanocrystals, Coherent Diffraction

Research Scope

This program applies state-of-the-art x-ray scattering techniques to the structure of materials, especially the strongly correlated electron materials of interest to the Condensed Matter Physics and Materials Science Division (CMPMSD) at Brookhaven National Laboratory. The long-term goal remains to seek structural explanations for the properties of correlated-electron “quantum” materials, including the roles of doping inhomogeneities, as well as magnetic and strained structural domains. Nanoscale fluctuations in strongly correlated systems are studied to understand their intrinsic properties and thermal excitation. We aim to understand phase transitions of materials through the role played by their nanoscale domains. Our experimental approach includes measuring hard and soft X-ray scattering from crystals, nanocrystals, superlattices, powders and thin films, augmented by neutron powder diffraction when scattering contrast is needed. X-ray coherence is critical to some of the methods we are developing, such as Bragg Coherent Diffraction Imaging (BCDI), X-ray ptychography and X-ray Photon Correlation Spectroscopy (XPCS). Our program contributes to the development of beamlines at the NSLS-II, especially the Coherent Soft X-ray (CSX), Coherent Hard X-ray (CHX), X-ray Powder Diffraction (XPD), Pair Distribution Function (PDF), Hard X-ray Nanoprobe (HXN) and Coherent Diffraction Imaging (CDI) beamlines.

Recent Progress

We have completed a combined PDF and BCDI study of nanocrystalline BaTiO₃ (BTO) using hydrothermally synthesized samples, similar to those used in multilayer capacitor technology. These materials are commonly considered to consist of either a single cubic average structural phase or a mixture of cubic and tetragonal phases. By combining PDF and BCDI, we could demonstrate that the material has local structural symmetry breaking throughout its structure and that its apparent cubic long-range symmetry arises from ~50 nm sized twin domains of tetragonal symmetry with 90° domain walls, shown in Fig 1, which interact to give the net cubic structure and residual strain. The BCDI images strongly support a model of domain wall migration in response to an electric field. This resolves a longstanding question of why nano-



BaTiO₃ has a strongly enhanced dielectric constant, which has important device applications [0].

By using combined powder 1D Pair Distribution Function (PDF) and single crystal 3D-PDF, we examined the evolution of local structure of RuP across its two-step electronic transition from high temperature metallic to a low temperature nonmagnetic insulating state via an intermediate pseudo-gap phase. In both experiments, we consistently found symmetry-breaking distortions, shown for 3D-PDF in Fig 2, in the metallic regime revealing electronic precursor states associated with orbital-charge trimerization, a fluctuation of pseudo-gap, representing the local response to the Fermi surface instability (narrow flat degenerate t_{2g} -bands). Since RuP is the parent of binary ruthenium pnictide superconductors where

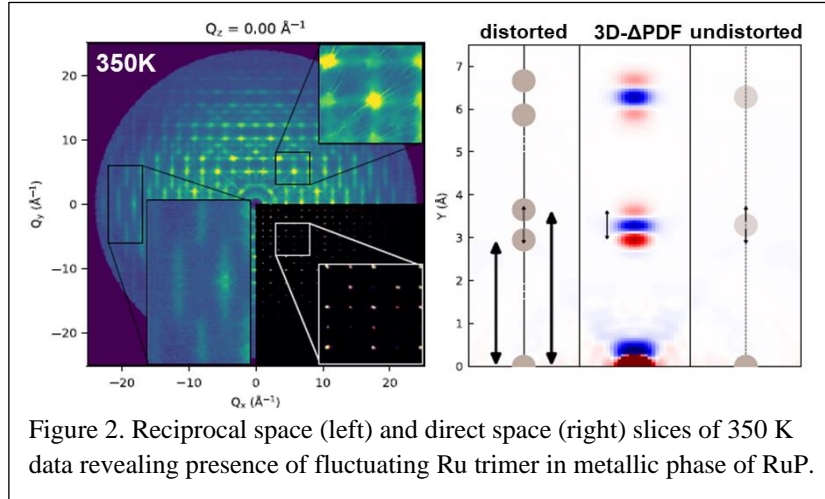


Figure 2. Reciprocal space (left) and direct space (right) slices of 350 K data revealing presence of fluctuating Ru trimer in metallic phase of RuP.

superconductivity emerges upon Ru/Rh substitution, with superconducting T_c maximized around the pseudo-gap quantum critical point, this discovery may be relevant to superconductivity.

We utilized temperature dependent X-ray PDF measurements to study local structure of AgGaTe₂, material exhibiting ultralow lattice thermal conductivity at elevated temperature. This tetragonal system shows negative thermal expansion (NTE) of the tetragonal axis in diffraction. The PDF analysis revealed a nanoscale symmetry broken state emerging from undistorted ground state on warming. Local distortions, which grow continuously with temperature are found to be correlated on sub-nanometer length scale, an effect leading to NTE behavior. Associated DFT calculations suggests that a large difference in energy between the s and d electron orbitals of the Ag leads to weak sd^3 orbital hybridization, which is the driving force of the local distortion of Ag. This causes strong acoustic–optical phonon coupling and ultralow lattice thermal conductivity. Observations provide a guideline to suppressing heat transport in diamondoid and other electronic materials.

In the layered 1T-TaS₂ charge density wave (CDW) system, we mapped out the detailed temperature evolution of the “star of David” (SoD) local distortion through its metallic, incommensurate, nearly commensurate and commensurate CDW phases. At 50 K we observe a novel response consistent with spin-singlet formation involving SoD orphan spins. At high temperature (metallic phase) we found signatures of polaron-like precursor. Upon heating above 630 K, seen in Fig 3, the signature signal drops to ~50% as TaS₂ passes through a polymorphic transformation involving a 50:50 mixture of 1T and 1H layers with octahedral and prismatic Ta coordination, respectively. The persistence of precursors in the 1T layers sandwiched between undistorted 1H layers unveil a 2D character of the underlying electronic instability. The findings are relevant for the recently observed coexistence of superconductivity and CDW in the 6R-TaS₂ polymorph.

In order to explore the time scales associated with phase transitions and to rationalize the complicated sequence of events taking place, we performed XFEL ultrafast X-ray Diffraction

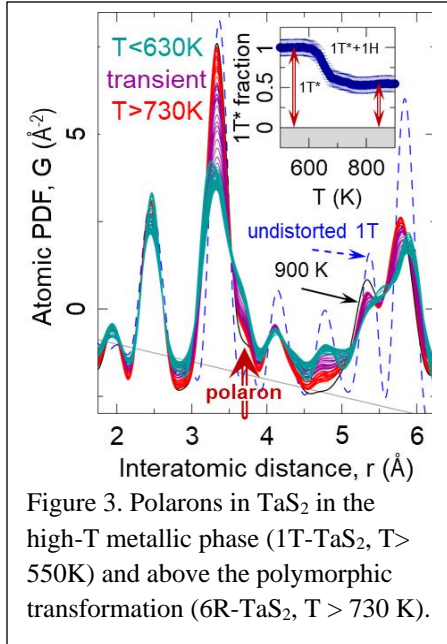


Figure 3. Polarons in TaS₂ in the high-T metallic phase (1T-TaS₂, T > 550K) and above the polymorphic transformation (6R-TaS₂, T > 730 K).

(XRD) experiments on Pd melting, both of which are explained by inhomogeneous spatial distribution of the electron-phonon coupling. Laser melting of 300nm Pd thin films was studied at the PAL-XFEL and found to show clear regimes of behavior in both time and fluence, with a film compression found at higher fluences, which was not seen in our earlier experiments on Au thin films. The inhomogeneity was unexpected because it was not seen in earlier experiments on Au melting. We found that Pd melts very differently from Au with the formation of a transient compression wave. We suspect the laser-generated electrons, responsible for carrying the heat away from the “skin depth,” cannot travel as far in Pd as in Au, which results in compression of the remainder of the material. We plan to transfer these ideas to understand the laser-driven behavior of Pd nanoparticles.

We explored whether the orbital degeneracy lifted (ODL) state is a peculiarity of weakly coupled electronic systems in

proximity to a localized-to-itinerant crossover, or if it is more common. To achieve this local structure of NaTiSi₂O₆ clinopyroxene Mott insulator is examined across its Ti-dimerization orbital-assisted Peierls transition at 210 K. Complementary X-ray and neutron PDF analyses reveal that, on warming, the dimers evolve into a short-range orbital degeneracy lifted state of dual orbital character, persisting up to the highest measured temperature. The state is correlated over the length scale spanning ~6 sites of the Ti zigzag chains. Our observations show that the ODL phenomenology does extend to strongly correlated electron systems.

We used high energy X-ray beamlines P07 and P21.1 at PETRA III at DESY to verify that the ODL precursor state, originally observed in polycrystalline CuIr₂S₄ exhibiting octamer orbital molecule singlet ground state, also occurs in a single crystal specimen. The study confirms the presence of local distortions in the crystal at room temperature and reveals three-dimensional character of the orbitally fluctuating state resembling orbital ice. The CuIr₂S₄ data were also utilized to examine diverse quite general but thus far unexplored aspects of reproducibility and relative importance of various processing protocols and parameters of the 3D-ΔPDF analysis. This was explicitly achieved by varying data-processing order and included analysis-steps. The final 3D-ΔPDF product is found to be remarkably robust, reinforcing confidence in this novel method.

Future Plans

We plan to combine PDF and BCDI to investigate domain formation (~100 nm) and the incommensurate character of the pseudo-gap phase of RuP implicated in HR-XRD. Other parents of binary ruthenium pnictides will be characterized, specifically RuSb, which exhibits a superconducting ground state in the absence of 2-step electronic transition. We will carry out local structure study of ZrTe₅ at 28-ID-1 of NSLS II in magnetic fields of up to 5 T, to explore the polaronic response, implicated by powder PDF, in relation to its reported giant magnetoresistance, manifested as a large enhancement of the resistivity anomaly peak. Single crystal X-ray diffuse scattering experiments on ZrTe₅ are also planned to corroborate the powder observations and establish the signatures of the Dirac polarons, and their response under uniaxial

strain. A detailed temperature study of 6R-TaS₂ is planned to further understand the coexistence of CDWs and superconductivity, in the context of the precursors observed in the 1T layers at high temperature. Several new candidates for emergent broken symmetry states in high performance thermoelectrics exhibiting ultralow thermal conductivity will also be screened for future detailed exploration.

Domain physics ideas will be developed using advanced sample preparation techniques, such as Focused Ion-Beam and Reactive Ion Etching, to explore domain formation in confined space and to understand pinning mechanisms using BCDI. We will develop in-situ methods to look at domain formation alongside the macroscopic electrical and magnetic responses of the materials. Domains of superstructure within the blocks will be imaged by BCDI and their temperature dependence will reveal the action of pinning forces arising at least from the cut surfaces and possibly from strain. Domains (for example, magnetic) of lower symmetry than the parent material will form twins whose spatial arrangement will inform us about strain relief mechanisms, which will be studied using the 3D-PDF method to understand how the internal strain patterns couple to the diffuse scattering. Epitaxial thin film superconductor devices, notably of La_{2-x}Sr_xCuO₄ (LSCO), show a remarkable angular variation in transverse electrical resistance, R_T, which is believed to be connected with the thin-film structure, but not yet completely understood [0]. Domains are known to form, associated with misfit dislocations in the atomic-layer epitaxial films provided by the Oxide MBE FWP in CMPMSD. We plan to start a new study of domain formation in such quantum materials, looking for a spatial pattern of structural domain walls that could play a role in explaining the variation of R_T. This will employ a 2D version of X-ray Bragg ptychography, taking advantage of the fact that thin-film diffraction is extended in the out-of-plane direction so only 2D coherent diffraction patterns are needed. This should lead to predictions of how R_T can ultimately be controlled for device applications.

References

1. A. F. Suzana, S. Liu, J. Diao, L. Wu, T. A. Assefa, M. Abeykoon, R. Harder, W. Cha, E. S. Bozin and I. K. Robinson, accepted in *Advanced Functional Materials* (2023)
2. J. Wu, A.T. Bollinger, X. He and I. Božović. *Spontaneous breaking of rotational symmetry in copper oxide superconductors*. *Nature* **547**, 432-435 (2017)

Publications

1. R. J. Koch, N. Aryal, O. Ivashko, Y. Liu, M. Abeykoon, E. D. Bauer, M. v. Zimmermann, W. Yin, C. Petrovic, E. S. Bozin. *Fluctuating Ru trimer precursor to a two-stage electronic transition in RuP*, *Phys. Rev. B* **106** 214516 (2022)
DOI: 10.1103/PhysRevB.106.214516
2. Y. Li, A. Sapkota, P. M. Lozano, Z. Du, H. Li, Z. Wu, A. K. Kundu, R. J. Koch, Lijun Wu, B. L. Winn, S. Chi, M. Matsuda, M. Frontzek, E. S. Božin, Y. Zhu, I. Božovic, A. N. Pasupathy, I. K. Drozdov, K. Fujita, G. D. Gu, I. A. Zaliznyak, Q. Li, and J. M. Tranquada, *Strongly overdoped La_{2-x}Sr_xCuO₄: Evidence for Josephson-coupled grains of strongly correlated superconductor*, *Phys. Rev. B* **106**, 224515 (2022).
DOI: 10.1103/PhysRevB.106.224515

3. G. Antonaropoulos, M. Vasilakaki, K. N. Trohidou, V. Iannotti, G. Ausanio, M. Abeykoon, E. S. Bozin, A. Lappas, Tailoring defects and nanocrystal transformation for optimal heating power in bimagnetic $\text{Co}_y\text{Fe}_{1-y}\text{O}@(\text{Co}_x\text{Fe}_{3-x})\text{O}_4$ particles, *Nanoscale* 14 382 (2022)
DOI: 10.1039/D1NR05172E
4. R.J. Koch, N. Roth, Y. Liu, O. Ivashko, A.-C. Dippel, C. Petrovic, B.B. Iversen, M. v. Zimmermann, and E. S. Bozin, On single-crystal total scattering data reduction and correction protocols for analysis in direct space, *Acta Crystallographica A* 77 611 (2021)
DOI: 10.1107/S2053273321010159
5. H. Xie, E.S. Bozin, Z. Li, M. Abeykoon, S. Banerjee, J.P. Male, G.J. Snyder, C. Wolverton, S.J.L. Billinge, M.G. Kanatzidis, Hidden Local Symmetry Breaking in Silver Diamondoid Compounds is Root Cause of Ultralow Thermal Conductivity *Advanced Materials* 34 2202255 (2022)
DOI: 10.1002/adma.202202255
6. M. W. Terban and Simon J. L. Billinge, Structural analysis of molecular materials using the pair distribution function *Chem. Rev.* 122 1208–1272 (2022)
doi: 10.1021/acs.chemrev.1c00237
7. S. Y. Harouna-Mayer, Songsheng Tao, ZiZhou Gong, Ann-Christin Dippel, Martin von Zimmermann, Dorota Koziej and Simon J. L. Billinge, Real space texture and pole figure analysis using the three-dimensional pair distribution function on a platinum thin film *IUCrJ* 9 594–603 (2022).
doi: 10.1107/S2052252522006674.
8. S. J. L. Billinge, Sandra H. Skjaervoe, Maxwell W. Terban, Songsheng Tao, Long Yang, Yevgeny Rakita, and Benjamin A. Frandsen Local structure determination using total scattering data *Comprehensive Inorganic Chemistry III*. ed. Angus Wilkinson, Paul R Raithby (2021)
doi: 10.1016/B978-0-12-823144-9.00040-6
9. A. K. C. Estandarte, Jiecheng Diao, Alice Llewellyn, Anmol Jnawali, Thomas M. M. Heenan, Sohrab R. Daemi, Joshua Bailey, Silvia Cipiccia, Darren Batey, Xiaowen Shi, Christophe Rau, Dan J. L. Brett, Rhodri Jervis, Ian K. Robinson and Paul R. Shearing, Operando Bragg Coherent Diffraction Imaging of $\text{LiNi}_{0.8}\text{Mn}_{0.1}\text{Co}_{0.1}\text{O}_2$ Primary Particles within Commercially Printed NMC811 Electrode Sheets *ACS Nano* 15 1321–1330 (2020).
DOI: 10.1021/acsnano.0c08575
10. J. Diao, Xiaowen Shi, Tadesse A. Assefa, Daniel S. Nunes, Darren Batey, Silvia Cipiccia, Christoph Rau, Ross Harder, Wonsuk Cha and Ian K. Robinson, Evolution of Ferroelastic Domain Walls during Phase Transitions in Barium Titanate Nanoparticles, *Physical Review Materials* 4 106001 (2020).
DOI: 10.1103/PhysRevMaterials.4.106001
11. A. F. Suzana, Longlong Wu, Tadesse A. Assefa, Benjamin P. Williams, Ross Harder, Wonsuk Cha, Chia-Kuang Tsung and Ian K. Robinson, Structure of a single palladium

nanoparticle and its dynamics during the hydride phase transformation *Nature Communications Chemistry* 4 64 (2020).

DOI: 10.1038/s42004-021-00500-7

12. T. A. Assefa, Ana Suzana, Longlong Wu, Rob Koch, LuXi Li, Wonsuk Cha, Ross Harder, Emil Bozin, Feng Wang, and Ian Robinson, Imaging the Phase Transformation of Single Particles of Lithium Titanate Anode Battery Material, *ACS Applied Energy Materials* 4 111-118 (2021).

DOI: 10.1021/acsaem.0c02010

13. R.J. Koch, R. Sinclair, M.T. McDonnell, R. Yu, M. Abeykoon, M.G. Tucker, A.M. Tsvetik, S.J.L. Billinge, H.D. Zhou, W.G. Yin, E.S. Bozin, Dual Orbital Degeneracy Lifting in a Strongly Correlated Electron System *Physical Review Letters* 126 186402 (2021).

DOI: 10.1103/PhysRevLett.126.186402

14. L. Yang, R.J. Koch, H. Zheng, J.F. Mitchell, W.G. Yin, M.G. Tucker, S.J.L. Billinge, E.S. Bozin, Two-orbital degeneracy lifted local precursor to a metal-insulator transition in *MgTi₂O₄* *Physical Review B* 102 235128 (2020).

DOI: 10.1103/PhysRevB.102.235128

15. Y. Hao, Zunpeng Feng, Soham Banerjee, Xiaohui Wang, Simon J. L. Billinge, Jiesu Wang, Kuijuan Jin, Ke Bi, and Longtu Li, Ferroelectric State and Polarization Switching Behaviour of Ultrafine BaTiO₃ Nanoparticles with Large-Scale Size Uniformity *Journal of Materials Chemistry C* 9 5267-5276 (2021).

DOI: 10.1039/D0TC05975G

16. J. L. Hitt, Yuguang C. Li, Songsheng Tao, Zhifei Yan, Yue Gao, Simon J. L. Billinge, and Thomas E. Mallouk, A High Throughput Optical Method for Studying Composition Effects in Electrochemical CO₂ Reduction Catalysts *Nature Communications* 12 1114 (2021).

DOI: 10.1038/s41467-021-21342-w

17. L. Wu, Shinjae Yoo, Ana F. Suzana, Tadesse A. Assefa, Jiecheng Diao, Ross J. Harder, Wonsuk Cha and Ian K. Robinson, 3D Coherent X-ray Imaging via Deep Convolutional Neural Networks *npj Computational Materials* 7 175 (2021)

DOI: 10.1038/s41524-021-00644-z

18. W. Wang, Lijun Wu, Junjie Li, Niraj Aryal, Xilian Jin, Yu Liu, Mikhail Fedurin, Marcus Babzien, Rotem Kupfer, Mark Palmer, Cedimir Petrovic, Weiguo Yin, Mark P. M. Dean, Ian Robinson, Jing Tao, Yimei Zhu, Photoinduced anisotropic lattice dynamic response and domain formation in thermoelectric SnSe *npj Quantum Materials* 6 97 (2021)

Doi: 10.1038/s41535-021-00400-y

19. M. G. Kim, A. Barbour, Wen Hu, S. B. Wilkins, Jiaqi Lin, I. K. Robinson, M. P. M. Dean, Choongjae Won, Junjie Yang, S.-W. Cheong, C. Mazzoli and V. Kiryukhin, Real-Space Observation of Fluctuating Antiferromagnetic Domain Walls *Science Advances* 8 eabj9493 (2022)

DOI: 10.1126/sciadv.abj9493

20. T. Liu, Jiajie Liu, Luxi Li, Lei Yu, Jiecheng Diao, Tao Zhou, Shunning Li, Alvin Dai, Wenguang Zhao, Yang Ren, Liguang Wang, Tianpin Wu, Rui Qi, Yinguo Xiao, Jiabin Zheng, Wonsuk Cha, Ross Harder, Ian Robinson, Jianguo Wen, Jun Lu, Feng Pan and Khalil Amine, Lattice displacement dictating the structure degradation of Li-rich layered oxide cathodes *Nature* 606 305–312 (2022)
DOI: 10.1038/s41586-022-04689-y
21. L. Wu, Yao Shen, Andi M. Barbour, Wei Wang, Dharmalingam Prabhakaran, Andrew T. Boothroyd, Claudio Mazzoli, John M. Tranquada, Mark P. M. Dean and Ian K. Robinson, Real Space imaging of Spin Stripe Domain Fluctuations in a Complex Oxide *Physical Review Letters* 127 275301 (2021)
DOI: 10.1103/PhysRevLett.127.275301
22. X. Liu, Xinwei Zhou, Qiang Liu, Jiecheng Diao, Chen Zhao, Luxi Li, Yuze Liu, Wenqian Xu, Amine Daali, Ross Harder, Ian K. Robinson, Mouad Dahbi, Jones Alami, Guohua Chen, Gui-Liang Xu and Khalil Amine, Multiscale understanding of surface structural effects on high-temperature operational resiliency of layered oxide cathodes *Advanced Materials* 34 2107326 (2021)
DOI: 10.1002/adma.202107326
23. N. Omori, Sara Mosca, Ines Lezcano-Gonzalez, Ian K. Robinson, Luxi Li, Alex G. Greenaway, Paul Collier, Andrew M. Beale, Alessia Candeo, A Multimodal Label-Free Imaging Study of Zeolite Crystals 2021 Conference on Lasers and Electro-Optics Europe and European Quantum Electronics Conference, CLEO/Europe-EQEC (2021)
https://opg.optica.org/abstract.cfm?URI=CLEO_Europe-2021-ch_9_6
24. A. Deltsidis, L. Simonelli, G. Vailakis, I. Capel Berdiell, G. Kopidakis, A. Krzton-Maziopa, E.S. Bozin, and A. Lappas, $\text{Li}_x(\text{C}_5\text{H}_5\text{N})_y\text{Fe}_2\text{-zSe}_2$: A Defect-Resilient Expanded-Lattice High-Temperature Superconductor *Inorganic Chemistry* 61 12797–12808 (2022)
DOI: 10.1021/acs.inorgchem.2c01906
25. I. Capel Berdiell, E. Pesko, E. Lator, A. Deltsidis, A. Krzton-Maziopa, A.M.M. Abeykoon, E.S. Bozin, and A. Lappas, In Situ Visualization of Local Distortions in the High-Tc Molecule Intercalated $\text{Li}_x(\text{C}_5\text{H}_5\text{N})_y\text{Fe}_2\text{-zSe}_2$ Superconductor *Inorganic Chemistry* 61 4350 (2022)
DOI: 10.1021/acs.inorgchem.1c03610
26. Q. Du, Y. Wang, Y. Wei, R. J. Koch, L. Wu, W. Zhang, T. C. Asmara, Z. Hu, E. S. Bozin, Y. Zhu, T. Schmitt, G. Kotliar, and C. Petrovic, Cascade of Spin-State Transitions in the Intermetallic Marcasite FeP_2 *Chemistry of Materials* 34 2025 (2022)
DOI: 10.1021/acs.chemmater.1c02569
27. B. A. Frandsen, Parker K. Hamilton, Jacob A. Christensen, Eric Stubbena, and Simon J. L. Billinge, DIFFPY.MPDF: Open-source software for magnetic pair distribution function analysis *J. Appl. Crystallography* 55 1377–1382 (2022)
doi: 10.1107/S1600576722007257

28. A. H. Slavney, Hong Ki Kim, Songsheng Tao, Mengtan Liu, Simon J. L. Billinge, and Jarad A. Mason, Liquid and Glass Phases of Alkylguanidinium Sulfonate Hydrogen-Bonded Organic Framework *J. American Chemical Society* 144 11064–11068 (2022)
doi: 10.1021/jacs.2c02918.
29. M. W. Terban, Leillah Madhau, Aurora J. Cruz-Cabeza, Peter O. Okeyo, Martin Etter, Armin Schulz, Jukka Rantanen, Robert E. Dinnebier, Simon J. L. Billinge, Mariarosa Moneghini, and Dritan Hasa, Controlling desolvation through polymer-assisted grinding *crystEngComm* 24 2305–2313 (2022).
url: <https://pubs.rsc.org/en/content/articlehtml/2022/ce/d2ce00162d>
30. E. Bennett, Matthew W. Greenberg, Abraham J. Jordan, Leslie S. Hamachi, Soham Banerjee, Simon J. L. Billinge, and Jonathan S. Owen, Size dependent optical properties and structure of ZnS nanocrystals prepared from a library of thioureas *Chem. Mater.* 34 706–717 (2022)
doi: 10.1021/acs.chemmater.1c03432
31. K. M. Ø. Jensen, Esther Rani Aluri, Enrique Sanchez Perez, Gavin B. M. Vaughan, Marco Di Michiel, Eleanor J. Schofield, Simon J. L. Billinge, and Serena A. Cussen, Location and characterization of heterogeneous phases within Mary Rose wood *Matter* 4 1–12 (2021).
doi: 10.1016/j.matt.2021.09.026
32. J. A. Kaduk, Simon J. L. Billinge, R. E. Dinnebier, Nathan Henderson, Ian Madsen, Radovan Cerny, Matteo Leoni, Luca Lutterotti, and Seema Thakral, Powder Diffraction *Nature Reviews Methods Primer* 1 77 (2021)
doi: 10.1038/s43586-021-00074-7
33. H. Miao, G. Fabbris, R. J. Koch, D. G. Mazzone, C. S. Nelson, R. Acevedo-Esteves, G. D. Gu, Y. Li, T. Yilimaz, K. Kaznatcheev, E. Vescovo, M. Oda, T. Kurosawa, N. Momono, T. Assefa, I. K. Robinson, E. S. Bozin, J. M. Tranquada, P. D. Johnson and M. P. M. Dean, Charge Density Waves in Cuprate Superconductors Beyond the Critical Doping, *npj Quantum Materials* 6 31 (2021).
DOI: 10.1038/s41535-021-00327-4
34. Y. Shen, G. Fabbris, H. Miao, Y. Cao, D. Meyers, D. G. Mazzone, T. A. Assefa, X. M. Chen, K. Kisslinger, D. Prabhakaran, A. T. Boothroyd, J. M. Tranquada, W. Hu, A. M. Barbour, S. B. Wilkins, C. Mazzoli, I. K. Robinson and M. P. M. Dean, Charge Condensation and Lattice Coupling Drives Stripe Formation in Nickelates, *Physical Review Letters* 126 177601 (2021).
<https://doi.org/10.1103/PhysRevLett.126.177601>
35. I. A. Zaliznyak, E. Bozin, A.V. Tkachenko, Comment on "Colossal Pressure-Induced Softening in Scandium Fluoride," *Physical Review Letters* 126, 179601 (2021).
DOI: 10.1103/PhysRevLett.126.179601
36. L. Wu, Pavol Juhas, Shinjae Yoo and Ian Robinson, Complex Imaging of Phase Domains by Deep Neural Network *IUCrJ* 8 12-21 (2021).
DOI: 10.1107/S2052252520013780

37. N. Nakamura, Laisuo Su, Han Wang, Noam Bernstein, Shikhar Krishn Jha, Elizabeth Culbertson, Haiyan Wang, Simon J. L. Billinge, C. Stephen Hellberg, and B. Reeja-Jayan, Linking Far-from-Equilibrium Defect Structures in Ceramics to Electromagnetic Driving Forces, *Journal of Materials Chemistry A* 9 8425-8434 (2021).
DOI: 10.1039/d1ta00486g
38. H. L. Andersen, Benjamin A. Frandsen, Haraldur P. Gunnlaugsson, Mads R. V. Jørgensen, Simon J. L. Billinge, Kirsten M. Ø. Jensen, and Mogens Christensen, Local and long-range atomic/magnetic structure of non-stoichiometric spinel iron oxide nanocrystallites, *IUCrJ* 8 2052–2525 (2021).
DOI: 10.1107/S2052252520013585.
39. N. Omori, Alessia Candeo, Sara Mosca, Ines Lezcano-Gonzalez, Ian K. Robinson, LuXi Li, Alex G. Greenaway, Paul Collier and Andrew M. Beale, Multimodal Imaging of Autofluorescent Sites Reveals Varied Chemical Speciation in SSZ-13 Crystals *Angewandte Chemie* 60 5125-5131 (2021).
DOI: 10.1002/anie.202015016

Nanoscale Structure and Motion of Non-collinear Spin Phases

Sujoy Roy

Lawrence Berkeley National Laboratory

*This program is part of the **Non-Equilibrium Magnetic Materials FWP** at LBNL
F. Hellman (PI), J. Bokor, P. Fischer, S. Griffin, S. Salahuddin*

Keywords

Chiral spin texture, Skyrmions, Domain fluctuation, Coherent X-ray scattering, X-ray Photon Correlation Spectroscopy

1. Research scope

This program is part of the BES funded FWP **Non-Equilibrium Magnetic Materials (NEMM)** in the Materials Sciences Division at LBNL. The overall mission of NEMM is to understand the fundamental science of magnetic materials and phenomena enabled by interfaces and spin-orbit coupling (SOC) through design, fabrication, measuring, modeling of static & dynamic properties of magnet/high SOC non-magnet heterostructures. The NEMM program addresses three interrelated Thrusts: i) understanding and controlling the free energy landscape of 2 and 3-dimensional chiral spin textures in thin films and multilayers, e.g. skyrmions, hopfions, chiral domain walls, that result from SOC plus inversion symmetry breaking; ii) designing magnet/non-magnet heterostructures with strong SOC that exhibit strong spin accumulation in response to a charge current to achieve current and voltage control of magnetization; and iii) producing highly non-equilibrium magnetic phases in these (hetero)structures by external excitation.

Within the NEMM program we lead the coherent X-ray scattering and X-ray Photon Correlation studies of magnetic thin films and heterostructures. The equilibrium or quasi-equilibrium phase of a system at non-zero temperature is determined in part by energetic considerations and in part by thermally driven fluctuations that store entropy. Magnetic skyrmions, for example, can be stabilized by either mechanism. Our goal is to understand and control the free energy landscape of chiral spin textures and address the effect of disorder and fluctuations which can lead to topological states and rich phase diagrams. Our work takes advantage of unique capabilities at the Advanced Light Source at LBNL and the LINAC Coherent Light Source at SLAC, and focuses on applying emerging soft x-ray tools to probe phases of magnetic films that exhibit non-collinear and topologically distinct spin structures, e.g., skyrmions and helical domain walls. We couple the high spin contrast of near-edge soft x-ray spectroscopies to imaging and scattering modalities to probe nanoscale spatial and temporal correlations in these spin structures.

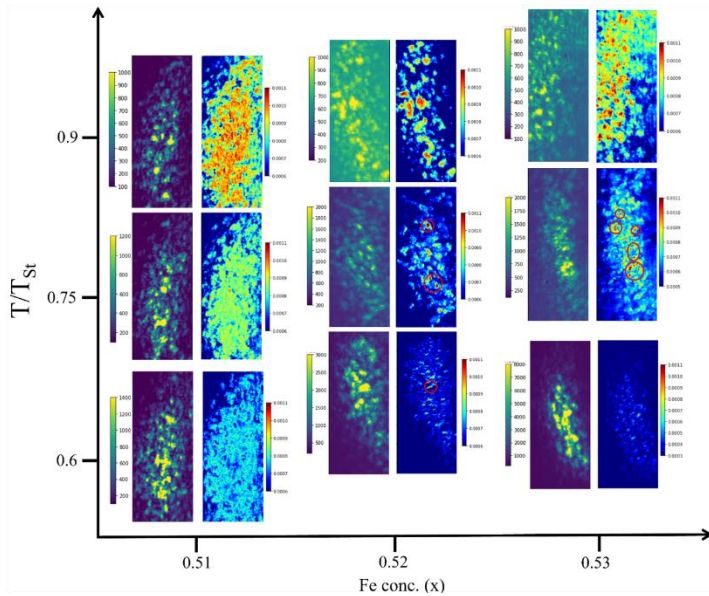
2. Recent Progress:

a. Temporal heterogeneity and power law dependence of fluctuation in amorphous Fe-Ge magnetic films

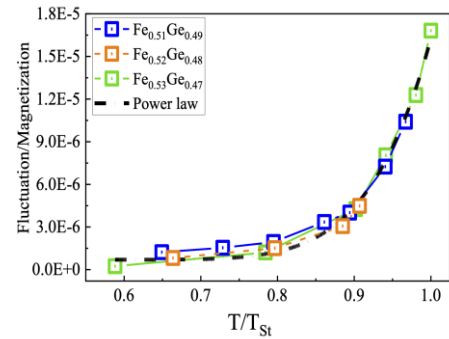
There is currently broad interest in utilizing the interesting properties of materials that exhibit topological solitary fields like skyrmions for advanced low power microelectronic applications. The NEMM group has applied a variety of tool to study *amorphous* $\text{Fe}_x\text{Ge}_{1-x}$ (*a*- $\text{Fe}_x\text{Ge}_{1-x}$) magnetic thin films. Amorphous $\text{Fe}_x\text{Ge}_{1-x}$ thin films allow us to control and tailor different spin textures and configurations by tuning its thickness, composition, applied magnetic field and temperature [1]. At low x , *a*- $\text{Fe}_x\text{Ge}_{1-x}$ is an insulator and non-magnetic; for increasing x , it first becomes metallic ($x \geq 0.2$), then magnetic ($x \geq 0.4$), then ferromagnetic for $x \geq 0.55$. We have

probed the magnetic phase behaviors of these films in the range $0.52 \leq x \leq 0.68$ with Fe L-edge resonant soft x-ray scattering, Lorentz TEM, and magnetic measurements with x-ray magnetic circular dichroism [2]. We showed that the samples have complex spin textures such as stripes, as well as isolated fluctuating skyrmions.

In a recent work we undertook coherent X-ray scattering and X-ray Photon Correlation Spectroscopy studies of a- $\text{Fe}_x\text{Ge}_{1-x}$, $x = 0.50, 0.51$ and 0.53 . In these concentrations the sample is a bad metal and magnetic interactions are weak. We obtained resonant diffraction images indicative of stripe domains. We found that there is an appreciable change in the intensity and full width half maximum (FWHM) of the peaks as a function of Fe concentration and that such disorder has a profound impact on the fluctuations.



Two-dimensional Q-space maps of the domain scattering and fluctuation heterogeneity in the stripe-phase as a function of Fe concentration (x). Red open-circles shown in two of these maps highlight the appearance of localized fluctuation “hot-spots”. (T/T_{st}) is reduced temperature where T_{st} is the stripe transition temp.



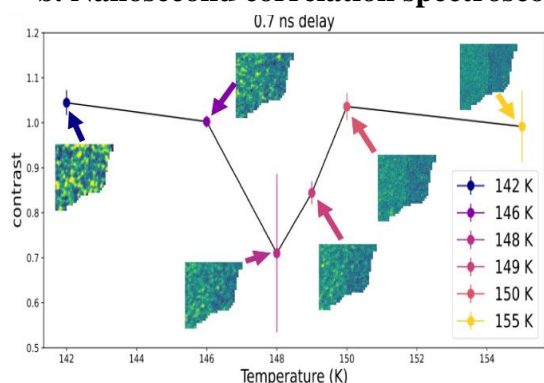
Fluctuation per unit magnetization as a function of reduced temperature. The three curves collapse together when normalized by their specific T_{st} and M_{s} .

We observe that well below the transition temperature, a small fraction of the sample fluctuates substantially (these are shown by red circles). As the temperature increases or the iron concentration decreases, the fluctuating fraction increases quickly eventually resulting in isotropic fluctuations. Interestingly, we find that the fluctuating fraction, when normalized to magnetization for different Fe concentrations, can be collapsed into a single power law behavior, suggesting that the nature of the transition can be fundamentally described in terms of the underlying spatiotemporal heterogeneity. This work has been submitted for publication.

We also showed that a one-dimensional stripe lattice in the dipolar Fe/Gd multilayer behaves like a finite-sized chiral soliton lattice, as observed in DMI based magnetic systems [4]. Discrete jumps in stripe-periodicity and intensity variation of 1st and 2nd order satellite diffraction peaks

of the stripe lattice follow a soliton sine-Gordon model even though the stripe phase in the Fe/Gd multilayer exhibits an equal population of coexisting opposite helicity spin-stripes.

b. Nanosecond correlation spectroscopy studies of *a*-Fe-Ge



Contrast as a function of temperature for a constant delay of 0.7 ns. The magnetic signal fluctuates as the sample passes through the phase transition around 148 K.

We continue to remain deeply engaged in the development of 2-pulse XPCS at LCLS2. We studied fluctuation of the domains in *a*-Fe_xGe_{1-x}, $x = 0.51$ as a function of temperature. We determined photon contrast as a function of delay for two different temperatures. At short time delays (around 350 ps), we found the contrast is higher indicating that the sample is static but as the delay between pulses is increased (~5-10 ns time scale), the sample starts to fluctuate. We also measured correlation as a function of temperature for a constant delay of 0.7 ns. An enhanced fluctuation near the transition temperature (around 148 K) was observed. This work is currently being prepared for publication.

3. Instrumentation development, collaborative and future work:

In the context of the NEMM science focus, we are actively planning for future developments in coherence resonant soft x-ray scattering techniques. We are actively collaborating with several groups (many of whom are PIs of X-ray program) and actively engaged in developing new techniques, and detectors. These efforts will be of major benefit to the task in the NEMM program and will take full advantage of the ALS upgrade to diffraction limited operation through the soft x-ray regime.

- One of the major future endeavors within the NEMM program is understanding and controlling the free energy landscape of chiral spin textures, and thus the emergence and stability of novel topological and complex spin textures and phases in amorphous materials. A particular focus is on identifying the role of disorder in amorphous material, investigate whether local symmetry breaking is impacted by topology. Various magnetic chiral systems are expected to host topological spin textures, and an underlying question will be, how chirality impacts or drives the topological properties and behavior. We will continue to use coherent X-ray scattering and XPCS to address above questions.
- In collaboration with Josh Turner at LCLS, we have been engaged in the development of the 2-pulse XPCS approach at LCLS2. Sub-Nanosecond XPCS opens up a new time regime to study fluctuations. These timescales for XPCS are not currently available at any other X-ray light source worldwide, since for current synchrotron signal levels, even with a fast CCD, the images do not contain enough photons for meaningful measurements in the short time scale regime. Along with equilibrium fluctuation studies, we would also like to pump the system to drive the magnetic state into a non-equilibrium state. We expect that a pump-XPCS probe experiment at sub-ns will shed light into the non-equilibrium relaxation behavior of the spin system.

- Complementing this 2-pulse XPCS program at LCLS, Roy is leading the commissioning of a new XPCS beamline and end station at the ALS. Multiple detectors, cryogenic temperature and applied magnetic field capabilities are available. PI within NEMM and several PIs of the X-ray Scattering program (Josh Turner (SLAC), Riccardo Comin (MIT), and Roopali Kukreja (UC Davis)) are already participating in early science commissioning experiments. The beamline is welcoming general users starting Jan 2023.
- Roy (lead PI), and others have funding from the BES Scientific User Facilities Division Detector R&D program to develop a Timepix based new class of fast soft x-ray XPCS detector that will, after ALS-U, probe the entire second-to-nanosecond XPCS time domain [4]. We are also developing new methods to calculate single-photon based correlation curves.
- In collaboration with Todd Hastings (U Kentucky), we fabricated a magnetic nanostructure with engineered defects and showed generation and control of X-ray orbital angular momentum beam using applied magnetic field and temperature [5]. Roy (lead PI) along with Hastings and Hellman (co-PI) have a LDRD from LBNL to carry out further work on interaction of X-ray OAM beam with magnetic and electronic orders in quantum materials.
- We have recently developed a probe that enables simultaneous measurement of X-ray scattering and transport data (anomalous and Topological Hall effect). This capability will allow us to correlate data from bulk with specific features on nanometer length scale. For example, our setup shows for the first time a clear topological Hall effect when a magnetic sample enters a skyrmion phase.

References

- [1]. D. S. Bouma, Z. Chen, B. Zhang, F. Bruni, M. E. Flatté, A. Ceballos, R. Streubel, **L. W. Wang**, R. Q. Wu, **F. Hellman**, Phys. Rev. B **101**, 014402 (2020).
- [2]. R. Streubel, D. S. Bouma, F. Bruni, X. Chen, P. Ercius, J. Ciston, A. T. N'Diaye, **S. Roy**, **S. D. Kevan**, **P. Fischer**, **F. Hellman**, Advanced Materials **33**, 2004830 (2021).
- [3]. A. Singh, M. K. Sanyal, J. C. T. Lee, J. J. Chess, R. Streubel, S. A. Montoya, M. K. Mukhopadhyay, B. J. McMorran, E. E. Fullerton, **P. Fischer**, **S. D. Kevan**, and **S. Roy**, Phys. Rev. B **105**, 094423 (2022).
- [4]. A. S. Tremsin, J.V. Vallergera, O.H.W. Siegmund, J. Woods, L.E. De Long, J.T. Hastings, R.J. Koch, S.A. Morley, Y.D. Chuang, **S. Roy**, J. Synchrotron Rad. **28**, 1069 (2021).
- [5]. Justin Woods, Xiaoqian Chen, Rajesh Vilas Chopdekar, Barry Farmer, Claudio Mazzoli, Roland Koch, Anton Tremsin, Wen Hu, Andreas Scholl, **Steve Kevan**, Stuart Wilkins, Wai-Kwong Kwok, Lance De Long, **Sujoy Roy**, and J. Todd Hastings, Phys. Rev. Lett., **126**, 117201 (2021).

Publications

- [1]. V. Esposito, X. Y. Zheg, M. H. Seaberg, S. A. Montoya, B. Holladay, A. H. Reid, R. Streubel, J. C. T Lee, L. Shen, J. D. Koralek, G. Coslovich, P. Walter, S. Zohar, V. Thampy, M. F. Lin, P. Hart, K. Nakahara, **P. Fischer**, W. Colocho, A. Lutman, F.-J. Decker, S. K. Sinha, E. E. Fullerton, **S. D. Kevan**, **S. Roy**, M. Dunn and J. J. Turner, Appl. Phys. Lett., **116**, 181901 (2020).

[2]. R. Streubel, D. S. Bouma, F. Bruni, X. Chen, P. Ercius, J. Ciston, A. T. N'Diaye, **S. Roy, S. D. Kevan, P. Fischer, F. Hellman**, “Chiral Spin Textures in Amorphous Iron–Germanium Thick Films” *Advanced Materials* **33**, 2004830 (2021).

[3]. A. Singh, M. K. Sanyal, J. C. T. Lee, J. J. Chess, R. Streubel, S. A. Montoya, M. K. Mukhopadhyay, B. J. McMorrان, E. E. Fullerton, **P. Fischer, S. D. Kevan**, and **S. Roy**, “Discretized evolution of solitons in the achiral stripe phase of a Fe/Gd thin film”, *Phys. Rev. B* **105**, 094423 (2022).

Note: The above publication is only the X-ray part of NEMM FWP.

Tracking intergranular strain dynamics with near-atomic scale coherent x-ray imaging at next generation light sources

PI: Richard L. Sandberg, Department of Physics and Astronomy, Brigham Young University

Collaborators: Robert M. Suter, Anthony D Rollett (Carnegie Mellon University), Anastasios Pateras (DESY), Stephan Hruszkewycz, Wonsuk Cha, Ross J. Harder (Argonne National Laboratory)

Self-identify keywords to describe your project: x-ray coherent diffraction strain imaging

Research Scope

We seek to advantage of revolutionary new coherent x-ray flux available at upgraded synchrotrons to develop inter- and intra-granular scale strain imaging of dislocation dynamics. A critical missing understanding for improvements in many technological materials, is how strain such interacts with grain boundaries in polycrystalline materials. An understanding of these strain dynamics across grain boundaries will be important for improving performance in additively manufactured structural materials and battery materials. We are working towards developing Bragg coherent diffraction imaging (BCDI) and combine it with other techniques such as high energy diffraction microscopy (HEDM through collaborator A. Rollet and B. Suter at Carnegie Mellon University) and high energy BCDI (HE-BCDI developed by collaborator S. Hruszkewycz at Argonne National Laboratory) to image dislocations as they transit or otherwise interact with grain boundaries. In order to accomplish this objective, the following key goals will need to be accomplished: (1) develop robust in situ x-ray grain orientation grain mapping (via Laue microscopy), (2) develop new BCDI algorithms for adjacent grains and atomic resolution, (3) image dislocation dynamics across grain boundaries during in situ tensile and compression, (4) perform complementary molecular dynamics studies, and (5) finally develop multi-detector/multi-peak BCDI to fully take advantage of the increasing available coherent flux.

Recent Progress

We have made major progress during our first full year in these areas: (1) making robust Laue microscopy for grain orientation mapping, (2) developing joint reconstructions of adjacent grains for BCDI and for atomic resolution, (3) and imaging strain dynamics across grain boundaries during in situ compression. However, first I will give a brief overview of the general accomplishments and progress during this year.

The major accomplishments this year included conducting 3 beamtimes at beamline 34-ID-C at the Advanced Photon Source (APS) at Argonne National Laboratory (1 was purely remote for BYU personnel, 2 with BYU personnel in person and virtually). Additionally, we developed a

process to make dewetted gold nanoparticles on electrically conductive niobium doped strontium-titanate (Nb:STO) single crystal substrates. These samples were developed by BYU undergraduate Landon Schnebly who will be working on a journal article manuscript of this result over the next few months. Development of the Au on Nb:STO samples also was critical to developing more robust Laue diffraction microscopy as it has allowed for samples that are more easily mapped with electron backscatter diffraction (EBSD) on a scanning electron microscope due to the reduced charging. Also, these samples are more robust to x-ray radiation pressure effects such as Au nanocrystal rotation and moving under the beamline pink beam illumination for Laue diffraction microscopy.

The next main progress we have made is with respect to goal (1) developing robust in situ Laue microscopy for grain orientation mapping at 34-ID-C. Recently, BYU graduate student Nick Porter has made the code more robust with the development of the LauePy [1], a rapid grain orientation mapping code that allows us to quickly find the location and orientation of grains. Our progress in developing robust Laue grain orientation mapping will be presented in the journal article currently under review [2].

The second major accomplishment this year was with respect to goal number (2) develop new BCDI algorithms for adjacent grains and atomic resolution. With Laue diffraction grain

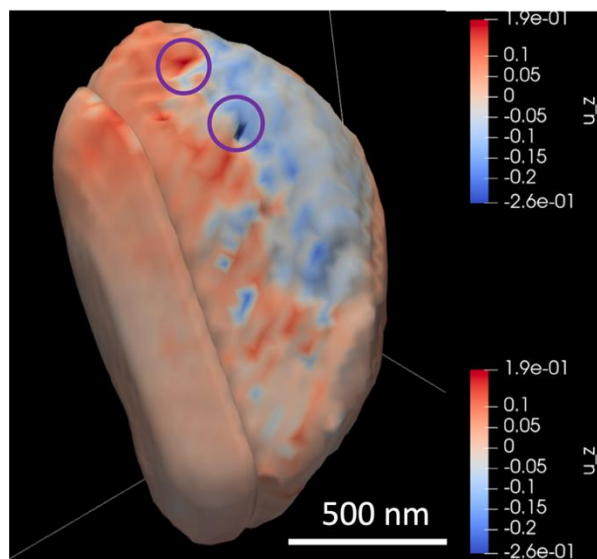


Fig. 2: Joint reconstruction of a twinned (111) oriented gold grains using recently developed joint reconstruction algorithm. The colors represent the atomic displacement field along the z or vertical direction. Four Bragg peaks were measured from each grain to image the complete strain tensor during repeated atomic force microscope (AFM) indentation. The right grain was indented with an AFM tip at two points indicated with purple circles. This data was taken in mid-December 2022 and ongoing efforts to understand the effects of the strain field across the grain boundary continue. This is the first demonstration of our multi-grain reconstruction during in situ indentation in support of object 3 in our proposal.

mapping was working more robustly, we have routinely able to find twined gold grains of dewetted gold on strontium titanate (STO) substrates. With the crystal orientations determined, we were able to easy maneuver the diffractometer to find several Bragg peaks from the parent grain and twinned grain (upwards of 6 peaks from each twin for a total of 12 peaks). In a recent beamtime we indented one of the grains with an atomic force microscope with up to 1 micro-Newton of force (see Fig. 1). This is a first demonstration for BCDI of reconstructing adjacent grains in a joint manner. This work was presented at the APS March meeting and in a paper soon to be submitted [3].

Finally, progress this year was made in phase retrieval development of atomic resolution BCDI (Goal #2) and develop complimentary molecular dynamics studies. BYU PhD student Jason Meziere has developed a phase retrieval algorithm that combines molecular dynamics in order to extract atomic positions from BCDI data (see Fig. 2). This work will be presented in papers soon to be submitted [4-5].

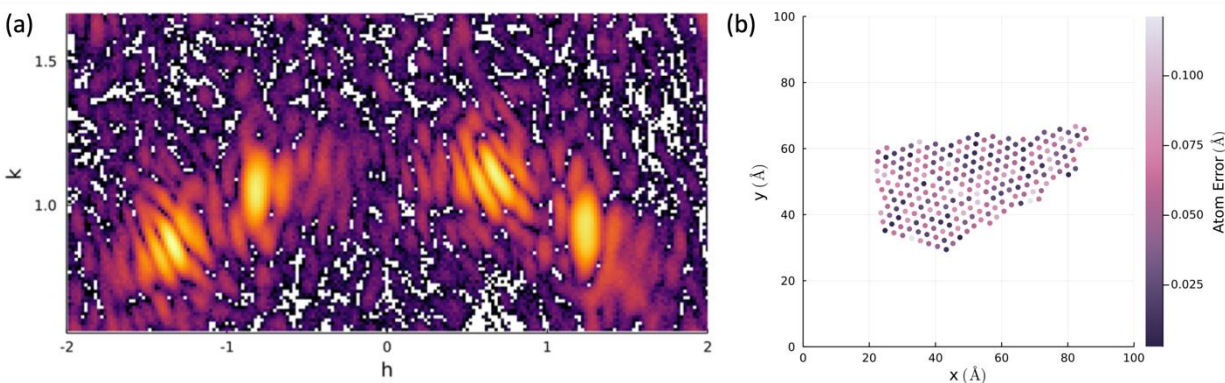


Fig. 2: Simulated 2D near atomic resolution BCDI: (a) Simulated (1, 1) and (-1, 1) Bragg peaks are used in the near atomic resolution BCDI development. Poisson noise is added to the peaks and then intensities less than a cutoff threshold are removed from the diffraction pattern. (b) The final reconstruction of the object from the Bragg peaks using the near atomic resolution BCDI algorithm. The colors show the atomic position error compared to the original object. As can be seen, the average error of about 0.05 Angstroms with the maximum error of any atom position at around 0.12 Angstroms.

Future Plans

In the second project year, we will continue to work on goals (1), (2), and (4) through our efforts in robust Laue diffraction grain mapping, joint reconstruction algorithms, and molecular dynamics simulations, but will also expand to work on the imaging of adjacent grains under strain and in multiple detector imaging. A significant, but planned, change in our project will be the one year shutdown of the Advanced Photon Source for the upcoming upgrade in 2023. We have one more beamtime in April of 2023 at APS. Therefore, we will submit beamtime proposals at the MAX-IV facility in Sweden and ID01 beamline at the EBS-ESRF facility in France. We do have a planned beamtime at EBS-ESRF with S. Hruszkewycz and S. Middali at Argonne to demonstrate HE-BCDI and HEDM for large adjacent grains. We also plan on submitting additional proposals to ESRF for atomic resolution BCDI.

References

- [1] J. Nicholas Porter, <https://github.com/jacione/lauepy> (2022).
- [2] Yueheng Zhang, Matthew J. Wilkin, Ross Harder, Wonsuk Cha, Landon Schnebley, Richard L. Sandberg, Robert Suter, Anastasios Pateras, and Anthony D. Rollett, “Automated Laue pattern

analysis for multi-peak strain imaging of nanocrystals at 34-ID-C,” submitted J. Synch. Rad (2022).

[3] Matthew J. Wilkin, Anastasios Pateras, Richard L. Sandberg, Nicholas Porter, Landon Schnebley, Ross Harder, Wonsuk Cha, Robert M. Suter, and Anthony D. Rollett, “3D strain imaging across a coherent twin boundary via Bragg Coherent X-ray Diffraction Imaging” in preparation (2022).

[4] Jason Meziere, Anastasios Pateras, Ross Harder, and Richard Sandberg, “Near-atomic Resolution Bragg Coherent Diffraction Imaging Phase Retrieval Utilizing Molecular Dynamics,” in preparation (2022).

[5] Anastasios Pateras, Henry Chapman, Ross Harder, Anthony D. Rollett, Richard L. Sandberg, “Simulations of First Experiments for Atomic-resolution 3D Bragg Coherent Diffraction Imaging” in preparation (2022).

Publications

[1] Yueheng Zhang, Matthew J. Wilkin, Ross Harder, Wonsuk Cha, Landon Schnebley, Richard L. Sandberg, Robert Suter, Anastasios Pateras, and Anthony D. Rollett, “Automated Laue pattern analysis for multi-peak strain imaging of nanocrystals at 34-ID-C,” submitted J. Synch. Rad (2022).

Electronic and Magnetic Properties of Quantum Materials

Zhi-xun Shen^{1,3}, T.P. Devereaux^{1,4}, B. Moritz¹, P.S. Kirchman¹, J.A. Sobota¹, M. Hashimoto^{1,2}, D.H. Lu^{1,2}

1. Stanford Institute for Materials and Energy Sciences, SLAC, Menlo Park, CA94025
2. Stanford Synchrotron Radiation Lightsource, SLAC, Menlo Park, CA94025
3. Department of Physics and Applied Physics, Stanford University, Stanford, CA 94305
4. Department of Materials Science and Engineering, Stanford University, Stanford, CA 94305

Self-identify keywords to describe your project: Quantum Materials, electronic and magnetic structure, photoemission spectroscopy, synchrotron radiation and x-ray free electron laser, theory/simulation

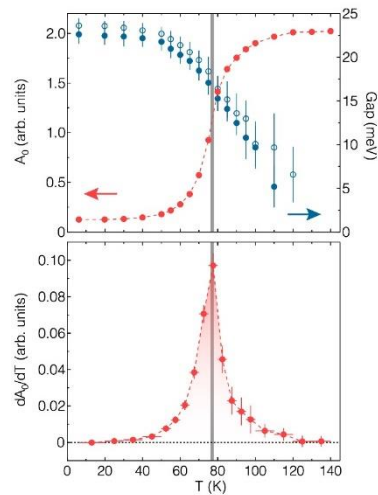
Research Scope

To develop a world class experimental and theoretical program in understanding the electronic and magnetic structures of quantum materials, to address BES grand scientific challenges through the utilization of DOE's x-ray user facilities and modern photoelectron spectroscopy with energy, momentum, and/or time and spin resolution. To complement these spectroscopy experiments with in-situ materials synthesis and characterization, and with advanced theoretical simulations. To complement experiments with theoretical investigations on key problems derived from experiments.

We aim at the highest precision measurements of an electron's energy, momentum, and spin quantum numbers and apply them to frontier quantum materials problems. We have had a number of important progresses over the past two years, including important publications in *Nature*, *Science* and *Review of Modern Physics*. Through these activities, we developed strong synergy with two major scientific user facilities at SLAC - LCLS and SSRL. In the following, we outline selected examples of our progresses.

Recent Progress

- **ARPES study of the high-T_c cuprate superconductors [1]**
 - o We extended the study of overdoped Bi2212 to span the entire Brillouin zone across T_c, aiming to understand the superconducting transition. We discovered that the transition temperature coincides with a rapid drop of zero-energy spectral intensity, with strong momentum anisotropy. Further, the specific heat is successfully reproduced from ARPES data, making a



Temperature evolution of the superconducting gap size and in-gap spectral intensity (A_0) in $(\text{Bi,Pb})_2\text{Sr}_2\text{CaCu}_2\text{O}_{8+\delta}$ (top). While the gap size evolves smoothly, the temperature derivative of A_0 (bottom) peaks at the superconducting transition marked by the vertical grey line.

direct connection between spectroscopy and thermodynamic experiments. This provides a critical missing link between thermodynamics and microscopic quantities that have eluded the community for more than three decades. Furthermore, the momentum dependence provides further insights not feasible from bulk measurements. These observations suggest that the superconducting transition in overdoped Bi2212 may be driven by phase fluctuations..

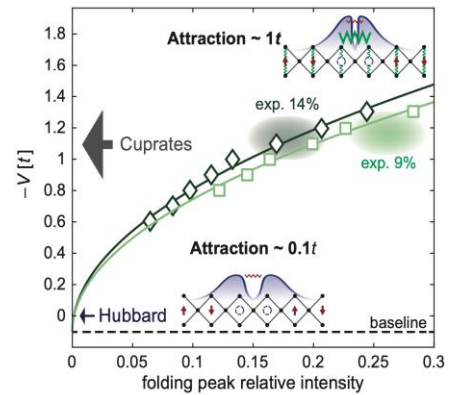
- **ARPES study of other strongly correlated materials [2]**

- o We investigated the electronic structure of superconducting Pr-nickelate thin films using resonant photoemission spectroscopy. The discovery of infinite-layer nickelate superconductors has spurred enormous interest. While the Ni^{1+} cations possess nominally the same $3d^9$ configuration as Cu^{2+} in cuprates, the electronic structure variances of the two remain elusive. By identifying the Ni character with resonant photoemission and comparison with density functional theory + U (on-site Coulomb repulsion energy) calculations, we estimate $U \sim 5$ eV, smaller than the charge transfer energy $\Delta \sim 8$ eV, confirming the Mott-Hubbard electronic structure in contrast to charge-transfer cuprates. Near the Fermi level (E_F), we observe a signature of occupied rare-earth states in the parent compound, which is consistent with a self-doping picture. Our results demonstrate a correlation between the superconducting transition temperature and the oxygen $2p$ hybridization near E_F when comparing hole-doped nickelates and cuprates.

- **ARPES studies of quantum thin films [3]**

- o Using in-situ oxide MBE method, we synthesized hole-doped 1D cuprate chains (9% to 40%) for the first time and conducted systematic *in situ* ARPES measurements. The availability of doped 1D material provides an opportunity to benchmark the applicability of the Hubbard model for cuprates, a long standing issues. Persistent spin-charge separation featured by separate holon and spinon spectral branches is observed up to 40% doping. A prominent holon folding spectroscopic feature is observed for the first time. It revealed an anomalously strong near-neighbor attraction V , which may arise from phonons within reasonable experimental parameters considering extended electron-phonon coupling. The resulting Hubbard+ V model likely provides a holistic picture for high- T_c cuprate physics.

- o We have synthesized and studied $\text{La}_{2-x}\text{Sr}_x\text{CuO}_4$ thin films over a wide range of doping ($x = 0.06 - 0.35$) using oxide MBE and performed *in situ* ARPES measurements. The reduced three-dimensionality in our $\text{La}_{2-x}\text{Sr}_x\text{CuO}_4$ thin films permitted an accurate determination of a Lifshitz transition in a doping range near $x = 0.21$. Using parameters determined from ARPES data, we were able to account for the observed specific heat maximum as a function of doping, excluding the need to invoke an additional



Comparison between the near-neighbor attraction strengths in the Hubbard model and in the real cuprate material. The real material manifest one order of magnitude stronger attractive interaction that the self generated super-exchange attraction.

quantum critical point to account for that anomaly. This has important implications on the relationship between quantum critical phenomena and cuprate superconductivity. [Y. Zhong *et al.*, *PNAS*. 119, 32 (2022)].

- **Spin-resolved ARPES instrument development and study of novel regimes of spin-orbit coupling and magnetism**
 - We used spin-resolved ARPES to characterize the spin texture of the Rashba semiconductor BiTeCl. The significantly higher resolution of the data allows us to detect an anomaly in the otherwise straightforward Rashba-like spin texture. We have successfully modeled this anomaly by invoking higher-order terms in the Rashba spin-orbit interaction Hamiltonian, constrained by the crystal point group symmetry. The symmetry of this Hamiltonian suggests that the observed states are localized surface states rather than delocalized quantum-well states, which had been an unsolved problem in the field. This work established a new data standard for spin resolved ARPES.
- **Time-resolved ARPES instrument development and studies [4]**
 - We continue to work closely with an international consortium to develop photoemission capability at LCLS-II using a momentum microscope based experimental end station. In the meantime, we have upgraded our UHV system and manipulator to accommodate in-plane sample rotations to fully leverage our newly developed bias capabilities that significantly expanded momentum space coverage for time resolved photoemission experiments using 6 eV ultrafast laser.
- **Theory Activities [5]**
 - We developed a minimal microscopic model in comparison with *in-situ* angle-resolved photoemission measurements in a doped 1D cuprate chain material. Simulations highlight the contributions from extended *e-ph* coupling, augmenting the standard Hubbard model. With couplings and phonon energies in reasonable ranges, we demonstrated that a strong attractive interaction exists between neighboring electrons. Considering chemical and structural similarities between 1D and 2D cuprate materials, a minimal model with extended *e-ph* coupling provided new insights on cuprate high- T_c superconductivity and related quantum phases [Ref 5, T. Tang *et al.*, *arXiv:2210.09288*].

Future Plans

- **Infrastructure and Equipment Development**
 - We will continue to develop and improve modalities of ARPES – small spot ARPES, time and spin-resolved ARPES, with the LCLS – *k* Microscope development being an important focus. We will continue to develop in-situ materials synthesis and numerical simulation capabilities in tandem with instrumental advancements.
- **ARPES study of novel superconductors**
 - We will continue to study the novel cuprate superconductors, expanding to electron doped and multilayer cuprates. We will investigate the connection between spectroscopy and thermodynamical quantities.
 - We plan to study the iron -based superconductors. An example is the heavily hole-doped $\text{Ba}_{1-x}\text{K}_x\text{Fe}_2\text{As}_2$ around the critical doping level of $x \sim 0.8$, at which a spontaneous breaking of time-reversal symmetry above the superconducting transition was reported recently.

- o Infinite layer nickelates is an important new superconducting material family. Through single crystals from the Max Planck Institute, we will perform ARPES studies of the electronic structure.
- **ARPES studies of quantum thin films**
 - o We will study electronic structure of multilayer oxides and material systems that cannot be prepared by bulk single crystal methods using our oxide MBE system and perform ARPES investigations. Following the success of synthesis of $\text{La}_{2-x}\text{Sr}_x\text{CuO}_4$ thin films, we will continue to explore other dopant and wider doping range for new phenomena. Other material examples include $\text{Sr}_{1-x}\text{La}_x\text{CuO}_2$ electron-doped infinite layer cuprate thin films and $\text{BaCuO}_{2+}/\text{SrCuO}_2$ superlattices.
- **ARPES studies of 2D and Topological Materials**
 - o We will investigate several important 2D and topological materials. This includes strongly correlated material families with both strong correlation and topological properties such as EuCd_2P_2 and EuCd_2As_2 , candidate topological insulator $\text{FeTe}_{0.5}\text{Se}_{0.5}$, exciton state of monolayer ZrTe_2 , and other transition metal multilayers made possible by our new materials preparation facility.
- **Time- and spin- resolved ARPES studies**
 - o We will investigate the coherent response in cuprate superconductors as function of the number of layers, i.e. compare the out-of-plane coherent phonons in Bi2201 , Bi2212 , Bi2223 to gauge changes of the electron-phonon coupling as function of the number of CuO_2 layers. Other systems include SmB_6 and $\text{FeTe}_{0.5}\text{Se}_{0.5}$.
- **Theory Activities**
 - o We will continue synergetic theoretical activities, including simulations for the single-band and multi-orbital Hubbard models, investigation of the influence of extended electron-phonon coupling, as identified from comparison to ARPES measurements, on various ordering tendencies, including superconductivity and charge-density-wave states, as well as polaron formation, using a combination of exact diagonalization, DQMC, and time-dependent density matrix renormalization group methods.

References [5 most relevant]

1. S.D. Chen, M. Hashimoto, Y. He, D. Song, J.-F. He, Y.-F. Li, S. Ishida, H. Eisaki, J. Zaanen, T.P. Devereaux, D.-H. Lee, D.-H. Lu, Z.-X. Shen. *Unconventional spectral signature of T_c in a pure d-wave superconductor*. *Nature* **601**, 562 (2022)
2. Z. Chen, M. Osada, D. Li, E. M. Been, S.D. Chen, M. Hashimoto, D. Lu, S.K. Mo, K. Lee, B.Y. Wang, F. Rodolakis, J. L. McChesney, C. Jia, B. Moritz, T. P. Devereaux, H. Y. Hwang, Z.-X. Shen. *Electronic structure of superconducting nickelates probed by resonant photoemission spectroscopy*. *Matter* **5**, 1806 (2022)
3. Z. Chen, Y. Wang, S.N. Rebec, T. Jia, M. Hashimoto, D. Lu, B. Moritz, R.G. Moore, T.P. Devereaux, and Z.X. Shen. *Anomalously strong near-neighbor attraction in doped 1D cuprate chains*. *Science* **373**, 1235 (2021).

4. N. Gauthier, J.A. Sobota, H. Pfau, A. Gauthier, H. Soifer, M.D. Bachmann, I.R. Fisher, Z.-X. Shen, P.S. Kirchmann. *Expanding the momentum field of view in angle-resolved photoemission systems with hemispherical analyzers*. Rev. Sci. Instrum. **92**, 123907 (2021)
5. Y. Wang, Z. Chen, T. Shi, B. Moritz, Z.-X. Shen, T.P. Devereaux. *Phonon-Mediated Long-Range Attractive Interaction in One-Dimensional Cuprates*. Phys. Rev. Lett. **127**, 197003 (2021)

Publications [10 most relevant]

1. T. Jia, Z. Chen, S. N. Rebec, M. Hashimoto, D. Lu, T. P. Devereaux, D.-H. Lee, R. G. Moore, Z.-X. Shen, *Magic Doping and Robust Superconductivity in Monolayer FeSe on Titanates*, Advanced Science **8**, 2003454 (2021)
2. J.A. Sobota, Y. He, and Z.-X. Shen, *Angle-Resolved Photoemission Spectroscopy Study of Quantum Materials*, Reviews of Modern Physics **93**, 025006 (2021)
3. Z. Chen, Y. Wang, S. N. Rebec, T. Jia, M. Hashimoto, D. Lu, B. Moritz, R. G. Moore, T. P. Devereaux, and Z.-X. Shen, *Anomalously Strong Near-Neighbor Attraction in Doped 1D Cuprate Chains*, Science **373**, 1235 (2021)
4. Y. He, S.-D. Chen, Z.-X. Li, D. Zhao, D. Song, Y. Yoshida, H. Eisaki, T. Wu, X.-H. Chen, D.-H. Lu, C. Meingast, T. P. Devereaux, R. J. Birgeneau, M. Hashimoto, D.-H. Lee, and Z.-X. Shen, *Superconducting fluctuations in overdoped $\text{Bi}_2\text{Sr}_2\text{CaCu}_2\text{O}_{8+\delta}$* , Phys Rev X **11**, 031068 (2021)
5. E. W. Huang, W. O. Wang, J. K. Ding, T. Liu, F. Liu, X.-X. Huang, B. Moritz, T. P. Devereaux, *Intertwined states at finite temperatures in the Hubbard model*, J. Phys. Soc. Jpn. **90**, 111010 (2021)
6. H. Pfau, M. Yi, M. Hashimoto, T. Chen, P.-C. Dai, Z.-X. Shen, S.-K. Mo, and D. Lu, *Quasiparticle coherence in the nematic state of FeSe*, Physical Review B **104**, L241101 (2021)
7. Yong Zhong, Zhuoyu Chen, Su-Di Chen, Ke-Jun Xu, Makoto Hashimoto, Yu He, Shin-ichi Uchida, Donghui Lu, Sung-Kwan Mo, Zhi-Xun Shen, *Differentiated roles of Lifshitz transition on thermodynamics and superconductivity in $\text{La}_{2-x}\text{Sr}_x\text{CuO}_4$* , Proc. Natl. Acad. Sci. **119**, e2204630119 (2022)
8. Jinwoong Hwang, Kyoo Kim, Canxun Zhang, Tiancong Zhu, Charlotte Herbig, Sooran Kim, Bongjae Kim, Yong Zhong, Mohamed Salah, Mohamed M El-Desoky, Choongyu Hwang, Zhi-Xun Shen, Michael F Crommie, Sung-Kwan Mo, *Large-gap insulating dimer ground state in monolayer IrTe₂*, Nature Communications **13**, 906 (2022)
9. Su-Di Chen, Makoto Hashimoto, Yu He, Dongjoon Song, Jun-Feng He, Ying-Fei Li, Shigeyuki Ishida, Hiroshi Eisaki, Jan Zaanen, Thomas P Devereaux, Dung-Hai Lee, Dong-

Hui Lu, Zhi-Xun Shen, *Unconventional spectral signature of T_c in a pure d -wave superconductor*, Nature **601**, 562-567 (2022).

- 10.** S. Sakamoto, N. Gauthier, P. S. Kirchmann, J. A. Sobota, and Z.-X. Shen, *Connection between coherent phonons and electron-phonon coupling in $Sb(111)$* , Physical Review B **105**, L161107 (2022)

Ultrafast Bursts of Coherent X-rays to Unveil Fluctuations in Quantum Matter

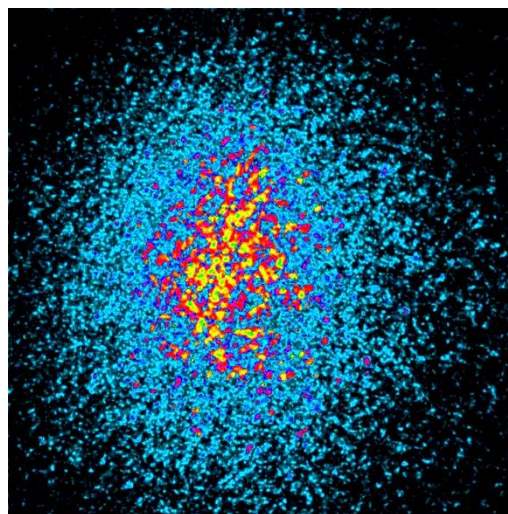
J. J. Turner, SIMES, Stanford University & SLAC National Accelerator Laboratory

keywords: Fluctuations, superconductivity, ultrafast, coherence, magnetic topology

Research Scope

We are developing novel ultrafast x-ray techniques to study fluctuations in quantum matter at times scales not accessible at traditional synchrotron sources. This is made possible by creating two X-ray Free Electron Laser (XFEL) pulses of femtosecond pulse duration, and varying them in time with respect to each other, on the relevant timescale of the physics one is after. This is only made possible with recent developments at XFEL facilities, such as the generation of fully coherent x-ray pulses, and the ability to adjust them on electronic time scales.

Though critical to many areas of science, one key area which will be impacted dramatically is unconventional superconductivity. This is because the pairing mechanism, and associated order parameters that have been shown to be important in these complex types of materials, can display fluctuations that are not well understood. Furthermore, many theories predict fluctuations are paramount to understanding these types of materials and their respective mechanisms which can host surprising physics.

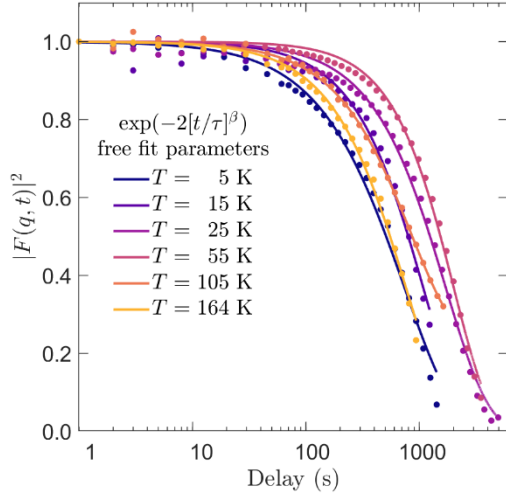


Orbital speckle pattern measured with soft x-rays at the Mn L-edge of $\text{Pr}_{0.5}\text{Ca}_{0.5}\text{MnO}_3$ at 205K at the ALS, featured in our review article [1] and in the latest Basic Energy Sciences Network Requirements Review [2].

The full scope of this activity is broad in nature. This includes, but is not limited to, working closely with accelerator physicists to deliver the necessary capabilities, design, construction and operation of new instruments to handle these types of experiments, work at other XFEL facilities in addition to LCLS and LCLS-II, coherent x-ray scattering work, materials characterization, and high-performance computing and sophisticated analysis techniques. Progress in all the above areas is necessary to push the envelope in demonstrating and making this capability routine for future XFEL experiments.

Recent Progress

The focal point of the research direction outlined above is to make scientific progress on our understanding of unconventional superconductivity with the tools we are developing. Because these tools are early in their development, and are dependent on XFEL technology and the requisite



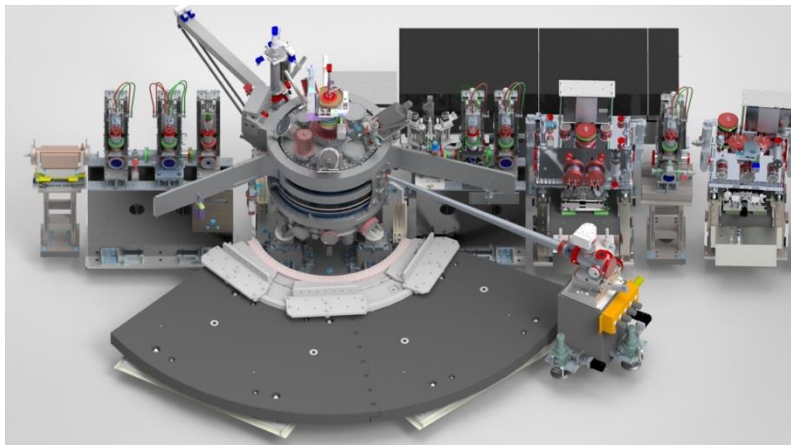
PRELIMINARY DATA. Correlation functions with temperature of $\text{YBa}_2\text{Cu}_3\text{O}_{6.67}$ measured at NSLS-II at beamline 11-ID, BNL.

sophisticated instruments, software, and analytical methods, we have specifically pushed the envelope in three focus areas: ultrafast x-ray measurements on unconventional superconductors, developing these two-pulse fluctuation methods on related systems, and measuring fluctuations in unconventional superconductors using synchrotrons at much longer timescales—providing learning which will be necessary to apply this to the faster timescales for fluctuation studies at future or upgraded XFELs. The first two are described in our recent publication Wandel et al. [3], and the DOE highlight entitled ‘Never frozen: skyrmion fluctuations’, respectively. The third area, measuring fluctuations in unconventional superconductors at slower times, has recently provided some very intriguing physics in this area.

As an example, we show a very preliminary figure, which should be noted has not been fully verified and has not yet been published in a peer-reviewed journal article. This was a measurement on the o-VIII doped YBCO system which shows superconductivity below $T_c=65\text{K}$, and a charge density wave (CDW) state at about $T_{\text{cdw}} \sim 130\text{K}$, which is thought to have a dynamic component. However, NMR studies have shown a static CDW order sets in at about $T_{\text{static}} \sim 50\text{K} \pm 10\text{K}$ [4]. We used XPCS to measure slow fluctuations of the lattice in this YBCO system near the (005) Bragg peak to directly measure how the lattice responds. This was carried out at the coherent beamline 11-ID at the NLSL-II DOE user facility, where speckle patterns were measured as a function of time after illuminating the system with a coherent x-ray beam. We found the temporal correlation functions were very dependent on the phase (see Fig.), even though the lattice is thought to be very robust. Furthermore, by extracting the correlation time as a function of temperature, preliminary data suggest a slowdown of the fluctuations centered around the onset temperature for the static CDW observed by NMR [4]. While still preliminary observations, it looks like the slowdown could be due to locking of the lattice to the CDW, while the fluctuations speed up on either side: above – as one moves away from the CDW state, and below – which could be due to competition with superconductivity.

Future Plans

We are in the process of solidifying the crowning achievement of this research activity, which is installing and commissioning a brand-new instrument at the LCLS-II which is focused on fluctuation phenomena in quantum materials, the X-ray Photon Fluctuation Spectroscopy (XPFS) instrument. This is funded through the BES Division of Materials Science and Engineering and will be a separate, stand-alone instrument designed by our BES-funded team, and will be stationed at the qRIXS beamline as part of the Resonant Inelastic X-ray Scattering (RIX) program, part of the new LCLS-II suite of instruments. This will consist of a UHV chamber which can accommodate either the latest SLAC-developed ePixM detector, or other options which may become available, such as the MCP-TimePix being developed at the Space Sciences Laboratory at the University of California at Berkeley. This chamber will be able to float across the floor to a



The design of the new XPFS chamber. This instrument is funded through the MSE part of BES at the DOE and will be compatible with the current sample system in place at the LCLS-II facility to measure first fluctuation studies at the high repetition rate offered by the upgraded LCLS-II facility.

precise location, while also being capable of being under UHV for soft x-ray scattering measurements at an arbitrary scattering angle. This is a significant upgrade from previous generations, which were proto-type versions constructed by our team [5], and could only operate in a forward scattering geometry, which has a more limited use for quantum materials studies. Once this system is constructed and in place, we plan on assisting with commissioning of the instrument and leading so-called ‘Early

Science’ activities for first measurements using this system and applying our new technique to exotic systems using the high-repetition rate of the LCLS-II.

Secondary to this instrumentation development, is the ongoing work being carried out by our team using the hard x-ray capability at the LCLS, with three future LCLS experiments being planned for the Spring of 2023. These include fluctuations at the ps timescale in LSCO to study the nature of the superconducting order, as well as the strongly spin-orbit coupled materials in the family of iridates, where the latter will be to demonstrate the equality of this type of method with the more traditional techniques such as RIXS. The final experiment planned this spring is in a completely different area of physics. Mainly funded by the Fusion Energy Sciences (FES) arm of the Office of Science, this project was initiated by a group at Oxford University in this area to use the methods we have been developing to measure viscosity in a high energy density system, important for this

field focused on fusion and shock wave physics in warm, dense states of matter. This effort, through collaboration with our team, has even recently received an invitation from the FES and National Nuclear Security Administration (NNSA) Defense Program to submit a new FOA to the DOE based on our experimental developments [6].

Parallel to our ongoing fluctuation studies are using the more traditional pump-probe studies run in a non-traditional way. For instance, our recent work on the high-temperature superconductor YBCO found a unique CDW state exists for a brief time period under optical excitation, when the superconductivity can be quenched [3]. The natural follow-up to this is to study fluctuations which occur in these new, transient states, using our methodology. This will also be explored in addition to the more traditional fluctuation spectra in equilibrium.

In addition to the mostly LCLS-centric activities, we are also thoroughly engaged in other synchrotron XPCS studies and other XFELs across the globe. One aspect of this that is addressed in our portfolio is how to handle large amounts of data and the need for high-performance computing (HPC), a critical aspect of these types of measurements. We have been especially interested in developing codes [7] and simulated data [8], both available on-line, to speed up the process of understanding the experiments ‘on-the-fly’. In a recent European XFEL experiment on a skyrmionic system, we collected 1PB of high-quality data. Handling this amount of data, transferring, reducing, and analyzing is a non-trivial task and is also helping us to develop computing expertise, and is furthermore helping us to prepare for the future of LCLS-II, when we reach the 1MHz data rates. This effort was presented recently at an invited talk at the HPC conference XLOOP, with a manuscript posted on the arXiv [9].

References

1. L. Shen, M. Seaberg, E. Blackburn and J. J. Turner, "[A snapshot review-Fluctuations in quantum materials: from skyrmions to superconductivity](#)", *MRS Adv.* **6**, 221–233 (2021) doi: 10.1557/s43580-021-00051-y
2. Carder, D.; Dart, E.; Graf, M.; Hawk, C.; Holder, A.; Jacob, D., et al. (2022). Basic Energy Sciences Network Requirements Review (Final Report). In *Basic Energy Sciences Network Requirements Review (Final Report)*. Lawrence Berkeley National Laboratory. Report #: LBNL-2001490/
3. S. Wandel, et al., "[Enhanced charge density wave coherence in a light-quenched, high-temperature superconductor](#)", *Science* **376**, 860 (2022) doi: 10.1126/science.abd7213
4. T. Wu, et al. “Magnetic-field-induced charge-stripe order in the high-temperature superconductor $\text{YBa}_2\text{Cu}_3\text{O}_y$ ”, *Nature* **477**, 191 (2011).
5. T. A. Assefa, et al., "[The fluctuation–dissipation measurement instrument at the Linac Coherent Light Source](#)", *Rev. Sci. Instrum.* **93**, 083902 (2022) doi: 10.1063/5.0091297
6. https://science.osti.gov/fes/-/media/grants/pdf/foas/2023/SC_FOA_0002884.pdf
7. Freely available *Python* code for analyzing single shot detector images for XPFS : https://github.com/slaclab/ml_xpfs

8. Freely available data set for simulation and algorithm testing:
<https://zenodo.org/record/6643622#.Y8CoO-zMKko>
9. Conference: <https://sc22.supercomputing.org/>, and paper can also be found here: H. Chen, et al. "Testing the data framework for an AI algorithm in preparation for high data rate X-ray facilities", <https://doi.org/10.48550/arXiv.2210.10137>

Publications

Put the list of publications in the recent 2-years SUPPORTED BY BES here.

1. N. G. Burdet, V. Esposito, M. H. Seaberg, C. H. Yoon and J. J. Turner, "[Absolute contrast estimation for soft X-ray photon fluctuation spectroscopy using a variational droplet model](#)", *Sci. Rep.* **11**, 19455 (2021) doi: 10.1038/s41598-021-98774-3
2. M. H. Seaberg, B. Holladay, S. A. Montoya, X. Y. Zheng, J. C. T. Lee, A. H. Reid, J. D. Koralek, L. Shen, V. Esposito, G. Coslovich, P. Walter, S. Zohar, V. Thampy, M. F. Lin, P. Hart, K. Nakahara, R. Streubel, S. D. Kevan, P. Fischer, W. Colocho, A. Lutman, F.-J. Decker, E. E. Fullerton, M. Dunne, S. Roy, S. K. Sinha and J. J. Turner, "[Spontaneous fluctuations in a magnetic Fe/Gd skyrmion lattice](#)", *Phys. Rev. Research* **3**, 033249 (2021) doi: 10.1103/PhysRevResearch.3.033249
3. R. M. Jay, S. Eckert, B. E. V. Kuiken, M. Ochmann, M. Hantschmann, A. A. Cordones, H. Cho, K. Hong, R. Ma, J. H. Lee, G. L. Dakovski, J. J. Turner, M. P. Minitti, W. Quevedo, A. Pietzsch, M. Beye, T. K. Kim, R. W. Schoenlein, P. Wernet, A. Föhlisch and N. Huse, "[Following Metal-to-Ligand Charge-Transfer Dynamics with Ligand and Spin Specificity Using Femtosecond Resonant Inelastic X-ray Scattering at the Nitrogen K-Edge](#)", *J. Phys. Chem. Lett.* **12**, 6676 (2021) doi: 10.1021/acs.jpcclett.1c01401
4. L. Shen, M. Seaberg, E. Blackburn and J. J. Turner, "[A snapshot review-Fluctuations in quantum materials: from skyrmions to superconductivity](#)", *MRS Adv.* **6**, 221–233 (2021) doi: 10.1557/s43580-021-00051-y
5. Y. Sun, V. Esposito, P. A. Hart, C. Hansson, H. Li, K. Nakahara, J. P. MacArthur, S. Nelson, T. Sato, S. Song, P. Sun, P. Fuoss, M. Sutton and D. Zhu, "[A Contrast Calibration Protocol for X-ray Speckle Visibility Spectroscopy](#)", *Appl. Sci.* **11**, 10041 (2021) doi: 10.3390/app11211004
6. F.-J. Decker, K. L. Bane, W. Colocho, S. Gilevich, A. Marinelli, J. C. Sheppard, J. L. Turner, J. J. Turner, S. L. Vetter, A. Halavanau, C. Pellegrini and A. A. Lutman, "[Tunable x-ray free electron laser multi-pulses with nanosecond separation](#)", *Sci. Rep.* **12**, (2022) doi: 10.1038/s41598-022-06754-y
7. S. Wandel, F. Boschini, E. H. de Silva Neto, L. Shen, M. X. N. Na, S. Zohar, Y. Wang, S. B. Welch, M. H. Seaberg, J. D. Koralek, G. L. Dakovski, W. Hettel, M.-F. Lin, S. P. Moeller, W. F. Schlotter, A. H. Reid, M. P. Minitti, T. Boyle, F. H. He, R. Sutarto, R. Liang, D. Bonn, W. Hardy, R. A. Kaindl, D. G. Hawthorn, J.-S. Lee, A. F. Kemper, A. Damascelli, C. Giannetti, J. J. Turner and G. Coslovich, "[Enhanced charge density wave](#)

- [coherence in a light-quenched, high-temperature superconductor](#)", *Science* **376**, 860 (2022) doi: 10.1126/science.abd7213
8. T. A. Assefa, M. H. Seaberg, A. H. Reid, L. Shen, V. Esposito, G. L. Dakovski, W. Schlotter, B. Holladay, R. Streubel, S. A. Montoya, P. Hart, K. Nakahara, S. Moeller, S. D. Kevan, P. Fischer, E. E. Fullerton, W. Colucho, A. Lutman, F.-J. Decker, S. K. Sinha, S. Roy, E. Blackburn and J. J. Turner, "[The fluctuation–dissipation measurement instrument at the Linac Coherent Light Source](#)", *Rev. Sci. Instrum.* **93**, 083902 (2022) doi: 10.1063/5.0091297
 9. S. R. Chitturi, N. G. Burdet, Y. Nashed, D. Ratner, A. Mishra, T. J. Lane, M. Seaberg, V. Esposito, C. H. Yoon, M. Dunne and J. J. Turner, "[A machine learning photon detection algorithm for coherent x-ray ultrafast fluctuation analysis](#)", *Struct. Dyn.* **9**, 054302 (2022) doi: 10.1063/4.0000161
 10. Ericmoore Jossou, Tadesse A. Assefa, Ana F. Suzana, Longlong Wu, Colleen Campbell, Ross Harder, Wonsuk Cha, Kim Kisslinger, Cheng Sun, Jian Gan, Lynne Ecker, Ian K. Robinson & Simerjeet K. Gill, "[Three-dimensional strain imaging of irradiated chromium using multi-reflection Bragg coherent diffraction](#)" *npj Materials Degradation*, **6**, 99 (2022) doi: <https://doi.org/10.1038/s41529-022-00311-8>

Automated sorting of coherent diffraction data from XFELs

Longlong Wu, Condensed Matter Physics and Materials Science Division, BNL

Ian Robinson, Condensed Matter Physics and Materials Science Division, BNL

Shinjae Yoo, Computational Science Initiative, BNL

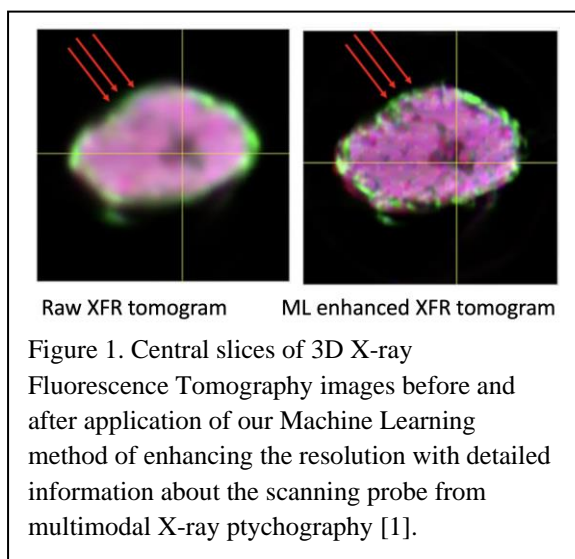
Yuewei Lin, Computational Science Initiative, BNL

Keywords: Machine Learning, Deconvolution, Cluster Analysis, Phase Retrieval, Inverse Problem

Research Scope

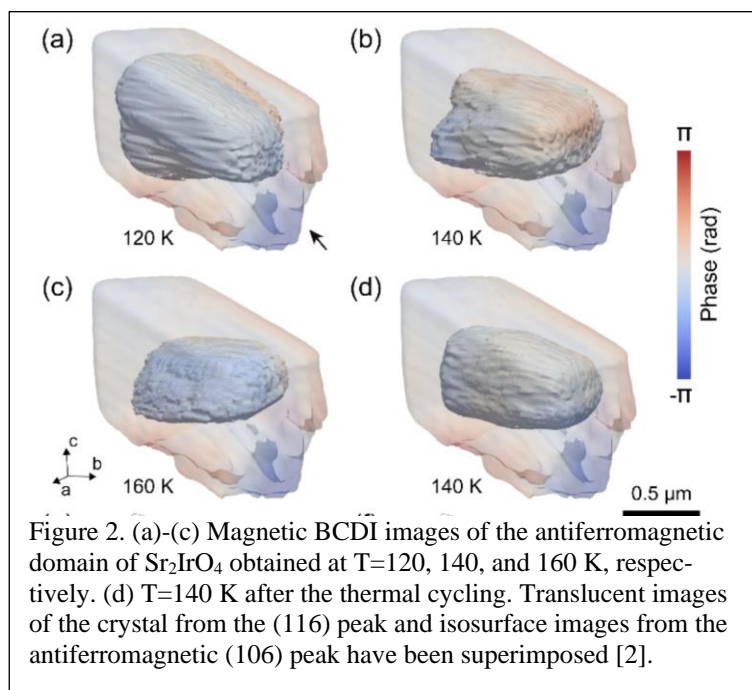
Coherent X-rays are routinely provided today by the latest Synchrotron and X-ray Free-electron Laser Sources (XFELs). When these diffract from a crystal containing defects, interference leads to the formation of a modulated diffraction pattern called "speckle". When the defects move around, they can be quantified by a correlation analysis technique called X-ray Photon Correlation Spectroscopy. But the speckles also change when the beam moves on the sample. By scanning the beam in a controlled way, the overlap between the adjacent regions gives redundancy to the data, which allows a solution of the inherent phase problem. This is the basis of the coherent X-ray ptychography method which can achieve image resolutions of 10 nm, but only if the probe positions are known. The goal of this project is to separate "genuine" fluctuations of a material sample from the inherent beam fluctuations at the high data rates of XFELs. Algorithms are being developed to calculate the correlations between all the coherent diffraction patterns arriving in a time series, then used to separate the two sources of fluctuation using the criterion that the "natural" thermal fluctuations do not repeat, while beam ones do. We attempt to separate the data stream into image and beam "modes" automatically.

Recent Progress



Under this FWP, we have made a significant enhancement of X-ray fluorescence microscopy which is widely used to study functional materials with variable compositions in 3D, both biological and composite materials. Currently, the spatial resolution for a hard X-ray nanoprobe fluorescence microscopy is limited to the X-ray probe size. We developed a machine learning (ML) model to overcome the resolution limit by deconvoluting the X-ray probe from the X-ray fluorescence (XRF) signal. To do this, we combined a multimodal, simultaneous measurement of the probe using X-ray ptychography [1]. The enhanced spatial

resolution was observed for both simulated and experimental XRF data, showing superior performance over the state-of-the-art scanning XRF method with different nano-sized X-ray probes. Enhanced spatial resolutions were also observed for the accompanying 3D tomographic reconstructions, such as that shown in Fig. 1 for an experimental $\text{LiNi}_{0.6}\text{Mn}_{0.2}\text{Co}_{0.2}\text{O}_2$ (NMC) battery cathode particle, 5 μm in diameter. It is anticipated that this probe profile deconvolution using the proposed ML solution to enhance the spatial resolution of an XRF microscope will be broadly applicable across both functional materials and biological imaging.

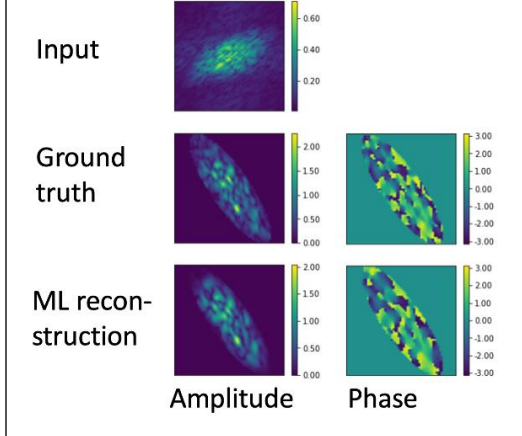


We also explored the temperature-dependent behavior of magnetic domains, which play an essential role in the magnetic properties of materials, leading to widespread applications. However, experimental methods to access the three-dimensional (3D) magnetic domain structures are very limited, especially for antiferromagnets. We investigated the spin-orbit Mott insulator iridate Sr_2IrO_4 which has an interesting magnetic structure because of its analogy to superconducting cuprates. We applied resonant X-ray magnetic Bragg coherent diffraction imaging

(BCDI) to track the real-space 3D evolution of antiferromagnetic ordering inside a Sr_2IrO_4 single crystal as a function of temperature, finding that the antiferromagnetic domain shows anisotropic changes. The anisotropy of the domain shape reveals the underlying anisotropy of the antiferromagnetic coupling strength within Sr_2IrO_4 . This is the first reported magnetic BCDI experimental result, which has taken repeated attempts at the state-of-the-art 34-ID-C beamline of APS. To get enough magnetic scattering signal, we had to carefully optimize the sample size using Focussed Ion Beam (FIB) sample cutting at the same time as enlarging the coherent beam size by closing the entrance slits. The size that worked best was a 1.3 μm cube, as shown in Fig 2.

We have performed data clustering of the XFEL data measured from $\text{La}_{2-x}\text{Sr}_x\text{CuO}_4$ (LSCO) epitaxial thin films in Hamburg. This was the original plan of our FWP proposal, which has brought together computational capabilities from the inverse problem, image clustering and data correlation fields. A distinct set of diffraction patterns, collected at the MID station of the European XFEL, has been merged together from raw data, selected by cross-correlation analysis. Stronger correlation was found between single XFEL shots within the same pulse train than

Figure 3. Testing of ML inversion of simulated data used to model the BCDI snapshot data obtained from LSCO thin films at the European XFEL. Ground truth and reconstructed amplitude and phase structures are reliably reproduced [3].



between trains. Recorded diffraction patterns were found to repeat over the full 30-minute run, rather than being clustered in time. This indicates the variations arise from beam/instrument stability rather than inherent fluctuations of the sample. The variations could be either beam movement or wavefront changes of the XFEL beam. Further, we have developed a Machine-Learning (ML) phasing algorithm which is reproducibly able to invert these data to images, shown in Fig. 3. This required an accurate forward model to describe the sample and diffraction process, which was then used to train a Complex-valued Convolutional Neural Network (CCNN). The major breakthrough was to develop a way to manage complex data arrays within the pyTorch package. By retaining the physical correspondence of the

amplitude and phase of the images as complex numbers (rather than separate channels in the earlier codes), the performance of the CCNN is significantly improved. We are therefore able to report the first time a beam-cut area of a sample has been successfully inverted in BCDI.

Future Plans

Because of the unknown beam position in the LSCO XFEL experiments as described above, we plan to work on training a CNN model to study the position information of input diffraction patterns. Diffraction patterns from overlapping cut-out regions of test images will be used for the ML model as training datasets. We can then learn the absolute position information for each diffraction pattern for the LSCO XFEL experiment described above. We will start with our developed phase-domain model for the ML model training. Whether the distance of separation or both its (x,y) coordinates will be recoverable is an important question to be answered. The success of the ML model will have a very broad application for the Synchrotron and X-ray Free-electron Laser Sources (XFELs), for example, beam position monitor.

There are further developments to make on the single shot imaging discussed above based on the CCNN. We plan to continue investigating the trade-offs associated with the size and shape of the real-space "support" function, which has a central role both in ML and classical iterative phasing methods. Use of a support reduces the number of degrees of freedom in the inverse problem, so a smaller support will improve the reliability and noise sensitivity, but at a cost of worse agreement with the data. Similarly, assumptions can be tested about the assumed structure of the phase domains in the sample, as well as other constraints. Generally, ML allows much more control of the physical description of the experiment (via the training) than the classical methods, so we are optimistic this will lead to further improvements.

We also plan to develop our previously published machine learning scheme for phasing experimental BCDI data [4]. Additions to the PyTorch package have been developed to handle complex numbers, which should greatly improve the performance of the method, which previously returned independent amplitude and phase images. We hope to expand the range of BCDI phasing problems to exceed what is possible using the classical iterative projection algorithms. This might include multiple-phase domain array structures which produce multi-centered diffraction patterns, which are found repeatedly in BCDI experiments on synthetic nanoparticles. We will start with the simpler problem of decomposing "twin" images of non-centrosymmetric objects, which currently do not perform well with the ML tools, and then move on to the phase domain array problem, which is famously intractable using the iterative methods. Because of the success reported above for the single-shot XFEL imaging of domains in LBCO thin films [4] and our experience on different ML approach for practical application [1, 3], we have some confidence that the ML approach, with sufficient training relevant to the samples under study, will lead to the improved capability of solving the "phase problem".

References

- [1] Longlong Wu, Seongmin Bak, Youngho Shin, Yong. S Chu, Shinjae Yoo, Ian K. Robinson and Xiaojing Huang, "Resolution-Enhanced X-ray Fluorescence Microscopy via Deep Residual Networks", under review at npj Computational Materials (2022)
- [2] Longlong Wu, Wei Wang, Tadesse A. Assefa, Ana F. Suzana, Jiecheng Diao, Gang Cao, Ross J. Harder, Wonsuk Cha, Kim Kisslinger, Mark P. M. Dean and Ian K. Robinson, "Anisotropy of Antiferromagnetic Domains in a Spin-orbit Mott Insulator", under review at Physical Review Letters (2022)
- [3] Xi Yu, Longlong Wu, Yuewei Lin, Jiecheng Diao, Jialun Liu, Jörg Hallmann, Ulrike Boesenberg, Johannes Möller, Anders Madsen, Tadesse Assefa, Emil S. Bozin, Yue Cao, Hoydoo You, Dina Sheyfer, Stephan Rosenkranz, Samuel Marks, Paul Evans, David Keen, Ivan Bozovic, Mark P.M. Dean, Shinjae Yoo, Ian K. Robinson, "Ultrafast Bragg Coherent Diffraction Imaging of Epitaxial Thin Films using Deep Complex-valued Neural Networks", in preparation for npj Computational Materials (2023)
- [4] Longlong Wu, Shinjae Yoo, Ana F. Suzana, Tadesse A. Assefa, Jiecheng Diao, Ross J. Harder, Wonsuk Cha and Ian K. Robinson, "3D Coherent X-ray Imaging via Deep Convolutional Neural Networks", npj Computational Materials 7 175 (2021)

Publications

- [1] Longlong Wu, Seongmin Bak, Youngho Shin, Yong. S Chu, Shinjae Yoo, Ian K. Robinson and Xiaojing Huang, "Resolution-Enhanced X-ray Fluorescence Microscopy via Deep Residual Networks", under review at npj Computational Materials (2022)

[2] Longlong Wu, Wei Wang, Tadesse A. Assefa, Ana F. Suzana, Jiecheng Diao, Gang Cao, Ross J. Harder, Wonsuk Cha, Kim Kisslinger, Mark P. M. Dean and Ian K. Robinson, "Anisotropy of Antiferromagnetic Domains in a Spin-orbit Mott Insulator", under review at Physical Review Letters (2022)

[3] Longlong Wu, Shinjae Yoo, Ana F. Suzana, Tadesse A. Assefa, Jiecheng Diao, Ross J. Harder, Wonsuk Cha and Ian K. Robinson, "3D Coherent X-ray Imaging via Deep Convolutional Neural Networks", npj Computational Materials 7 175 (2021)

DOI: 10.1038/s41524-021-00644-z

[4] Longlong Wu, Yao Shen, Andi M. Barbour, Wei Wang, Dharmalingam Prabhakaran, Andrew T. Boothroyd, Claudio Mazzoli, John M. Tranquada, Mark P. M. Dean and Ian K. Robinson, "Real Space imaging of Spin Stripe Domain Fluctuations in a Complex Oxide", Physical Review Letters 127 275301 (2021)

DOI: 10.1103/PhysRevLett.127.275301

[5] Ana F. Suzana, Sizhan Liu, Jiecheng Diao, Longlong Wu, Tadesse A. Assefa, Milinda Abeykoon, Ross Harder, Wonsuk Cha, Emil S. Bozin and Ian K. Robinson, "Structural explanation of the dielectric enhancement of barium titanate nanoparticles grown under hydrothermal conditions", accepted in Advanced Functional Materials (2022)

[6] Ericmoore Jossou, Tadesse A. Assefa, Ana F. Suzana, Longlong Wu, Colleen Campbell, Ross Harder, Wonsuk Cha, Kim Kisslinger, Cheng Sung, Jian Gang, Lynne Ecker, Ian K. Robinson and Simerjeet K. Gill, "Three-dimensional strain imaging of irradiated chromium using multi-reflection Bragg coherent diffraction", accepted in npj Materials Degradation (2022)

[7] Wei Wang, Lijun Wu, Junjie Li, Niraj Aryal, Xilian Jin, Yu Liu, Mikhail Fedurin, Marcus Babzien, Rotem Kupfer, Mark Palmer, Cedomir Petrovic, Weiguo Yin, Mark P. M. Dean, Ian Robinson, Jing Tao, Yimei Zhu, "Photoinduced anisotropic lattice dynamic response and domain formation in thermoelectric SnSe", npj Quantum Materials 6 97 (2021)

Doi: 10.1038/s41535-021-00400-y

[8] Min Gyu Kim, A. Barbour, Wen Hu, S. B. Wilkins, Jiaqi Lin, I. K. Robinson, M. P. M. Dean, Choongjae Won, Junjie Yang, S.-W. Cheong, C. Mazzoli and V. Kiryukhin, "Real-Space Observation of Fluctuating Antiferromagnetic Domain Walls", Science Advances 8 eabj9493 (2022)

DOI: 10.1126/sciadv.abj9493

[9] Tongchao Liu, Jiajie Liu, Luxi Li, Lei Yu, Jiecheng Diao, Tao Zhou, Shunning Li, Alvin Dai, Wenguang Zhao, Yang Ren, Liguang Wang, Tianpin Wu, Rui Qi, Yinguo Xiao, Jiaxin Zheng,

Wonsuk Cha, Ross Harder, Ian Robinson, Jianguo Wen, Jun Lu, Feng Pan and Khalil Amine, “Lattice displacement dictating the structure degradation of Li-rich layered oxide cathodes”, *Nature* 606 305–312 (2022)

DOI: 10.1038/s41586-022-04689-y

[10] Xiang Liu, Xinwei Zhou, Qiang Liu, Jiecheng Diao, Chen Zhao, Luxi Li, Yuze Liu, Wenqian Xu, Amine Daali, Ross Harder, Ian K. Robinson, Mouad Dahbi, Jones Alami, Guohua Chen, Gui-Liang Xu and Khalil Amine, “Multiscale understanding of surface structural effects on high-temperature operational resiliency of layered oxide cathodes”, *Advanced Materials* 34 2107326 (2021)

DOI: 10.1002/adma.202107326

[11] Naomi Omori, Sara Mosca, Ines Lezcano-Gonzalez, Ian K. Robinson, Luxi Li, Alex G. Greenaway, Paul Collier, Andrew M. Beale, Alessia Candeco, “A Multimodal Label-Free Imaging Study of Zeolite Crystals”, 2021 Conference on Lasers and Electro-Optics Europe and European Quantum Electronics Conference, CLEO/Europe-EQEC (2021)

https://opg.optica.org/abstract.cfm?URI=CLEO_Europe-2021-ch_9_6

[12] Ruyi Lian, Bingyao Huang, Ligu Wang, Qun Liu, Yuewei Lin and Haibin Ling, "End-to-end orientation estimation from 2D cryo-EM images", *Acta Cryst. D78*, 174–186 (2022).

<https://doi.org/10.1107/S2059798321011761>

[13] Hao Huang, Tapan Shah and Shinjae Yoo, "Deep Time Series Sketching and Its Application on Industrial Time Series Clustering", *IEEE BigData 2022*, (accepted)

*University
Abstracts*

Emergent and Tunable Properties in Ultrathin Film Structures

Tai Chang Chiang, Department of Physics, University of Illinois at Urbana-Champaign, Urbana, IL 61822

Self-identify keywords to describe your project: thin films, quantum materials, heterostructures, emergency, electronic structure

Research Scope

Our research is to explore emergent properties in ultrathin film structures made of charge density wave compounds, magnetic materials, superconductors, and topological materials. Quantum confinement and proximity coupling in these structures can lead to competition and entanglement of the different ordering effects and give rise to novel functionality. Samples are prepared by molecular beam epitaxy (MBE) and the flip-chip method [1,2]; the latter allows heterostructures to be prepared from chemically reactive component materials, which are incompatible with MBE growth. We employ angle-resolved photoemission spectroscopy (ARPES) for characterizing the electronic structure, including band gaps, band splittings, and surface states. X-ray diffraction is utilized to characterize atomic displacements resulting from electron-lattice and electron-phonon coupling as commonly observed in charge density wave systems. We also collaborate with leading experts in scanning tunneling microscopy and theoretical simulations for greater impact. The synthesis, spectroscopic, scattering, and simulation work paves the way for advanced measurements including (1) ultrafast x-ray scattering at free-electron-laser facilities, which yields information about the dynamics of the competing ordering effects, and (2) double photoemission spectroscopy, which yields information about particle-particle correlation, pairing mechanisms, magnetic exchange coupling, etc.

Recent Progress

Our work has resulted in a number of publications as listed below. A common theme of the publications is preparation of materials and ultrathin films and studies of entanglement and competition of electron and lattice ordering effects. Particularly notable are the following three projects:

1. Coherent electronic band structure of $\text{TiTe}_2/\text{TiSe}_2$ moiré bilayer [3]: Moiré structures, with their often unusual properties, have attracted much interest in recent years. Our study of $\text{TiTe}_2/\text{TiSe}_2$, formed by sequential growth of TiSe_2 and TiTe_2 monolayers, shows coherent emergent electronic structure as evidenced by ARPES band mapping (Fig. 1). The two monolayers adopt the same lattice orientation but incommensurate lattice constants. Despite the lack of translational symmetry, sharp dispersive bands are observed. The dispersion relations are distinct from those of

the component monolayers alone. Theoretical calculations illustrate the formation of composite bands by coherent electronic coupling despite the weak van der Waals interlayer bonding, which leads to band renormalization and energy shifts. The work illustrates the rich physics in moiré structures and the potential of creating novel properties from atomic layer engineering.

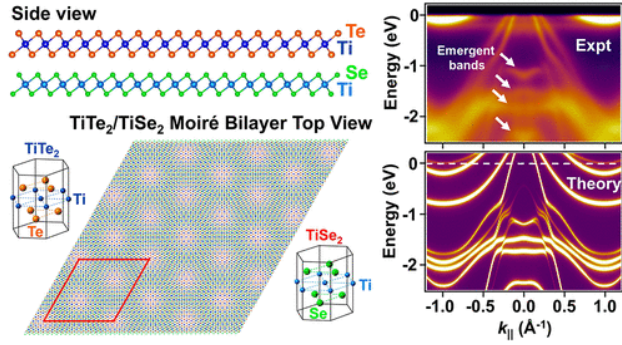


Fig. 1 Left: schematic atomic structure of TiTe₂/TiSe₂ moiré bilayer and the TiTe₂ and TiSe₂ unit cells. Lattice mismatch between the two materials results in moiré modulation. Right: experimental and theoretical ARPES band structures.

2. Emergent and tunable topological surface states in complementary Sb/Bi₂Te₃ and Bi₂Te₃/Sb thin-film heterostructures [4]: Epitaxial thin-film heterostructures offer a versatile platform for realizing topological surface states (TSSs) that may be emergent and/or tunable by tailoring the atomic layering in the heterostructures. Sb and Bi₂Te₃ thin films with closely matched in-plane lattice constants are chosen to form two complementary heterostructures: Sb overlayers on Bi₂Te₃ (Sb/Bi₂Te₃) and Bi₂Te₃ overlayers on Sb (Bi₂Te₃/Sb), with the overlayer thickness as a tuning parameter. In the bulk form, Sb (a semimetal) and Bi₂Te₃ (an insulator) both host TSSs with the same topological order but substantially different decay lengths and dispersions, whereas ultrathin Sb and Bi₂Te₃ films by themselves are fully gapped trivial insulators. ARPES, aided by theoretical calculations, confirm the formation of emergent TSSs in both heterostructures (see Fig. 2). The energy position of the topological Dirac point varies as a function of overlayer thickness, but the variation is non-monotonic, indicating nontrivial effects in the formation of topological heterostructure systems. The results illustrate the rich physics of engineered composite topological systems that may be exploited for nanoscale spintronics applications.

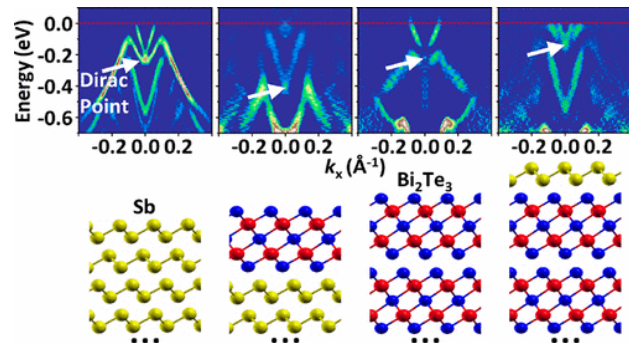


Fig. 2 ARPES band mapping of Sb/Bi₂Te₃ and Bi₂Te₃/Sb thin-film heterostructures reveals a topological Dirac point (indicated by an arrow), which moves in response to changes in the layering configuration; the nontrivial evolution agrees with first-principles simulations.

3. Dirac nodal line in hourglass semimetal Nb₃SiTe₆ [5]: Glide-mirror symmetry in nonsymmorphic crystals can foster the emergence of novel hourglass nodal loop states. We have performed detailed ARPES band mapping of a predicted topological hourglass semimetal phase in Nb₃SiTe₆ (see Fig. 3). Linear band crossings are observed at the zone boundary, which could be the origin of the nontrivial Berry phase and are consistent with a predicted glide quantum spin Hall effect; such linear band crossings connect to form a nodal loop. The saddle-like Fermi surface of

Nb_3SiTe_6 observed in our results helps unveil linear band crossings that could be easily missed in typical ARPES settings. In-situ alkali-metal doping of Nb_3SiTe_6 facilitated the observation of other band crossings and parabolic bands at the zone center correlated with accidental nodal loop states. Overall, our results complete the system's band structure description, help explain prior Hall measurements, and suggest the existence of a nodal loop at the zone center of Nb_3SiTe_6 .

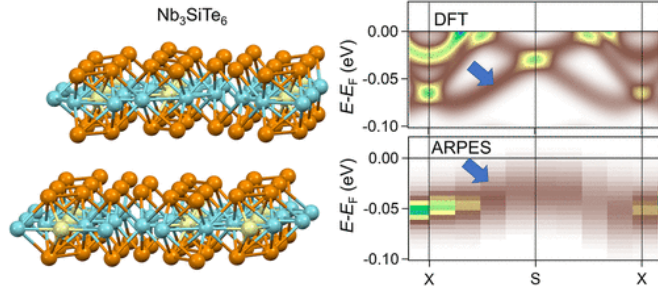


Fig. 3 Left: schematic showing the layered structure of the topological hourglass semimetal Nb_3SiTe_6 . Right: ARPES band mapping confirms the predicted Dirac nodal line band structure.

Future Plans

Our future plans include: (1) continued research on, and developing improved procedures for the creation of, novel materials and composite thin film systems prepared by molecular beam epitaxy (MBE) and the flip-chip method [1,2], (2) dynamic studies at the femtosecond time scale at free electron laser facilities, and (3) measurements using double photoemission spectroscopy to extract information about particle-particle correlations, pairing mechanisms, and magnetic exchange coupling effects, etc.

The flip chip method allows the creation of novel heterostructures from a broad selection of component quantum materials including charge density wave compounds, magnetic materials, superconductors, and topological materials. Competition and entanglement of the different ordering effects are expected to give rise to emergent properties and novel functionality. A new Nb sputtering source has just been added to our system, which allows the preparation of fresh Nb layers in situ. Nb is a superconductor with the highest transition temperature in the periodic table. We will test the Nb-based samples for superconducting proximity effects. A nitrogen gas line has been added for the preparation of NbN, which has a much higher superconducting transition temperature than that of Nb. We also plan to add an iron (Fe) sputtering source, which will allow us to incorporate ferromagnetic Fe into our flip chips. The exchange splitting in Fe is ~ 2 eV, a large effect easy to detect with ARPES and spin-ARPES. One experiment under planning is to couple Fe to ultrathin films of VSe_2 , which is predicted to be on the verge of a magnetic instability, to create a ferromagnetic 2D system. A few other candidate materials in the VSe_2 family will also be tested for emergent magnetic and spin properties when they are coupled to Fe. We will look for signatures of a topological ferromagnet, which is a subject matter of great prevailing interest.

Future studies will include dynamic measurements at the femtosecond time scale at free electron laser facilities. We (Yue Cao, Paul Evans, myself, and other collaborators) just finished a run at EuroXFEL on the incommensurate charge density wave compound TaS_2 . Of interest is the depinning and sliding of charge density waves under an applied electric field. The motions can be

explored by measuring the dynamical behavior of speckle diffraction patterns. While beam time at free electron laser facilities is still in short supply, the situation should improve as LCLS-II becomes available.

In many quantum materials, electron-electron correlation effects play a key role in giving rise to unusual and useful properties. Examples include the pairing interaction in superconductors, exchange interactions in magnetic materials, metal-insulator transitions, strange metal behavior, and band structure renormalization in general. Traditional spectroscopic methods (such as ARPES) yield a single-particle spectral function; the particle-particle correlation effects are averaged out. To extract the detailed two-particle correlation, double ARPES is a promising method. We are developing techniques and instruments for this purpose. The first step is to perform such measurements using laboratory laser sources. On the longer term, it would be very desirable to develop a special beam line based on a single-bunch mode at a synchrotron. We will begin with a conceptual development.

References

1. D. Flötotto, Y. Ota, Y. Bai, C. Zhang, K. Okazaki, A. Tsuzuki, T. Hashimoto, J. N. Eckstein, S. Shin, and T.-C. Chiang, "Superconducting pairing of topological surface states in bismuth selenide films on niobium," *Sci. Adv.* **4**, eaar7214 (2018).
2. Joseph A. Hlevyack, Sahand Najafzadeh, Meng-Kai Lin, Takahiro Hashimoto, Tsubaki Nagashima, Akihiro Tsuzuki, Akiko Fukushima, Cédric Bareille, Yang Bai, Peng Chen, Ro-Ya Liu, Yao Li, David Flötotto, José Avila, James N. Eckstein, Shik Shin, Kozo Okazaki, and T.-C. Chiang, "Massive suppression of proximity pairing in topological $(\text{Bi}_{1-x}\text{Sb}_x)_2\text{Te}_3$ films on niobium," *Phys. Rev. Lett.* **124**, 236402 (2020).
3. Meng-Kai Lin, Tao He, Joseph A. Hlevyack, Peng Chen, Sung-Kwan Mo, Mei-Yin Chou, and T.-C. Chiang, "Coherent electronic band structure of $\text{TiTe}_2/\text{TiSe}_2$ moiré bilayer," *ACS Nano* **15**, 3359 (2021).
4. Yao Li, John W. Bowers, Joseph A. Hlevyack, Meng-Kai Lin, and Tai-Chang Chiang, "Emergent and tunable topological surface states in complementary $\text{Sb}/\text{Bi}_2\text{Te}_3$ and $\text{Bi}_2\text{Te}_3/\text{Sb}$ thin-film heterostructures," *ACS Nano* **16**, 6, 9953 (2022).
5. Ro-Ya Liu, Angus Huang, Raman Sankar, Joseph Hlevyack, Chih-Chuan Su, Shih-Chang Weng, Meng-Kai Lin, Peng Chen, Cheng-Maw Cheng, Jonathan Denlinger, Sung-Kwan Mo, Alexei Fedorov, Chia-Seng Chang, Horng-Tay Jeng, Tien-Ming Chuang, and Tai-Chang Chiang, "Dirac nodal line in hourglass semimetal Nb_3SiTe_6 ," *Nano Lett.* **XX**, XXXX (2022).

Publications

1. Joseph A. Hlevyack, Liang Ying Feng, Meng Kai Lin, Rovi Angelo B. Villaos, Ro Ya Liu, Peng Chen, Yao Li, Sung Kwan Mo, Feng Chuan Chuang, and T.-C. Chiang, "Dimensional

- crossover and band topology evolution in ultrathin semimetallic NiTe₂ films," *npj 2D Mater. Appl.*, **5**, 40 (2021).
2. Rongjing Guo, Tai-Chang Chiang, and Huan-hua Wang, "Modulating effect of evanescent waves on thin-film growth," *Phys. Rev. B* **104**, 115429 (2021).
 3. Meng-Kai Lin, Tao He, Joseph A. Hlevyack, Peng Chen, Sung-Kwan Mo, Mei-Yin Chou, and T.-C. Chiang, "Coherent electronic band structure of TiTe₂/TiSe₂ moiré bilayer," *ACS Nano* **15**, 3359 (2021).
 4. Yi Wu, Wenhao Zhang, Yuan Fang, Shuai Lu, Li Wang, Peng Li, Zhongzheng Wu, Zhiguang Xiao, Chao Cao, Xiaoxiong Wang, Fang-Sen Li, Yi Yin, Tai-Chang Chiang, and Yang Liu, "Interfacial electron-phonon coupling and quantum confinement in ultrathin Yb films on graphite," *Phys. Rev. B* **104**, L161402 (2021).
 5. Hawoong Hong, Xinye Fang, Friederike Wrobel, Meng-Kai Lin, Zhan Zhang, Kevin Peterson, Anand Bhattacharya, Dillon Fong, Tai Chang Chiang, "On the development of order and interfaces during growth of ultrathin La₂CuO₄ films by molecular beam epitaxy," *ACS Applied Electronic Materials* (on line Nov. 8, 2021).
 6. Qiangsheng Lu, Jacob Cook, Xiaoqian Zhang, Kyle Y. Chen, Matthew Snyder, Duy Tung Nguyen, P. V. Sreenivasa Reddy, Bingchao Qin, Shaoping Zhan, Li-Dong Zhao, Pawel J. Kowalczyk, Simon A. Brown, Tai-Chang Chiang, Shengyuan A. Yang, Tay-Rong Chang, and Guang Bian, "Realization of unpinned two-dimensional dirac states in antimony atomic layers," *Nature Commun.* **13**, 4603 (2022).
 7. Joseph A. Hlevyack, Yang-Hao Chan, Meng Kai Lin, Tao He, Wei Hsiang Peng, Ellen C. Royal, Mei-Yin Chou, and T. C. Chiang, "Emergence of topological and trivial interface states in VSe₂ Films Coupled to Bi₂Se₃," *Phys. Rev. B* **105**, 195119 (2022).
 8. Meng-Kai Lin, Jun Zhao, Joseph A. Hlevyack, and T.-C. Chiang, "Cloning the Dirac cones of bilayer graphene to the zone center by selenium adsorption," *npj 2D Mater. Appl.* **6**, 78 (2022).
 9. Qiangsheng Lu Ching-Kai Chiu, Congcong Le, Jacob Cook, Xiaoqian Zhang, Xiaoqing He, Mohammad Zarenia, Paul F. Miceli, Chang Liu, Tai-Chang Chiang, Giovanni Vignale, and Guang Bian, "Dirac fermion cloning, moiré flat bands and magic lattice constants in epitaxial monolayer graphene," *Adv. Mater.* **34**, 2200625 (2022).
 10. Sean Howard, Arjun Raghavan, Davide Iaia, Caizhi Xu, David Flötotto, Man-Hong Wong, Sung-Kwan Mo, Bahadur Singh, Raman Sankar, Hsin Lin, Tai-Chang Chiang, and Vidya Madhavan, "Observation of a tunable isolated Dirac point in Ge(Bi_xSb_{1-x})₂Te₄," *Phys. Rev. Mat.* **6**, 044201 (2022).
 11. P. Chen, Y.-H. Chan, R.-Y. Liu, H. T. Zhang, Q. Gao, A.-V. Fedorov, M. Y. Chou, and T.-C. Chiang, "Dimensional crossover and symmetry transformation of the charge density waves in VSe₂," *Phys. Rev. B* **105**, L161404 (2022).
 12. Yao Li, John W. Bowers, Joseph A. Hlevyack, Meng-Kai Lin, and Tai-Chang Chiang, "Emergent and tunable topological surface states in complementary Sb/Bi₂Te₃ and Bi₂Te₃/Sb thin-film heterostructures," *ACS Nano* **16**, 6, 9953 (2022).

13. Meng-Kai Lin, Guan-Hao Chen, Ciao-Lin Ho, Wei-Chen Chueh, Joseph A. Hlevyack, Chia-Nung Kuo, Tsu-Yi Fu, Juhn-Jong Lin, Chin-Shan Lue, Wen-Hao Chang, Noriaki Takagij, Ryuichi Arafune, Tai-Chang Chiang, and Chun-Liang Lin, "Tip-mediated bandgap tuning for monolayer transition metal dichalcogenides, ACS Nano, **16**, 9, 14918 (2022).
14. Ro-Ya Liu, Angus Huang, Raman Sankar, Joseph Hlevyack, Chih-Chuan Su, Shih-Chang Weng, Meng-Kai Lin, Peng Chen, Cheng-Maw Cheng, Jonathan Denlinger, Sung-Kwan Mo, Alexei Fedorov, Chia-Seng Chang, Horng-Tay Jeng, Tien-Ming Chuang, and Tai-Chang Chiang, "Dirac nodal line in hourglass semimetal Nb₃SiTe₆," Nano Lett. XX, XXXX (2022).

Optical models and sample environments for resonant soft X-ray scattering of carbon nanostructured materials

Brian A. Collins, Washington State University

Resonant Soft X-ray Scattering (RSoXS), aqueous micelle nanocarriers, spectral analysis, density functional theory optical tensor, organic electronic nanostructure

Research Scope

The interactions and structures of organic small molecules and polymers on the nano-to-mesoscale drive materials properties and represent a critical realm for investigation of new technologies and medicines. For example, successful OLED displays and organic

photovoltaics represent a new class of printable and flexible devices that continue to drive technological innovation, while polymer nanoparticles (now used in some vaccines) hold a significant potential for next generation smart medicines or environmental remediation. In all cases, molecular-to-mesoscale assembly and ordering are critical for materials performance. In particular non-crystalline molecular orientation has been shown to significantly affect electronic processes at junctions within organic electronic devices. [1] Unfortunately, traditional techniques to probe nanostructure suffer from poor resolution and/or contrast, resulting in little information or requiring laborious and disruptive labeling. Near edge X-ray absorption fine structure (NEXAFS) spectroscopy can distinguish molecular species and bond orientation and has been demonstrated to be potentially powerful in revealing such information at a local level when paired with scattering. [1,2] Such unique sensitivity is limited, however, by the low penetration depth of soft X-rays and the delicate nanostructures involved that often require specific (aqueous) environments to form. The objective of the program is to develop an environmental control platform and scattering analysis methods for resonant soft X-ray scattering (RSoXS) [3] that enable the quantitative measurement of molecular identities, concentrations, relative orientations, and conformations within composite and hierarchical structures. In particular, local information of molecular orientation and conformation without crystallinity is a capability not possible with any other technique, but currently lacks detailed analysis methods. On the side of sample environment, we aim to develop and demonstrate microfluidic liquid flow cells that enable soft X-ray penetration while actively controlling temperature, flow, mixing, and concentration as well as applying electrostatic fields. Toward novel analyses methods, we aim to develop optical tensors from density functional theory (DFT) that quantitatively capture the near edge absorption fine structure, are chemically traceable, and enable characterization of molecular orientation within nanostructures. Such models and methods will be immediately applied to better understand the

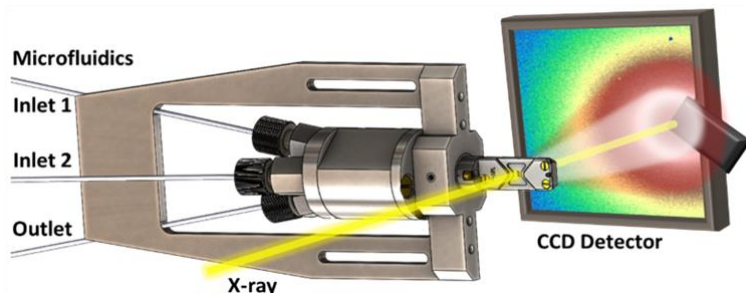


Figure 1: Microfluidic flow cell enabling sample environmental control in RSoXS.

ordering mechanisms of self-assembled molecular nanostructures and electronic devices such as transistors, solar cells, and aqueous nanocarriers.

Recent Progress

In the past two years, we have made considerable progress in advancing the capability of using microfluidic flow cells for soft X-ray scattering to investigate the structure of self-assembled polymer nanocarriers. **Figure 1** shows the microfluidic setup that mimics in-situ cells developed for electron microscopy. In our initial demonstration [4] we investigated the in-situ structure and dynamics of aqueous nanocarriers based on a block-copolymer micelle used as a delivery vehicle in applications such as medical therapeutics and oil-spill cleanup for environmental remediation. [5] The self-assembly and dynamic internal structure of these nanoparticles are critical for hydrocarbon encapsulation, where, for example, the hydrophobic core must be accessed by the target molecule for capture and released under controlled conditions. Dynamic details of the core diameter and target concentrations in the core under various conditions are inaccessible by any direct-measurement technique. Small angle neutron scattering (SANS) has been historically used to probe micelles' internal structure, using deuteration of either the molecule or the solvent environment. However, this chemical labeling is known to alter the structure in either case. [6,7] Furthermore, the multiple samples required and slow nature of SANS precludes monitoring dynamics. RSoXS at the carbon edge is particularly well suited for label-free investigations of dynamics within these structures.

Our initial study on these showed that this technique, combined with a new spectral analysis (see **Figure 2a**) could indeed fully characterize spatiochemical information – including quantifying chemical concentrations within the micelle corona. Impressively, the singular methyl group difference between the corona and core blocks of the polymer in the micelle (**Figure 2b** inset) provided sufficient contrast to extract this information. This bodes well for more complex multispecies nanostructures involving target encapsulants and functionalization moieties. We, furthermore, were able to demonstrate characterization of micelle dynamics in this study. Utilizing the dual microfluidic supply lines, we rapidly varied the concentration of micelles while monitoring the micelle-micelle interactions. Through this experiment, we revealed characteristic dynamics on the order of 10 seconds as well as several minutes (see **Figure 2b**).

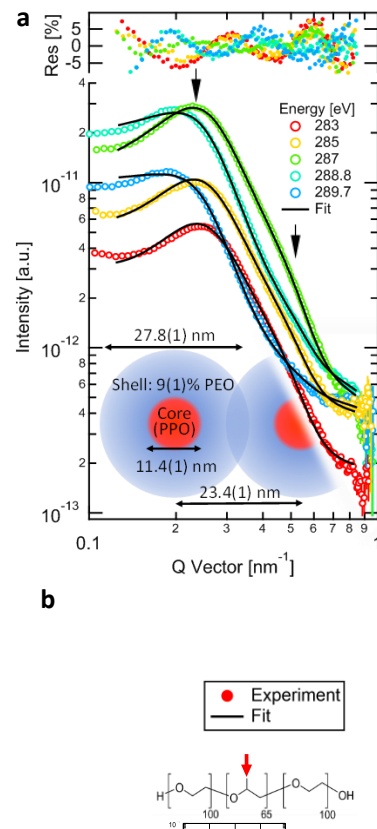


Figure 2: RSoXS spectral analysis can extract quantitative molecular composition inside nanostructures. (a) Simultaneous multi-resonance fit to extract both structural statistics and molecular composition (inset) of a Plurionics F127 organic nanocarrier used in drug-delivery. (b) F127 dynamics captured in a dual-flow experiment fit to a double exponential model. Inset is the F127 molecular structure, highlighting the single identifying chemical moiety – a methyl.

Finally, we have continued to apply this technique to novel charged polysoap micelles developed for oil spill remediation. [8] These micelles offer single molecule (unimeric) structures that enhance surface area for capture by orders of magnitude. Our analysis of multiple molecular weights and concentrations indicate an advantageous persistence of the micelle structure that may be dictated by the electric double layer of charge that stabilizes the structure. [9] This provides evidence for a design principle to enhance hydrocarbon capture of these nanoparticles.

Previous work on DFT-based optical tensors for RSoXS, established the Transition-Potential method as superior for qualitative accuracy of X-ray optical properties for molecular and polymeric systems. However, even these calculations would require refining the remaining inaccuracies with angle-resolved NEXAFS measurements for quantitative agreement if they were to be used in analyses of molecular orientation and conformation in resonant X-ray techniques. To accomplish this, we proposed possible clustering algorithms to reduce the numerous DFT molecular orbital (MO) transitions to a set of parameters that could be refined to spectroscopy measurements. Recently, we have explored and identified an algorithm that best groups and refines the transitions into principle features for a single optical model in quantitative agreement with angle-resolved NEXAFS spectroscopy of these

molecules in different packing structures (see **Figure 3**). [10] This model strategically includes transition dipole moments (TDM) that can be used to extract molecular orientation or molecular conformation from flexible molecules. Each TDM is additionally assigned to a major MO that is chemically traceable to moieties within the molecule (**Figure 3** inset) to aid in identification of chemical substituents involved in emergent electronic structures from conformational effects.

Future Plans

Moving forward in our development of in-situ RSoXS capabilities we plan to branch out in two primary ways. The first is to further develop our spectral analysis to quantify systems with many unique molecular components to enable routine investigation of target concentrations in complex nanocarrier systems. This leap would require combining our measurements with absolute

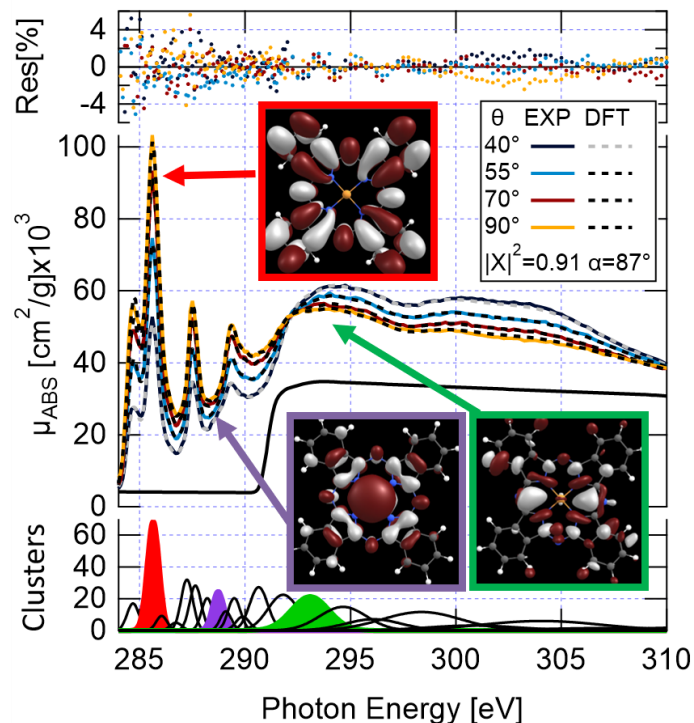


Figure 3: Experimentally Refined DFT Optical Tensor of Cu-Phthalocyanine. Transitions are algorithmically clustered into principle features retaining chemical origin and TDMs from the primary MO (examples inset & color coded). Inaccuracies of the model (dashed lines) are refined to angle-resolved NEXAFS spectroscopy (solid lines) for quantitative agreement.

scattering calibration. We have accomplished this in a separate previous study and are ready to combine it here. We plan to demonstrate this analysis on micelles containing molecular cargo and cross compare with other less-direct methods measuring uptake. The other branch advancing this technique is to develop capabilities to control sample temperature and electric fields. This will enable investigations of micelle stability and ion/electron transport in organic electronic materials. Both heating and field capabilities have been developed for analogous electron microscopy instruments involving electrodes-deposited on the SiN-windowed cells. Our custom system already incorporates electrical feedthroughs for these anticipated capabilities. We expect that temperature studies will reveal polymer architectures leading to ideal stability of micelle nanocarriers at body temperatures or even pH and temperature-triggered capture and release molecular of cargo. Studies investigating mixed conduction in organic electronic devices will target localization of ion transport within the polymer nanostructure.

Next steps in our optical model development involve further demonstrating the power of optical sensors we have generated in resonant X-ray reflectivity measurements on organic electronic thin film devices and RSoXS orientation characterization within organic nanostructures. Here we target prototypical systems and devices such as phthalocyanine small molecular transistors and thiophene based organic photovoltaics. Molecular orientation has been shown to be important in such devices, [1] but quantitative characterization of orientation angle, population, and proximity to device interfaces has not been possible to date. In addition, we will continue to expand the library of organic molecules with chemically traceable optical sensors, and in doing so, develop standard best practices for accurately and easily generating these X-ray optical models such that the practice can be utilized by other scientific fields studying molecular materials.

References

- [1] J. R. Tumbleston, B. A. Collins, L. Yang, A. C. Stuart, E. Gann, W. Ma, W. You, and H. Ade, *The Influence of Molecular Orientation on Organic Bulk Heterojunction Solar Cells*, *Nat. Photonics* **8**, 385 (2014).
- [2] B. A. Collins, J. E. Cochran, H. Yan, E. Gann, C. Hub, R. Fink, C. Wang, T. Schuettfort, C. R. McNeill, M. L. Chabiny, and H. Ade, *Polarized X-Ray Scattering Reveals Non-Crystalline Orientational Ordering in Organic Films*, *Nat. Mater.* **11**, 536 (2012).
- [3] B. A. Collins and E. Gann, *Resonant Soft X-Ray Scattering in Polymer Science*, *J. Polym. Sci.* **60**, 1199 (2022).
- [4] T. McAfee, T. Ferron, I. A. Cordova, P. D. Pickett, C. L. McCormick, C. Wang, and B. A. Collins, *Label-Free Characterization of Organic Nanocarriers Reveals Persistent Single Molecule Cores for Hydrocarbon Sequestration*, *Nat. Commun.* **12**, 1 (2021).
- [5] A. M. Bodratti and P. Alexandridis, *Formulation of Poloxamers for Drug Delivery*, *J. Funct. Biomater.* **9**, (2018).
- [6] T. P. Russell, *Changes in Polystyrene and Poly(Methyl Methacrylate) Interactions with Isotopic Substitution*, *Macromolecules* **26**, 5819 (1993).
- [7] N. J. Chang and E. W. Kaler, *The Structure of Sodium Dodecyl Sulfate Micelles in Solutions of H₂O and D₂O*, *J. Phys. Chem.* **89**, 2996 (1985).
- [8] P. D. Pickett, C. R. Kasprzak, D. T. Siefker, B. A. Abel, M. A. Dearborn, and C. L.

- Mccormick, *Amphoteric, Sulfonamide-Functionalized “Polysoaps”*: CO₂-Induced Phase Separation for Water Remediation, *Macromolecules* **51**, 9052 (2018).
- [9] D. Grabner, P. D. Pickett, T. R. McAfee, C. L. McCormick, C. Wang, and B. A. Collins, *Molecular Weight-Independent Anionic Polymer Micelles Characterized via in-Situ RSoXS*, Prep. (2023).
- [10] V. Murcia, O. Alqahtani, and B. A. Collins, *Merging Experiment and Theory for Chemically Traceable and Quantitatively Accurate X-Ray Optical Tensors of Organic Molecules*, Prep. (2023).

Publications

1. T. McAfee, T. Ferron, I. A. Cordova, P. D. Pickett, C. L. McCormick, C. Wang, and B. A. Collins, *Label-Free Characterization of Organic Nanocarriers Reveals Persistent Single Molecule Cores for Hydrocarbon Sequestration*, *Nat. Commun.* **12**, 1 (2021).
2. B. A. Collins and E. Gann, *Resonant Soft X-Ray Scattering in Polymer Science*, *J. Polym. Sci.* **60**, 1199 (2022).
3. D. Grabner, P. D. Pickett, T. R. McAfee, C. L. McCormick, C. Wang, and B. A. Collins, *Molecular Weight-Independent Anionic Polymer Micelles Characterized via in-Situ RSoXS*, In Preparation (2023).
4. V. Murcia, O. Alqahtani, and B. A. Collins, *Merging Experiment and Theory for Chemically Traceable and Quantitatively Accurate X-Ray Optical Tensors of Organic Molecules*, In Preparation. (2023).
5. N. Tokmoldin, B. Sun, F. Moruzzi, A. Patterson, O. Alqahtani, R. Wang, B. A. Collins, I. McCulloch, L. Luer, C. J. Brabec, D. Neher, and S. Shoaee, *On the Impact of the Energy Level Offset on Carrier Recombination and Fill-Factor in Organic Solar Cells*, In Preparation. (2023).

Resonant coherent diffractive imaging of complex materials

Riccardo Comin, Massachusetts Institute of Technology

Keywords: Resonant X-ray scattering; lensless Bragg imaging; single-shot imaging; electronic/magnetic textures.

Research Scope

This project is centered on the development of new X-ray microscopy methodologies combining resonant X-ray scattering and coherent lensless imaging to visualize nanoscale charge/spin textures in complex materials. Strongly correlated electron systems host various forms of electronic symmetry breaking which can be directly accessed in reciprocal space, but whose granular real-space domain structure is beyond the reach of scattering probes. The main goal of this research work is to develop and apply new X-ray microscopy approaches for spatial and spatiotemporal imaging of quantum materials at the nanoscale. We focus on two main directions: (1) establishing robust resonant coherent imaging methods to map out electronic domains in symmetry-broken quantum solids with finite-Q orders (charge-density-waves; antiferromagnetism; skyrmions); (2) developing single-shot phase retrieval approaches to perform stroboscopic imaging on non-isolated samples using ultrafast X-ray probes.

Currently, most efforts are directed at the demonstration of Bragg imaging and single-shot imaging using a Randomized Probe Imaging (RPI) approach that we developed at the start of this research program [1,2], alongside other efforts including maskless Fourier transform holography [3]. RPI relies on a special type of structured illumination to enable solving the phase problem from a single X-ray diffraction (speckle) pattern. The probe carries the information that produces redundancy in the experimental dataset and obviates the need for use of multiple exposures (as done, e.g., in ptychography) or support constraints (e.g., use of prepatterned masks). RPI is being actively used within this project for both projects (1) and (2). At the ALS, we are working in collaboration with S. Roy and D. Shapiro at the COSMIC beamline to demonstrate single-frame Bragg imaging with synchrotron X-rays. On a parallel track, we have been developing special optics to demonstrate single-shot imaging using RPI at free electron laser sources.

These ongoing efforts are timely as they are poised to leverage the recent developments of new highly coherent X-ray sources at both synchrotron (APS-U, ALS-U) and free-electron-laser facilities (LCLS-II). Developing new X-ray tools for the visualization of electronic textures at the nanoscale remains a major frontier that has already revealed key details of functional materials (semiconductor chips, batteries, catalysts, etc.), and whose application to quantum solids is the main scope of this work.

Recent Progress

To push forward the use of Randomized Probe Imaging (RPI) for stroboscopic X-ray microscopy, in 2022 we performed a demonstration experiment at the DiProI beamline of the FERMI Free Electron Laser (XFEL). Single-shot imaging is essential for studying the dynamical evolution of electronic and magnetic domains at the nanoscale and in systems undergoing spontaneous (thermal) fluctuations or subject to external drives such as photoexcitation or current/voltage bias. Because RPI operates based on single frames, it is natural to implement it for single-shot spatiotemporal imaging applications at FEL sources.

FEL sources are ideal for dynamical X-ray studies with high temporal resolution, however, they suffer from a variety of issues that are uncommon at synchrotron-based sources. The primary challenge is the instability of the photon beam between consecutive pulses (shot-to-shot variations), due to the stochastic nature of the lasing process. This is a potential issue for propagation-based phase contrast imaging methods [4], and also for RPI, which requires a detailed calibration of the input wavefield to operate. Consequently, we designed this experiment to study the feasibility and limitations of performing RPI at FEL sources. We succeeded in demonstrating that, on strongly scattering samples, it is straightforward to achieve the numerical-aperture (NA) limited resolution of RPI, even without correcting for wavefront variations. We imaged a Siemens star test target, using 20 nm light, achieving a 400 nm full-pitch resolution over a 40 μm field of view [Fig 1a]. This corresponds to a space-bandwidth product of over 30,000, nearly an order of magnitude larger than the highest space-bandwidth product achieved using CDI at an FEL [5]. Furthermore, we demonstrated that, with an addition to the algorithm that account for unstable illumination, we could recover the shot-to-shot variations in the input illumination [Fig 1b]. Finally, we turned to a weakly scattering magnetic multilayer of Co/Pt, imaged under circularly polarized illumination to reveal the magnetic domain structure. While these samples could not be imaged to an NA-limited resolution, we found that the RPI reconstructions “failed gracefully”, by producing shot-noise limited images with a lower effective resolution. This contrasts with methods like CDI, which typically fail by completely failing to converge.

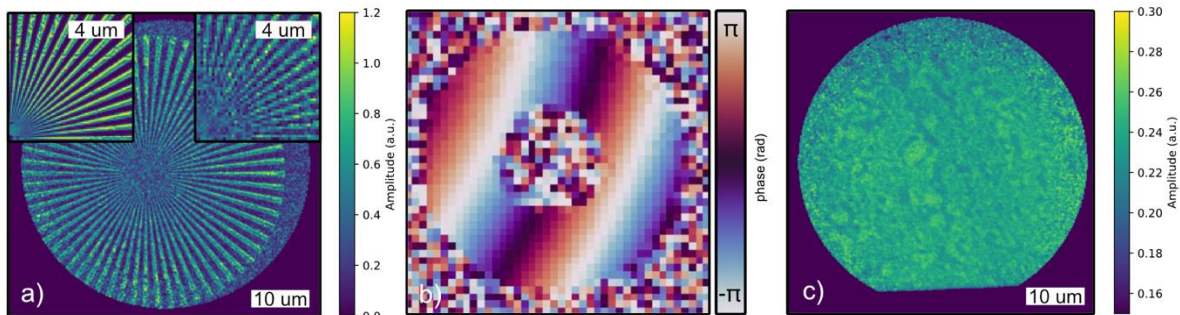


Figure 1 a) An example single-shot RPI reconstruction of the Siemens Star, with ptychography in the upper left for comparison. b) The distorted phase of the recovered illumination of a single FEL pulse. c) An RPI reconstruction of magnetic domains in a Co/Pt sample, synthesized from 200 shots.

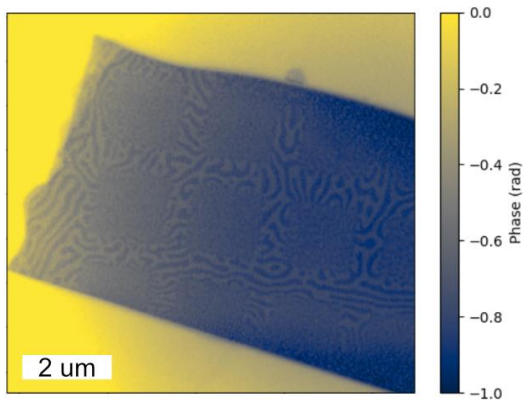


Figure 2 The reconstructed phase of a flake of Fe_3GeTe_2 containing doped regions, showing the magnetic domain texture

To highlight the broader applicability of ptychography based on randomized illumination, we studied thin samples of exfoliated 2D magnet Fe_3GeTe_2 using the COSMIC-Imaging beamline of the ALS, where we imaged their magnetic domain structure. In this case, the ptychography imaging was accelerated by the large, highly structured probe, and RPI was used to speed up alignment and overview scans following temperature steps. The sample itself contained pristine regions, as well as regions which had been modified using Au implantation via focused ion beam. We obtained clear images of the magnetic domain structure at a variety of temperatures [Fig 2], as well as evidence

that the domain structure changes as the Curie temperature is approached. We are currently analyzing these data to generate full images at each temperature point and understand the scientific implications of our measurements.

We have also been working to enable Bragg imaging of electronic phases with symmetry-breaking orders. The prototype system that our work has oriented around is NdNiO_3 , a rare earth nickelate which undergoes a transition from a paramagnetic metal to antiferromagnetic insulating state. This is an interesting system to study because the antiferromagnetic order produces a magnetic Bragg peak which is well-separated from the structural diffraction, and existing resonant X-ray scattering experiments and nanodiffraction confirm the presence of a rich nanoscale domain structure.

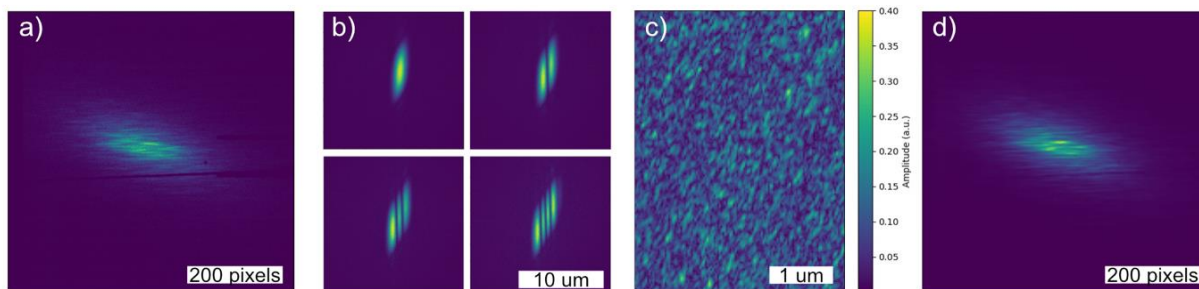


Figure 3 a) An example exposure from the Bragg ptychography dataset, showing the smearing due to the energy bandwidth. b) The top four modes of the reconstructed probe, used to allow for simultaneous incoherence and instability. c) An example reconstruction of the object, showing a realistic texture that nonetheless is not repeatably reconstructed. d) Diffraction data simulated from the texture in c, showing the plausibility (but not uniqueness) of the result.

In previous years, we had collected several datasets from thin films of NdNiO_3 on NdGaO_3 substrates, using 850 eV light tuned to the Ni L_3 edge. These data suffered from several issues, the

most egregious being a worse-than-nominal energy bandwidth, and instability in photon beam energy. This caused smearing of the diffraction pattern along a characteristic direction, while simultaneously inducing the diffraction pattern to jitter [Fig 3a]. Because of these issues, the data resisted analysis with basic ptychography algorithms. More recently, we worked to develop an algorithm capable of modeling and (in principle) overcoming this kind of simultaneous instability and incoherence. Reanalyzing the original data using this algorithm revealed insights into the structure of the probe [Fig 3b] but failed to produce interpretable images of the sample due to the significant degradation of the data.

Future Plans

We have a manuscript currently in preparation, reporting on our single-shot RPI experiments at the FERMI FEL. Our results realize the highest space-bandwidth product phase images ever extracted from single-shot x-ray experiments at a comparable resolution, and we are thus excited about the applications of this method as we continue to develop it, improving its quality and resolution. We have proposed further work at the same beamline, this time to incorporate this method into a pump-probe experiment to study the dynamics of ultrafast demagnetization. We intend to continue refining and supporting this application until we can be allocated time. Further, we will be applying to other FELs to extend our method to higher energies (soft X-rays).

Regarding the Bragg imaging project, we have been performing pilot experiments at the COSMIC-Scattering beamline of the ALS, as part of an ongoing collaboration with Sujoy Roy that will continue for the foreseeable future. This project builds on the methodological improvements taking place at this beamline to enable high-quality ptychography data in the Bragg geometry. The PI has been involved in the development of the science case for the future FLEXON beamline of the ALS-U, and these pilot experiments are an important part of this process. We are excited about the prospects of applying our improved algorithms to fresh data coming from these experiments.

References

1. K. Keskinbora, A. L. Levitan, R. Comin. *Maskless Fourier Transform Holography*. Optics Express **30**, 403 (2022).
2. Z. Guo, A. Levitan, G. Barbastathis, and R. Comin, *Randomized probe imaging through deep k-learning*, Optics Express **30**, 2247 (2022).
3. A. Levitan, K. Keskinbora, U. Sanli, M. Weigand, R. Comin. *Single-frame far-field diffractive imaging with randomized illumination*. Optics Express **28**, 37103 (2020).
4. Buakor, K., *et al.* *Shot-to-shot flat-field correction at X-ray free-electron lasers*. Opt. Express **30**, 10633 (2022).
- 5f. Kobayashi, A., *et al.* *Common architectures in cyanobacteria Prochlorococcus cells visualized by X-ray diffraction imaging using X-ray free electron laser*. Sci Rep **11**, 3877 (2021).

Publications

1. Z. Guo, A. Levitan, G. Barbastathis, and R. Comin, *Randomized probe imaging through deep k -learning*, Optics Express **30**, 2247 (2022).
2. A. Levitan, R. Comin, *Error metrics for partially coherent wavefields*, Optics Letters **47**, 2322 (2022).

Elucidating structural changes and nonradiative pathways of semiconductor nanocrystals under photoexcitation

Benjamin Cotts, Assistant Professor, Department of Chemistry and Biochemistry, Middlebury College

Jihong Ma, Assistant Professor, Department of Mechanical Engineering, University of Vermont

Keywords: Semiconductor Nanocrystals, time-resolved X-ray scattering, pair distribution function analysis, Molecular Dynamics simulations

Research Scope

This program focuses on investigating the structural signatures of nonradiative relaxation in colloidal semiconductor nanocrystals as a function of composition and ligand chemistry. Studies have shown that a nanocrystal's surface dramatically impacts exciton-phonon coupling and carrier cooling in nanocrystals, including the availability of nonradiative recombination pathways [1]. By employing ultrafast structural techniques at DOE user facilities combined with all-optical correlative measurements and atomistic simulations, we aim to quantify the structural features and origins of colloidal semiconductor nanocrystal nonradiative pathways. We make use of the user facilities at Argonne National Laboratory Advanced Photon Source as well as the SLAC MeV Ultrafast electron diffraction instrument (MeV-UED, part of SLAC LCLS user facility) to measure the nanocrystal structure under non-equilibrium conditions. Systematic variation of sample preparation is monitored with quantum yield as well as time- and temperature-resolved fluorescence spectroscopy to work towards generalizable design principles. Close theoretical feedback is provided by collaboration between Middlebury College and University of Vermont researchers.

Recent Progress (FY2023)

Time-resolved X-ray Diffraction measurements. In collaboration with Burak Guzelturk at Argonne National Laboratory we recently conducted preliminary measurements of semiconductor nanocrystals in a liquid jet at BL 11-ID-D. Strong signal was observed and analysis is ongoing to connect transient disorder to the surface chemistry, composition, and size of the nanocrystal samples. In particular, in collaboration with the Olshansky group at Amherst College, we have

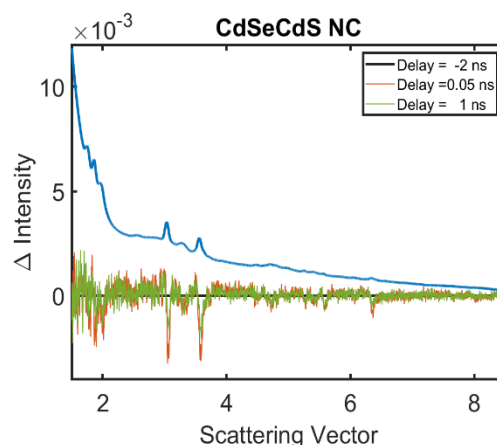


Figure 1. CdSe:CdS transient x-ray diffraction data. Scaled down reference integrated intensity vs. scattering vector data is shown in blue. Differential intensity at a time delay of 50 ps is plotted in red followed by a time delays of 1000 ps in green. The strong differential signal to noise is indicative of our ability to discern transient structural changes to the NC. Data was taken at ANL APS BL 11-ID-D in 2022.

varied the surface chemistry of CdSe:CdS nanocrystals to systematically control their radiative efficiency and measure the resulting samples at BL 11-ID-D.

Correlative in situ pair distribution function measurements and molecular dynamics simulations. In collaboration with Uta Ruett and Olaf Borkiewicz at Argonne National Laboratory's BL 11-ID-B as well as beamline scientist Burak Guzelturk, we recently conducted temperature-dependent pair distribution function measurements of nanocrystal samples as a function of size and surface chemistry. These studies will provide valuable inputs into our molecular dynamics simulations and help us to deconvolve thermal and exciton-phonon coupling effects on nanocrystal structure following photoexcitation.

Molecular Dynamics Simulations to understand atomistic structural changes. We employ molecular Dynamics (MD) simulations to help understand the atomistic origins of the time-dependent structural response of the NCs. Our goal is to acquire an atomistic understanding of the differences between baseline simple Debye-Waller heating responses and anomalous non-thermal results arising from strong exciton-phonon coupling. Large-scale simulations are carried out with equilibrium molecular dynamics (MD) using LAMMPS [2]. Current efforts are focused on adapting published potentials to fit our needs for the systems of interest. An example preliminary differential pair distribution function ($\Delta G(r, \Delta T)$) of PbS nanocrystals is included in Figure 2. This simulation focuses on a 5.7 nm PbS nanocrystal containing 4151 atoms, equilibrated in vacuum at 20 K using the Langevin thermostat implemented in LAMMPS. The same thermostat was subsequently applied to heat the nanocrystal to 298K, 318K, 338K, and 358K in 1 million timesteps, with each timestep of 1 fs.

A snapshot of an equilibrated nanocrystal at 338 K is presented in Figure 2. A 1.5-million-timestep of equilibration was conducted at each temperature before the radial distribution function [$g(r)$] calculation, which was averaged over 1 ns. The Velocity-Verlet time integration algorithm was applied throughout the simulation.

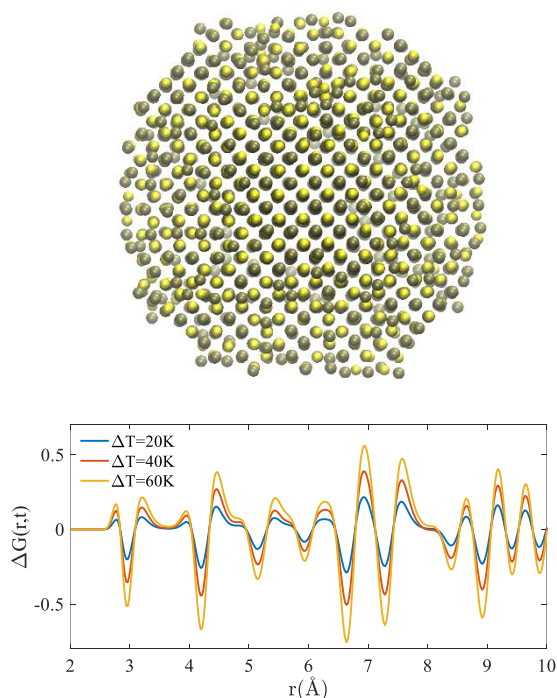


Figure 2. A MD snapshot of a bare equilibrated PbS QD with diameter ~ 5.7 nm. A differential pair distribution function ($\Delta G(r, \Delta T)$) for representative temperature jumps of 20, 40, and 60 K is included.

Future Plans

Future work includes further time-resolved and temperature-resolved photoluminescence studies to prepare optimized samples for study at DOE user facilities. We plan to continue to use correlative measurements such as *in situ* pair distribution function measurements in order to tune our atomistic simulations to our target systems and understand their fundamental behavior. Further simulation work will target a better understanding of the thermal relaxation behavior of nanocrystal thin films following photoexcitation.

In collaboration with Burak Guzelturk at Argonne National Laboratory's Advanced Photon Source, we plan to carry out time-resolved X-ray diffraction measurements of semiconductor nanocrystals in liquid jet and thin-film samples using the higher energy of the upgraded time-resolved research beamline at BL 25-ID. We aim to understand the prevalence of transient disorder and nonradiative recombination pathways as function of semiconductor nanocrystal surface chemistry.

References

1. B. Guzelturk, B. L. Cotts, D. Jasrasaria, J. P. Philbin, D. A. Hanifi, B. A. Koscher, A. D. Balan, E. Curling, M. Zajac, S. Park, N. Yazdani, C. Nyby, V. Kamysbayev, S. Fischer, Z. Nett, X. Shen, M. E. Kozina, M.-F. Lin, A. H. Reid, S. P. Weathersby, R. D. Schaller, V. Wood, X. Wang, J. A. Dionne, D. V. Talapin, A. P. Alivisatos, A. Salleo, E. Rabani & A. M. Lindenberg *Dynamic lattice distortions driven by surface trapping in semiconductor nanocrystals*. Nat. Commun. **12**, 1860 (2021).
2. S. Plimpton. Fast parallel algorithms for short-range molecular dynamics. Journal of computational physics, **117**(1), 1-19 (1995).

Publications

This is a new program (October 2022), with no publications currently.

Multidimensional Coherent Spectroscopy of van der Waals materials and heterostructures

Steven T. Cundiff, Department of Physics, University of Michigan

Keywords: transition metal dichalcogenides; spectroscopy; excitons; heterostructures; ultrafast optics; ultrafast microscopy

Research Scope

Although stable bulk materials provide a rich palette with diverse properties, man made nanostructures provide an avenue to achieving properties and functionality that cannot be found in bulk materials. Examples include semiconductor quantum wells, semiconductor quantum dots and recently, van der Waals heterostructures [3-1]. Nanostructures display not only unique static properties, but, in addition, the excitation dynamics can be strongly modified from that of the constituent materials.

Optical spectroscopy is particularly well suited to studying excitation dynamics in nanostructures because the dynamics often occur on ultrafast time scales (roughly defined as being less than a few picoseconds) and optical methods based on ultrashort light pulse are usually the best, if not the only, method of accessing these timescales. In semiconductor nanostructures, the optical response is often dominated by the formation of excitons, Coulomb bound electron-hole pairs, because excitons have a large oscillator strength, and therefore interact strongly with light causing them to display a nonlinear response at relatively low excitation levels. In traditional semiconductor nanostructures the exciton binding energy is of order 10 meV, so the excitonic response is only important at low temperatures. However, in transition metal dichalcogenides (TMDCs) the exciton binding energy is much larger, such that excitons are stable even at room temperature for single monolayers.

The excitonic resonances serve as sensitive probe of material properties, but are also very sensitive to many-body interactions. For example, the excitonic resonance often displays inhomogeneous broadening due to structural disorder in nanostructures because fluctuations in size result in fluctuations in the quantum confinement energy, which in turn causes the optical transition frequency to fluctuate. Since the exciton binding energy is sensitive to the dielectric environment, in 2D layered materials such as TMDCs, it can vary dramatically depending on the substrate and the presence of any adjacent layers. TMDC heterostructures can be made by stacking [3-1, 4-2]. Typically the excitonic resonance is sensitive to excitation level, shifting and/or broadening as the number of carriers changes.

While linear optical spectroscopy, such as absorption spectroscopy or photoluminescence spectroscopy, can provide significant information about exciton resonances, coherent spectroscopy provides a more complete picture, in part because of its ability to remove the effects of inhomogeneous broadening. The most common forms of coherent spectroscopy, generally based on transient four-wave-mixing, have been used for several decades to study excitonic

resonances in semiconductors. However over the last decade, multidimensional coherent spectroscopy (MDCS) has become the dominant method [6-3].

In conventional approaches to coherent spectroscopy, including MDCS, a coherent signal is separated from the excitation beams by arranging for it to be emitted in a unique direction. This “wavevector selection” of the signal restricts the smallest spot size that can be used because a tightly focused spot requires a large range of wave-vectors, which is incompatible with having well defined wavevectors for the excitation beams and signal.

We have developed and implemented a new approach to MDCS that relies on frequency selection, rather than wavevector selection, to separate the signal from the incident pulses. In this approach, the incident pulses are “frequency tagged” such that the coherent signal has a frequency that is unique from all of the incident pulses and all pair-wise interactions of them. This approach allows all the beams to be co-propagating, along with the signal and focused down to a diffraction limited spot. The observable can be a coherent signal [8-4], which is heterodyne detected, or a photocurrent or luminescence signal.

Performing MDCS with diffraction limited spots is critical for studying TMDCs because these layered two-dimensional materials have an indirect band gap in the bulk, but a single monolayer has a direct gap, resulting in strong photoluminescence. However, single monolayers are typically prepared by exfoliation, just like graphene, resulting in relatively small flakes, of order a few microns to a few 10s of microns. While traditional MDCS with wavevector selection has been performed on TMDCs, much of the work has been done on CVD grown samples where the spot spanned multiple flakes, possibly adding extrinsic broadening and dynamics due to flake boundaries. Thus realizing MDCS with diffraction limited spots is necessary to observe the intrinsic response. In addition, four-wave-mixing microscopy results show significant variation within a single flake.

In this project, we apply these recently developed methods for performing MDCS with diffraction limited spots to TMDC heterostructures, including heterostructures that display lateral confinement due to moiré effects. In the TMDCs we will address fundamental questions regarding nature of the broadening of the excitonic and trion resonances, how the broadening depends on the dielectric environment, on temperature, on excitation density and on material quality.

Recent Progress

This project started last year, thus this is the first update for it. Prior to it start, we built laser-scanning microscopy setup and demonstrated it use on TMD monolayers and heterostructures [5]. This work demonstrated that there is significant heterogeneity in the optical properties of the materials. For some optical parameters (e.g., homogeneous and inhomogeneous widths) the properties maybe (anti)correlated. Some parameters, such the coupling between layers, is remarkably robust and shows much less spatial heterogeneity.

As the first result supported by this project, we demonstrated rapid imaging based on four-wave mixing (FWM) by assessing the quality of TMD materials through measurement of their nonlinear response, exciton dephasing, and exciton lifetimes. We use a WSe₂ monolayer grown by chemical vapor deposition as a canonical example to demonstrate these capabilities. By comparison, we show that extracting material parameters such as FWM intensity, dephasing times, excited state lifetimes, and distribution of dark/localized states allows for a more accurate assessment of the quality of a sample than current prevalent techniques, including white light microscopy and linear micro-reflectance spectroscopy. We further discussed future improvements of the ultrafast FWM techniques by modeling the robustness of exponential decay fits to different spacing of the sampling points. Employing ultrafast nonlinear imaging in real-time at room temperature bears the potential for rapid in-situ sample characterization of advanced materials and beyond. The experimental concept for FWM imaging is shown in Fig. 1.

An image of the sample acquired with a conventional white-light microscope is shown in Fig. 2(a). The sample is a commercially available CVD-grown flake of WSe₂ (6Carbon Technologies), grown on a separate substrate and transferred onto a new substrate of SiO₂/Si. The monolayer shows an uneven structure due to residue remaining from the transfer process, a common problem in CVD-grown materials. A resonant (with the exciton) integrated reflectance image is shown in Fig. 2(b). Here, we use a sample point on the substrate to reference a reflectance of one and integrate over the laser spectrum spanning a range from 1600 meV to 1700 meV. The sample reflectance is influenced by both reflections from the sample and the back-reflected signal from the substrate that is absorbed in the sample. The spatial structure of the integrated reflectance coincides with the spatial structure visible in the white light microscopy image in Fig. 2(a). Nonetheless, differences (e.g., at the bottom of the sample) remain. A FWM intensity image of the sample is shown in Fig. 2(c). It indicates a strong spatial dependence of the FWM strength, which has been attributed to local strain profiles, changes in the dielectric environment, doping, trapped charges, impurities, defect densities, and distribution of dark states. Some regions of stronger FWM correlate with areas of weaker reflectance (e.g., the bright center structure). In contrast, some areas of weaker reflectance (e.g., towards the center-left of the sample) show an overall weaker FWM

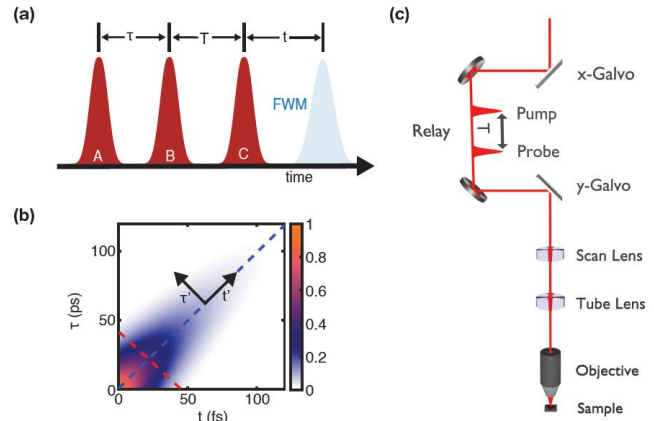


Fig. 1. (a) Schematic of a three-pulse FWM experiment. The FWM is emitted after the third pulse *C*. By varying different time delays, we can access the dephasing of the exciton coherence and decay of the exciton density. (b) Temporal evolution of the FWM signal for varying τ and t delays. Dephasing time and inhomogeneous linewidth can be extracted by taking slices along the axes spanned by the blue and red dashed lines. (c) Schematic of the custom-built laser-scanning microscope. The *x*- and *y*-Galvos are relayed onto each other using off-axis parabolic mirrors before being relayed onto the back of the microscope objective with a combination of scan and tube lens.

signal. Moreover, some areas of stronger reflectance, such as the bottom of the sample, show a stronger FWM signal. These observations highlight one of the benefits of nonlinear FWM imaging: while white light microscopy and even resonant linear micro-reflectance spectroscopy can be helpful for sample characterization, the

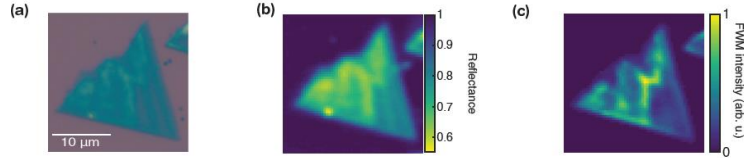


Fig. 2. (a) White-light microscopy image (false color) of a CVD-grown WSe_2 monolayer. (b) Resonant integrated reflectance from 1600 meV to 1700 meV of the WSe_2 monolayer. Here, we set the substrate to have a reflectance of one. (c) FWM intensity image of the WSe_2 monolayer.

sensitivity of FWM to material changes, including doping, defects, strain, dielectric environment, and dark state distribution changes, yields more detailed information about the quality of a sample.

Future Plans

We have begun efforts to study an new van der Waals material, NiPS_3 , which shows strong exciton-phonon coupling. It has a much weaker optical nonlinearity, thus we were not able to obtain a signal. We discovered a digital signal processing artifact that was producing a false signal, setting a detection threshold, we have developed a solution. However the cryostat failed, so we are currently waiting for it to be returned by the manufacturer before we can try again to measure spectra and images from the NiPS_3 sample. In addition, we are planning to study TMD heterostructures that show hybridized electronic states.

References

Put the list of references here using Times New Roman 10 pt. Please limit to no more than 5 papers. Provide full citation, including title and full author list.

1. K. Geim and I. V. Grigorieva, "Van der Waals heterostructures," *Nature* **499**, 419-425 (2013).
2. Q. Tong, H. Yu, Q. Zhu, Y. Wang, X. Xu, and W. Yao, "Topological mosaics in moiré superlattices of van der Waals heterobilayers," *Nat. Phys.* **13**, 356-362 (2016).
3. S. T. Cundiff and S. Mukamel, "Optical multidimensional coherent spectroscopy," *Phys. Today* **66**(7), 44-49 (2013).
4. E. W. Martin and S. T. Cundiff, "Inducing coherent quantum dot interactions," *Phys. Rev. B* **9**, 081301(R) (2018).
5. T. L. Purz, E. W. Martin, W. G. Holtzmann, P. Rivera, A. Alfrey, K. M. Bates, H. Deng, X. Xu and S. T. Cundiff, "Imaging dynamic exciton interactions and coupling in transition metal dichalcogenides," *J. Chem. Phys.* **156**, 214704 (2022).

Publications

1. T.L Purz, B.T. Hipsley, E.W. Martin, R. Ulbricht and S.T. Cundiff, "Rapid multiplex ultrafast nonlinear microscopy for material characterization," *Opt, Expr.* **30**, 45008 (2022).

Detecting Indistinguishable Photons at an X-ray Synchrotron Source

PI: Stephen M. Durbin, Department of Physics and Astronomy, Purdue University
Collaborators: XianRong Huang, Thomas Gog, Zahir Islam, & Jorg Stempfer, Argonne

Keywords: Multi-photon interference, photon degeneracy, indistinguishable x-rays, entanglement

Research Scope

Indistinguishable photons are a prerequisite for observing certain quantum optical behaviors, including the creation of entangled photon pairs with an interferometer. X-ray synchrotrons should produce indistinguishable photons; the probability that a given x-ray photon has an indistinguishable counterpart depends on the photon degeneracy factor n_{ph} , which is proportional to brightness. This factor exceeds 10% for 8 keV x-rays at the APS, so in principle the APS is already a copious source of indistinguishable x-ray photon pairs. This research effort aims to make the first observation of indistinguishable synchrotron x-ray photons by taking advantage of multi-photon interference: two indistinguishable x-ray photons at 8 keV, for example, will diffract from a crystal as if they were one photon with an energy of 16 keV (a phenomenon previously observed with optical photons). This is an example of multi-photon interference.¹ We utilize an x-ray interferometer to produce monochromatic x-rays, and a simple analyzer crystal to search for photons that diffract as if they had double the single photon energy.²

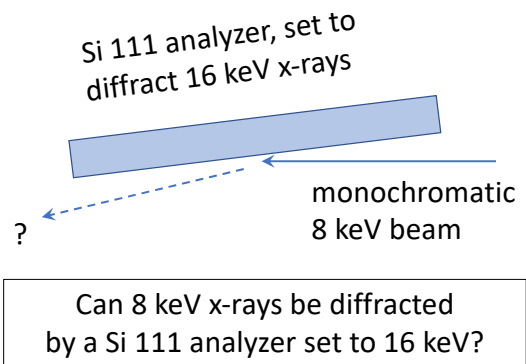


Figure 1: Analyzer crystal configuration for observing multi-photon interference. A Si (111) crystal is oriented to diffract 16 keV x-rays; single 8 keV photons will not be diffracted. The observation of diffracted 8 keV photons indicates a multi-photon response.

Recent Progress

A preliminary experimental test was conducted at the APS Sector 6 ID beamline in December 2022. A Si (220) Bonse-Hart Laue interferometer, fabricated by collaborators at the APS, was installed and set to diffract the 8 keV incident beam (plus harmonics) from the upstream Si (111) monochromator. An interferometer was utilized only because it could be a future testbed for creating entangled photons; a simpler diffractive element would likely suffice for this study. The forward-diffracted Laue beams were subsequently analyzed by a Si (111) crystal. The detector was a scintillator/photomultiplier tube with energy discrimination that distinguished between 8 and 16 keV pulses. When the analyzer Bragg angle was set for 8 keV, the detector observed the expected 8 keV peak plus a contribution from harmonics (16, 24 keV). When setting the analyzer angle to diffract at 16 keV, however, none of the 8 keV photons are expected to diffract from it. Preliminary results show rather convincingly that a significant peak at 8 keV is routinely observed.

This is taken as initial evidence for multi-photon diffraction at an x-ray synchrotron beamline, a signature of indistinguishable photons generated by a synchrotron source.

Future Plans

The preliminary results suggest that multi-photon diffraction is readily observable at the APS. These results should be taken with caution, however, since nothing like this has been previously reported. Our group will be repeating and extending these measurements at the APS some time before the long shutdown for the APS-U begins this April.

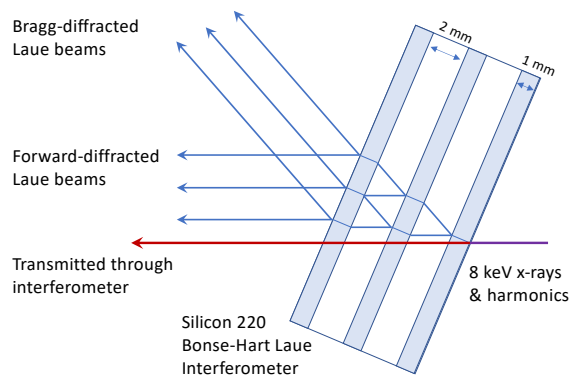


Figure 2: Configuration of the Bense-Hart Laue interferometer for generating diffracted beams for subsequent multi-photon diffraction analysis (see Fig. 1). The three forward-diffracted Laue beams were then diffracted by a Si (111) analyzer set to 16 keV.

References

1. J. Stohr, *Overcoming the diffraction limit by multi-photon interference: a tutorial*, *Advances in Optics and Photonics* **11**, 215 (2019).
2. S. M. Durbin, *Proposal for entangled x-ray beams*, *Journal of Applied Physics* **131**, 224401 (2022).

Publications

(None supported by BES in last two years.)

Dynamics of Complex Magnetic and Ferroelectric Polarization Configurations

Paul G. Evans, University of Wisconsin-Madison, pgevans@wisc.edu

Keywords: Dynamics, magnetism and ferroelectricity, coherence, nanodiffraction

1. Research Scope

Our program has the goal of developing novel x-ray scattering methods and applying them to challenging scientific problems in the materials science and materials physics of complex oxide electronic materials exhibiting magnetic or ferroelectric order. We take advantage particularly of recent advances ultrafast x-ray scattering methods to study the structural evolution and dynamics of thin-film oxide materials. The project considers three interconnected and related problems in the structure and dynamics of nanoscale order in ferroic materials:

1. Characterization of nanoscale structural and magnetic coupling in magnetic insulators. X-ray nanobeam magnetic diffraction and nanobeam imaging methods allow unanswered questions in the nanoscale magnetism of thin-film magnetic insulators to be addressed. X-ray magnetic diffraction techniques provide precise local magnetic information from materials and devices with nanoscale dimensions, a regime in which combined structural and magnetic information has not been previously available.
2. Understanding and controlling the dynamics of structural features associated with nanoscale ferroelectricity. Recent developments in materials design and epitaxial synthesis techniques have made it possible to create systematic variations in the orientation of oxygen octahedra with perovskite oxide thin films. Control of the octahedral orientation promises to yield a new approach to the control of functional properties such as ferroelectricity and magnetism, but systematic exploration faces artifacts due to subtle variations among substrates with different strain and symmetry. The project employs ultrafast time-resolved diffraction techniques to probe the rotation of octahedra systematically as a function of ultrafast optically induced distortion in BiFeO_3 , a model perovskite for which octahedral rotation predictions are already available. The resulting structural probe promises to be widely applied to problems associated with octahedra in thin films and at interfaces, including in improper ferroelectricity in superlattices.
3. Finite-wavevector magnetic dynamics and magnetic excitations. We are characterizing the magnetic excitations of thin-film magnetic materials using a novel combination of the developments in x-ray magnetic diffraction and ultrafast methods described in the previous two activities. Previous work has shown that the acoustic phonon dispersion can be accurately measured using high-dynamic range thin-film diffraction techniques. This ultrafast scattering approach is being combined with magnetic diffraction to measure the dispersion of spin waves in magnetic garnets. The dispersion and lifetimes of these excitations are key components underpinning models of spintronic devices based on the spin-Seebeck effect but are presently out of reach for optical probes and inelastic x-ray or neutron scattering techniques.

Together, these experiments present new directions in both x-ray scattering and materials research. The complementary use of ultrafast and nanobeam-related techniques allows these problems to be addressed in ways that would not otherwise be possible. The research directions benefit from recent developments in the capabilities of x-ray sources, particularly through the dramatic recent

improvement in the emittance of electron-storage-ring based synchrotron light sources and the femtosecond time resolution of free-electron lasers (FELs).

2. Recent Progress

2.1 Optically induced stress and distortion in ferroelectric thin films

We have conducted a series of studies that probe, describe, and exploit the distortion arising from optical excitation of ferroelectric and multiferroic oxides. The optical excitation of ferroelectrics leads to a non-equilibrium distribution of electrons among excited states. These states have a wide range of energies, up to approximately 1 eV above the band edge. The non-equilibrium electron population leads to the development of a mechanical stress and a resulting strain. Recent theory and computation studies have predicted that stress depends in detail on which states are populated.

We have used FEL x-ray diffraction at the Pohang Accelerator Laboratory to study the distortion arising from femtosecond optical excitation of the multiferroic complex oxide BiFeO₃. The combination of the experimental results and a detailed acoustic model reveal that a large component of the stress develops at sub-picosecond timescales. This component of the stress develops before the relaxation of the excited electrons to the band edge and provides insight into the mechanism through which the carriers couple to mechanical stress [P1].

The properties of the BiFeO₃ layers depend sensitively on the structure of the material, in particular, on the orientation of the FeO₆

oxygen octahedra within the rhombohedral unit cell. A second experiment at the Pohang Accelerator Laboratory FEL showed that the intensities of the x-ray reflections associated with the oxygen octahedral rotation vary after optical excitation. These experiments and the subsequent analysis were challenging because the reflections have low intensity and thus required the development of precise data normalization and analysis techniques. An analysis of the intensities of several x-ray reflections has shown that the intensity variation is a systematic function of the strain. We are in the process of comparing the observed intensity variation with density-functional-theory predictions of the dependence of the octahedral orientation on strain [R1].

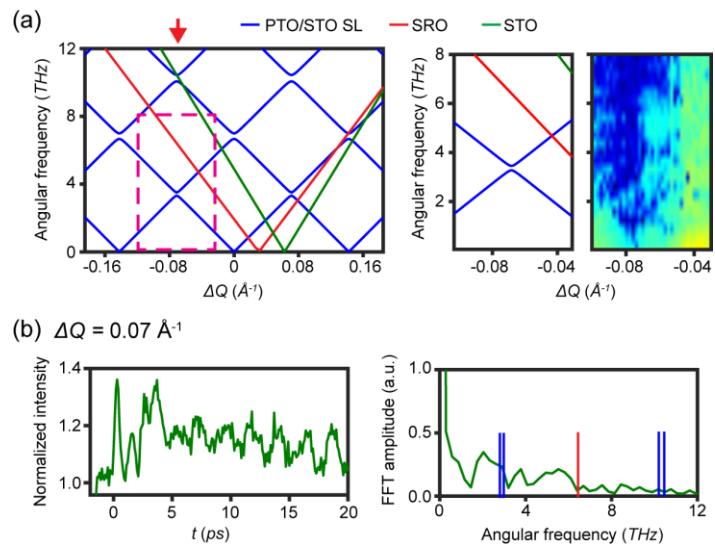


Figure 1. Dispersion of excitations in PTO-STO superlattice.

(a) Schematic of phonon dispersion a PTO-STO superlattice on an SRO bottom electrode on an STO substrate and time-domain Fourier-transform of intensity in the indicated wavevector-frequency range. (b) Dynamics at the value of ΔQ indicated by the arrow in (a). A new mode at 1.5 THz does not appear in the predicted dispersion.

2.2 Polarization and excitation dynamics in ferroelectric/dielectric superlattices

The ferroelectric polarization in ferroelectric/dielectric superlattices with nanoscale periodicities has a complex configuration. We have completed a series of studies of the dynamics of the polarization in these materials. The first two of these studies were conducted in oxide heterostructures with a metallic SrRuO₃ (SRO) bottom electrode layer, a key experimental detail. Optical absorption in the SRO layer is extremely strong, resulting in a distinct mechanical

arrangement. The optical pulse launches an intense strain pulse from the SRO layer, which perturbs the structure of the ferroelectric/dielectric heterostructure. The decoupling of structural and ferroelectric responses was a key component of a collaborative study of the THz-pumped dynamics of ferroelectric vortices at LCLS [P2]. The Q -dependence of the intensity oscillations due to the propagating strain pulse follows the phonon dispersion (Fig. 1(a)), providing the means to probe this dispersion experimentally. The time-dependence of the intensity at a wavevector corresponding to the mini-Brillouin zone center, measured at LCLS, is shown in Fig. 1(b). The Fourier transform of this intensity reveals a new mini-Brillouin-zone-center mode of excitation, also shown Fig. 1(b) [R3].

Crucially, however, the optically induced screening effect also induces polarization phenomena in the ferroelectric/dielectric superlattices. A series of experiments at the PAL XFEL revealed a polarization rotation phenomenon in a $\text{PbTiO}_3/\text{SrTiO}_3$ (PTO/STO) superlattice that led to a distinctive variation of the x-ray scattering from the ferroelectric domain pattern [P3]. In comparison with the PTO/STO system, $\text{BaTiO}_3/\text{CaTiO}_3$ (BTO/CTO) superlattices exhibit far stronger electrical coupling between the component layers. The optical screening induces a unique effect in BTO/CTO: an optically induced expansion in the BTO layer and a compression of the CTO [P4].

2.3 Magnetic dynamics and time-domain studies of magnetic excitations

Magnetic dynamics in ferrimagnetic and ferromagnetic materials underpins important magnetic and magnetoelectric phenomena, including notably the spin-Seebeck effect and other spin-caloritronic phenomena. There is a significant challenge in understanding the magnetic excitations of these systems because previous probes rely on magneto-optical effects limited to a narrow range of wavevectors near the center of the Brillouin zone. We have developed time-resolved x-ray magnetic diffraction techniques with the ultimate goal of probing magnetic dynamics, including possibly the spectrum of spin-wave excitations. The spin-wave excitations, often termed the magnon dispersion, across a wide range of wavevectors and are particularly important in insulating crystalline magnetic materials. We are focusing on epitaxial gadolinium iron garnet (GdIG) thin film, for which magnon-mediated spin transport is a proposed mechanism for the spin-Seebeck effect.

We conducted an experiment at LCLS in December, 2022 using an ultrafast optical pulse to generate an acoustic excitation in a Pt/GdIG thin film heterostructure. We had already conducted a time-resolved diffraction study at the FemtoMAX facility of the MAX-IV light source to determine the thermal properties of the Pt/GdIG/GGG heterostructure [P5]. We have further conducted a low temperature magnetic scattering study at the APS to verify the predicted temperature dependence of the magnetic scattering signal. Based on those studies, we have hypothesized that the acoustic excitation is transferred to a broad spectrum of magnetic dynamical phenomena via

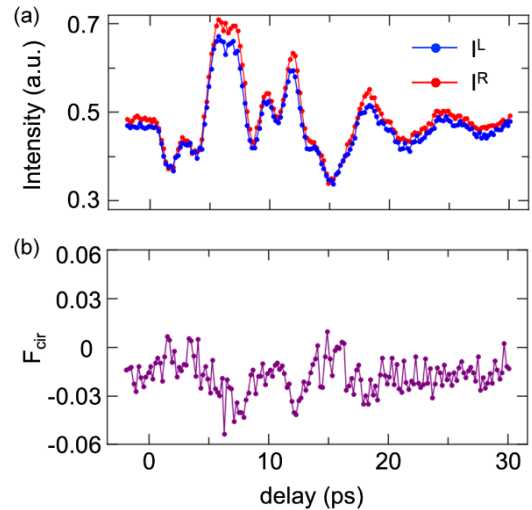


Figure 2. Magnetic dynamics in GdIG. Dynamics following optical excitation of a surface Pt layer at $t=0$ acquired finite $\Delta Q=5 \ 2\pi/d$ from a GdIG thin film with thickness $d=70$ nm. (a) Intensity at fixed ΔQ with left (L) and right (R) circular polarization. (b) The circular flipping ratio $(I_L - I_R)/(I_L + I_R)$ reflects the excitation of magnetic dynamics following optical excitation.

inverse magnetostriction phenomena. Magnetic information can be readily separated from the simultaneous measurements of the acoustic distortion. Both effects are measured simultaneously. Notably, a less-often-used π -polarized linear polarization contrast is available in Bragg diffraction geometries and provides complementary information [P6]. This work builds on our previous detailed x-ray magnetic diffraction and nanobeam characterization of thin GdIG layers at the ESRF [P6] and APS. The LCLS experiments included fabricating and characterizing a small in-vacuum electromagnet at the University of Wisconsin-Madison. The magnet was employed to establish the initial magnetic configuration of the GdIG thin film and to switch the magnetic state between initial configurations of opposite magnetization. The measurements shown in Fig. 2(a) employed a field saturating the magnetization of the GdIG layer in a direction maximizing the magnetic cross section and simplifying the analysis of the magnetic scattering signal. Measurements were conducted using left and right polarizations generated using a recently constructed x-ray phase plate setup at the LCLS's XPP beamline. Measurements with opposite magnetization (not shown) show approximately opposite values of the flipping ratio. Initial analysis of the results of the LCLS experiments show that there are both acoustic and magnetic effects and reveal signatures of the coupling between them. In Fig. 2(b), for example, the magnetic contrast F_{cir} varies during the period from 0 to 20 ps in which the acoustic pulse is propagating through the GdIG layer.

3. Future Plans

3.1 Magnetic dynamics

We plan to follow up the ultrafast magnetic diffraction experiments shown in Fig. 2 through analysis extracting the magnetic dynamics. Further experiments will expand the range of magnetic dynamic phenomena, for example, through probes of magnetic heterostructures, with a broader range of temperatures, and in systems relevant to magneto-optical phenomena.

3.2 Magnetic contrast in coherent scattering

We have conducted a resonant Bragg-diffraction ptychography experiment to probe the magnetic microstructure of GdIG. The experiment used the same GdIG L2 resonance as our previous nanobeam diffraction study [P6] and the December, 2022 LCLS experiment. The ptychography experiment was conducted in June 2021 at the European Synchrotron Radiation Facility (ESRF) in collaboration with Dr. Danny Mannix (European Spallation Source), Dr. Gerardina Carbone (MAX-IV), and Prof. Virignie Chamard (Aix Marseille University). The ptychography experiments relied on the large increase in brilliance arising from the upgrade of the ESRF to a multi-bend achromat storage ring. An initial analysis of the results has shown that the reconstruction of the structure (i.e. the conventional Bragg ptychography) was excellent. Analysis of the magnetic contribution to the signal is continuing.

References and Publications in Preparation

[R1] N. Li, H. J. Lee, D. Sri Gyan, Y. Ahn, E. C. Landahl, J. Carnis, J. Y. Lee, T. Y. Kim, S. Unithrattil, J. Y. Jo, S. H. Chun, S. Kim, S.-Y. Park, I. Eom, C. Adamo, D. G. Schlom, H. Wen, and P. G. Evans, “*Ultrafast optically induced perturbation of oxygen octahedral rotations in multiferroic BiFeO₃ thin films,*” in preparation (2023).

[R2] Y. Ahn, J. Zhang, D. A. Walko, S. O. Hruszkewycz, E. E. Fullerton, P. G. Evans, and H. Wen, “*Ultrafast switching of interfacial thermal conductance,*” in preparation (2023).

[R3] D. Sri Gyan, H. J. Lee, Y. Ahn, S. D. Marks, M. H. Yusuf, M. Dawber, D. Zhu, T. Sato, S. Song, H. Wen, and P. G. Evans, “*Terahertz Acoustics in Ferroelectric/Dielectric Superlattice,*” in preparation (2023).

Publications Supported by BES

- P1. H. J. Lee, Y. Ahn, S. D. Marks, D. Sri Gyan, E. C. Landahl, J. Y. Lee, T. Y. Kim, S. Unithrattil, S. H. Chun, S. Kim, S.-Y. Park, I. Eom, C. Adamo, D. G. Schlom, H. Wen, S. Lee, J. Y. Jo, and P. G. Evans, “*Sub-Picosecond Optical Stress Generation in Multiferroic BiFeO₃*” *Nano Lett.* **22**, 4294 (2022). <https://doi.org/10.1021/acs.nanolett.1c04831>.
- P2. Q. Li, V. Stoica, M. Pasciak, Y. Zhu, Y. Yuan, M. R. McCarter, S. Das, A. K. Yadav, S. Park, C. Dai, T. Yang, H. Jun Lee, Y. Ahn, S. D. Marks, T. Sato, M. C. Hoffmann, M. Chollet, M. E. Kozina, S. Nelson, D. Zhu, D. A. Walko, M. Trigo, A. M. Lindenberg, P. G. Evans, L.-Q. Chen, R. Ramesh, L. W. Martin, V. Gopalan, J. W. Freeland, J. Hlinka, and H. Wen, “*Observation of tunable collective excitations in polar vortices*,” *Nature* **592**, 376 (2021).
- P3. H. J. Lee, Y. Ahn, S. D. Marks, E. C. Landahl, S. Zhuang, M. H. Yusuf, M. Dawber, J. Y. Lee, T. Y. Kim, S. Unithrattil, S. H. Chun, S. Kim, I. Eom, S.-Y. Park, K. S. Kim, S. Lee, J. Y. Jo, J. Hu, and P. G. Evans, “*Structural Evidence for Ultrafast Polarization Rotation in Ferroelectric/Dielectric Superlattice Nanodomains*,” *Phys. Rev. X* **11**, 031031 (2021). <https://doi.org/10.1103/PhysRevX.11.031031>.
- P4. D. Sri Gyan, H. J. Lee, Y. Ahn, J. Carnis, T. Y. Kim, S. Unithrattil, J. Y. Lee, S. H. Chun, S. Kim, I. Eom, M. Kim, S.-Y. Park, K. S. Kim, H. N. Lee, J. Y. Jo, and P. G. Evans, “*Optically Induced Picosecond Lattice Compression in the Dielectric Component of a Strongly Coupled Ferroelectric/Dielectric Superlattice*,” *Adv. Electron. Mater.* **8**, 2101051 (2022). <https://doi.org/10.1002/aelm.202101051>.
- P5. D. Sri Gyan, D. Mannix, D. Carbone, J. L. Sumpter, S. Geprägs, M. Dietlein, R. Gross, A. Jurgilaitis, V.-T. Pham, H. Coudert-Alteirac, J. Larsson, D. Haskel, J. Stremper, and P. G. Evans, “*Low-Temperature Nanoscale Heat Transport in a Gadolinium Iron Garnet Heterostructure Probed by Ultrafast X-ray Diffraction*,” *Struct. Dyn.* **9**, 045101 (2022). <https://doi.org/10.1063/4.0000154>.
- P6. P. G. Evans, S. D. Marks, S. Geprägs, M. Dietlein, Y. Joly, M. Dai, J. Hu, L. Bouchenoire, P. B. J. Thompson, T. U. Schüllli, M.-I. Richard, R. Gross, D. Carbone, and D. Mannix, “*Resonant Nanodiffraction X-ray Imaging Reveals Role of Magnetic Domains in Spin Caloritronics*,” *Sci. Adv.* **6**, aba9351(2020).
- P7. Y. Ahn, M. J. Cherukara, Z. Cai, M. Bartlein, T. Zhou, A. DiChiara, D. A. Walko, M. Holt, E. E. Fullerton, P. G. Evans, and H. Wen, “*X-ray nanodiffraction imaging reveals distinct nanoscopic dynamics of an ultrafast phase transition*,” *Proc. Natl. Acad. Sci. USA* **119**, e2118597119 (2022). <https://doi.org/10.1073/pnas.2118597119>.
- P8. T. D. Frazer, Y. Zhu, Z. Cai, D. A. Walko, C. Adamo, D. G. Schlom, E. E. Fullerton, P. G. Evans, S. O. Hruszkewycz, Y. Cao, and H. Wen, “*Optical transient grating pumped x-ray diffraction microscopy for studying mesoscale structural dynamics*,” *Scientific Rep.* **11**, 19322 (2021). <https://doi.org/10.1038/s41598-021-98741-y>.
- P9. Y. Ahn, A. S. Everhardt, H. J. Lee, J. Park, A. Pateras, S. Damerio, T. Zhou, A. D. DiChiara, H. Wen, B. Noheda, and P. G. Evans, “*Dynamic Tilting of Ferroelectric Domain Walls via*

Optically Induced Electronic Screening,” Phys. Rev. Lett. **127**, 097402 (2021).
<https://doi.org/10.1103/PhysRevLett.127.097402>.

Helical dichroism and coherent diffractive imaging with twisted x-ray beams

PI: Edwin Fohtung¹, Co-PI: Jian Shi¹

fohtue@rpi.edu; shij4@rpi.edu

¹Dept. of Materials Science and Engineering, Rensselaer Polytechnic Institute

Self-identify keywords to describe your project: orbital angular momentum, coherent diffractive imaging, helical dichroism, twisted x-ray beams, chiral materials

Research Scope

The objective of this program is to develop and exploit x-ray scattering and coherent diffractive imaging techniques that rely on twisted x-ray beams that carry orbital angular momentum (OAM) with opposite phase helicity to probe chirality in structural and electronic order parameters. An important manifestation of chirality is the interaction between materials and photons with handedness. The focus of this project is to develop new, coherent scattering and CDI techniques, whose scattering contrast mechanism relies on x-ray helical dichroism and circular helical dichroism of resonant scattering on elemental edges. The project will integrate theory and computational methods of electronic properties of chiral crystals, synthesis of chiral structures with the desired blueprint, and novel x-ray characterization techniques of such crystals using twisted x-ray beams to develop a new contrast mechanism. Our approach will be to utilize x-ray optics such as spiral zone plates that produce x-ray beams with OAM at synchrotrons and XFELs to probe prototypical and emergent materials that host chirality in either the structural and/or electronic phases.

Recent Progress

Probing the domain structure of DyMnO₃ : hosting chiral magnetoelectric vortex lines

We start by using Ptychographic X-ray Computed Tomography (PXCT) and X-ray fluorescent tomography with twisted beams to probe the structure of DyMnO₃ (DMO) at the CSAXS beamline of the Swiss light source. Hexagonal manganites RMnO₃ (R= Ho, Y, Dy) belong to an exciting class of *ferroic* materials exhibiting strong interactions between a highly frustrated magnetic system, the ferroelectric polarization, and the lattice. DMO possesses two major microscopic mechanisms for ferroelectricity (FE) generation, i.e., the inverse Dzyaloshinskii–Moriya interaction between Mn spin pairs and the exchange striction between Dy–Mn spin pairs, making it an aggressive model to address various opportunities for magnetoelectric (ME) controls. However, experimental research on operando probing of microscopic effects

associated with ME such as the local domain (FE, and ME) structure is hindered by technical the limitation of available optical, electron and standard x-ray diffraction probes. This motivated us to attempt to resolve the chiral vortex lines in bulk DMO crystals at Synchrotrons.

Our first attempt at the CSAXS beamline was to resolve the structure of a bulk DMO using twisted X-ray beams with no external perturbations such as electric or magnetic field on the sample. This will allow us to understand the strengths and limitations of X-ray twisted light matter interaction. Our core assumption is that the interaction of twisted wavefront of X-rays with a singularity-like changes in the materials complex electron density (associated with dislocation cores or the cores of topological polar vortices) will manifest different X-ray scattering signal for different helicity of the beam.

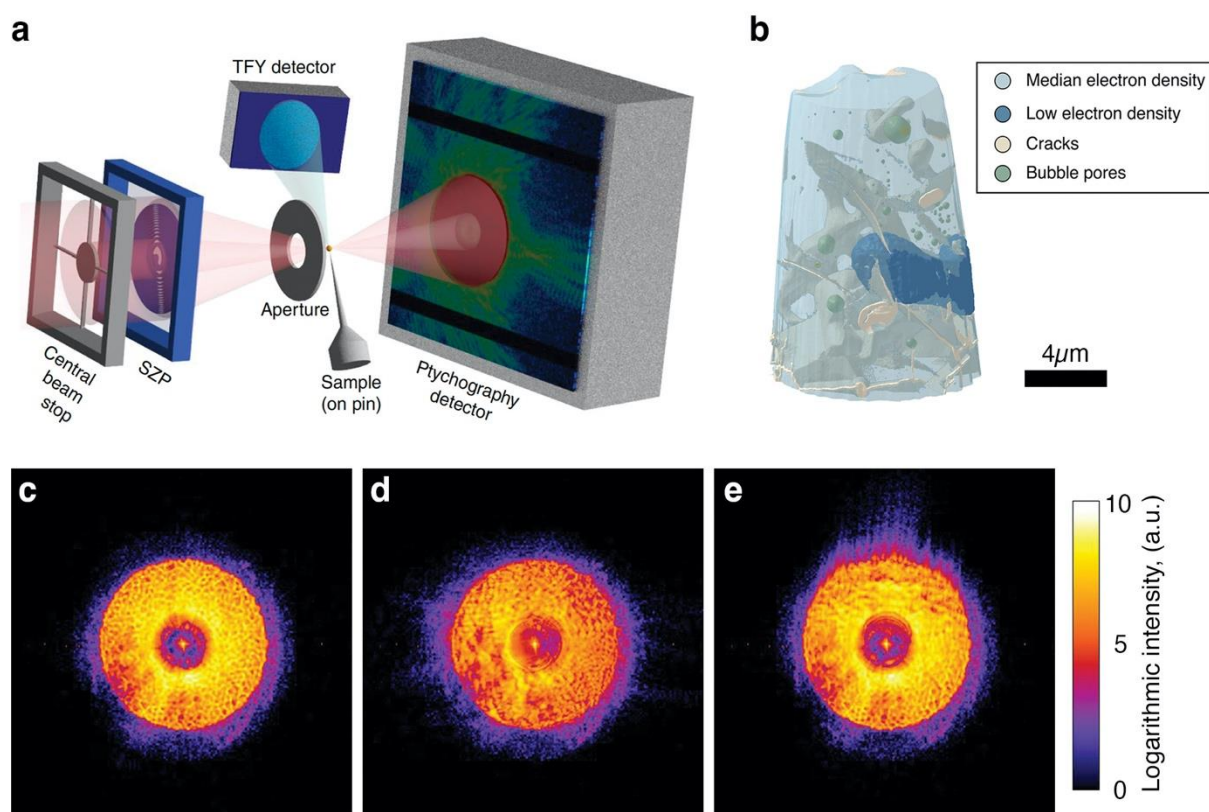
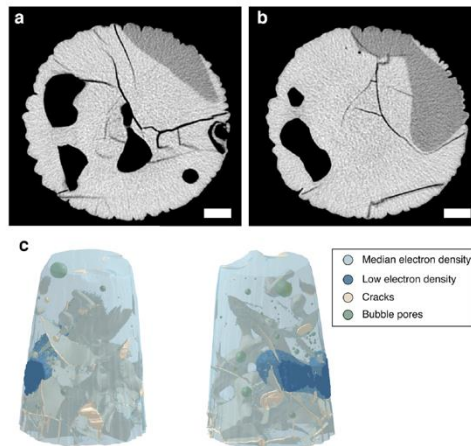


Figure 1. (a) Spiral Fresnel Zone Plates (SFZ) are used to generate X-ray beam carrying OAM. A central beam stop and an aperture ensure that only the first diffraction order of the zone plate reaches the sample, which is brought into the focus of the beam in solid form on a pin. Spectra are recorded using a total fluorescence yield (TFY) detector that is mounted on the side close to the DMO sample.(b) volume rendering of DMO. (c-e) Measured transmission intensity for different OAM of beam.

Ptychographic X-ray Computed Tomography (PXCT) and X-ray fluorescent tomography with twisted beams

In order to perform high-resolution ptychographic tomography the entire sample volume needs to be confined within a cylinder with a maximum diameter of about 100 microns, such that there is air at both sides of sample for all rotation angles from 0 to 180 degrees. We used focused ion beam (FIB) to cut a portion of a bulk DMO sample. Fig. 1a displays the PXCT acquisition setup: a Pilatus 2M detector was positioned 7.2 m downstream the DMO sample with a flight tube in between filled with helium. Another 500k Eiger detector (see Fig. 1a) was positioned at ~ 90 degrees from the sample at a distance of 70 mm for the total fluorescence yield (TFY) measurements. The hard X-ray regime offers two major advantages. First, the increased amplitude of the wave vector k has the consequence that higher multiples can contribute to the measured signal. These higher multiples interact with spatial derivatives of the exciting fields and are thus more sensitive to their spatial variation, that is, the phase vortex in the present case. Second, the short wavelengths of X-rays enable much smaller focal spots than in the optical domain, leading to a phase gradient in the illuminated area that is orders of magnitude higher. This enhanced phase gradient is favorable since, in actual experiments, the vortex beam and the chiral DMO under investigation are not perfectly aligned.



At CSAXS we acquired multiple datasets of ptychographic X-ray computed tomography and X-ray fluorescent tomography with twisted beams of different helicity from a sample of DMO shaped into a pillar by FIB. The data quality appears to be sufficient for the evaluation of the stated experimental goal. Currently we've reconstructed high quality ptychographic data with resulted resolution of 50nm (see Figure 2a & b). With this resolution we can clearly identify the overall structures of the DMO sample such as pores, cracks and regions of lower electron density (see Figure 2c). We can also resolve the sub-micron textures of the material. This data will be used to interpret the tomograms acquired in fluorescence mode where we expect signatures of the topological defects.

Figure 2. Preliminary analysis of acquired data. (a) and (b) are the slices through reconstructed tomograms of the electron density. Scale bars are 1 μ m. (c) is the 3D rendering of the sample volume acquired with ptychographic computed X-ray tomography.

Future Plans

We are currently working on the alignment, fitting, and analysis of the fluorescence data from DMO sample. The beamline apparatus delivered exceptional data quality that allowed us to

reconstruct and visualize the mesoscale defects such as internal cracks and pores with ~50nm spatial resolution.

The next step is to collect and analyze helical dichroism for different X-ray beam helicity as a function of energy. We shall probe across the Dy L₃ (7.790 keV, & L₂ (8.581 keV), Mn (K, L-edges if attainable). Next, we shall attempt operando (electric and/or magnetic field) BCDI using twisted X-ray beams collected in the vicinity of specific (h, k, l) reflection in individual grains or nanocrystals. BCDI will provide much higher spatial resolution and we anticipate to see the manifestation and cross-coupling of chirality in each of these individual ferroic orders. For instance, in ferroelectric domains, chirality can manifest itself in the spontaneous ferroelectric polarization order parameter as a self-organized array of vortices (left-handed) and antivortices (right-handed) sub-nm structures formed at the intersection of FE domain walls.

Such vortex/antivortex core are expected to be in the paraelectric phase in the monolith of ferroelectric nanocrystals. Also, in hexamanganites, the structural phase transition from one space group to another may lead to structural trimerization with six anti-phase domains (α^+ , β^+ , γ^+ , α^- , β^- , γ^-). We shall study the nature of FE domains near the observed pores and voids. We used BCDI to probe possible materials that could potentially harbor chirality in the electronic and/or structural order parameter(see publication #1 and Publication #2)

Once the methodology is understood, we shall use twisted X-ray beam to study other chiral systems using helical dichroic (B)CDI and other new techniques at synchrotrons such as the ALS, PSI, SOLEIL, MAX-IV, and the ESRF.

Publications from work supported by the DOE BES grant

1. Elijah Schold, Zachary Barringer, Xiaowen Shi, Skye Williams, Nimish Prashant Nazirkar, Yiping Wang, Yang Hu, Jian Shi & Edwin Fohtung. "*Three-dimensional morphology and elastic strain revealed in individual photoferroelectric SbSI nanowire.*" [*MRS Bulletin*,48 \(2022\)](#).

Abstract: Antimony sulfoiodide (SbSI) exhibits great promise for photovoltaic applications due to it being optically active in its ferroelectric phase. Previous studies on the SbSI system have relied largely on ensemble-averaging techniques and/or computational studies, wherein true volumetric enumeration of atomic displacement has remained ambiguous at the nanoscale. Here, we have mapped strain and the complex Bragg electronic density among the (002) planes in an individual SbSI nanowire using Bragg coherent diffractive imaging in hopes of guiding efforts to strain engineered SbSI

nanostructures for photovoltaic and other optoelectronic applications. We have found that the as-grown nanowire showed sharp faceting and high crystallinity, with no evidence of point or line mechanical defects in the (002) atomic displacement map (u_{002}). There is evidence, however, of planar defects in the wire that separate regions of positive and negative shear strain (τ_{32}) where these domain walls are parallel to the (011)-type facets. Increased Bragg electronic density near the center of the nanowire shows that the nanowires could have additional dangling bonds present there, increasing the likelihood that shells could bond to the wire for strain-engineering purposes.

Acknowledgements: E.F. and J.S. acknowledge support from the US Department of Energy, Award No. DE-SC0023148, and from the National Science Foundation under Award No. 2024972. E.F. also acknowledges funds from Rensselaer Polytechnic Institute. This research used resources of the Advanced Photon Source (APS), a US Department of Energy (DOE) Office of Science User Facility operated for the DOE Office of Science by Argonne National Laboratory (ANL) under Contract No. DE-AC02-06CH11357. We thank the staff at ANL and the APS for their support.

2. Xiaowen Shi, Nimish Nazirkar, Zach Barringer, Skye Williams, Ross Harder, and Edwin Fohtung. "*Topological defects and ferroelastic twins in ferroelectric nanocrystals.*" [*MRS Advances* 10 \(1557\), 2022.](#)

Topological defects (TDs) are at the heart of many intriguing phenomena in fields as diverse as biology and materials science. Emergent functionalities emanating from topological defects—such as the ability of domain walls to host itinerant electrons—make them potential hosts for charge conductivity, as well as superconductivity, as measured in twinned crystals of WO_3 . Thus, ferroelastic domains and domain boundaries are intriguing objects of study in fundamental and applied sciences. Here, we utilized Bragg coherent diffractive imaging (BCDI) to capture ferroelastic twins in an individual $\text{BaFe}_{12}\text{O}_{19}$ nanocrystal. BCDI is a lens-less diffractive imaging technique that relies on coherent properties of X-ray beams to resolve deformation fields in individual nanocrystals from measured coherent diffraction pattern. Here, we reconstruct the morphology and displacement field of (200) planes. Our reconstructions identify ferroelastic domains with homogenous displacement fields separated by domain boundaries. The efficacy of BCDI in studying TDs in three dimensions is demonstrated.

Acknowledgements: This work was supported by the US Department of Energy (DOE) Office of Science under award No. DE-SC0023148. This research used resources of the

Advanced Photon Source (APS), a US Department of Energy (DOE) Office of Science User Facility operated for the DOE Office of Science by Argonne National Laboratory (ANL) under contract No. DE-AC02-06CH11357. The Bragg coherent Diffraction Experiments were carried out at the Advanced photon source. Raw data were measured at the Advanced Photon Source Sector 34-ID-C and are permanently deposited there. The data supporting the findings of this study are available from the corresponding author upon request. We thank the staff at ANL and the APS for their support.

Ultrafast Electronic and Structural Dynamics in Quantum Materials

Nuh Gedik, MIT

Keywords: Photoinduced phase transitions, time and angle resolved photoemission spectroscopy, high harmonic generation, ultrafast electron diffraction

Research Scope

Discovery and control of novel phases of quantum materials has been a long-standing goal in condensed matter physics. Historically, a plethora of exotic phenomena has been realized by inducing phase transitions in thermal equilibrium through chemical substitution or via the application of external stimuli such as pressure or magnetic field. With the advent of time resolved techniques based on ultrafast laser pulses, realizing novel phases through nonequilibrium phase transitions induced by light has become a hotly researched frontier. These “light-induced phase transitions” can lead to new states that may or may not exist in thermal equilibrium.

Despite several examples of this phenomena in different systems, there are still many unanswered questions and the overarching principles (if any) that govern these phase changes are still not well known. For example, what are the similarities and differences in terms of physical mechanisms between the regular phase transitions and the ones that are induced by light? How do the properties of new phases created by light compare to the equilibrium phases that may exist in different parts of the equilibrium phase diagram? What determines the relaxation timescales and under what circumstances can these phases be made metastable? Could the coherence of light be utilized to engineer new band structures to facilitate these phase transitions?

The goal of this program is to answer these and related questions in light induced phase transitions and optical manipulation of order parameters. This is done by using and developing advanced time resolved optical and electron-based spectroscopies. Our main scientific trusts are studying photoinduced phase transitions in model charge density wave systems, using light to optically manipulate order parameters of complex phases, and realizing Floquet topological phases. In terms of technique development, we are working to improve the capabilities of high harmonic generation-based time and angle resolved photoemission spectroscopy (trARPES). Below, we will present examples of one published work and one ongoing work.

1. **Role of equilibrium fluctuations in light-induced order (*PRL* 127, 227401 (2021))**

Engineering novel states of matter with light is at the forefront of materials research. An intensely studied direction is to realize broken-symmetry phases that are “hidden” under equilibrium conditions but can be unleashed by an ultrashort laser pulse. Despite a plethora of experimental discoveries, the nature of these orders and how they transiently appear remain unclear. To this end, we investigate the rare-earth tritellurides ($R\text{Te}_3$), in which we have previously reported a

nonequilibrium charge density wave (CDW) that is suppressed in equilibrium and only appears after photoexcitation¹.

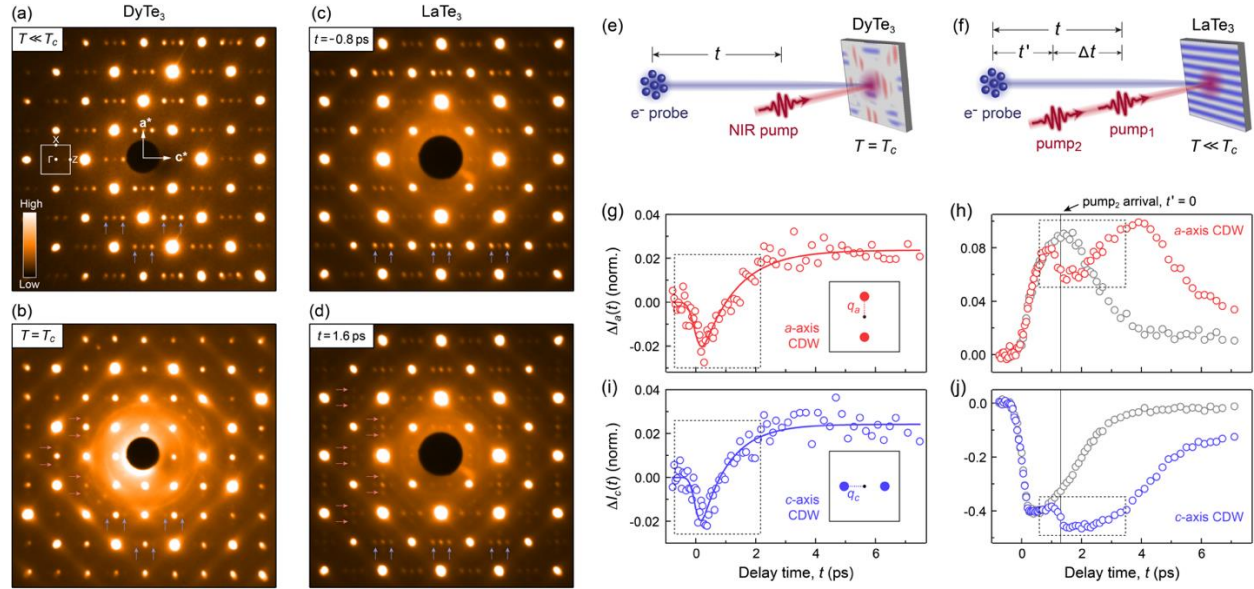


Figure 1 | Parallels between critical state in equilibrium and light-induced state out of equilibrium. (a)(b) Static electron diffraction patterns of DyTe₃ ($T_c = 306 \pm 3$ K) at 100 K and 307 K. (c)(d) Time-resolved diffractions of LaTe₃ before (c) and after (d) photoexcitation by an 80-fs, 800-nm laser pulse, measured at 307 K. Blue and red arrows indicate the CDW peaks along the c - and a -axis, respectively. (e)(f) Schematic UED setups for DyTe₃ and LaTe₃. Both samples were kept at 307 K. The incident fluence was 3.3 mJ/cm^2 in (e) and 1.0 mJ/cm^2 for each pump in (f). (g)–(j) Changes in the integrated intensities for a - and c -axis diffuse CDW peaks after photoexcitation. Integration areas are marked by solid circles in the insets. Traces are normalized by the average value of I_c before photoexcitation. In (h)(j), vertical lines indicate the arrival time of pump₂ at $\Delta t = 1.3$ ps. For reference, dynamics in the absence of pump₂ is shown in gray.

This light-induced CDW is evidenced in ultrafast electron diffraction (UED) measurements on LaTe₃ [Fig. 1(c)(d)], where photoexcitation gives rise to new CDW peaks along the crystallographic a -axis (red arrows) while the equilibrium CDW peaks along the c -axis are transiently suppressed (blue arrows). Remarkably, we found that the diffraction pattern of this photoinduced state is almost indistinguishable from that of a critical state in DyTe₃ near the CDW transition temperature (T_c) in equilibrium [Fig. 1(b)], both of which carry the hallmark of a restored symmetry between the a - and c -axes. Motivated by this parallel between the critical state in equilibrium and the photoexcited state out of equilibrium, we further perturbed these two states with a femtosecond near-IR pulse and compared their responses [Fig. 1(e)(f)]. Again, the photoinduced dynamics in these two regimes bear striking similarities, both featuring a transient reduction of the peak intensity followed by a swift recovery, an evolution perfectly mirrored in both a - and c -axes [see dashed rectangles in Fig. 1(g)–(j)].

Our results offer a generic mechanism for the creation of photoinduced states, which can emerge as order parameter fluctuations in the absence of long-range order. This insight suggests that

materials with strong fluctuations in equilibrium are promising platforms to host “hidden” orders after laser excitation. Similar to an equilibrium critical point, this out-of-equilibrium phenomenology should hold regardless of microscopic details, providing a guiding principle in our search for other light-induced orders.

2. Investigation of Floquet-Bloch states in graphene

Floquet-Bloch states are photon-dressed Bloch states which appear as replicas of the electronic band structure in energy axis. Just as spatially periodic crystal structure results in electronic bands that replicate along the momentum axis, temporally periodic electric field of a pump beam gives rise to band structure that repeats itself in the energy axis. Previously, we have observed Floquet-Bloch states using time- and angle-resolved photoemission spectroscopy (tr-ARPES) on the two-dimensional surface state of a topological insulator, Bi_2Se_3 ² and, we succeeded in separating them from Volkov states which are photon-dressed states of photo-emitted electrons³.

Although the manifestations of the Floquet-Bloch states have since been detected in other materials such as graphene and transition metal dichalcogenides, direct observation using tr-ARPES has not been conclusively achieved yet in systems beyond topological insulators. Recently, there was an attempt to observe Floquet-Bloch states at room temperature⁴ in graphene. The authors could not detect Floquet-Bloch states and attributed it to a short scattering time which destroys the Floquet-Bloch states.

We performed tr-ARPES measurements on graphene on SiC using linearly polarized 0.6 eV pump and 26.4 eV probe pulses at a temperature of about 35 K. Fig. 2a present the static spectra showing the Dirac cone at the K point. In Fig. 2b, the delay time snapshots with S-polarized pump pulses show the birth and decay of the replica as a function of delay time (static bands were cut in this figure to improve the visibility of the replica bands). To understand if the replica bands are caused by Floquet-Bloch or Volkov states, we searched for hybridization gaps. We did not observe hybridization gaps possibly due to low fluence of the available pump intensity. We are currently working on alternative ways of differentiating the signatures of Floquet-Bloch states. In particular, the intensity distribution of replica in constant energy cuts evolves as the pump polarization rotates.

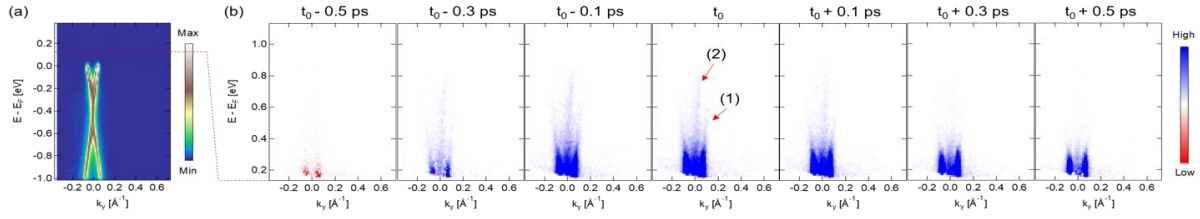


Figure 2 | Light dressed electronic bands in graphene (a) E- k_y cut from static spectrum. (b) E- k_y cuts from delay time snapshots. t_0 is the delay time when pump and probe pulses overlap. Note that the vertical axis ranges in E- k_y cuts of (a) and (b) are different. The color scale in (b) is saturated to clearly show the weak replicated bands. The color scale ranges for E- k_y cuts in (b) are all same. In (b), at t_0 , (1) indicates the excited states of the original band and (2) indicates the replica of the original band and the excited states.

We currently believe that parts of features in the evolution cannot be explained if we only consider Volkov states. To check whether this can be explained by Floquet-Bloch states, we are currently collaborating with theorists to perform simulations.

Future Plans

We will continue to investigate coherent light-matter interaction and light-induced phase transitions in different materials. In particular, in order to increase the visibility of Floquet-Bloch states in graphene and other materials, we will significantly improve our tr-ARPES setup by installing a second synchronized laser that will be dedicated for generating low frequency high fluence pump pulses. Secondly, we will use combination of ultrafast electron diffraction and tr-ARPES to study the competing a and c axis charge density waves in $R\text{Te}_3$. We will focus on the members of the $R\text{Te}_3$ family that display both orders in equilibrium. We will track evolution of these orders by overserving the gaps in the electronic dispersion and the satellite peaks in the diffraction. Beyond the charge density waves in $R\text{Te}_3$, we will also Finally, we will investigate the possibility of realizing a light induced topological phase transition in in situ grown thin films using molecular beam epitaxy (MBE). We will specifically focus on topological crystalline insulator $\text{Pb}_{(1-x)}\text{Sn}_x\text{Se}$ in which there exist a temperature and doping induced topological phase transition.

References

1. Kogar, A. *et al.* Light-induced charge density wave in LaTe_3 . *Nat Phys* **16**, 159–163 (2020).
2. Wang, Y. H., Steinberg, H., Jarillo-Herrero, P. & Gedik, N. Observation of floquet-bloch states on the surface of a topological insulator. *Science (1979)* **342**, 453–457 (2013).
3. Mahmood, F. *et al.* Selective scattering between Floquet-Bloch and Volkov states in a topological insulator. *Nat Phys* **12**, 306–310 (2016).
4. Aeschlimann, S. *et al.* Survival of Floquet-Bloch States in the Presence of Scattering. *Nano Lett* **21**, 5028–5035 (2021).

Publications

1. “Coherent detection of hidden spin-lattice coupling in a van der Waals antiferromagnet” Emre Ergeçen , Batyr Ilyas , Junghyun Kim , Jaena Park , Mehmet B. Yilmaz , Tianchuang Luo , Di Xiao , Satoshi Okamoto , Je-Geun Park , Nuh Gedik, PNAS, in print, (2023)
2. “Experimental realization of a single-layer multiferroic” Qian Song, Connor A. Occhialini, Emre Ergeçen, Batyr Ilyas, Kenji Watanabe, Takashi Taniguchi, Nuh Gedik, Riccardo Comin, *Nature* **602**, 601–605 (2022) ([pdf](#))
3. “Unconventional hysteretic transition in a charge density wave” B. Q. Lv, Alfred Zong, D. Wu, A.V. Rozhkov, Boris V. Fine, Su-Di Chen, Makoto Hashimoto, Dong-Hui Lu, M. Li, Y.-B. Huang, Jacob P. C. Ruff, Donald A. Walko, Z. H. Chen, Inhui Hwang, Yifan Su, Xiaozhe Shen, Xirui Wang, Fei Han, Hoi Chun Po, Yao Wang, Pablo Jarillo-Herrero, Xijie Wang, Hua Zhou, Cheng-Jun Sun, Haidan Wen, Zhi-Xun Shen, N. L. Wang, Nuh Gedik *Phys. Rev. Lett.* **128**, 036401 (2022) ([pdf](#))
4. “Magnetically brightened dark electron-phonon bound states in a van der Waals antiferromagnet” Emre Ergeçen, Batyr Ilyas, Dan Mao, Hoi Chun Po, Mehmet Burak Yilmaz, Junghyun Kim, Je-Geun Park, T. Senthil and Nuh Gedik *Nature Communications* **13**, Article number: 98 (2022) ([pdf](#))
5. “A versatile sample fabrication method for ultrafast electron diffraction”, Bie, Y. Q., Zong, A., Wang, X., Jarillo-Herrero, P., & Gedik, N., *Ultramicroscopy*, **230**, 113389 (2021) ([pdf](#))
6. “Role of equilibrium fluctuations in light-induced order” Alfred Zong, Pavel E. Dolgirev, Anshul Kogar, Yifan Su, Xiaozhe Shen, Joshua A. W. Straquadine, Xirui Wang, Duan Luo, Michael E. Kozina, Alexander H. Reid, Renkai Li, Jie Yang, Stephen P. Weathersby, Suji Park, Edbert J. Sie, Pablo Jarillo-Herrero, Ian R. Fisher, Xijie Wang, Eugene Demler, Nuh Gedik *Phys. Rev Lett.* **127**, 227401 (2021) ([pdf](#))
7. “Trimeron-phonon coupling in magnetite” Przemysław Piekarczyk, Dominik Legut, Edoardo Baldini, Carina A. Belvin, Tomasz Kołodziej, Wojciech Tabiś, Andrzej Kozłowski, Zbigniew Kakol, Zbigniew Tarnawski, José Lorenzana, Nuh Gedik, Andrzej M. Oleś, Jürgen M. Honig, and Krzysztof Parlinski *Phys. Rev. B* **103**, 104303 (2021) ([pdf](#))
8. "Exciton-driven antiferromagnetic metal in a correlated van der Waals insulator" Carina A. Belvin, Edoardo Baldini, Ilkem Ozge Ozel, Dan Mao, Hoi Chun Po, Clifford J. Allington, Suhan Son, Beom Hyun Kim, Jonghyeon Kim, Inho Hwang, Jae Hoon Kim, Je-Geun Park, T. Senthil, Nuh Gedik, *Nature Communications* **12**, 4837 (2021) ([pdf](#))
9. “Phonoritons as Hybridized Exciton-Photon-Phonon Excitations in a Monolayer h-BN Optical Cavity” Simone Latini, Umberto De Giovannini, Edbert J. Sie, Nuh Gedik, Hannes Hübener, Angel Rubio, *Phys. Rev Lett.* **126**, 227401 (2021) ([pdf](#))
10. “Unconventional ferroelectricity in moiré heterostructures” Zhiren Zheng, Qiong Ma, Zhen Bi, Sergio de la Barrera, Ming-Hao Liu, Nannan Mao, Yang Zhang, Natasha Kiper, Kenji Watanabe, Takashi Taniguchi, Jing Kong, William A Tisdale, Ray Ashoori, Nuh Gedik, Liang Fu, Su-Yang Xu, Pablo Jarillo-Herrero, *Nature* **588**, 71–76 (2020) ([pdf](#))

Elucidating Emergence in Strongly Coupled Hierarchical Functional Materials

Naomi Ginsberg, PI, David Limmer, co-PI, University of California, Berkeley; Dmitri Talapin, co-PI, University of Chicago; Samuel Teitelbaum, co-PI, Arizona State University

Research Scope

This project aims to establish new pathways to control emergence of structure and function in optically driven bottom up assembly of nanomaterials. We focus on important emerging complex material heterostructures where symmetries and bonding interactions are important on multiple scales: *strongly coupled nanocrystal superlattices in ionic solutions*. We seek to relate the structure and symmetries of the individual components of the heterostructure to the structure and symmetries of the superlattice that emerges. We study the bottom up self-assembly of superlattices made from a promising new form of Coulomb-stabilized nanocrystals and how laser illumination can aid this self-assembly. To do so requires probing the structural and electronic properties over multiple scales in space and time, which we do by using and advancing a series of complementary X-ray scattering experiments. Primarily, we characterize the microscopic fluctuations of the solution of nanocrystals using MHz X-ray photon correlation spectroscopy (XPCS); we characterize the transient charge restructuring of the electrolyte at the nanocrystal surface using time-resolved wide angle X-ray scattering (TR-WAXS); and we characterize the unusual structural and mechanical properties of the superlattices with coherent diffractive imaging (CDI) and time-resolved small angle X-ray scattering (TR-SAXS). We support and test our models derived from these XFEL measurements that we are advancing with *in situ* SAXS and in-house optical studies of the self-assembly phase transition, both with and without optical illumination. The ability to not only observe but to also develop new strategies to create and control emergent phenomena and functional materials will open new possibilities for complex materials functionalities from renewable energy supply and storage to ultra-selective catalysts.

Recent Progress

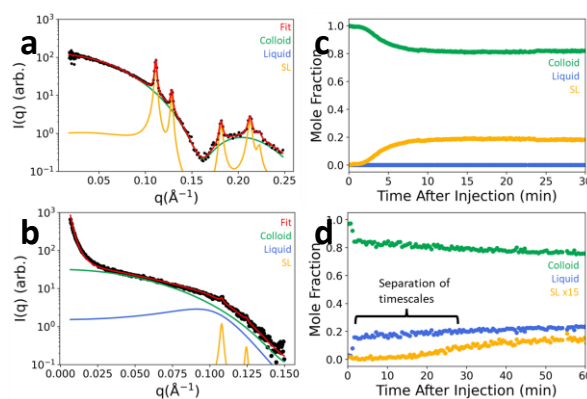


Figure 1. SAXS patterns of superlattices forming from colloid (a) and from liquid (b). Kinetics of one-step (c) and two-step (d) superlattice formation associated with SAXS patterns in a and b.

Strongly-coupled superlattice formation mechanisms. Elucidating the formation pathways of strongly-coupled superlattices from electrostatically stabilized nanocrystals in electrolytic solutions serves as a foundation for all XFEL studies by enabling targeting of specific solution, liquid, and solid phases to be studied. To do so, we developed a novel apparatus for use in *in situ* SAXS at the Stanford Synchrotron Radiation Lightsource (SSRL) and the Advanced Light Source (ALS). This enabled us to finely tune external control parameters like the solution conditions while obtaining SAXS patterns with ms time resolution. We developed quantitative

analysis approaches and fit time-dependent scattering patterns to determine the relative proportions of different phases as a function of time throughout the assembly process. We discovered that superlattices can form via a one-step process (superlattices form directly from colloidal phase) or a two-step process in which a metastable colloidal liquid forms from the colloidal phase and then the superlattices nucleate from within the liquid. This enabled us to determine the phase diagram and the kinetics of the associated assembly processes that target specific locations on the phase diagram for this enigmatic system. By directly validating these results with theoretical simulations, we uncovered the thermodynamic and kinetic parameters, e.g. nanocrystal density and solution properties, that determine the one-step or two-step formation pathway of superlattices and their associated design principles [1]. This effort allows us not only to exquisitely predict and control the products of self-assembly but also to develop analysis tools to rapidly identify phase diagram locations during XFEL experiments to ensure efficiency and success.

Microsecond XPCS of 3-phase colloidal nanocrystal system. *In situ* SAXS experiments revealed kinetics on timescales of ms-min of transitions between colloidal nanocrystal, liquid, and superlattice phases. To uncover the dynamics of these phases and the fluctuations associated with transitions between them, we used MHz XPCS at the European XFEL (EuXFEL). MHz XPCS enables determination of μs dynamical time scales on nm length scales, which is well-matched to the characteristic fluctuations of diffusing nanocrystals. By taking time autocorrelation functions of the coherently scattered X-ray patterns as a function of μs delay time, we uncovered sub- μs time scales associated with nanocrystal diffusion and $> 1 \mu\text{s}$ time scales associated with fluctuations of the metastable liquid phase that are distinct from free nanoparticle diffusion in solution. This is the first example of XPCS on a liquid that accesses the constituent particle scales, and we hope to extract microscopic details of the nanocrystal interactions within the liquid phase with further experiment and simulation.

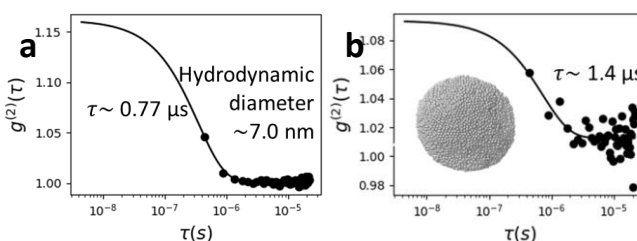


Figure 2. MHz XPCS of PbS nanocrystal colloid and liquid phases at $q = 0.01625 \text{ \AA}^{-1}$. Intensity-intensity autocorrelation functions with fits of colloid (a) and liquid (b) phases.

Ion restructuring. While high dielectric nanocrystals like PbS ($\epsilon \sim 170$) self-assemble into superlattices, nanocrystals of semiconductors with more typical dielectric constants like CdSe ($\epsilon \sim 10$) aggregate. Simulations [2] suggest that when the dielectric of the nanocrystal is larger than that of the solvent, ions in solution form shells of ion density at the nanocrystal surface. We have carried out static WAXS at NSLS-II to obtain pair distribution functions (PDFs) of ion reorganization at the surface of PbS (Fig. 3a) and CdSe (Fig. 3b) nanocrystals. Ions around PbS nanocrystals exhibit radially decaying oscillations of ion density, while ions around CdSe surfaces show no radial dependence, supporting our hypothesis that differences in ion density at the nanocrystal surface lead to differences in self-assembly of high- and low-dielectric nanocrystals.

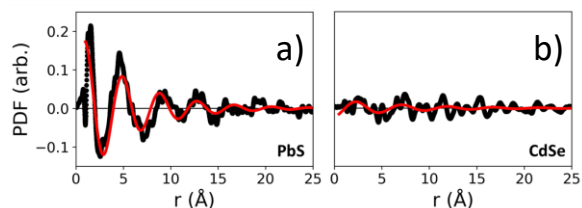


Figure 3: PDFs of ion reconstruction at the surface of a) high dielectric and b) low dielectric nanocrystals from static WAXS.

Quantitative measurements of nanocrystal interactions. Exact interaction potentials between highly charged nanocrystals is not possible to determine, but the integrated potential can be estimated by a Zimm analysis of X-ray scattering that is represented as the second virial coefficient (B2).[3] We find that for PbS nanocrystals, the repulsive potential is significantly higher using charged ligands in polar solvents than with native organic ligands in non-polar solvents. Interestingly, the B2 dependence on nanocrystal size reveals opposite behavior between the two different surface chemistries, decreasing (increasing) as nanocrystal size increases for charged (organic) surface ligands. This diverging behavior at small sizes may suggest that charged ligands organize themselves with a higher density around smaller nanocrystals leading to a higher surface charge density. Quantitative measurements of nanocrystal interactions have rarely been reported and provide new insight into the nanocrystal surface chemistry which ultimately determine the solution properties of these materials.

Theory. In the last year, the Limmer group in close collaboration with the Talapin and Ginsberg groups has continued to develop computational approaches for inverting time dependent X-ray scattering measurements to real space structure evolution in the context of driven colloidal assembly. These efforts have been partitioned into two thrusts. In the first, we have developed coarse-grained modeling approaches to simulate colloidal assembly *in silico*. Structures sampled from these dynamic models form a basis for fitting scattering patterns. Such a basis has allowed us to extract mechanistic information, allowing for the first time the demonstration of nonclassical two-step nucleation. Validating the structures with the scattering patterns also admits real space interpretation, as the full configuration space and all of its corresponding many body correlation functions are measurable within the molecular dynamics simulations. In the second thrust, we have further developed simulation tools to allow for the study of rare events in driven systems. This is a canonically hard problem, as traditional equilibrium tools used to span timescales in thermal systems require knowledge of the specific form of the stationary distribution and the ability to bias it directly. Leveraging recent advances in machine learning techniques, we have developed methodologies to access rare but important events in driven, assembling systems of colloids. This technique employs reinforcement learning approaches to optimize a guiding force that, when acting upon the system, drives it through the rare fluctuation in a manner consistent with the way the system would have naturally accessed the rare fluctuation. This has been used to begin studying in more detail the nonclassical nucleation pathways discovered previously in this collaboration.

Future Plans

Extending MHz XPCS. Our results at EuXFEL show that we can correctly quantify the fluctuations associated with nanocrystal diffusion and more complex phases using XPCS. While we were able to obtain dynamical timescales for the colloidal and metastable liquid phases, these were acquired at small wavevector ($Q = 0.01625 \text{ \AA}^{-1}$). By performing more measurements and optimizing our analysis pipelines, we will obtain timescales at higher wavevectors approaching the interparticle separation between nanocrystals in liquid and superlattice phases. This will enable us to determine key features of the interparticle interactions that we can directly compare with simulation to uncover the key dynamical processes that enable self-assembly of high-dielectric nanocrystal superlattices. We will compare these results with XPCS of low-dielectric nanocrystals to uncover the microscopic processes leading to arrest, which will help inform our nonequilibrium illumination protocols.

Photoinduced effects on TR-WAXS. Following our recent work on WAXS-PDF reconstructions of ion organization around PbS and CdSe nanocrystals, we intend to gain insight into how light can mediate self-assembly through photoexcitation driving ion reconstruction. Our hypothesis is that photoexcitation will increase the dielectric constant of the nanocrystal, thereby triggering a rearrangement of the surrounding ions to generate more distinct ion solvation shells characteristic of what is at a metallic nanocrystal surface. We were recently awarded beamtime at APS BioCARS beamline (14-ID-C) to perform TR-WAXS with sub-nanosecond temporal resolution and have pending sub-picosecond proposals at XFELs for TR-WAXS to extend these results, especially at LCLS, where the new undulators enable high-flux 25 keV photon energy capabilities for liquid scattering are a promising approach to reveal ion shell rearrangements that may mediate light-driven self-assembly.

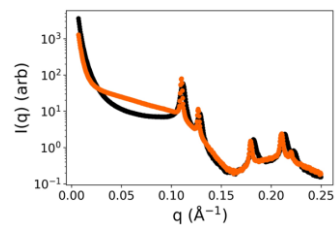


Figure 4: SAXS pattern of PbS nanocrystals self-assembled with and without CW, above-bandgap laser illumination.

Photoinduced effects on self-assembly. Recently, we carried out preliminary work using *in situ* SAXS at ALS to study the effect of continuous wave (CW), above-bandgap excitation on self-assembly of PbS nanocrystals. We found that photoexcitation slowed assembly kinetics and led to more ordered superlattices with larger lattice constants (**Fig. 4**), suggesting that the laser manipulates the interactions between nanocrystals due to some combination of heating and electronic effects. In upcoming experiments at SSRL, we will vary the illumination period and wavelength to elucidate the role of heating vs. electronic effects. We will also study the potential of illuminating CdSe nanocrystals to alter their interactions to promote self-assembly.

Far-from-equilibrium self-organization of magnetically driven nanoparticles. The combination of tight synthetic control of nanocrystal size and shape, colloidal stability, and precisely engineered magnetic properties make nanocrystals a unique platform for in-depth studies of non-equilibrium active matter. Although some encouraging results have been reported for driven micron-size particle realizations of active matter and chiral fluids, nanocrystals have several advantages owing to the higher tunability of their chemistry and interactions [1,4,5]. We will perform SAXS and XPCS of the structure factor $S(q)$ and dynamics of magnetically-driven superparamagnetic Fe_3O_4 colloidal nanocrystals to reveal yet unknown relations between activity, structural correlations, possible order formation and energy dissipation rate. The experimental data will be analyzed using theoretical methods developed by the Limmer group.

References

- [1] I. Coropceanu, E. M. Janke, J. Portner, D. Haubold, T. D. Nguyen, A. Das, C. Tanner, J. K. Utterback, S. Teitelbaum, M. Hudson, N. Sarma, A. M. Hinkle, C. Tassone, A. Eychmüller, D. Limmer, M. Olvera de la Cruz, N. Ginsberg, D. V. Talapin. Self-assembly of nanocrystals into strongly electronically coupled all-inorganic supercrystals. *Science* **2022**, 375, 1422-1426.
- [2] Guerrero García, G. I. and Olvera de la Cruz, M. “Polarization effects of dielectric nanoparticles in aqueous charge-asymmetric electrolytes.” *J. Phys. Chem. B* 118 (2014): 8854–8862.

[3] A. E. Saunders, and B. A. Korgel. Second Virial Coefficient Measurements of Dilute Gold Nanocrystal Dispersions Using Small-Angle X-ray Scattering. *J. Phys. Chem. B* **2004**, *108*, 16732-16738.

[4] Vishal Soni, Ephraim S. Bililign, Sofia Magkiriadou, Stefano Sacanna, Denis Bartolo, Michael J. Shelley, and William T.M. Irvine. *Nature Physics* **2019**, *15*, 1188-1194.

[5] I. Coropceanu, M. A. Boles, D. V. Talapin. Systematic Mapping of Binary Nanocrystal Superlattices: The Role of Topology in Phase Selection. *J. Am. Chem. Soc.* **2019**, *141*, 5728–5740.

Publications (past 2 years)

1. Coropceanu, Igor, et al. "Self-assembly of nanocrystals into strongly electronically coupled all-inorganic supercrystals." *Science* 375.6587 (2022): 1422-1426.

2. Das, A., Rose, D. C., Garrahan, J. P., & Limmer, D. T. (2021). Reinforcement learning of rare diffusive dynamics. *The Journal of Chemical Physics*, *155*(13), 134105.

3. Das, Avishek, and David T. Limmer. "Variational design principles for nonequilibrium colloidal assembly." *The Journal of chemical physics* 154.1 (2021): 014107.

4. J. M. Kurley, J.-A. Pan, Y. Wang, H. Zhang, J. C. Russell, G. F. Pach, B. To, J. M. Luther, D. V. Talapin. Roll-to-Roll Friendly Solution-Processing of Ultrathin, Sintered CdTe Nanocrystal Photovoltaics. *ACS Appl. Mater. Interfaces* 2021, *13*, 44165–44173.

5. J. K. Utterback, A. Sood, I. Coropceanu, B. Guzelturk, D. V. Talapin, A. M. Lindenberg, N. S. Ginsberg. Nanoscale Disorder Generates Subdiffusive Heat Transport in Self-Assembled Nanocrystal Films. *Nano Letters* 2021, *21*, 3540–3547.

Transient and Metastable Order Created by Ultrafast Light (DE-SC0012375)

V. Gopalan (Penn State, Lead), Y. Cao (MSD, ANL), L. Q. Chen (Penn State), J. W. Freeland (APS, ANL), A. M. Lindenberg (Stanford), L. W. Martin (LBNL/U. C. Berkeley), Vladimir Stoica (Penn State), H. Wen (MSD, ANL).

Keywords: Polar Supertextures, ferroelectric heterostructures, XFEL, Synchrotron, ultrafast optics

Research Scope

The central focus of the current project is to study the emergence and dynamics of a rich portfolio of complex topological structures. The ongoing project (DE-SC0012375) was triggered by experimental successes of members of this team in designing polar complexity in $(\text{PbTiO}_3)_m/(\text{SrTiO}_3)_n$ oxide superlattices that led to the emergence of supercrystals,¹ polar vortices,² and skyrmions³. These first-of-their-kind synthetic topological polar structures are collectively dubbed *polar supertextures*.

These polar textures involve structural modulations ranging from sub-angstrom-to-tens of nanometer scales and are created in a succession of stimulated phenomena from femtoseconds to milliseconds. The design space in these prototypical testbed structures is large enough (*e.g.*, materials, substrate strain, duty cycle, m/n , periodicity, and $m+n$) and the underlying physical interactions are established enough (*i.e.*, ferroelectricity, elasticity, electrostriction, boundary conditions) to poise the system on the verge of instability. We then drive such a system with an appropriate impulse (*i.e.*, an ultrafast pulse of light and/or field) to realize a very rich spectrum of complexity. It is essential to monitor ultrafast light-matter interaction processes at relevant timescales using state-of-the-art experiments at synchrotron (at Advanced Photon Source and, during the APS upgrade, at NSLS-II and SSRL) and XFEL (at LCLS, Spring-8, and PAL) facilities complemented with ultrafast optics and atomic and mesoscale computational methods. Using such an integrated approach, our team has uncovered the intricate structure of a polar supercrystal and emergent collective dynamics of polar vortices and skyrmions. This has driven our efforts in the past two years towards a deeper understanding of the science behind the emergence of these complex, extended structures as well as their collective behavior that is more the sum of its components.

Recent Progress

Our current grant (DE-SC 0012375) has been boosted by a current *LCLS Campaign* which has granted us six runs since 2018 for a total number of 25 shifts (eight runs since 2016 for a total of 32 shifts). This has led to some spectacular results and stimulated our ideas for renewal presented below. These runs were complemented with time at the SACLA, FERMI, PAL, and Paul Scherer XFELs and over 40 runs at the APS. Besides the published work (see annual report and

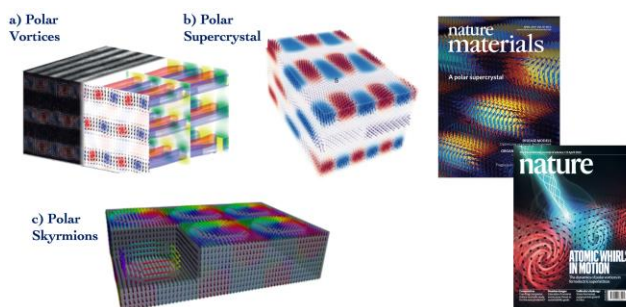


Fig. 1: Ferroelectric Supertextures in $(\text{PbTiO}_3)_m/(\text{SrTiO}_3)_n$ where the polarization can twist, turn and tumble in the form of (a) vortices, (b) supercrystal (c) skyrmions.¹⁻³

separate document of publications list), we highlight below three exciting discoveries relevant to the renewal that are in the final stages of manuscript preparation:

(1) Single-shot studies of supercrystal formation: We investigated the irreversible dynamics of supercrystal formation using single-shot measurements at LCLS and SACLA. These experiments are based on the ability of LCLS to measure the evolution of lattice structure with a single X-ray pulse by combining 100's of such spots on the sample to reconstruct the dynamics of an irreversible phase conversion process. The early moments (fs-ps) in the creation of the supercrystal using ultrafast light reveals the critical role of the initial microstructure as well as that of charge transfer to the interfaces on sub-ps time scales in driving a deterministic pathway that evolves over timescales into the msec regime where the new phases form. In the regime of optical excitation that promotes the supercrystal formation, we identified a decoupled sub-ps collapse of phases, where the emergent vortex phase responds faster (at ~ 0.5 ps) than the ferroelectric (a_1/a_2 in-plane polarized nanodomains) phase (at ~ 1 ps) (**Fig. 2b**).

The sub-ps dynamical response of the polar superstructures shows the critical role of charge migration towards the superlattice interfaces. The resulting photoinduced electron population in the conduction band is accumulated rapidly in the interfacial region assisted by the photovoltaic effect and further transferred to the SrTiO₃ layers to become long-lived therein (**Fig. 2a**). Furthermore, before the supercrystal nucleation and growth is observed at the tens of ns timescale and beyond, we have recorded the formation of transient metastable states such as a high-temperature vortex-like (V) phase where it should have been erased in equilibrium as well as a transient labyrinth phase (L) as indicated by experimental result (inset, **Fig. 2b**). The transient L phase is erased by the spatially adjacent V phase that subsumes the L phase into a new vortex supercrystal (VSC) phase. Dynamical phase-field modeling (**Fig. 2c**) describes the spatial and temporal evolution of charge carriers and the strain relaxation, predicts the evolution of heterogeneous polarization, charge, and strain dynamics.

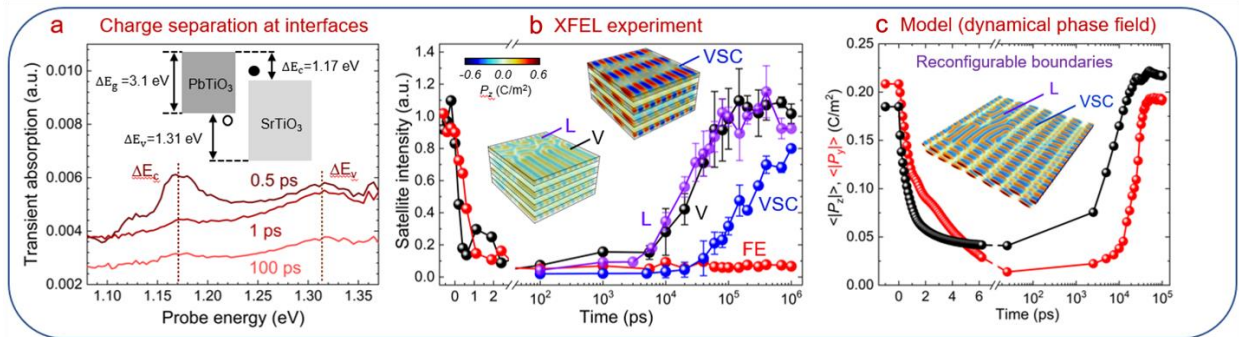


Fig. 2: The genesis of a supercrystal: (a) Photocarrier redistribution at the [(SrTiO₃)₁₆/(PbTiO₃)₁₆]_{7.5} interfaces across the derived bandstructure using stroboscopic transient absorption spectroscopy that recorded the time dependence of enhanced carrier concentration at the band offsets of the interfaces as indicated by the dashed lines. (b) The satellite peak dynamics captured with single shot XFEL measurements of irreversible phase conversion dynamics stimulated with optical pulses. (c) A dynamical phase field modeling capturing the underlying dynamics.

(2) Single-shot XPCS reveals hidden fluctuation dynamics: A new approach for visualizing dynamic heterogeneity and the internal structure and motion of domain walls is established in the creation of a supercrystal through single shot X-ray photon correlation spectroscopy (XPCS) that is missed in tracking standard diffraction intensity.

Figure 3 shows the results of probing the nucleation and growth of the supercrystal phase within a $(\text{PbTiO}_3)_{16}/(\text{SrTiO}_3)_{16}$ superlattice in a single-shot geometry. From the measurement of transient speckle patterns (**Fig. 3a**), a time-dependent correlation analysis reveals new dynamics unresolved by standard crystallographic analyses (*e.g.*, integrated Bragg peak intensity) (**Fig. 3b**). We further find that this two-time correlation analysis provides a direct window into the dynamical heterogeneity of the phase transition, showing sensitivity to the nucleation and growth of the new phase, the merging of different spatially separated domains, and direct sensitivity to the nanoscale structure of the domain walls (**Fig. 3c,d**). This approach provides a first attempt to connect temporal and spatial evolution in such complex structures and represents a new tool in our ultrafast arsenal to probe materials.

(3) Ultrafast coherent dynamics of polar skyrmions:

We have revealed unique terahertz phason modes in polar skyrmions. Our first-of-its-kind study of THz dynamics of polar vortices⁴ (cover of *Nature*, 2021; **Fig. 1**) revealed a sub-Terahertz **vortexon mode** where, upon THz excitation, adjacent vortices twist counterclockwise relative to each other producing a mode that carries angular momentum. We have also explored the THz dynamics of skyrmions, which are quasi-0D objects. To characterize the ultrafast structural dynamics of polar skyrmions, we have performed THz-pump, femtosecond X-ray

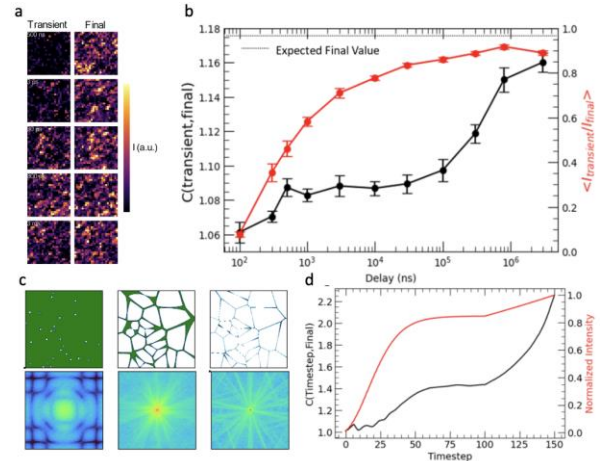


Fig.3: Hidden domain wall dynamics revealed by XPCS: a) transient speckle patterns at various time scales. b) Comparison of Bragg peak integrated intensity (red) to dynamic two-time correlation function analysis (black) showing new dynamics extending to millisecond time scales not resolved by standard crystallographic approaches. (c,d) Simulation involving nucleation and coarsening of heterogeneous bubbles of new phase which closely matches experimental data.

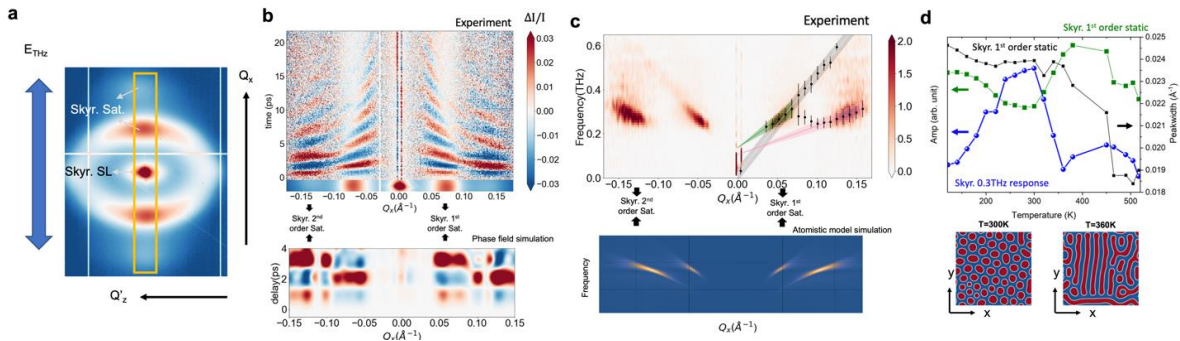


Fig. 4: Ultrafast phason mode observed in polar skyrmions: (a) Diffraction pattern around one of the 004 $(\text{PbTiO}_3)_{16}/(\text{SrTiO}_3)_{16}$ superlattice Bragg peaks (log scale). (b) Top: Differential diffraction intensity with THz excitation as a function of delay at 220 K. Bottom: Dynamical phase-field simulation showing the diffraction intensity changes as a function of time. (c) Top: The FFT spectrum of the top panel in (b) that shows the dispersion of the observed modes. The dashed lines are color coded to show the dispersion relation probed at the 1st and 2nd diffraction satellites. The slopes of the dispersion relation correspond to the speed of acoustic modes. Bottom: The atomistic simulation that shows the collective modes dispersion of a vortexon-like mode at the 1st diffraction satellite and a phason mode at the 2nd satellite. (d) Top: Temperature-dependence of the mode amplitude (left axis) and the skyrmion satellite diffraction intensity (left axis) and peak width (right axis). Bottom: phase-field simulation captures a topology change from the polar skyrmions at 300K to labyrinth-like structures at 360K.

diffraction probe measurements at the XPP end-station of the LCLS. The average in-plane polar skyrmion spacing is ~ 9 nm, which gives rise to the satellite diffraction about the 004-Bragg peak (**Fig. 4a**). The intensity oscillation between +1 and -1 order as well as between +1 and +2 order are π out of phase, indicating a transient symmetry breaking by the THz field (**Fig. 4b**). The Q_x -dependent Fourier spectra showed the dispersion relation of these modes (**Fig. 4c**). The dispersion curves (dashed lines) do not extend to the origin but across 0.15 THz at zero Q_x . Recent atomistic simulations in collaboration with J. Hlinka (Czech Academy of Sciences) shows that one of these modes is **a unique vortexon-like mode** like that seen in vortices, and an additional **unique phason mode** arising from inhomogeneous phase of the domain-wall vibrations in the skyrmions (**Fig. 4c**). We further found that the mode amplitudes were reduced drastically at 360 K (blue dots, **Fig. 4d**), accompanied by a sharp reduction in the skyrmion 1st order satellite peakwidth (black squares, **Fig. 4d**) and increase in intensity (green squares, **Fig. 4d**). This ultrafast phase transformation has been identified by phase-field modeling as the skyrmions undergoing a merging to form long labyrinth-like domains (**Fig. 4d**).

Future Plans

Beyond publishing the above works, as described in our renewal white paper submitted recently, we propose to further explore three science drivers:

(1) What are the atomic and mesoscale stochastic processes that can be collectively excited along deterministic energy pathways towards the emergence of these polar supertextures? This includes mapping out the phase space of many new supertextures we have observed with small changes in the experiments, more deeply probing photoinduced interface carrier dynamics on sub-ps time scales and probing stochastic processes underpinning the emergence of order using XFEL and ultrafast optics.

(2) How can we harness novel static and ultrafast dynamic properties of these emergent supertextures? This includes driving topological transformations using nonlinear phononics, ultrafast achiral symmetry breaking in supertextures using circularly polarized THz, and exciting coherent hybrid acoustic-polarization modes in supertextures.

(3) How can we design new heterostructures that exhibit expanded structural and functional couplings beyond the $(\text{PbTiO}_3)_m/(\text{SrTiO}_3)_n$ prototypical system? Here we propose coupling polar and magnetic orders in $(\text{PbTiO}_3)_m/(\text{SrRuO}_3)_n$ heterostructures, as well as exploring predicted supertextures in $\text{KNbO}_3/\text{KTaO}_3$ heterostructures.

References

1. Stoica, V. A. *et al.* Optical creation of a supercrystal with three-dimensional nanoscale periodicity. *Nat Mater* **18**, 377–383 (2019).
2. Yadav, A. K. *et al.* Observation of polar vortices in oxide superlattices. *Nature* **530**, 198–201 (2016).
3. Das, S. *et al.* Observation of room-temperature polar skyrmions. *Nature* **568**, 368–372 (2019).
4. Li, Q. *et al.* Subterahertz collective dynamics of polar vortices. *Nature* **592**, 376–380 (2021).

Publications

1. *Light-driven polarization manipulation in a relaxor ferroelectric*, Suji Park, Bo Wang, Tiannan Yang, Sahar Saremi, Jieun Kim, Wenbo Zhao, Burak Guzelurk, Aditya Sood, Clara Nyby, Marc Zajac, Xiaozhe Shen, Mike Kozina, Alex Reid, Stephen Weathersby, Xijie Wang, **Lane W. Martin, Long-Qing Chen, Aaron Lindenberg**, <https://doi.org/10.1021/acs.nanolett.2c02706> (2022), This work was supported by the U.S. Department of Energy, Office of Science, Office of Basic Energy Sciences, under Award Number DE-SC-0012375. SLAC MeV-UED is supported in part by the DOE BES SUF Division Accelerator & Detector R&D program, the LCLS Facility, and SLAC under Contract Nos. DE-AC02-05-CH11231 and DE-AC02-76SF00515. B.G., A.S., C.N., and M.Z. acknowledge support by the Department of Energy, Office of Science, Office of Basic Energy Sciences under contract DE-AC02-76SF00515.
2. *Large Itinerant Electron Exchange Coupling in the Magnetic Topological Insulator $MnBi_2Te_4$* , Hari Padmanabhan, **Vladimir A. Stoica**, Peter Kim, Maxwell Poore, Tiannan Yang, Xiaozhe Shen, Alexander H. Reid, Ming-Fu Lin, Suji Park, Jie Yang, Huaiyu Wang, Nathan Z. Koocher, Danilo Puggioni, Lujin Min, Seng-Huat Lee, Zhiqiang Mao, **James M. Rondinelli, Aaron M. Lindenberg, Long-Qing Chen**, Xijie Wang, **Richard D. Averitt, John W. Freeland**, and **Venkatraman Gopalan**, *Advanced Materials* (2022). *Advanced Materials* (2022). <https://doi.org/10.1002/adma.202202841> H.P., V.A.S., H.W., P.K., M.P., N.Z.K., A.M.L., R.D.A., J.M.R., J.W.F., and V.G. acknowledge support from the DOE-BES grant DE-SC0012375. H.P., T.Y., L-Q.C., and V.G. acknowledge support from the DOE Computational Materials program, DE-SC0020145. Support for crystal growth and characterization was provided by the National Science Foundation through the Penn State 2D Crystal Consortium-Materials Innovation Platform (2DCC-MIP) under NSF cooperative agreement DMR-1539916. D.P. was supported by the Army Research Office (ARO) under grant no. W911NF-15-1-0017. SLAC MeV-UED is supported in part by the DOE BES SUF Division Accelerator & Detector R&D program, the LCLS Facility, and SLAC under Contract Nos. DE-AC02-05-CH11231 and DE-AC02-76SF00515.
3. *Tunable nanoscale evolution and topological phase transitions of a polar vortex supercrystal*, C. Dai, **V. A. Stoica**, S. Das, Z. Hong, **L. W. Martin**, R. Ramesh, **J. W. Freeland, H. Wen, V. Gopalan, L-Q. Chen**, *Advanced Materials*, 2106401 (2021) <https://doi.org/10.1002/adma.202106401>, C.D., V.A.S., J.W.F., H. W., V.G., L.W.M., and L.Q.C. acknowledge the support of U.S. Department of Energy, Office of Science, Office of Basic Energy Sciences, under Award Number DE-SC-0012375 for the simulation and diffraction-based study of these materials. R.R. and S.D. acknowledge support from the Office of Basic Energy Sciences, US Department of Energy (DE-AC02-05CH11231). L.W.M. and R.R. also acknowledge partial support of the Army Research Office under the ETHOS MURI via cooperative agreement W911NF-21-2-0162 for the development of similar superlattice materials. This research used resources of the Advanced Photon Source, a U.S. Department of Energy (DOE) Office of Science User Facility operated for the DOE Office of Science by Argonne National Laboratory under Contract No. DE-AC02-06CH11357, with data collected at X-ray Science Division beamlines 7ID-C and 33ID-B.
4. *Interlayer magnetophononic coupling in $MnBi_2Te_4$* , Hari Padmanabhan, Maxwell Poore, Peter Kim, Nathan Z. Koocher, **Vladimir A. Stoica**, Danilo Puggioni, Hugo Wang, Xiaozhe Shen, Alexander H. Reid, Mingqiang Gu, Maxwell Wetherington, Seng Huat Lee, Richard Schaller,

Zhiqiang Mao, **Aaron M. Lindenberg**, Xijie Wang, **James M. Rondinelli**, **Richard Averitt**, **Venkatraman Gopalan**. *Nature Commun.* <https://doi.org/10.1038/s41467-022-29545-5>, arXiv:2104.08356v1 [cond-mat.mtrl-sci] H.P., V.A.S., H.W., P.K., M.P., N.Z.K., R.A., J.M.R., and V.G. acknowledge support from the DOE-BES grant DE-SC0012375. H.P. acknowledges partial support from the DOE Computational Materials program, DE-SC0020145. Support for crystal growth and characterization was provided by the National Science Foundation through the Penn State 2D Crystal Consortium-Materials Innovation Platform (2DCC-MIP) under NSF cooperative agreement DMR-1539916. D.P. was supported by the Army Research Office (ARO) under grant no. W911NF-15-1-0017. SLAC MeV-UED is supported in part by the DOE BES SUF Division Accelerator & Detector R&D program, the LCLS Facility, and SLAC under Contract Nos. DE-AC02-05-CH11231 and DE-AC02-76SF00515.

5. *Magnetic order driven ultrafast phase transition in NdNiO₃*, V. A. Stoica, D. Puggioni, J. Zhang, R. Singla, G. L. Dakovski, G. Coslovich, M. H. Seaberg, M. Kareev, S. Middey, P. Kissin, R. D. Averitt, J. Chakhalian, H. Wen, J. M. Rondinelli, and J. W. Freeland, *Phys. Rev. B* **106**, 165104 (2022) J.W.F. wants to acknowledge the help with science and data analysis from N. Laanait. V.A.S., J.Z., R.D.A., J.C., H.W., J.M.R., and J.W.F. were supported by the Department of Energy Grant No. DE-SC0012375 for work with ultrafast x-ray and optical experiments and analysis of the data with theoretical support. D.P. was supported by the Army Research Office (Grant No. W911NF-15-1-0017). J.C. was also supported by DOD-ARO under Grant No. 0402-17291 and by the Gordon and Betty Moore Foundation's EPiQS Initiative through Grant No. GBMF4534. Work at the Advanced Photon Source, Argonne was supported by the U.S. Department of Energy, Office of Science under Grant No. DEAC02-06CH11357. Use of the Linac Coherent Light Source (LCLS), SLAC National Accelerator Laboratory, which is a DOE Office of Science User Facility, was under Contract No. DE-AC02-76SF00515. Electronic structure calculations were performed using computational resources provided by the DOD-HPCMP. J.W.F. would like to acknowledge many insightful conversations with A. J. Millis and D. Khomskii.
6. *Sub-Terahertz collective dynamics of polar vortices*. Q. Li, V. Stoica, M. Pasciak, Y. Zhu, Y. Yuan, T. Yang, M. R. McCarter, S. Das, A. K. Yadav, S. Park, C. Dai, H. J. Lee, Y. Ahn, S. D. Marks, T. Sato, M. C. Hoffmann, M. Chollet, M. E. Kozina, S. Nelson, D. Zhu, D. A. Walko, **A. M. Lindenberg**, P. G. Evans, **L.-Q. Chen**, R. Ramesh, **L. W. Martin**, **V. Gopalan**, **J. W. Freeland**, J. Hlinka, **H. Wen**, *Nature* **592**, 376-380 (2021). [DOI: 10.1038/s41586-021-03342-4] This work was primarily supported by the US Department of Energy, Office of Science, Basic Energy Sciences, Materials Sciences and Engineering Division: experimental design, data collection, data analysis, and part of simulations by Q.L. and H.W. were supported under the DOE Early Career Award; **ultrafast measurements and sample synthesis by V.A.S., Y.Y., S.P., L.W.M., C.D., S.Y., A.L., L.-Q.C., V.G., J.W.F. and H.W. were supported under award no. DE-SC-0012375**; ancillary ultrafast X-ray measurements by H.L., S.M., Y.A. and P.E. were supported under award no. DE-FG02-04ER46147. M.M., S.D., and R.R. acknowledge support for part of sample synthesis through the Quantum Materials programme (KC 2202) funded by the US Department of Energy, Office of Science, Basic Energy Sciences, Materials Sciences Division under contract no. DE-AC02-05-CH11231. J.H. and M.P. were supported by the Czech Science Foundation (project no. 19-28594X) and acknowledge the access to computing facilities owned by parties and projects contributing to the National Grid Infrastructure MetaCentrum, provided under programme no. Cesnet LM2015042. T.Y. and L.-

Q.C. acknowledge partial support from the US Department of Energy, Office of Science, Basic Energy Sciences, under award n0. DE-SC0020145 as part of the Computational Materials Sciences Program and from NSF under award DMR-1744213. Y.Z. and H.W. acknowledge support by ANL-LDRD for preliminary X-ray measurements. Q.L. acknowledges support by the Basic Science Center Project of NSFC under grant no. 51788104 for completing phase-field simulations at Tsinghua University. S.M. acknowledges support from the Office of Science Graduate Student Research (SCGSR) programme (DOE contract no. DE-SC0014664) and from the UW-Madison Materials Research Science and Engineering Center (NSF DMR-1720415). H.L. acknowledges support by the National Research Foundation of Korea under grant 2017R1A6A3A11030959. Use of the Linac Coherent Light Source is supported by the US Department of Energy, Office of Science, Office of Basic Energy Sciences under contract no. DE-AC02-76SF00515. Use of the Advanced Photon Source is supported by the US Department of Energy, Office of Science, Office of Basic Energy Sciences under contract no. DE-AC02-06CH11357.

7. *Structural Chirality of Polar Skyrmions Probed by Resonant Elastic X-Ray Scattering*, Margaret R. McCarter, Kook Tae Kim, **Vladimir A. Stoica**, Sujit Das, Christoph Klewe, Elizabeth P. Donoway, David M. Burn, Padraic Shafer, Fanny Rodolakis, Mauro A. P. Gonçalves, Fernando Gómez-Ortiz, Jorge Íñiguez, Pablo García-Fernández, Javier Junquera, Stephen W. Lovesey, Gerrit van der Laan, Se Young Park, **John W. Freeland**, **Lane W. Martin**, Dong Ryeol Lee, and Ramamoorthy Ramesh, *Phys. Rev. Lett.* 129, 247601 (2022). M.R.M. and R.R. were supported by the Quantum Materials program from the Office of Basic Energy Sciences, U.S. Department of Energy (DE-AC02-05CH11231). V. A. S., J. W. F., and L. W. M. acknowledge the U.S. Department of Energy, Office of Science, Office of Basic Energy Sciences, under Award No. DE-SC-0012375 for support to study complex-oxide heterostructure with x-ray scattering. L. W. M. and R. R. acknowledge partial support from the Army Research Office under the ETHOS MURI via cooperative agreement W911NF-21-2-0162. J. Í. acknowledge financial support from the Luxembourg National Research Fund through project FNR/C18/MS/ 12705883/REFOX. Diamond Light Source, UK, is acknowledged for beam time on beam line I10 under proposal NT24797. K. T. K., S. Y. P., and D. R. L. acknowledge support from the National Research Foundation of Korea, under Grant No. NRF-2020R1A2C1009597, NRF-2019K1A3A7A09033387, and NRF-2021R1C1C1-009494. M. A. P. G. acknowledges support by the Czech Science Foundation (Project No. 19-28594X). This research used resources of the Advanced Light Source, a U.S. DOE Office of Science User Facility under Contract No. DE-AC02-05CH11231. This research used resources of the Advanced Photon Source, a U.S. Department of Energy (DOE) Office of Science User Facility at Argonne National Laboratory and is based on research supported by the U.S. DOE Office of Science-Basic Energy Sciences, under Contract No. DE-AC02-06CH11357. S. D. gratefully acknowledges a start-up grant from Indian Institute of Science, Bangalore, India. F.G.-O., P.G.-F., and J.J. acknowledge financial support from Grant No. PGC2018-096955-B-C41 funded by MCIN/AEI/10.13039/501100011033 and by ERDF “A way of making Europe,” by the European Union. F. G.-O. acknowledges financial support from Grant No. FPU18/04661 funded by MCIN/AEI/10.13039/501100011033.
8. *Chiral structures of electric polarization vectors quantified by X-ray resonant scattering*, K.T. Kim, M.R. McCarter, **V.A. Stoica**, S. Das, C. Klewe, E. Donoway, D. Burn, P. Shafer, F. Rodolakis, M. Gonçalves, F. Gómez-Ortiz, J. Íñiguez, P. Garcia-Fernandez, J. Junquera, S. Lovesey, G. van der Laan, L.W. Martin, A.Y. Park, J.W. Freeland, R. Ramesh, *Nature*

Communications, <https://doi.org/10.1038/s41467-022-29359> (2022). K.T.K., S.Y.P., and D.R.L. acknowledge financial support by National Research Foundation of Korea (Grant No. NRF-2020R1A2C1009597, NRF-2019K1A3A7A09033387, and NRF-2021R1C1C1009494). M.M., and R.R. were supported by the Quantum Materials program from the Office of Basic Energy Sciences, US Department of Energy (DE-AC02-05CH11231). V.A.S., J.W.F., and L.W.M. acknowledge the U.S. Department of Energy, Office of Science, Office of Basic Energy Sciences, under Award Number DE-SC-0012375 for support to study complex-oxide heterostructure with X-ray scattering. L.W.M. and R.R. acknowledge partial support from the Army Research Office under the ETHOS MURI via cooperative agreement W911NF-21-2-0162. J.Í. acknowledge financial support from the Luxembourg National Research Fund through project FNR/C18/MS/12705883/REFOX. Diamond Light Source, UK, is acknowledged for beamtime on beamline I10 under proposal NT24797. Use of the Advanced Light Source, Lawrence Berkeley National Laboratory, was supported by the U.S. Department of Energy (DOE) under contract no. DE585 AC02-05CH11231, and use of the Advanced Photon Source was supported by DOE's Office of Science under contract DE-AC02-06CH11357.

9. *Condensation of collective polar vortex modes*, Tiannan Yang, Cheng Dai, Qian Li, **Haidan Wen, and Long-Qing Chen**, *Phys. Rev. B* **103**, L220303, DOI: <https://doi.org/10.1103/PhysRevB.103.L220303>, We thank Venkatraman Gopalan and Jirka Hlinka for helpful discussions and comments on the work. The work is primarily supported as part of the Computational Materials Sciences Program funded by the US Department of Energy, Office of Science, Basic Energy Sciences, under Award No. DE-SC0020145. The authors also acknowledge partial support from the National Science Foundation under Award No. DMR-1744213 for the early effort on the development of dynamical phase-field model, the US Department of Energy under Award No. DE-SC-0012375 on the experimental effort, and computational resource provided by the Institute for CyberScience at the Pennsylvania State University. H.W. acknowledges the support from the US Department of Energy, Office of Science, Basic Energy Sciences, Materials Sciences and Engineering Division.
10. *Local negative permittivity and topological-phase transition in polar skyrmions*. S. Das, Z. Hong, **V. A. Stoica**, M. A. P. Gonçalves, T. Y. Shao, E. Parsonnet, E. J. Marksz, S. Saremi, M. McCarter, A. Reynoso, C. J. Long, A. M. Hagerstrom, D. Meyers, V. Ravi, B. Prasad, H. Zhou, Z. Zhang, H. Wen, F. Gómez-Ortiz, P. García-Fernández, J. Bokor, J. Íñiguez, **J. W. Freeland**, N. D. Orloff, J. Junquera, **L-Q. Chen**, S. Salahuddin, D. A. Muller, **L. W. Martin**, R. Ramesh, *Nature Mater.* **20**, 194-201 (2021). [DOI: 10.1038/s41563-020-00818-y]. This work was supported by the Quantum Materials program of the Office of Basic Energy Sciences, US Department of Energy (DE-AC02-05CH11231). M.A.P.G. and J.Í. were funded by the Luxembourg National Research Fund through the CORE program (Grant FNR/C15/MS/10458889 NEWALLS). **J.W.F., V.A.S., H.W. and L.W.M. acknowledge support from the US Department of Energy, Office of Science, Office of Basic Energy Sciences (Award number DE-SC-0012375) for the development and study of ferroic heterostructures.** The phase-field simulations at Penn State were supported as part of the Computational Materials Sciences Program funded by the US Department of Energy, Office of Science, Basic Energy Sciences (Award number DE-SC0020145) and the Extreme Science and Engineering Discovery Environment (XSEDE) cluster, which is supported by the National Science Foundation (Grant ACI-1548562), and specifically, it used the Bridges system, which is supported by the NSF (Award number ACI-1445606) at the Pittsburgh Supercomputing

Center (PSC), under allocation DMR170006. F.G.O., P.G.F. and J.J. acknowledge financial support from the Spanish Ministry of Economy and Competitiveness (Grants FIS2015-64886-C5-2-P and PGC2018-096955-B-C41), and P.G.F. acknowledges support from Ramón y Cajal Foundation (Grant RyC-2013-12515). V.A.S., M.R.M., S.D., H.W., Z.Z., J.W.F. and H.Z. acknowledge use of the Advanced Photon Source, a US Department of Energy, Office of Science User Facility operated for the DOE Office of Science by Argonne National Laboratory under contract no. DE-AC02-06CH11357. V.A.S. and H.W. thank Q. Li and S. Marks for kind assistance in operating the XNOM station at the 7-ID-C beamline of APS. Y.T.S. and D.A.M. acknowledge support from the AFOSR Hybrid Materials MURI (Award number FA9550-18-1-0480). We acknowledge the electron microscopy facility of the National Science Foundation (Award numbers DMR-1719875 and DMR-1429155). E.J.M., C.J.L. and N.D.O. acknowledge J. C. Booth for establishing the high-frequency testing facility at NIST, funding E.J.M. and developing the original on-wafer techniques.

Emergent Phenomena at Mott Interfaces – a Time- and Depth-Resolved Approach

Alexander Gray, Department of Physics, Temple University

Keywords: x-ray scattering, x-ray photoemission, THz pulses, oxide interfaces, magnetism

Research Scope

This research program aims at addressing the scientific questions related to the time-dependent emergence and control of non-equilibrium electronic phases of matter in strongly-correlated Mott oxides and their interfaces. We are focusing specifically on exploiting the interfaces in heterostructures and superlattices containing strongly-correlated manganites and nickelates because, in such systems, precise control of electronic and magnetic structure in the ground state can be achieved through dimensionality, heterostructuring, interface termination, and lattice strain [1-3]. One of the main objectives of this program is to develop a suite of complementary ultrafast x-ray scattering techniques which probe the three-dimensional nanoscale evolution of materials' properties as the electronic and spin states are driven out of equilibrium by ultrafast external stimuli such as intense THz electric fields [4]. Ångstrom-level depth resolution in such measurements is achieved by utilizing the x-ray standing-wave method, wherein the intensity profile of the probing x-ray radiation is tailored and translated vertically within the sample [5]. As a key part of this project, we are working to marry this methodology, which is presently being utilized only in equilibrium, with the ultrafast FEL- and synchrotron-based pump-probe techniques. This will result in the development of a powerful new experimental platform that can be used to study electronic systems driven out of equilibrium with depth resolution. The new depth-resolved ultrafast x-ray scattering techniques and instrumentation developed in the course of this program will be generalizable for immediate use at the DOE's synchrotron and FEL facilities.

Recent Progress

During the recent two years of this research program, we continued to expand our experimental activities related to the ultrafast THz *E*-field control of magnetic and electronic interactions at Mott interfaces containing CaMnO₃ and LaNiO₃ thin films. These activities are directly related to the two major goals of this project - (1) to disentangle, understand, and harness control over the intricate competing interactions responsible for emergent interfacial magnetism, and (2) to develop a suite of ultrafast experimental techniques to probe the time-dependent evolution of electronic and spin states that are driven out of equilibrium by ultrafast external stimuli such as intense THz *E*-fields.

Motivated by these challenges, we have combined two static x-ray and two ultrafast THz pump-probe techniques to obtain a comprehensive depth- and time-resolved picture of the electronic and magnetic interactions leading to the stabilization and control of the interfacial ferromagnetic state at the CaMnO₃/LaNiO₃ interface. Specifically: (1) soft x-ray standing-wave photoemission was used to probe the interfacial charge transfer resulting in the ferromagnetic

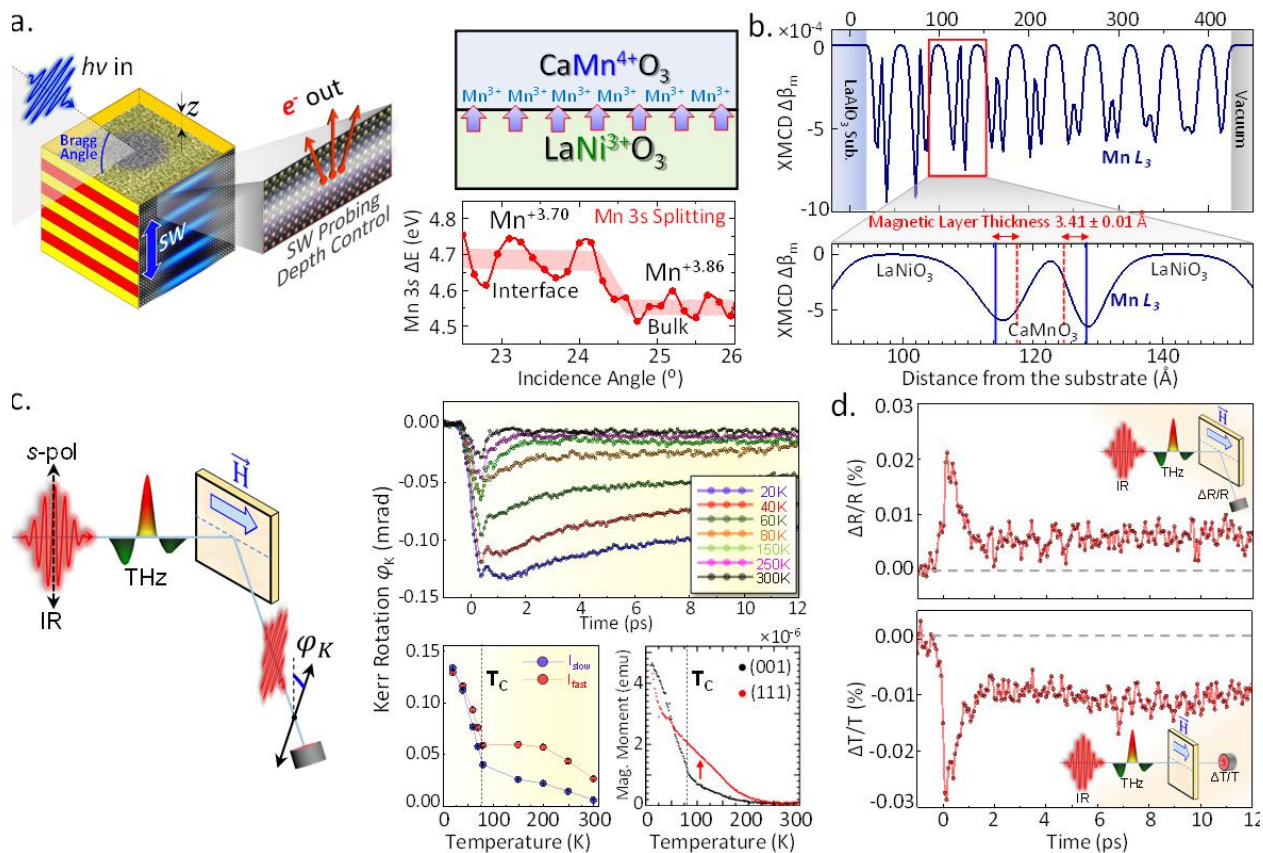


Figure 5 | **a.** Schematic diagram of the standing-wave photoemission experiment and the depth-resolved evolution of the Mn valence state near the interface, as probed via the measurement of the Mn 3s core-level multiplet splitting. Bulk-like CaMnO_3 exhibits a near-stoichiometric effective valence-state of $\text{Mn}^{+3.86}$, while the interfacial CaMnO_3 exhibits a higher abundance of the Mn^{3+} sites and, thus, a reduced effective valence-state of $\text{Mn}^{+3.70}$. An increased concentration of the Mn^{3+} cations at the interface creates an electronic environment favorable for the emergence of interfacial ferromagnetism mediated via the Mn^{4+} - Mn^{3+} ferromagnetic double exchange. **b.** The resultant magnetic profile of the superlattice, as probed using soft x-ray resonant magnetic scattering. The effective thickness of the interfacial ferromagnetic layer was determined to be approximately 3.41 \AA (one unit cell), consistent with the standing-wave measurements shown in (a). **c.** Schematic diagram of the THz-pump tr-MOKE probe experimental setup and the temperature-dependent delay traces showing evolution of the magnetic state following THz excitation. Amplitudes of the two dynamic processes observed in the delay traces follow the temperature dependence of the interfacial magnetic moment, with the T_C of approximately 75 K . **d.** Ultrafast evolution of the IR reflectivity and transmissivity suggests transient THz-induced metallization of the superlattice.

double-exchange interaction, (2) soft x-ray resonant magnetic scattering was utilized to derive a sub-Ångstrom-resolution depth profile of the resulting interfacial magnetic moment, (3) ultrafast THz-pump tr-MOKE spectroscopy was used to trigger and observe the ultrafast demagnetization of the interface, and (4) ultrafast THz-pump IR reflectivity and transmissivity spectroscopies were utilized concomitantly to observe the evolution of the electronic properties. Some of the key results are shown in Figure 1 with more technical details described in the figure caption.

In order to probe the non-equilibrium dynamics of this emergent interfacial state, we had to tackle a major technical challenge of combining several THz-pump ultrafast-probe detection techniques in one experimental setup, including reflection- and transmission-based tr-MOKE, as

well as polarization-dependent reflectivity and transmissivity. The setup had to facilitate cryogenic temperatures of down to 20 K and an applied magnetic field of up to 1 T.

By combining advanced x-ray spectroscopic and scattering techniques (standing-wave photoemission and resonant magnetic scattering) with ultrafast THz-pump IR-probe spectroscopies, we established an important link between the electronic and magnetic degrees of freedom that explain the emergence of the interfacial ferromagnetic ground state in this archetypal Mott oxide heterostructure. Our findings suggest an avenue for efficient electric-field switching of two-dimensional ferromagnetic states at oxide interfaces.

To gain a deeper understanding of the interactions between the electronic and magnetic phenomena in the $\text{LaNiO}_3/\text{CaMnO}_3$ superlattices, we have continued our ongoing experimental activities utilizing in-situ PLD growth combined with ARPES and spin-ARPES to probe the electronic structure of the ultrathin LaNiO_3 layers. We focused on exploring the x-ray polarization dependence of the ARPES data, as well as spin resolution, to build up a complete picture of the spin and orbital makeup of the interfacial states. One of the key discoveries of this reporting cycle was the orbital-dimensional crossover (from 3D to 2D) with the reduced thickness of LaNiO_3 thin films in the $\text{LaNiO}_3/\text{CaMnO}_3$ superlattices. Such orbital reconstruction is a viable candidate mechanism for controlling interfacial magnetism, independently of the metal-insulator transition.

Finally, as an exploratory direction of this project, we have carried out the first successful proof-of-principle experiments adding quantitative depth resolution to the photoemission microscopy (PEEM) studies of 2D van der Waals materials. The methodology used in these experiments, standing-wave SW-PEEM, utilizes kinetic-energy-filtered x-ray photoemission microscopy and was first demonstrated by the PI and collaborators at BESSY II. The standing-wave approach enables truly depth-selective and non-destructive investigation of the interface-specific and two-dimensional electronic phenomena and is ideally suited for the depth-resolved studies of layered van der Waals materials and heterostructures.

Future Plans

In the near future, we are planning to continuously shift the emphasis of our research efforts toward the lab- and FEL-based ultrafast THz studies of the electronic, magnetic, and structural properties of the strongly-correlated materials and superlattices. Specifically, we are planning to transfer this suite of techniques to LCLS-II, and to carry out THz-pump x-ray-scattering measurements on the $\text{LaNiO}_3/\text{CaMnO}_3$ superlattices. The main motivation for this is the element-specificity and the nm-scale spatial resolution accessible in the soft x-ray regime. These key capabilities will enable us to dynamically probe the $\text{Ni} \rightarrow \text{Mn}$ charge transfer mechanism, which lies at the core of the interfacial ferromagnetism phenomena.

As an exploratory direction, we are currently also working on the development of a suite of complementary x-ray scattering and imaging techniques that are based on *momentum microscopy* and designed to probe the spin and orbital-resolved electronic band structure of quantum materials and heterostructures. We anticipate that, with the proliferation of momentum microscopy in the U.S. and the world, these techniques will become widespread in both

synchrotron and FEL settings and will pave the way to the discovery of new classes of materials for quantum computing.

References

1. R. U. Chandrasena, W. Yang, Q. Y. Lei, M. U. Delgado-Jaime, K. Wijesekara, M. Golalikhani, B. A. Davidson, E. Arenholz, K. Kobayashi, M. Kobata, F. M. F. de Groot, U. Aschauer, N. A. Spaldin, X. X. Xi, and A. X. Gray, *Strain-Engineered Oxygen Vacancies in CaMnO₃ Thin Films*, Nano Lett. **17**, 794 (2017).
2. M. Golalikhani, Q. Lei, R. U. Chandrasena, L. Kasaei, H. Park, J. Bai, P. Orgiani, J. Ciston, G. Sterbinsky, D. A. Arena, P. Shafer, E. Arenholz, B. Davidson, A. J. Millis, A. X. Gray, and X. X. Xi, *Nature of the metal-insulator transition in few-unit-cells-thick LaNiO₃ films*, Nature Comm. **9**, 2206 (2018).
3. R. U. Chandrasena, C. L. Flint, W. Yang, A. Arab, S. Nemšák, M. Gehlmann, V. B. Özdöl, F. Bisti, K. D. Wijesekara, J. Meyer-Ilse, E. Gullikson, E. Arenholz, J. Ciston, C. M. Schneider, V. N. Strocov, Y. Suzuki, and A. X. Gray, *Depth-resolved charge reconstruction at the LaNiO₃/CaMnO₃ interface*, Phys. Rev. B **98**, 155103 (2018).
4. A. X. Gray, M. C. Hoffmann, J. Jeong, N. P. Aetukuri, D. Zhu, H. Y. Hwang, N. C. Brandt, H. Wen, A. J. Sternbach, S. Bonetti, A. H. Reid, R. Kukreja, C. Graves, T. Wang, P. Granitzka, Z. Chen, D. J. Higley, T. Chase, E. Jal, E. Abreu, M. K. Liu, T.-C. Weng, D. Sokaras, D. Nordlund, M. Chollet, H. Lemke, J. Glowonia, M. Trigo, Y. Zhu, H. Ohldag, J. W. Freeland, M. G. Samant, J. Berakdar, R. D. Averitt, K. A. Nelson, S. S. P. Parkin, H. A. Dürr, *Ultrafast Terahertz Field Control of Electronic and Structural Interactions in Vanadium Dioxide*, Phys. Rev. B **98**, 045104 (2018).
5. A. X. Gray, S. Nemšák, C. S. Fadley, *Combining hard- and soft- x-ray photoemission with standing-wave excitation, resonant excitation and angular resolution*, Synchrotron Rad. News **31**, 42 (2018).

Publications Supported by BES (recent 2 years):

1. J. Wang, Y. Shin, J. R. Paudel, J. D. Grassi, R. K. Sah, W. Yang, E. Karapetrova, A. Zaidan, V. N. Strocov, C. Klewe, P. Shafer, A. X. Gray, J. M. Rondinelli, and S. J. May, *Strain-induced anion ordering in perovskite oxyfluoride films*, Chem. Mater. **33**, 1811 (2021).
2. C. Kalhaz, N. K. Fernandez, P. Bhatt, F. O. L. Johansson, A. Lindblad, H. Rensmo, L. Zendejas Medina, R. Lindblad, S. Siol, L. P. H. Jeurgens, C. Cancellieri, K. Rossmagel, K. Medjanik, G. Schonhense, M. Simon, A. X. Gray, S. Nemšák, P. Lomker, C. Schlueter, and A. Regoutz, *Hard X-ray Photoelectron Spectroscopy: A Snapshot of the State-of-the-Art in 2020*, J. Phys.: Condens. Matter **33**, 233001 (2021).
3. A. Rattanachata, L. Nicolai, H. P. Martins, G. Conti, M. J. Verstraete, M. Gehlmann, S. Ueda, K. Kobayashi, I. Vishik, C.M. Schneider, C. S. Fadley, A. X. Gray, J. Minar, and S. Nemšák,

- Bulk Electronic Structure of Lanthanum Hexaboride (LaB₆) by Hard X-ray Angle-Resolved Photoelectron Spectroscopy*, Phys. Rev. Mater. **5**, 055002 (2021).
4. M. Chrysler, J. Gabel, T.-L. Lee, A. N. Penn, B. E. Matthews, D. M. Kepaptsoglou, Q. M. Ramasse, J. R. Paudel, R. K. Sah, J. D. Grassi, Z. Zhu, A. X. Gray, J. M. LeBeau, S. Spurgeon, S. A. Chambers, P. V. Sushko, and J. H. Ngai, *Tuning band alignment at a semiconductor-crystalline oxide heterojunction via electrostatic modulation of the interfacial dipole*, Phys. Rev. Mat. **5**, 104603 (2021).
 5. C.-T. Kuo, G. Conti, J. E. Rault, C. M. Schneider, S. Nemšák, and A. X. Gray, *Emergent phenomena at oxide interfaces studied with standing-wave photoelectron spectroscopy*, J. Vac. Sci. Technol. A **40**, 020801 (2022).
 6. Y. Yang, M. Han, C. E. Shuck, R. K. Sah, J. R. Paudel, A. X. Gray, Y. Gogotsi, and S. J. May, *Correlating electronic properties with M-site composition in solid solution Ti_yNb_{2-y}CT_x MXenes*, 2D Mater. **10**, 014011 (2023).
 7. W. Yang, L. Kasaei, H. Hijazi, S. Rangan, Y.-W. Yeh, R. K. Sah, J. R. Paudel, K. Chen, A. X. Gray, P. Batson, L. C. Feldman, and X. X. Xi, *Ultra-thin Epitaxial MgB₂ on SiC: Substrate Surface Polarity Dependent Properties*, Phys. Rev. Mater., accepted (2023). arXiv:2301.01669
 8. D. Mondal, S. Mahapatra, A. M. Derrico, R. Rai, J. R. Paudel, C. Schlueter, A. Gloskovskii, F. M. F. DeGroot, D. D. Sarma, A. Narayan, P. Nukala, A. X. Gray, and N. P. B. Aetukuri, *Modulation-Doping a Correlated Electron Insulator*, Science, submitted (2023). arXiv: submit/4680978

Novel topological and superconducting materials and their excitation properties

P.I.: M. Zahid Hasan (Princeton University)

Keywords: Quantum Materials, ARPES, X-ray spectroscopy, Nonlinear Optics, Ultrafast Properties

Research Scope

One of the goals in modern science is to identify, understand and explore novel states of matter and excitation (including ultrafast) dynamics that are possible in quantum materials. After the initial discovery of topological insulators and related materials, the field has greatly expanded to consider all possible combinations of symmetry and topology to classify quantum matter and subsequently identify their surface/bulk ground-state order and excitation including their novel ultrafast properties. Our early works on this topic under this grant have received more than 50,000 peer citations reflecting the level of follow up research activity and the broader impact on the field. Our program focused on discovery and understanding of novel topological materials using advanced spectroscopic techniques and develop the techniques and methodologies further in certain directions. We combine FP-DFT/TBT calculation techniques to discover novel topological materials harboring new protected quantum properties then probe and explore suitable materials primarily via ARPES, X-ray scattering and Ultrafast techniques. Currently we are also working on developing a novel ultrafast technique suitable for the study of photo-induced changes and nonlinear optical properties in topological matter. The general focus of this proposal is to carry out novel and potentially high-impact experiments to advance the fundamental science frontier on quantum materials.

Recent Progress

Our research in the current cycle continues towards the discovery of materials that embody novel symmetry, topology and dynamics using photon based spectroscopies. We identified new classes of topological matter and phenomena beyond the Z_2 materials and explored their novel quantum and ultrafast properties. Recent research focuses on a few classes of materials:

(1) **Novel Weyl/Chiral materials:** Recent advances in ARPES have allowed spatially-resolved measurements using a micron-sized beam-spot, in situ gating and other improvements in control of beam and also sample, granting access to new quantum phenomena. Utilizing these novel advanced in instrumentations we studied electronic states and excitations in Co_2MnGa which is governed by a set of nodal loops, termed Weyl loops and topological surface states and drive a giant anomalous Hall effect [1]. New classes of topological surface states are observed our linked nodal loops materials – the topological Seifert surface states. The Seifert surface encodes information about the linking (Knot) number. We explored the Seifert surfaces in linked nodal loop materials with state-of-the-art ARPES/spin-ARPES (I. Belopolski et.al., NATURE 604, 647-652 (2022)) [1].

(2) **Kagome magnets:** Intrinsic Chern quantum phases are possible in kagome lattices. The hard magnet TbMn_6Sn_6 system has been shown to hosting ideal spin-orbit-coupled magnetic kagome lattices in the previous cycle. We currently explore in-plane spin-momentum locking with spin-resolved ARPES to develop understanding of Chern phases in the generalized R- Mn_6Sn_6 family [2]. Another kagome material, KV_3Sb_5 which seems to exhibit unconventional charge order which also becomes weakly magnetic and opens a gap near the Fermi level that we currently study. (J. Yin et.al., NATURE 612, 647-657 (2022); X. Teng et.al., NATURE 609, 490-495 (2022)) [2].

(3) **Topological superconductor candidates:** We continued to search for intrinsic topological superconductors in candidate materials including KV_3Sb_5 which reveal some exotic quantum many-body phenomena (C. Mielke et.al, NATURE 602, 245-250 (2022); X. Yang et.al., Phys. Rev. Letts (in press) (2023)) [2, 3].

(4) **Ultrafast dynamics:** Dirac-Weyl, kagome and related chiral materials discovered under this grant are being further studied to explore their ultrafast/dynamical properties using an ultrafast Tr-ARPES spectrometer instrument. We are also studying the nonlinear optical CPGE (circular photogalvanic effect) response which is expected to reveal novel excitation dynamics and help develop ultrafast control of topological materials. (M. Yahyavi et.al, “Transverse circular photogalvanic effect associated with Lorentz-violating Weyl fermions” arXiv:2301.00958 (2023); N. Sirica et.al., “Photocurrent-driven transient symmetry breaking in the Weyl semimetal TaAs” Nature Materials 21, 62–66 (2022)).

Future Plans

We continue to identify new classes of topological matter beyond \mathbb{Z}_2 topological insulators and explore their novel quantum properties. Future research focuses on a few classes of target materials: (1) Novel Weyl/Chiral materials: During the previous cycle, we have predicted that the ferromagnet PrAlGe realizes a magnetic Weyl semimetal. Recent advances in ARPES have allowed spatially-resolved measurements using a micron-sized beam-spot, in situ gating and other improvements in control of beam and also sample, granting access to new quantum (topological) phenomena. Utilizing these advances we plan to study electronic states and excitations in MnCoGa and related materials including (Pr/Ce) AlGe series which is governed by a set of nodal loops, termed Weyl loops and topological surface states and drive a giant anomalous Hall effect. New classes of topological surface states may arise in linked nodal loops-topological Seifert surface states. The Seifert surface encodes information about the linking (Knot) number. We plan to explore the Seifert surfaces in linked nodal loop materials with state-of-the-art ARPES/spin-ARPES and ultrafast Tr-ARPES. (2) Kagome magnets: Intrinsic Chern quantum phases are possible in kagome lattices. The hard magnet TbMn_6Sn_6 system has been shown to hosting ideal spin-orbit-coupled magnetic kagome lattices in previous cycle. We plan to explore in-plane spin-momentum locking with spin-resolved ARPES to develop understanding of Chern phases in the entire R- Mn_6Sn_6 and KV_3Sb_5 families. Resolving the spin-texture of the unconventional charge order gap or the bands associated with it by spin-resolved ARPES will provide smoking-gun

evidence for the time-reversal symmetry breaking and will help elucidate its microscopic origin as we plan to carry out in the next cycle. (3) Search for topological superconductors: As in the last cycle, we plan to continue to search for intrinsic topological superconductors in some materials including KV₃Sb₅ [2] and also explore new materials Sn_{1-x}In_xTe and SrPtAs. (4) Ultrafast dynamics: Dirac-Weyl, kagome and related chiral materials discovered under this grant will be further studied to explore their ultrafast/dynamical properties using a novel ultrafast instrument which was funded during the last cycle but the project got delayed due to COVID shutdown. Once completed (expected around late 2023) the setup is expected to reveal novel excitation dynamics and ultrafast control of topological materials [4,5]. (5) Nonlinear optical responses of quantum materials have recently undergone dramatic developments to unveil nontrivial geometry and topology. A remarkable example is the quantized longitudinal circular photogalvanic effect (CPGE) associated with the Chern number of Weyl fermions, while the physics of transverse CPGE in Weyl semimetals remains exclusive. We recently showed theoretically that the transverse CPGE of Lorentz invariant Weyl fermions is forced to be zero. We find that the transverse photocurrents of Weyl fermions are associated not only with the Chern numbers but also with the degree of Lorentz-symmetry breaking in topological materials. Based on the generic two-band model analysis, we provided a powerful method to simulate the transverse CPGE based on the tilting and warping terms of Weyl fermions. Our results are more capable in designing large transverse CPGE of Weyl semimetals in experiments and are applied to more than tens of Weyl materials to estimate their photocurrents that we plan to study. Our method paves the way to study the CPGE of massless or massive quasiparticles to design next-generation ultrafast and quantum optoelectronics [4].

References

1. Ilya Belopolski, Guoqing Chang, Tyler A. Cochran, Zi-Jia Cheng, Xian P. Yang, Cole Hugelmeier, Kaustuv Manna, Jia-Xin Yin, G. Cheng, Daniel Multer, Maksim Litskevich, Nana Shumiya, Songtian S. Zhang, Chandra Shekhar, N. Schröter, Alla Chikina, Craig Polley, Balasubramanian Thiagarajan, Mats Leandersson, Johan Adell, Shin-Ming Huang, Nan Yao, Vladimir N. Strocov, Claudia Felser, and M. Zahid Hasan, *Observation of a linked loop quantum state*, NATURE **604**, 647-652 (2022).
2. Jia-Xin Yin, Biao Lian, M. Zahid Hasan *Topological kagome magnets and superconductors*, NATURE **612**, 647-657 (2022).
3. Xian P. Yang, Yigui Zhong, Sougata Mardanya, Tyler A. Cochran, Ramakanta Chapai, Akifumi Mine, Junyi Zhang, Jaime Sánchez-Barriga, Zi-Jia Cheng, Oliver J. Clark, Jia-Xin Yin, Joanna Blawat, Guangming Cheng, Ilya Belopolski, Tsubaki Nagashima, Najafzadeh Sahand, Shiyuan Gao, Nan Yao, Arun Bansil, Rongying Jin, Tay-Rong Chang, Shik Shin, Kozo Okazaki and M. Zahid Hasan,

Coexistence of bulk-nodal and surface-nodeless Cooper pairings in a superconducting Dirac semimetal,

Phys. Rev. Letts. (in press) (2023).

4. Mohammad Yahyavi, Yuanjun Jin, Yilin Zhao, Zi-Jia Cheng, Tyler A. Cochran, Yi-Chun Hung, Tay-Rong Chang, Qiong Ma, Su-Yang Xu, Arun Bansil, M. Zahid Hasan, Guoqing Chang,
Transverse circular photogalvanic effect associated with Lorentz-violating Weyl fermions,
arXiv:2301.00958 (2023).
5. Nicholas Sirica, Peter P Orth, MS Scheurer, YM Dai, M-C Lee, Prashant Padmanabhan, LT Mix, SW Teitelbaum, Mariano Trigo, LX Zhao, GF Chen, Bing Xu, Run Yang, Bing Shen, Chaowei Hu, C-C Lee, Hsin Lin, TA Cochran, SA Trugman, J-X Zhu, MZ Hasan, Ni Ni, XG Qiu, AJ Taylor, DA Yarotski, RP Prasankumar
"Photocurrent-driven transient (ultrafast) symmetry breaking in the Weyl semimetal TaAs"
Nature Materials **21**, 62-66 (2022).

Publications

2022

1. Jia-Xin Yin, Biao Lian, M Zahid Hasan *"Topological kagome magnets and superconductors"* Nature 612, 647-657 (2022)
2. Mohammad Yahyavi, Yuanjun Jin, Yilin Zhao, Zi-Jia Cheng, Tyler A. Cochran, Yi-Chun Hung, Tay-Rong Chang, Qiong Ma, Su-Yang Xu, Arun Bansil, M. Zahid Hasan, Guoqing Chang *"Transverse circular photogalvanic effect associated with Lorentz-violating Weyl fermions"* arXiv:2301.00958 (submitted 2022)
3. Daniel Multer, Jia-Xin Yin, Md. Shafayat Hossain, Xian Yang, Brian C Sales, Hu Miao, William R Meier, Yu-Xiao Jiang, Yaofeng Xie, Pengcheng Dai, Jianpeng Liu, Hanbin Deng, Hechang Lei, Biao Lian, M. Zahid Hasan *"Imaging real-space flat band localization in kagome magnet FeSn"* arXiv:2212.12726
4. Nana Shumiya, Jia-Xin Yin, Guoqing Chang, Meng Yang, Sougata Mardanya, Tay-Rong Chang, Hsin Lin, Md Shafayat Hossain, Yu-Xiao Jiang, Tyler A. Cochran, Qi Zhang, Xian P. Yang, Youguo Shi, M. Zahid Hasan; *"Evidence for electronic signature of magnetic transition in topological magnet HoSbTe"* 10.1103/PhysRevB.106.035151
5. Xiaokun Teng, Lebing Chen, Feng Ye, Elliott Rosenberg, Zhaoyu Liu, Jia-Xin Yin, Yu-Xiao Jiang, Ji Seop Oh, M. Zahid Hasan, Kelly J. Neubauer, Bin Gao, Yaofeng Xie, Makoto Hashimoto, Donghui Lu, Chris Jozwiak, Aaron Bostwick, Eli Rotenberg, Robert J. Birgeneau, Jiun-Haw Chu, Ming Yi, Pengcheng Dai; *"Discovery of charge density wave in a correlated kagome lattice antiferromagnet"* Nature 609, 490-495 (2022)
6. Jia-Xin Yin, Yu-Xiao Jiang, Xiaokun Teng, Md. Shafayat Hossain, Sougata Mardanya, Tay-Rong Chang, Zijin Ye, Gang Xu, M. Michael Denner, Titus Neupert, Benjamin

- Lienhard, Han-Bin Deng, Chandan Setty, Qimiao Si, Guoqing Chang, Zurab Guguchia, Bin Gao, Nana Shumiya, Qi Zhang, Tyler A. Cochran, Daniel Multer, Ming Yi, Pengcheng Dai, M. Zahid Hasan; “*Discovery of charge order and corresponding edge state in kagome magnet FeGe*” Phys. Rev. Lett. 129, 166401 (2022)
7. Xian P. Yang, Harrison LaBollita, Zi-Jia Cheng, Hari Bhandari, Tyler A. Cochran, Jia-Xin Yin, Md. Shafayat Hossain, Ilya Belopolski, Qi Zhang, Yuxiao Jiang, Nana Shumiya, Daniel Multer, Maksim Liskevich, Dmitry A. Usanov, Yanliu Dang, Vladimir N. Strocov, Albert V. Davydov, Nirmal J. Ghimire, Antia S. Botana, M. Zahid Hasan; “*Visualizing the out-of-plane electronic dispersions in an intercalated transition metal dichalcogenide*” 10.1103/PhysRevB.105.L121107 Physical Review B
 8. Ilya Belopolski, Guoqing Chang, Tyler A. Cochran, Zi-Jia Cheng, Xian P. Yang, Cole Hugelmeyer, Kaustuv Manna, Jia-Xin Yin, Guangming Cheng, Daniel Multer, Maksim Litskevich, Nana Shumiya, Songtian S. Zhang, Chandra Shekhar, Niels B. M. Schröter, Alla Chikina, Craig Polley, Balasubramanian Thiagarajan, Mats Leandersson, Johan Adell, Shin-Ming Huang, Nan Yao, Vladimir N. Strocov, Claudia Felser, M. Zahid Hasan; “*Observation of a linked loop quantum state*” Nature 604, 647-652 (2022)
 9. Zijin Ye, Aiyun Luo, Jia-Xin Yin, M Zahid Hasan, Gang Xu; *Structural instability and charge modulations in the Kagome superconductor AV3Sb5*; 10.1103/PhysRevB.105.245121
 10. Yaofeng Xie, Yongkai Li, Philippe Bourges, Alexandre Ivanov, Zijin Ye, Jia-Xin Yin, M Zahid Hasan, Aiyun Luo, Yugui Yao, Zhiwei Wang, Gang Xu, Pengcheng Dai; *Electron-phonon coupling in the charge density wave state of CsV3Sb5* Phys. Rev. B 105, L140501 (2022)
 11. Nana Shumiya, Md Shafayat Hossain, Jia-Xin Yin, Zhiwei Wang, Maksim Litskevich, Chiho Yoon, Yongkai Li, Ying Yang, Yu-Xiao Jiang, Guangming Cheng, Yen-Chuan Lin, Qi Zhang, Zi-Jia Cheng, Tyler A. Cochran, Daniel Multer, Xian P. Yang, Brian Casas, Tay-Rong Chang, Titus Neupert, Zhujun Yuan, Shuang Jia, Hsin Lin, Nan Yao, Luis Balicas, Fan Zhang, M. Z. Hasan *Room-temperature quantum spin Hall edge state in a higher-order topological insulator Bi4Br4*; Nature Materials 21, 1111–1115 (2022)
 12. Haoxiang Li, Yu-Xiao Jiang, J. X. Yin, Sangmoon Yoon, Andrew R. Lupini, Y. Pai, C. Nelson, A. Said, Y. M. Yang, Q. W. Yin, C. S. Gong, Z. J. Tu, H. C. Lei, Binghai Yan, Ziqiang Wang, M. Z. Hasan, H. N. Lee, H. Miao; “*Spatial symmetry constraint of charge-ordered kagome superconductor CsV3Sb5*” Nature Communications 13:6348 (2022)
 13. C. Mielke III, D. Das, J. -X. Yin, H. Liu, R. Gupta, Y. -X. Jiang, M. Medarde, X. Wu, H. C. Lei, J. J. Chang, P. Dai, Q. Si, H. Miao, R. Thomale, T. Neupert, Y. Shi, R. Khasanov, M. Z. Hasan, H. Luetkens, Z. Guguchia; “*Time-reversal symmetry-breaking charge order in a kagome superconductor*” Nature 602, 245-250 (2022)

2021

1. M. Zahid Hasan, Guoqing Chang, Ilya Belopolski, Guang Bian, Su-Yang Xu, Jia-Xin Yin “*Weyl, Dirac and high-fold chiral fermions in topological quantum materials*” Nature Reviews Materials 6, 784–803 (2021)
2. Z. Guguchia, H. Zhou, C. N. Wang, J. -X. Yin, C. Mielke III, S. S. Tsirkin, I. Belopolski, S. -S. Zhang, T. A. Cochran, T. Neupert, R. Khasanov, A. Amato, S. Jia, M. Z. Hasan, H. Luetkens; “*Putative helimagnetic phase in the kagome metal $Co_3Sn_2-xIn_xS_2$* ” npj Quantum Materials 6, 50 (2021)
3. Zhiwei Wang, Yu-Xiao Jiang, Jia-Xin Yin, Yongkai Li, Guan-Yong Wang, Hai-Li Huang, Sen Shao, Jinjin Liu, Peng Zhu, Nana Shumiya, Md Shafayat Hossain, Hongxiong Liu, Youguo Shi, Junxi Duan, Xiang Li, Guoqing Chang, Pengcheng Dai, Zijin Ye, Gang Xu, Yanchao Wang, Hao Zheng, Jinfeng Jia, M. Zahid Hasan, and Yugui Ya. *Electronic nature of chiral charge order in the kagome superconductor CsV_3Sb_5* . Phys. Rev. B **104**, 075148 (2021). 10.1103/PhysRevB.104.075148
4. Daniel Multer, Jia-Xin Yin, Songtian S. Zhang, Hao Zheng, Tay-Rong Chang, Guang Bian, Raman Sankar, and M. Zahid Hasan. *Robust topological state against magnetic impurities observed in the superconductor $PbTaSe_2$* . Phys. Rev. B **104**, 075145 (2021). 10.1103/PhysRevB.104.075145
5. Nana Shumiya, Md. Shafayat Hossain, Jia-Xin Yin, Yu-Xiao Jiang, Brenden R. Ortiz, Hongxiong Liu, Youguo Shi, Qiangwei Yin, Hechang Lei, Songtian S. Zhang, Guoqing Chang, Qi Zhang, Tyler A. Cochran, Daniel Multer, Maksim Litskevich, Zi-Jia Cheng, Xian P. Yang, Zurab Guguchia, Stephen D. Wilson, and M. Zahid Hasan. *Intrinsic nature of chiral charge order in the kagome superconductor RbV_3Sb_5* . Phys. Rev. B **104**, 035131 (2021). 10.1103/PhysRevB.104.035131
6. Wenlong Ma, Xitong Xu, Jia-Xin Yin, Hui Yang, Huibin Zhou, Zi-Jia Cheng, Yuqing Huang, Zhe Qu, Fa Wang, M. Zahid Hasan, and Shuang Jia. *Rare Earth Engineering in RMn_6Sn_6 ($R=Gd-Tm, Lu$) Topological Kagome Magnets*. Phys. Rev. Lett. **126**, 246602 (2021).
7. Yu-Xiao Jiang, Jia-Xin Yin, M. Michael Denner, Nana Shumiya, Brenden R. Ortiz, Gang Xu, Zurab Guguchia, Junyi He, Md Shafayat Hossain, Xiaoxiong Liu, Jacob Ruff, Linus Kautzsch, Songtian S. Zhang, Guoqing Chang, Ilya Belopolski, Qi Zhang, Tyler A. Cochran, Daniel Multer, Maksim Litskevich, Zi-Jia Cheng, Xian P. Yang, Ziqiang Wang, Ronny

- Thomale, Titus Neupert, Stephen D. Wilson, M. Zahid Hasan. *Unconventional chiral charge order in kagome superconductor KV_3Sb_5* . Nat. Mater. **20**, 1353–1357 (2021).
8. Ilya Belopolski, Tyler A. Cochran, Xiaoxiong Liu, Zi-Jia Cheng, Xian P. Yang, Zurab Guguchia, Stepan S. Tsirkin, Jia-Xin Yin, Praveen Vir, Gohil S. Thakur, Songtian S. Zhang, Junyi Zhang, Konstantine Kaznatcheev, Guangming Cheng, Guoqing Chang, Daniel Multer, Nana Shumiya, Maksim Litskevich, Elio Vescovo, Timur K. Kim, Cephise Cacho, Nan Yao, Claudia Felser, Titus Neupert, and M. Zahid Hasan. *Signatures of Weyl Fermion Annihilation in a Correlated Kagome Magnet*. Phys. Rev. Lett. **127**, 256403 (2021).
 9. M. Zahid Hasan, Guoqing Chang, Ilya Belopolski, Guang Bian, Su-Yang Xu, Jia-Xin Yin. *Weyl, Dirac and high-fold chiral fermions in topological quantum matter*. Nat Rev Mater **6**, 784–803 (2021).
 10. Jia-Xin Yin, Shuheng H Pan, M Zahid Hasan. *Probing topological quantum matter with scanning tunnelling microscopy*. Nat Rev Phys **3**, 249–263 (2021). 10.1038/s42254-021-00293-7
 11. H. Miao, Y. L. Wang, J.-X. Yin, J. Zhang, S. Zhang, M. Z. Hasan, R. Yang, X. C. Wang, C. Q. Jin, T. Qian, H. Ding, H.-N. Lee, and G. Kotliar. *Hund's superconductor $Li(Fe,Co)As$* . Phys. Rev. B **103**, 054503 (2021).
 12. Ming-Chien Hsu, Hsin Lin, M Zahid Hasan, Shin-Ming Huang. *Topologically distinct Weyl fermion pairs*. Sci Rep **11**, 416 (2021). 10.1038/s41598-020-79977-6
 13. Titus Neupert, M. Michael Denner, Jia-Xin Yin, Ronny Thomale, and M. Zahid Hasan. *Charge order and superconductivity in kagome materials*. Nat. Phys. (2021). 10.1038/s41567-021-01404-y
 14. C. Mielke, III, Y. Qin, J.-X. Yin, H. Nakamura, D. Das, K. Guo, R. Khasanov, J. Chang, Z. Q. Wang, S. Jia, S. Nakatsuji, A. Amato, H. Luetkens, G. Xu, M. Z. Hasan, and Z. Guguchia. *Nodeless kagome superconductivity in $LaRu_3Si_2$* . Phys. Rev. Materials **5**, 034803 (2021). 10.1103/PhysRevMaterials.5.034803
 15. N Sirica, P. P. Orth, M. S. Scheurer, Y.M. Dai, M.-C. Lee, P. Padmanabhan, L.T. Mix, S.W. Teitelbaum, M. Trigo, L.X. Zhao, G.F. Chen, B. Xu, R. Yang, B. Shen, C. Hu, C.-C. Lee, H. Lin, T.A. Cochran, S.A. Trugman, J.-X. Zhu, M.Z. Hasan, N. Ni, X.G. Qiu, A.J. Taylor, D.A. Yarotski, R.P. Prasankumar. *Photocurrent-driven transient symmetry breaking in the Weyl semimetal $TaAs$* . Nat. Mater. **21**, 62–66 (2021).

Ultrafast enhancement of antiferromagnetic second-harmonic generation in BiFeO₃

Wanzheng Hu, Boston University

Keywords: multiferroics, nonlinear phononics

Research Scope

Ferroelectric materials have an intrinsic spontaneous electric polarization that can be switched by electric field. Ultrafast switching of ferroelectric polarization is appealing for developing non-volatile ultrafast memory unit. A recent theory work¹ predicted that a sub-picosecond reversal of the ferroelectric polarization can be achieved by driving the highest energy infrared-active phonon in perovskite transition-metal ferroelectrics. The switching is bidirectional and the switched state is long-lived. However, a pioneering experiment on LiNbO₃ showed only a partial polarization switching can be induced by phonon pumping, and the original phase was rapidly restored within 0.5 picoseconds.²

We aim at exploring ultrafast switching of ferroelectric polarization in a broad category of ferroelectrics using coherent phonon excitations. We start from bismuth ferrite (BiFeO₃), one of the most widely studied room-temperature multiferroics with large spontaneous polarization, strong optical nonlinearities, and strong couplings of the lattice structure, electronic and magnetic properties to external fields. Our goal is to search for light-controlled long-lived ferroelectric switching at room temperature. Our experiment will provide a new perspective to understand the fundamental interactions which controls ferroelectricity in perovskite oxides. Since bismuth ferrite allows more than one ferroelectric polarization directions within the unit cell, this research may enable multi-bit information encoding in a single ferroelectric domain.

Recent Progress

Magnetoelectric multiferroics simultaneously exhibit ferroelectric and magnetic order that are intrinsically coupled to each other within a single phase. These couplings allow for the control of magnetization and polarization through respective cross-coupled electric and magnetic fields, which makes them appealing candidates for encoding and accessing information using two order parameters at a time. Instead of applying static external fields, one can imagine to couple to the multiferroic order parameters using the electromagnetic field components of light, which would allow for remote and all optical control of the magnetoelectric phases. Here, we show that ferroelectric polarization and antiferromagnetism can be enhanced simultaneously by laser excitation of optical phonons in the prototypical multiferroic material BiFeO₃. Specifically, we use time-resolved second harmonic generation (tr-SHG) to probe the dynamics of the crystal lattice and magnetic order in response to the coherent excitation of fully-symmetric phonon modes with ultrashort mid-infrared pulses at room temperature.

We find that ferroelectric polarization and antiferromagnetic order in BiFeO₃ can be enhanced simultaneously through nonlinear excitation of phonons. We coherently excite the high-frequency fully symmetric (A₁) modes of the system with ultrashort mid-infrared pulses and probe the evolution of the structural and antiferromagnetic state using time-resolved second-harmonic generation (tr-SHG). As shown in Fig. 1, when the mid-infrared pump pulses is polarized along the ferroelectric polarization direction, the SHG intensity has a maximum 1.5% transient enhancement; when the mid-infrared field is orthogonal to the ferroelectric polarization, no pump-induced change is observed. The lifetime of the transient state closely follows the pump pulse duration, similar to what was observed in LiNbO₃.²

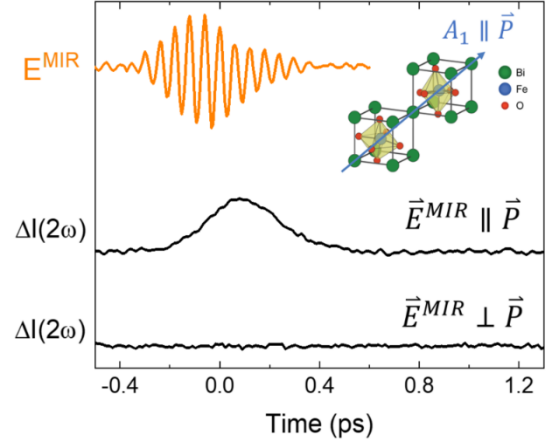


Figure 1 Phonon-driven enhancement of the second-harmonic generation in BiFeO₃ (unpublished data).

The SHG process in a crystal depends on its point group symmetry. It is a sensitive probe for ferroelectricity (which breaks space-inversion symmetry) and magnetic ordering (which breaks time-inversion symmetry). The SHG intensity, $I(2\omega)$, is proportional to $|P(2\omega)|^2$, where $P(2\omega)$ is the light-induced nonlinear polarization:

$$P_i(2\omega) \propto \left(\chi_{ijk}^{(i)} + \chi_{ijk}^{(c)} \right) E_j(\omega) E_k(\omega)$$

with $E(\omega)$ the incident light field and χ the SHG tensor. Each of i, j, k represent the direction of polarization of the relevant fields. $\chi_{ijk}^{(i)}$ and $\chi_{ijk}^{(c)}$ are the crystallographic and magnetic SHG susceptibility tensor components, respectively. For BiFeO₃, $\chi_{ijk}^{(i)}$ represents the ferroelectric contribution and is the leading term for SHG process; $\chi_{ijk}^{(c)}$ is the antiferromagnetic susceptibility tensor component. The point-group symmetry of a crystal determines its set of non-zero SHG tensors. At room temperature, the crystal lattice of BiFeO₃ is rhombohedral (space group R3c), with 3m point-group symmetry. The antiferromagnetic order in the bulk crystal shows an additional long-range magnetic modulation with three equivalent wave vectors (τ_1, τ_2, τ_3) perpendicular to ferroelectric polarization. Our sample is a predominantly single ferroelectric and single- τ magnetic domain crystal. The single- τ magnetic wave vector lifts the three-fold rotation symmetry around P , and lowers the symmetry to monoclinic, with a point group m . Therefore, information on ferroelectricity and antiferromagnetic ordering is encoded in the symmetry of SHG intensity, which can be probed experimentally by varying the polarization of the fundamental beam.

Figure 2a shows the probe polarization dependence of the SHG signal at equilibrium. In the s-probe channel, the SHG signal has four lobes, with a small asymmetry along the 60° and 240° directions. This asymmetry comes from the time-noninvariant part of the SHG signal (antiferromagnetic contribution, white area), which arises from symmetry lowering by the single magnetic domain. Figure 2b shows the s-probe SHG polar plot in the phonon-driven state at maximum pump probe response. The maximum transient SHG enhancement is along 60° and 240° , where the antiferromagnetic contribution dominates. The maximum light-induced changes in the SHG intensity, $\Delta I_{\text{max}} / \Delta I$, is 1.5%. Probing antiferromagnetic order has always been a hard task, due to the exact cancellation of its internal magnetization. To our knowledge, this is the first experimental observation of an enhanced magnetic SHG signal in the phonon driven state.

We also conducted SHG measurements for the p-probe channel, which is dominated by the ferroelectric contribution. Our data shows an enhanced ferroelectric contribution to the SHG signal (data not shown here) with $\Delta I_{\text{max}} / \Delta I = 1.5\%$.

We perform phonon dynamics simulations supported by density functional theory calculations. Our calculations indicate that nonlinear phonon coupling leads to a rectification of the A1 modes of the system that modifies the second-order susceptibility tensors by about 2%, which account for the increase in the ferroelectric polarization. The antiferromagnetic order in BiFeO₃ has an additional long-range modulation. However, simulation of the antiferromagnetic order is beyond the capability of density functional calculations. We speculate the enhanced antiferromagnetic SHG signal also comes from the enhanced second-order susceptibility tensors.

Future Plans

Magnetic SHG is a powerful probe of complex magnetic distributions. Our results on BiFeO₃ show that antiferromagnetic order can be probed by SHG polarimetry, and mid-infrared pulses with peak electric field exceeding several megavolts per centimeter can modify the magnetic order within picosecond time scales. We plan to use magnetic SHG to probe novel spin

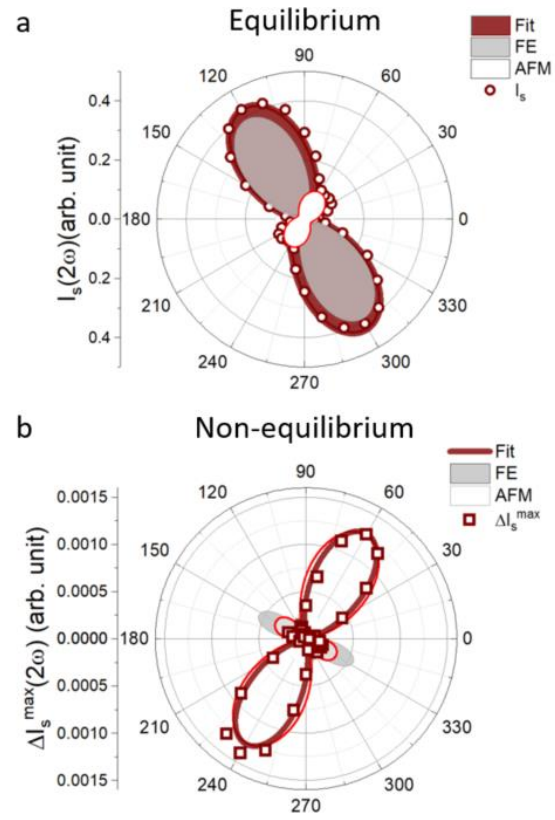


Figure 2 Probe polarization dependence of the second-harmonic signal (a) at equilibrium and (b) in the phonon driven state (unpublished data).

order in materials with centrosymmetric lattice structure, from which the second-harmonic generation is purely magnetic in origin. Our plan is to (1) probing magnetic SHG in helical spin state in centrosymmetric lattice, and (2) control helical spin state with circularly polarized light pumping.

References

1. Alaska Subedi, *Proposal for ultrafast switching of ferroelectrics using midinfrared pulses*, Phys. Rev. B **92**, 214303 (2015).
2. R. Mankowsky, A. von Hoegen, M. Först, and A. Cavalleri, *Ultrafast Reversal of the Ferroelectric Polarization*, Phys. Rev. Lett. **118**, 197601 (2017).

Publications

Manuscript to be submitted:

Daniel Alejandro Bustamante Lopez, Dominik Maximilian Juraschek, Xianghan Xu, Sang-Wook Cheong, and Wanzheng Hu, *Ultrafast enhancement of antiferromagnetic second-harmonic generation in BiFeO₃*.

Probing Twisted 2D Heterostructures using Focused Photoemission Spectroscopy

Jyoti Katoch, Carnegie Mellon University

Keywords: 2D materials, twisted vdW heterostructures, *in-operando* micro- and nano-ARPES

Research Scope

Vertical stacking of atomically thin two-dimensional (2D) crystals to engineer atomically precise van der Waals (vdW) heterostructures, provides a unique opportunity to study designer quantum matter which can host novel physical phenomena. The vdW heterostructures with small lattice mismatch and a relatively small twist angle between the constituent layers, have shown to exhibit coexisting complex phases of matter including Mott insulating state, superconductivity, bound quasiparticles, and topological states [1]. To understand the origin of complex phases of matter that exists in vdW heterostructures and their dependence on twist angle, this project seeks to directly probe the spatially resolved band structure of mesoscopic sized 2D quantum materials based heterostructures using the state-of-the-art angle-resolved photoemission spectroscopy with focused spatial resolution (microARPES and nanoARPES). In addition, planned research aims at developing a capability to perform nanoARPES measurement under non-equilibrium conditions – like when an external lateral electric field is applied to a 2D system. This enables direct investigation of the changes to electronic states and chemical potential in 2D quantum material-based nanoscale devices under non-equilibrium conditions [2]. This research is a crucial step towards the utilization of the 2D materials for future technological applications in electronics, opto-electronics, photonics, and spintronic devices. In last two years, we investigated the twist angle dependence on the electronic states of different 2D based heterostructure and their devices.

Recent Progress

1. Visualizing band structure hybridization and superlattice effects in twisted MoS₂/WS₂ heterobilayers [Jones *et. al.*, *2D Mater.*, 9 015032 (2022)]

Stacking of two-dimensional (2D) van der Waals (vdW) materials is a promising avenue for engineering electronic states for device applications. A mismatch of atomic registries between single-layer transition metal dichalcogenides (TMDs) in a vdW heterostructure produces a moiré superlattice with a periodic potential which can be fine-tuned by introducing a twist angle between the materials. This approach is promising both for controlling the interactions between the TMDs and for engineering their electronic band structures, yet direct observation of the changes to the electronic structure introduced by the moiré have so far been missing. Here, we utilize microARPES) on a 2D material based heterostructure which consists of three monolayer MoS₂ islands laid on monolayer WS₂ all placed on hBN and doped TiO₂ (Fig. 1a-b). We began investigating the quasiparticle dynamics by determining the twist angle between each MoS₂/WS₂ combination as knowing their twist angle, we can examine how it influences the heterostructure's quasiparticle dispersion. Our measurements reveal each MoS₂ island has a unique rotational alignment to the WS₂, which were found to be $2.0 \pm 0.5^\circ$, $13.0 \pm 0.5^\circ$, and $20.0 \pm 0.5^\circ$. Furthermore, we observe strong hybridization effects between MoS₂ and WS₂ bands at the Γ -point of the Brillouin zone (BZ), characterized by a strong bonding/antibonding energy splitting of (548 ± 33) meV (Fig. 1c). This splitting is found to be independent of the twist angle and leads to a transition from a direct bandgap in the SL TMDs to an indirect bandgap in our heterostructures. Apart from this transition, we observe replica bands around the Γ -point for the 20° and 13° sample which are highlighted in the top right of Fig. 1d-f. Each of these replica bands, whose location is tunable with twist angle, allow for additional optical transitions between the valence and conduction bands.

These moiré effects are not observed in the 2° heterostructure which is consistent with expected locations because the brightest replica's position in momentum space overlays the primary Γ -point peak.

We compared our experimental dispersion with density functional theory (DFT) calculations of unfolded superlattice electronic bands in relaxed MoS_2/WS_2 structures with commensurate stacking near our experimental twist angles. We find agreement between experimental and theoretical bands, which strongly suggests that the measured minibands arise from

the inherent moiré potential. The calculations provide an estimate for the conduction band dispersion and, in combination with the measured valence band dispersion, reveal optical transitions caused by the superlattice. The direct to indirect band gap transition and appearance of twist angle dependent replica bands highlight the possibility to engineer optoelectronic properties of TMD heterostructures using the twist angle-tunable superlattice dispersion. This study gives novel and detailed insight to the quasiparticle dynamics as the twist angle evolves.

2. *In-operando* nanoARPES: Spatial Mapping of the Electronic Structure of Twisted Bilayer Graphene [Majchrzak et al., *Small Sci.*, 1, 2000075 (2021)]

In twisted bilayer graphene (TBLG), superlattices can be induced and tuned by varying the interlayer rotation θ between two graphene layers. Extensive work has been done to investigate the influence of varied twist angle and doping on the transport and optical properties of TBLG, revealing its potential for versatile applications. In this work, we demonstrate the strength of the *in-operando* nanoARPES technique by mapping and analyzing the Dirac cones in a TBLG device under different device conditions. This gives us a unique view into how microscopic rotational domains influence the operation of the device and the states that govern it. We show that these features are characterized by significant energy- and momentum-dependent displacements of the Dirac cones when a current is applied, which we attribute to strong local electric field enhancements. Finally, we find that this behavior is also strongly dependent on the electrostatic gate voltage applied to dope the TBLG, thereby revealing a complex interplay of structural inhomogeneity, transport properties and electronic structure using *in operando* nanoARPES.

The mapping of the device was carried out in the presence of gate-induced doping and source–drain currents thereby combining the two standard modes of operation of a device with the nanoARPES capability. We developed an analysis method that is capable of extracting maps

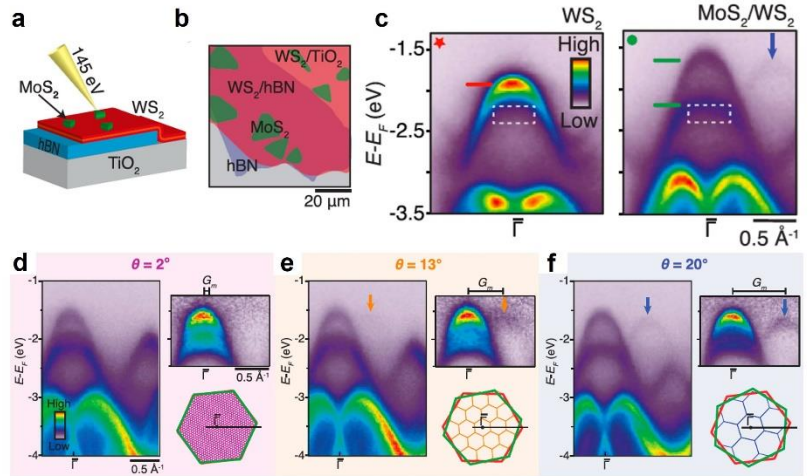


Figure 1: (a) Schematic showing ARPES measurements on the heterostructure consisting of SL MoS_2 islands, SL WS_2 , and thick hBN, on a n-doped TiO_2 substrate. (b) Sketch of the heterostructure with labels that correspond to the different parts of the sample identified. (c) Dispersion of WS_2 on hBN directly compared to the MoS_2/WS_2 with a 20° twist. (d-f) Dispersion near the Gamma point of the MoS_2/WS_2 heterostructures with 2° , 13° , and 20° twist angles, respectively. In each section, there is an insert in the top right displaying an image with high contrast which highlights the presence of replica bands coming from moiré effect.

composed of the position-dependent variations in Dirac cone dispersion and linewidth, leading to the identification of rotational domain boundaries and impurities within the device. We find the presence of rotational domains (9.8 to 12.7 degrees) within the active region of graphene device and how they correspond with the twisted domain boundaries of the heterostructure. With the twist angle boundaries investigated in full, we seek out how they influence the operation of the device by applying a current of 314 μA and gate voltage to tune the carrier density. The main effect of a current is the position dependent rigid energy shift of the spectra caused by the local potential ϕ , but by taking the gradient of the potential we can reveal the local electric field which reveals a more intricate texture across the device (Fig 2). Interestingly, in the middle of the device, where a rotational domain boundary is seen to perforate the TBLG from top to bottom edges, the electric field exhibits a substantial increase, reaching a maximum strength of 0.75 $\text{V}/\mu\text{m}$. This abrupt change is directly visible in the corresponding ARPES spectrum from this region in Fig. 2b where a faint replica of the top Dirac cone, rigidly shifted in energy by 0.44 eV is observed. This effect arises because the light spot is large enough to illuminate the sharp boundaries between two regions with different local potential, leading to the incoherent superposition of the intensity from the two sides of the boundary. Our work reveals that advanced 2D heterostructures that combine materials with variable electron- and hole-type doping along the device will display complex transport properties that emerge from the local electronic structure, which can be uncovered by in-operando nanoARPES.

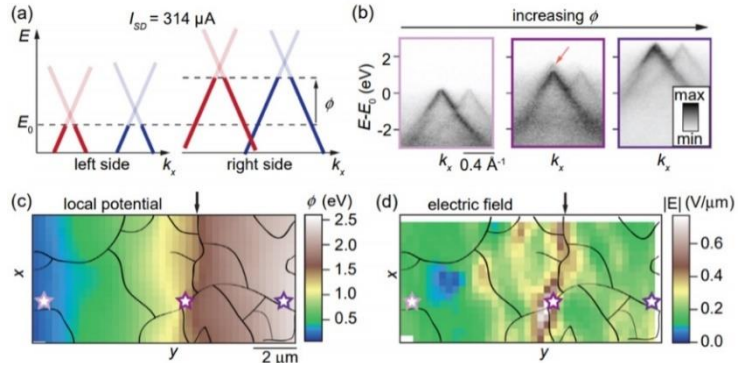


Figure 2: (a) Model nanoARPES spectrum from the TGB sample as a current of 314 μA is applied from left to right. (b) Measured nanoARPES spectrum from the device. Notice the arrow in the middle panel showing a superposition of signals at a rotation boundary. (c) Mapping the local potential of the current carrying device (d) The local electric field of the device.

The main effect of a current is the position dependent rigid energy shift of the spectra caused by the local potential ϕ , but by taking the gradient of the potential we can reveal the local electric field which reveals a more intricate texture across the device (Fig 2). Interestingly, in the middle of the device, where a rotational domain boundary is seen to perforate the TBLG from top to bottom edges, the electric field exhibits a substantial increase, reaching a maximum strength of 0.75 $\text{V}/\mu\text{m}$. This abrupt change is directly visible in the corresponding ARPES spectrum from this region in Fig. 2b where a faint replica of the top Dirac cone, rigidly shifted in energy by 0.44 eV is observed. This effect arises because the light spot is large enough to illuminate the sharp boundaries between two regions with different local potential, leading to the incoherent superposition of the intensity from the two sides of the boundary. Our work reveals that advanced 2D heterostructures that combine materials with variable electron- and hole-type doping along the device will display complex transport properties that emerge from the local electronic structure, which can be uncovered by in-operando nanoARPES.

3. Observation of novel quasi-particle in doped graphene/tungsten disulfide heterostructure [To be submitted]

Ability to tune the charge carrier densities in TMDCs enables the modulation of many-body interactions and quasiparticle dynamics, which can have huge impact on their electronic and optoelectronic properties [3]. In this study, we have investigated the effect of electron doping via potassium atom deposition on the electronic structure of SL-graphene/ WS_2 heterostructure on hBN placed on TiO_2 substrate. Upon electron doping via potassium evaporation, we observe the emergence of electronic states near Fermi level at K. The analysis reveals that the structure of these electron states is caused by the formation of quasi particle-polarons upon electron doping. We now discuss the evolution and origin of the polaron on electron doping in graphene/ WS_2 heterostructure as shown in Fig. 3. The Fig. 3(a) shows the evolution of a feature that has narrow band with a broad tail towards the higher binding energy, with increased electron doping (left to right). The EDC at K in Fig. 3(b) shows a main peak along with satellite peaks whose energy position is evenly spaced out. The overlaid purple line is the best fit whose intensity follows the Poisson

distribution. This spectral function has previously been attributed to Frölich polarons. Fig. 3(c) shows the evolution of the EDC intensity at K as a function of electron doping. From this we extract the evenly spaced-out energy position (ΔE) as a function of charge carrier density in graphene (Fig. 3(d)) and fitting follows the $\sqrt{n_G}$ -dependence (black dashed line), suggesting coupling to a single plasmon mode. The formation of strongly coupled plasmon-induced polarons with graphene is not well-established in bare WS₂, despite expected stronger screening with graphene. This sheds light into the critical role played by many body interactions in the formation of 2D plasmonic polarons, which is important for understanding the excitation dynamics and charge carrier transport.

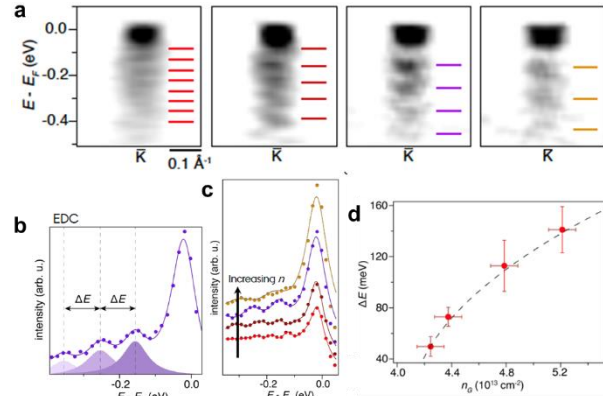


Figure 3: (a) The dispersion of SL graphene/WS₂ around K point as a function of increased n doping from left to right. The colored lines indicate the equal spacing in energy position (ΔE) which is clearly seen as satellite peaks separation along with main peak in (b). The intensity of EDCs as a function of electron doping is shown in (c). (d) ΔE as a function of charge carrier density in graphene.

Future Plans

Focused ARPES, i.e., microARPES and nanoARPES, will be employed to directly “see” the tunable electronic structure of different combination of TMDCs. Homo- and hetero-bilayers of TMDCs and twisted graphene sheets will be investigated to probe many body effects (MBEs). MBEs can give rise to many exotic quantum phenomena in twisted 2D heterostructures, such as flattening of bands and superconductivity, and lead to the formation of quasiparticles such as plasmons (collective excitations of electron density), polarons (a composite particle consisting of an electron with an attached phonon cloud), excitons (bound electron-hole pair) and trions (bound excitations of electron-hole-hole or electron-electron-hole composite particles). We will also investigate the electronic band structure of operating 2D devices, with current and gate voltage applied, to understand the complex role played by many-body interactions on the transport properties. In addition, we will probe adatom induced MBEs in TMDCs/h-BN heterostructures. Atomically clean 2D systems will be exposed to controlled amounts of adatoms (alkali metals) in the nanoARPES chamber. After each exposure, the transport and photoemission measurements will be performed to gain insight into the impact of atoms (or defects) on the average transport properties and changes to the band structure. During the last reporting cycle, we have worked with beamline scientists at the nanoARPES end-station to test the electron doping, using in-situ alkali metal evaporation, of mono- and bi-layer graphene devices to study the impact of many-body interactions on their electronic structure.

Reference

1. S.K. Behura, A. Miranda, S. Nayak, K. Johnson, P. Das and N. R. Pradhan, “Moiré physics in twisted van der Waals heterostructures of 2D materials”, *Emergent Materials* 4, 813-826 (2021).
2. P. Hofmann “Accessing the spectral function of *in operando* devices by angle-resolved photoemission spectroscopy”, *AVS Quantum Sci.* 3, 021101 (2021).
3. N. P. Wilson, W. Yao, J. Shan, and X. Xu, “Excitons and emergent quantum phenomena in stacked 2D semiconductors”, *Nature* 599, 383-392 (2021).

Publications

1. Alfred J H Jones, Ryan Muzzio, Sahar Pakdel, Deepnarayan Biswas, Davide Curcio, Nicola Lanatà, Philip Hofmann, Kathleen M McCreary, Berend T Jonker, Kenji Watanabe, Takashi Taniguchi, Simranjeet Singh, Roland J Koch, Chris Jozwiak, Eli Rotenberg, Aaron Bostwick, Jill A Miwa, **Jyoti Katoch*** and Søren Ulstrup, “Visualizing band structure hybridization and superlattice effects in twisted MoS₂/WS₂ heterobilayers”, **2D Mater.**, **9** 015032 (2022). [*Corresponding author]
2. Paulina Majchrzak, Ryan Muzzio, Alfred J. H. Jones, Davide Curcio, Klara Volckaert, Deepnarayan Biswas, Jacob Gobbo, Simranjeet Singh, Jeremy T. Robinson, Kenji Watanabe, Takashi Taniguchi, Timur K. Kim, Cephise Cacho, Jill A. Miwa, Philip Hofmann, **Jyoti Katoch***, and Søren Ulstrup* “In Operando Angle-Resolved Photoemission Spectroscopy with Nanoscale Spatial Resolution: Spatial Mapping of the Electronic Structure of Twisted Bilayer Graphene”, *Small Sci.*, **1**, 2000075 (2021). [*Corresponding author].
3. Davide Curcio, Alfred J. H. Jones, Ryan Muzzio, Klara Volckaert, Deepnaryan Biswas, Charlotte E. Sanders, Pavel Dudin, Cephise Cacho, Simranjeet Singh, Kenji Watanabe, Takashi Taniguchi, Jill A. Miwa, **Jyoti Katoch**, Soren Ulstrup, and Philip Hofmann “Accessing the Spectral Function in a Current-Carrying Device”, *Physical Review Letters*, **125**, 236403 (2020).

ULTRAFAST COHERENT X-RAY STUDIES OF QUANTUM MATERIALS

Roopali Kukreja,

Material Science and Engineering, University of California Davis

Self-identify keywords to describe your project: Coherent X-ray scattering, Quantum Materials, Thin Films, X-ray Photon Correlation Spectroscopy, Fluctuations

Research Scope: This project focuses on utilizing x-ray photon correlation spectroscopy (XPCS) at synchrotron sources and upcoming x-ray free electron sources (XFEL) to access both nanoscale lengthscales and fundamental timescales to investigate fluctuations of electronic and magnetic order across phase transitions as well as their behavior under external stimuli such as optical laser. Emergence of ‘exotic’ quantum states under non-equilibrium conditions in quantum materials challenges the limits of our understanding at microscopic length scales and ultrafast time scales. Fundamental understanding of the role of nanoscale heterogeneities and fluctuations in quantum materials has been impeded by the lack of experimental methods which can access both characteristic lengthscales and timescales. The project utilizes recently developed and upcoming user facilities such as National Synchrotron Light Source II (NSLS II), Linac Coherent Light Source (LCLS) and LCLS II as well as existing facilities such as Advanced Photon Source (APS). Coherent x-ray scattering measurements will be used to achieve insights into both thermal and ultrafast fluctuations of electronic and magnetic order across phase transitions. Ground state of the samples will be controlled via structural parameters (epitaxial strain, stoichiometry and doping) to study the relationships between lattice with specific quantum behavior (spin, charge). These studies will allow us to develop mesoscale understanding of fluctuations emerging from interplay between charge, spin and lattice order parameters.

Recent Progress:

A. Emergent electronic behavior at nanoscale: Recently, we have performed optically driven ultrafast studies as well as thermally driven measurements on magnetite highlighting that the role of phase separation and domain dynamics cannot be excluded from the description of phase transitions, and can in fact dictate the timescales of emergent metallic phase [22, 43]. For both optically and thermally driven transition, we observed that the insulating long-range trimeron ordering (three-Fe-site distortions) gets destroyed and the timescales of emergent metallic phase are dictated by coalescing of remaining trimerons leading to phase separation of insulating and metallic domains. However, surprisingly, orbital fluctuations seen at Fe L_3 edge were not observed at the oxygen K-edge indicating the fact that the orbital fluctuations are localized and purely electronic in nature, and not structural which would have resulted in fluctuations at oxygen K-edge. In order to further clarify the nature of these fluctuations, we utilized the split-pulse delay system at the Coherent X-ray Scattering (CXS) Hutch at LCLS with the split-delay varying from femtoseconds to nanoseconds. We tracked the evolution of

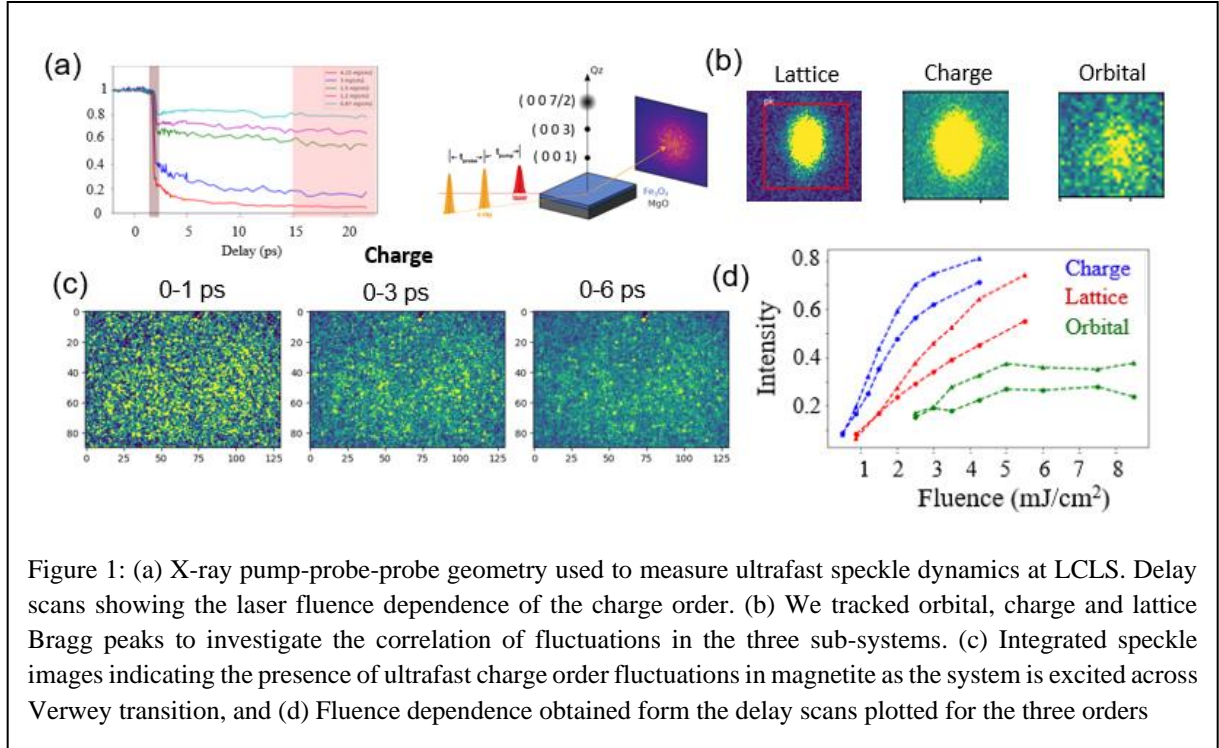


Figure 1: (a) X-ray pump-probe geometry used to measure ultrafast speckle dynamics at LCLS. Delay scans showing the laser fluence dependence of the charge order. (b) We tracked orbital, charge and lattice Bragg peaks to investigate the correlation of fluctuations in the three sub-systems. (c) Integrated speckle images indicating the presence of ultrafast charge order fluctuations in magnetite as the system is excited across Verwey transition, and (d) Fluence dependence obtained from the delay scans plotted for the three orders

the speckle pattern of the (003) charge order peak, (007/2) orbital order peak at the resonant iron edge and compared with speckle evolution of (001) lattice peak. While our measurement on speckle pattern of orbital order need further analysis, the measurements on charge order show distinct fluctuations on picosecond timescales (see Figure 1(a)). Furthermore, additional pump-probe studies at SwissFEL, revealed a surprising resilience of orbital order to laser fluence compared to both structural and charge order (see Figure 1(d)). This is strikingly different than previous studies performed on bulk magnetite and potentially highlights the route to tune ultrafast orbital ordering via strain engineering.

B. Emergent structural behavior and correlations with charge and magnetic ordering

Another aspect we focused on is to utilize XPCS to investigate the coupling of magnetic and electronic degrees of freedom in thermally driven phase transitions. If the two degrees of freedom are indeed decoupled or coupled in these systems, the nature of fluctuations, their evolution as a function of temperature, would be different or similar, respectively. Rare-earth nickelates provide an ideal system to study this phenomenon, as different types of rare earth cation (RNiO_3 , where R is rare earth Nd, Sm) provide a way to tune the tolerance factor to achieve coupled insulator-to-metal transition and Neel temperatures, $T_{\text{MIT}}=T_{\text{N}}$ (i.e. NdNiO_3 (NNO)) or systems where $T_{\text{MIT}}\neq T_{\text{N}}$ (i.e. SmNiO_3 (SNO)). To this effect, we have recently measured thermally driven XPCS studies for both NNO and SNO. We tuned to (002) and (105) Bragg peaks to measure both structural and electronic ordering. Specifically, for structural, **this information will be correlated to variation** in Ni-O stretching mode or rotation of NiO_6 octahedra to map out the structural evolution as a function of time. Figure 2 shows our preliminary studies on NNO grown on SrTiO_3 (STO) performed by accessing (105) peak showing structural fluctuations in the material system.

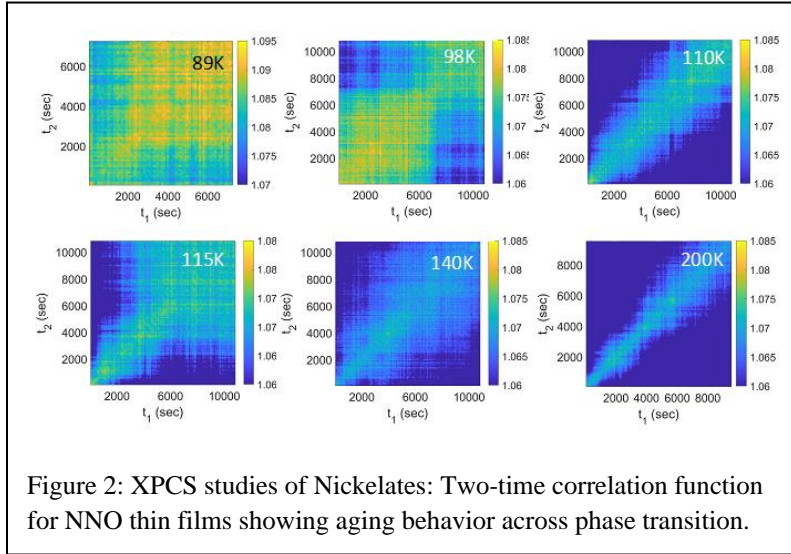


Figure 2: XPCS studies of Nickelates: Two-time correlation function for NNO thin films showing aging behavior across phase transition.

Interestingly, even at non-resonant energy (~ 8 keV) we observed speckle fluctuations in both metallic and insulating state ($T_{MIT}=T_N \sim 150$ K). This is in striking contrast with results obtained in magnetite where no structural fluctuations have been observed. Furthermore, aging dynamics is observed as shown in two time-correlation function (Figure 2). Our XPCS studies also show that faster structural fluctuations are observed in NNO

compared to SNO, pointing towards role of magnetism and structural correlations which is not present in SNO. In fact, coupled recovery of magnetism and structural order parameter has been recently observed in our time-resolved pump probe studies in nickelates [3].

Future Plans: We plan to work on adapting droplet-analysis algorithms [4] for quantum materials which will also enable analysis of both electronic and orbital order data measured at LCLS. Comparison of this analysis for different resonant edges and multiple scattering peaks will provide further insights into the coupling of magnetic and electronic degrees of freedom in quantum materials. Additional ultrafast XPCS studies are also planned to develop complete overview of the electronic distortions at ps timescale. We also have upcoming beamtimes both at NSLS-II (CHX and CSX) and ALS (COSMIC) to utilize XPCS to capture the evolution of electronic and magnetic fluctuations in nickelate family as a function of sample parameter phase space.

References

1. Kukreja, R., Hua, N., Ruby, J., Barbour, A., Hu, W., Mazzoli, C., Wilkins, S., Fullerton, E. F., & O.G. Shpyrko. Orbital domain dynamics in magnetite below the Verwey transition. *Phys. Rev. Lett.*, 121, 177601 (2018)
2. Christiansen-salameh, J., Yang, M., Rippy, G., & Li, J. Cai, Z., Holt, M. Agnus, G. Maroutian, T. Lecoer, P., Matzen, S., Kukreja, R. Understanding nanoscale structural distortions in and clustering algorithm analysis research papers. *Journal of Synchrotron Radiation* 28, 207–213 (2021).
3. Y. Sun, N. Wang, S. Song, P. Sun, M. Chollet, T. Sato, T. B. van Driel, S. Nelson, R. Plumley, J. Montana-Lopez, S. W. Teitelbaum, J. Haber, J. B. Hastings, A. Q. R. Baron, M. Sutton, P. H. Fuoss, A. Robert and D. Zhu, A compact hard x-ray split-delay system based on variable-gap channel-cut crystals, *Opt. Lett.* 44, 2582 (2019)

4. Fluence dependent switching of structural dynamics in NNO/STO thin films, Jugal Mehta, Jianheng Li, Scott Smith, Rahul Jangid, Nadia Albayati, Kenneth Ainslie, Don Walko, Haidan Wen, Roopali Kukreja, PR Materials (in review, 2023)

Publications

1. Discerning orbital fluctuations in Fe₃O₄ below the Verwey transition, Nelson Hua, Jianheng Li, Stjepan B. Hrkac, Andi Barbour, Wen Hu, Claudio Mazzoli, Stuart Wilkins, Roopali Kukreja, Eric E. Fullerton, Oleg G. Shpyrko Physical Review Materials (accepted, 2023)

Ultrafast control of spin fluctuations in light-driven quantum materials

Matteo Mitrano, Harvard University, Department of Physics (Principal Investigator)

Keywords: Ultrafast spin dynamics, strongly correlated systems, light-matter interaction, quantum entanglement, time resolved x-ray spectroscopy.

Research Scope

Quantum materials feature subtly interacting lattice, orbital, charge, and spin degrees of freedom. The delicate balance among these interactions makes these systems extremely susceptible to external stimuli and is key to the appearance of emergent quantum phases such as superconductivity, magnetism, and charge order. Manipulating spins via ultrafast light-matter interaction is a promising route to dynamically control quantum materials' properties and induce light-matter hybrid states. However, understanding how lasers modify the microscopic spin dynamics in quantum materials is still a challenge, mainly due to the lack of momentum sensitivity of ultrafast optical probes.

Our program tightly integrates advanced ultrafast optical spectroscopy and time-resolved x-ray scattering methods with the goal to address the microscopic physics of light-driven spin fluctuations in quantum materials and their role in the appearance of nonequilibrium quantum phases. We investigate paradigmatic examples of effective spin $S=1/2$ (or pseudospin $J_{\text{eff}}=1/2$) Mott insulators in quasi-one-dimensional (1D), quasi-two-dimensional (2D), and frustrated lattices, with a focus on light-induced phenomena such as (1) the reshaping of short-range spin fluctuations, (2) nonequilibrium spin entanglement dynamics, (3) dynamical quantum criticality and (4) photoinduced spin liquidity.

This research makes use of transformative new spectroscopic capabilities at x-ray free electron laser (XFEL) facilities, such as LCLS-II and EuXFEL, and is poised to advance our understanding of light-matter interaction processes in interacting electron systems. The results of these studies will drive the synthesis of light-driven states of matter without equilibrium analogues and the realization of next-generation quantum technologies.

Recent Progress

During year 1 of this research program (started in July 2022), we focus on the light control of effective interactions and of spin fluctuations in quasi-one-dimensional model systems, such as the spin-1/2 Heisenberg chain Sr_2CuO_3 (SCO). Our goals are to (1) demonstrate a light-induced renormalization of the finite-momentum spin fluctuation spectrum, and (2) establish spectroscopic protocols to certify the presence of spin entanglement in the light-driven state.

Key to the first aim is achieving a transient renormalization of the superexchange energy $J=4t^2/U$, which sets the energy scale of the spin fluctuations (t being the electron hopping energy and U is the onsite Coulomb repulsion). The superexchange energy can be either modified via transient distortions of the lattice via resonant vibrational excitations or through a nonresonant Floquet dressing of the effective electronic interactions U or t . Following our recent experimental demonstration of a dynamical renormalization of the effective Hubbard U in the cuprate superconductor $\text{La}_{2-x}\text{Ba}_x\text{CuO}_4$ [1], we have performed time-resolved x-ray absorption (trXAS) and

time-resolved resonant inelastic x-ray scattering (trRIXS) experiments on Sr_2CuO_3 to accurately map transient changes of its electronic structure.

By exciting SCO with 1.55 eV pulses, we observe transient dynamics at odds with 2D cuprates. We measure the onset of hidden many-body transitions suggesting a rearrangement of the charge carriers beyond a simple renormalization of the Hubbard U . Furthermore, we measured trRIXS spectra at $q = (0.3, 0.0)$ r.l.u. along the chain direction and under the same excitation conditions with a grating spectrometer (0.65 eV resolution) to monitor changes of spinon continuum and dd excitations. Both trXAS and trRIXS data, acquired at the Pohang XFEL and at the LCLS-II (respectively), together with time-dependent density functional theory calculations will allow us to quantify the transient renormalization of the effective Hamiltonian of this model 1D system.

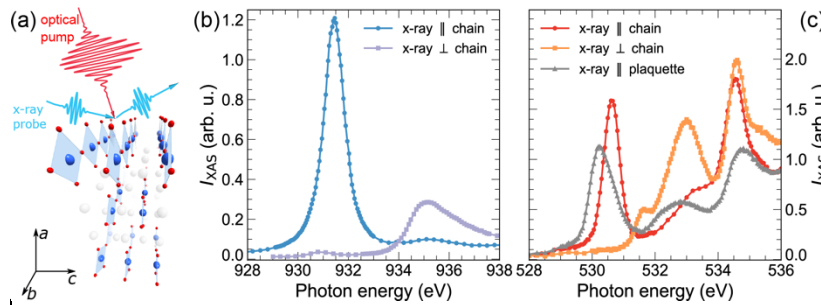


Fig. 1. (a) Sketch of the trXAS experiment on Sr_2CuO_3 (SCO). (b)-(c) Equilibrium XAS spectrum of SCO along different crystal directions at Cu L- and O K-edges, measured at the Pohang XFEL.

The renormalized Hamiltonian modifies the spin entanglement, which we aim to extract from trRIXS experiments. One relevant form of quantum entanglement in many-body systems is the so-called multipartite entanglement. A quantum system is n -particle entangled if it contains at least one state with n particles which

cannot be factorized, or, in other words, if its wavefunction contains a quantum superposition of n subsystems. Normally probed via tomographic methods in few-particle systems such as cold atoms in optical lattices, multipartite spin entanglement can also be experimentally quantified in solids through scattering experiments and the use of specific figures of merit known as *entanglement witnesses* [2]. At equilibrium, this is made possible by the existence of a fundamental relationship between a specific sum rule integral of the dynamical susceptibility and a multipartite entanglement witness, the Quantum Fisher Information F_q , which in tandem with operator-specific quantum bounds can be used to determine whether a state is n -partite entangled.

We have, therefore, investigated the applicability of this approach to quantify multipartite entanglement in quantum systems driven out of equilibrium. By using both exact diagonalization and density matrix renormalization group calculations, we have numerically calculated the time-dependent quantum Fisher information of a paradigmatic one-dimensional fermion chain undergoing a time-dependent change of the Coulomb interaction. Further, we have determined a self-consistent procedure to extract F_q from trRIXS spectra. Our results show that the quantum Fisher information can witness distinct signatures of multipartite spin entanglement both near and far from equilibrium that are robust against decoherence. Further, we have defined a protocol to extract this entanglement witness in upcoming trRIXS experiments at XFELs.

Future Plans

Building on this research, we plan to perform high energy resolution trRIXS experiments on quasi-one-dimensional and quasi-two-dimensional cuprates. Our work will provide a first mapping of finite-momentum spin fluctuations in these materials and contribute to the construction of a microscopic theory of light-driven superconductivity. Furthermore, the manipulation of spin

fluctuations and effective interactions in quasi-one-dimensional cuprates could lead to the observation of nonequilibrium doublon condensation at finite momentum (h -pairing).

More specifically, these experiments will be fielded at the qRIXS spectrometer of LCLS-II, both at the early science stage (Spring 2023) and as regular proposals (Fall 2023-Spring 2024), and at the EuXFEL/hRIXS endstation (possibly in Fall 2023). Our group will also lead a pilot trRIXS experiment on a quasi-one-dimensional ladder cuprate at the SwissFEL/Furka beamline in July 2023.

Finally, the detection of entanglement in equilibrium RIXS spectra of quasi-1D and quasi-2D systems will be supported by experiments at NSLS-II/SIX in collaboration with M. P. M. Dean and V. Bisogni.

References

1. D. R. Baykusheva, H. Jang, A. A. Husain, S. Lee, S. F. R. TenHuisen, P. Zhou, S. Park, H. Kim, J.-K. Kim, H.-D. Kim, M. Kim, S.-Y. Park, P. Abbamonte, B. J. Kim, G. D. Gu, Y. Wang, and M. Mitrano, *Ultrafast Renormalization of the On-Site Coulomb Repulsion in a Cuprate Superconductor*, *Phys. Rev. X* **12**, 011013 (2022).
2. P. Hauke, M. Heyl, L. Tagliacozzo, and P. Zoller, *Measuring multipartite entanglement through dynamic susceptibilities*, *Nat. Phys.* **12**, 8 (2016).

Publications

1. D. R. Baykusheva, M. H. Kalthoff, D. Hofmann, M. Claassen, D. M. Kennes, M. A. Sentef, M. Mitrano, *Witnessing nonequilibrium entanglement dynamics in a strongly correlated fermionic chain*, arXiv: 2209.02081 (2022).
2. J. Hales, U. Bajpai, T. Liu, D. R. Baykusheva, M. Li, M. Mitrano, Y. Wang, *Witnessing Light-Driven Entanglement using Time-Resolved Resonant Inelastic X-Ray Scattering*, arXiv:2209.02283 (2022).

Ultrafast Probing and Manipulation of Magnetic Materials using Polarization-Shaped Laser and Coherent Soft X-Ray Beams

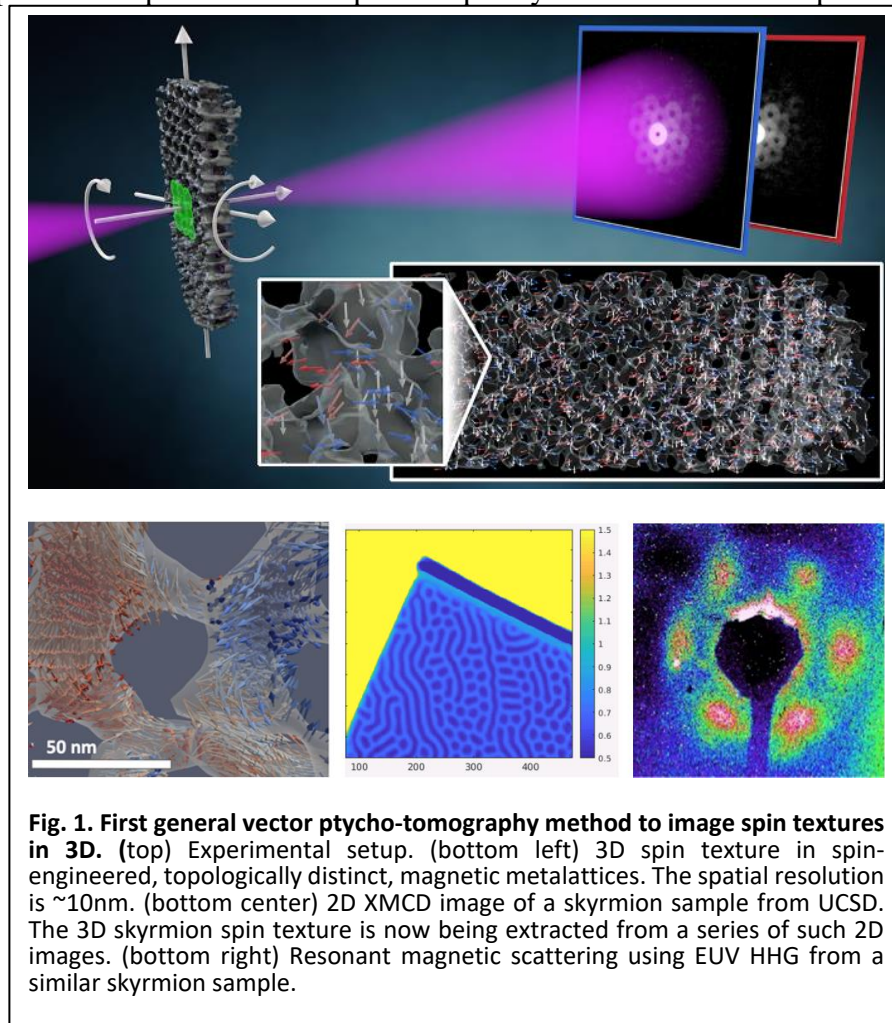
Margaret Murnane and Henry Kapteyn, Department of Physics and JILA, University of Colorado and NIST, Boulder, CO 80309, USA

Research Scope

A detailed understanding of nanoscale magnetism has become more critical in the 21st century in support of fundamental science and next-generation energy-efficient nanotechnologies. A comprehensive microscopic model of how spins, electrons, photons and phonons interact does not yet exist. This understanding is fundamentally constrained in large part by a limited ability to directly observe magnetism on all relevant time and length scales. Fortunately, by combining high harmonic (HHG) sources with new spectroscopic techniques, we have achieved fundamentally new insights into spin dynamics and textures.[1-9] This is because ultrafast extreme UV (EUV) and X-ray pulses make it possible to probe element-specific spin dynamics in multi-component magnetic systems, providing rich new information not accessible using visible light. In particular, tabletop high harmonic (HHG) sources are unique as a probe of magnetic dynamics since they can capture the fastest spin dynamics in multiple elements (sites or layers) simultaneously.

Recent Progress

In a series of exciting developments supported by this grant, we used tabletop high harmonic probes as well as DOE facilities to extract fundamental new



understanding of magnetic materials, as well as new capabilities for probing spin textures and dynamics.[1-9] Thus, trainees supported by this grant performed research using DOE facilities, as well as tabletop-scale high harmonic sources.

Vector 3D imaging of magnetic textures; Dynamic EUV RMS [1,11]: Our group was part of a very large team that participated in 6 beamtimes at the DOE LBNL COSMIC facility (ALS). In an exciting series of experiments soon to be published in Nature Nanotechnology and also in preparation, trainees supported by this DOE SXR scattering grant joined with a team led by STROBE to help commission the new COSMIC imaging beamline at the ALS for vector ptycho-

tomographic imaging of a topologically constrained 3D magnetic field in magnetic metalattices. (STROBE is an NSF Science and Technology Center with Murnane serving as Director). This 3D spin texture research effort required a large team to run 24-7 to take hundreds of 2D scans for the vector tomography imaging (5-11 TB of data during two different beam times). Our group suggested this experiment and sample (Murnane and Kapteyn), UCLA contributed advanced algorithms (Miao and Osher groups), Berkeley hosts the facility (Shapiro), while Penn State (Badding group) provided the magnetic metalattice samples. This allowed us to image nanostructured, topologically distinct, magnetic metalattice materials using a new and general vector ptycho-tomography method to image spin textures in 3D, with the highest ~10 nm spatial resolution to date (previous record was ~100 nm), and without any prior knowledge about the sample (Fig. 1). [1]

In a second series of experiments, we performed the same experiments on skyrmion samples from UCSD.[11] The 3D skyrmion spin texture is now being extracted from a series of such 2D images – however, the data from the skyrmion sample is much more challenging to extract because the sample only has magnetic contrast, so aligning the different images requires new approaches.

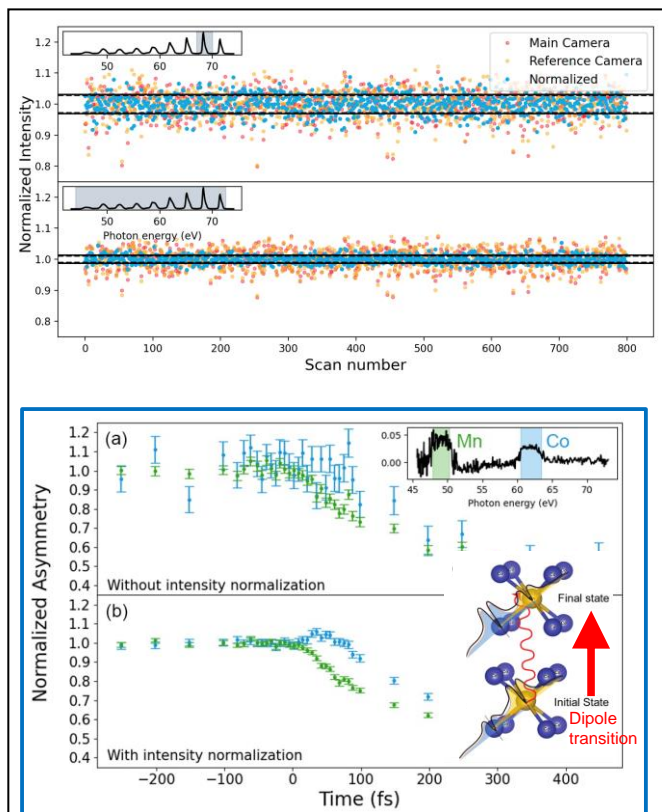


Fig. 2. High quality EUV MOKE data using new intensity-normalized HHG beamline. (top) Normalization of a single 66 eV harmonic, and of all harmonics simultaneously. For the 66 eV harmonic, the % RMS noise on the sample camera is 4.29% before normalization and 3.19% after normalization. The % RMS noise of all harmonics on the sample camera is 3.06% before normalization and 1.18% after normalization. (bottom) Magnetization dynamics of the Co and Mn in the Co_2MnGe Heusler alloy, showing enhanced ability, in x10 less time, to capture how optical pumping directly and immediately transfers magnetization from Mn (green) to Co (blue).

Shot-noise-limited high harmonic beamline for probing spin dynamics in magnetic materials [2,5,7-9,12]: High harmonic generation (HHG) makes it possible to measure spin and charge dynamics in materials on femtosecond to attosecond timescales. However, the extreme nonlinear nature of the high harmonic process means that intensity fluctuations can limit measurement sensitivity. In work soon to be published in the Review of Scientific Instruments,[2] we developed a noise-cancelled, tabletop high harmonic beamline for time-resolved reflection mode spectroscopy of magnetic materials. We use a reference spectrometer to independently normalize the intensity fluctuations of each harmonic order and eliminate long term drift, allowing us to make spectroscopic measurements near the shot noise limit. These improvements allow us to significantly reduce the integration time required for high signal-to-noise (SNR) measurements of element-specific spin dynamics (Fig. 2). In particular, we are probing the different mechanisms underlying direct light-induced spin transfer on ultrafast, few-femtosecond, timescales.[7-9,12] Looking forward, improvements in the HHG flux, optical coatings, and grating design can further reduce the acquisition time for high SNR measurements by 1-2 orders of magnitude, enabling dramatically improved sensitivity to spin, charge and phonon dynamics in magnetic materials. In ongoing work in preparation for publication, we are using this low-noise beamline to compare spin dynamics in different Heusler alloys in collaboration with theory experts from Germany and Sweden. Another high-flux EUV HHG beamline is being used to capture the dynamic resonant magnetic scattering from other magnetic and skyrmion samples.[10,11]

Participation in experiments at LCLS and other DOE-related collaborations [3]: Our group participated in beamtimes with Tom Silva (NIST) and Erik Fullerton (UCSD) and others that used the LCLS XFEL to show that spin transport leads to non-uniform magnetization dynamics of domains. This work was recently published in Phys. Rev. B, highlighted as an Editor's Choice.

In addition, we wrote a Physics Viewpoint highlight for research performed at the ALS source, and a News and Views article on advanced electron imaging of spin textures.[4, 6] Finally, several Kapteyn-Murnane group members joined DOE laboratories - most recently Dr. Quynh Nguyen, who was awarded a Stanford Q-FARM Bloch Postdoctoral Fellowship at SLAC.

Future Plans

We will explore exciting new directions, taking advantage of both tabletop HHG sources as well as DOE facilities. First, we will explore the fundamental mechanisms underlying the fastest light-induced spin manipulation in materials, from single element, to more-complex materials such as spin-polarized Heusler alloys, as well as 2D magnets. We already have samples from several groups. Second, will expand our studies of magnetically ordered systems to develop new characterization techniques. Third, we will complement our nanoscale static 3D imaging of spin textures at the ALS, by using HHG to capture spin dynamics using EUV and SXR scatterometry. We will also use our ability to create polarization and phase structured HHG beams (SAM, OAM) to enhance contrast and probe chiral texture.

References to Publications supported by BES X-Ray Scattering

1. *Direct observation of 3D topological spin textures and their interactions using soft x-ray vector ptychography*, A. Rana*, C.T. Liao*, E. Iacocca, J. Zou, M. Pham, E. Cating Subramanian, Y. Lo, S. Ryan, X. Lu, C. Bevis, R. Karl Jr, A. Glaid, Y. Yu, P. Mahale, D. Shapiro, S. Yazdi, T. Mallouk, S. Osher, H. Kapteyn, V. Crespi, J. Badding, Y. Tserkovnyak, M. Murnane, J. Miao, in press, *Nature Nanotechnology* (2023). arxiv.2104.12933
2. *A beamline for ultrafast extreme ultraviolet magneto-optical spectroscopy in reflection near the shot noise limit*, P. Johnsen, S. Ryan, C. Gentry, A. Grafov, H. Kapteyn, M. Murnane, in press, *Rev. Scientific Instrum.* (2023).
3. *Ultrafast perturbation of magnetic domains by optical pumping in a ferromagnetic multilayer*, D. Zusin, E. Iacocca, L. Le Guyader, A. Reid, W. Schlotter, T. Liu, D. Higley, P. Tengdin, S. Patel, A. Shabalin, N. Hua, S. Hrkac, H. Nembach, J. Shaw, S. Montoya, A. Blonsky, C. Gentry, M. Hofer, M. Murnane, H. Kapteyn, E. Fullerton, O. Shpyrko, H. Durr, T. Silva., *Physical Review B* **106**, 144422 (2022). *Selected as Editor's suggestion.*
4. *A closer look at spin textures*, J. Miao, M. Murnane, *Nature Nanotech.* 10.1038/s41565-022-01262-6 (2022)
5. *Probing and manipulating magnetic and 2D quantum materials using ultrafast laser and high harmonic sources*, M. Murnane, X. Shi, H. Kapteyn, *Journal of Physics: Condensed Matter* **33**, 353001 (2021).
6. *Switching the Twist in X-rays with Magnets*, C.T. Liao, C. Hernandez-Garcia, M. M. Murnane, *Physics Viewpoint, Physics* **14**, 34 (2021). DOI: 10.1103/Physics.14.34
7. *Attosecond light science and its application for probing quantum materials*, X. Shi, C. Liao, Z. Tao, E. Cating, M. Murnane, C. Hernandez-Garcia, H. Kapteyn, Invited *JPhys Photonics/JPhys B Atto issue* **53**, 184008 (2020).
8. *Direct light-induced spin transfer between different elements in a spintronic Heusler material via femtosecond laser excitation*, P. Tengdin, C. Gentry, A. Blonsky, D. Zusin, M. Gerrity, L. Hellbruck, J. Shaw, Y. Kvashnin, E. Delczeg-Czirjak, M. Arora, H. Nembach, T. Silva, S. Mathias, M. Aeschlimann, H. C. Kapteyn, D. Thonig, K. Koumpouras, O. Eriksson, M. Murnane, *Science Advances* **6**, eaaz1100 (2020). DOI: 10.1126/sciadv.aaz1100
9. *Ultrafast optically induced spin transfer in ferromagnetic alloys*, M. Hofherr, S. Huser, J. Dewhurst, P. Tengdin, S. Sakshath, H. Nembach, S. Weber, J. Shaw, T. Silva, H. Kapteyn, M. Cinchetti, B. Rethfeld, M. Murnane, D. Steil, B. Stadtmüller, S. Sharma, M. Aeschlimann, S. Mathias, *Science Advances* **6**, eaay8717 (2020).
10. *Hyperspectral Interferometric EUV Magnetic Imaging*, N. Brooks et al., in prep. (2023).
11. *Capturing the 3D spin texture and dynamics of skyrmions*, I. Binnie et al., in prep. (2023).
12. *Light-induced spin transfer in Heusler compounds*, S. Ryan et al., in prep. (2023).

Multimodal Quantum Material Control Monitored with Ultrafast Coherent X-rays

**Keith A. Nelson, Riccardo Comin, MIT; James Freericks, Georgetown University
David Reis, Mariano Trigo, SLAC; Nicholas Sirica, LANL**

Keywords: XFEL; Terahertz; Quantum phases; Ultrafast; Multimodal control

Research Scope

Based on progress during an initial grant period, our recently renewed multi-institutional program is designed to advance our ability to induce, probe, and theoretically model novel quantum phases of matter. We aim to use multiple dynamic stimuli to control multiple coupled modes including optical and acoustic phonons, magnons, and low-frequency electronic excitations associated with charge-density waves and superconductivity. Terahertz-frequency (THz) and long-wavelength IR excitation fields are used to drive optical phonons, magnons, and electronic responses; optical pulses to excite selected acoustic waves that deliver specified in-plane or through-plane uniaxial strains; and crossed X-ray pulses to drive material responses with specified nanoscale spatial modulations comparable to those that form spontaneously in many quantum phases. We probe the dynamic material responses with ultrashort coherent X-ray probe pulses, whenever possible at the LCLS X-ray free-electron laser (XFEL) at SLAC National Accelerator Laboratory. We also probe the dynamics with pulses in THz through visible spectral regions in tabletop ultrafast laser systems. We study material systems hosting emergent quantum phases including multiferroic materials, charge-density wave (CDW) phases, and superconducting phases. In many cases, our multimode excitation may induce transformations of matter into new states with altered structural, electronic, and/or magnetic characteristics. X-ray diffraction and diffuse scattering, X-ray absorption, and resonant X-ray scattering measurements may be conducted to monitor the formation and duration of these states including their nanoscale textures.

Much of our progress is enabled by novel experimental methods for excitation and control of the samples and for measurement of the dynamic sample responses. In some cases, sequences of multiple THz pulses may be used to guide the sample from its initial state, through collective motions of its electrons and ions that are monitored by ultrashort-duration X-ray pulses, into a new crystalline phase with different lattice structure, electrical conductivity, and/or magnetization. THz excitation may be supplemented by acoustic waves that strain the sample to match the lattice dimensions of the new crystal structure, assisting the material transformation. Excitation with spatially periodic X-ray patterns may be used to generate new material states with nanoscale features. First-principles theoretical modeling guides the design of excitation light frequencies, spatial patterns, and pulse sequences that can achieve our control objectives. Theoretical modeling also guides the interpretation of our experimental results, yielding fundamental understanding of quantum phases and the coupled degrees of freedom involved in their interconversion. Light-induced phases may be transient or long-lived, pointing toward practical applications in energy-

efficient ultrafast modulation and switching. We will develop methods that allow time-dependent X-ray measurements to be conducted in a single laser shot in order to characterize the dynamics and understand the mechanisms of photoinduced transitions into persistent metastable phases.

Recent Progress

The results from years 2021-present include those from our original project period as well as our renewal project that began in September 2022. We summarize several examples of current work, emphasizing methodological developments as well as the scientific insights they yield.

1. X-ray excitation and probing of SrTiO_3 and KTaO_3

a. THz field-induced ferroelectric transition in quantum paraelectric SrTiO_3 . Early in the initial project period, we reported tabletop experiments in which a strong single-cycle THz field was used to drive SrTiO_3 (STO) from its low-temperature quantum paraelectric (QPE) phase into a transient ferroelectric (FE) phase, revealed through time-resolved optical birefringence and second harmonic generation measurements [1]. Molecular dynamics simulations included in the report confirmed that a short-duration electric field like that of the THz pulse could drive collective motion of the polar soft mode that would move the ions into their positions in a ferroelectric structure. We have since conducted X-ray diffraction measurements of THz-driven STO at the LCLS XPP hutch. Measurement of signals from the (3.5 1.5 4.5) tetragonal peak showed coherent oscillations of an antiferrodistortive (AFD) mode that is anharmonically coupled to the soft mode and that the MD simulations showed would undergo displacements following THz driving of the soft mode. XRD measurements from the (-3 3 3) cubic Bragg peak were collected using THz pulses generated from two different lithium niobate crystals with opposite ferroelectric polarities, yielding THz fields with opposite polarities. See Fig. 1.

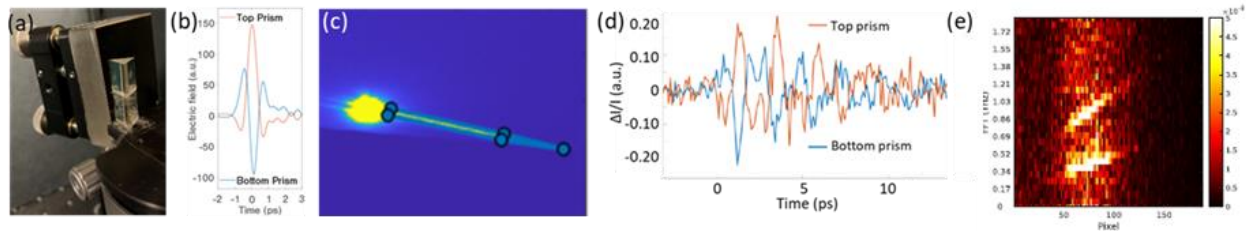


Figure 1. (a) Two LN crystal prisms mounted with opposite ferroelectric polarity and with vertical translation so one or the other could be used for THz generation at LCLS. (b) THz fields of opposite polarity generated using the two LN crystals. (c) SrTiO_3 XRD from (-3 3 3) cubic Bragg peak and nearby wavevectors up to $\sim 0.6 \text{ nm}^{-1}$. (d) Time-resolved XRD integrated over the off-Bragg scattering wavevectors shown in (c), following THz excitation of STO at 20 K with both polarities. The soft mode oscillatory signals are inverted, showing that odd-symmetry soft mode displacements are observed. No odd-symmetry signals were observed at zone center. (e) Frequencies extracted from data like that in (d) as a function of wavevector difference from the Bragg peak. The FE soft mode and a piezoelectrically coupled transverse acoustic mode dispersion are observed.

The measurements revealed key information that could not be extracted from all-optical tabletop measurements. Odd-symmetry displacements of the soft mode and a coupled transverse acoustic mode were revealed through inversion of the time-dependent XRD signals induced by the

opposite-polarity THz fields. The signals were observed only at off-Bragg scattering wavevectors, indicating heterodyning with signals from pre-existing polar nanoregions of roughly 10-nm dimensions in which global centrosymmetry was already broken. The use of inverted driving fields may have broad applicability in unveiling nanoscale structural, magnetic, or electronic features and dynamics in quantum phases.

b. X-ray probing and excitation of $KTaO_3$ (KTO) and STO. Diffuse X-ray scattering measurements of STO (at SwissFEL) and KTO (at LCLS) revealed strong coupling between a LWIR-pumped 16-THz optical phonon mode of STO and zone boundary acoustic phonons (Publication list #29) and demonstrated UV-induced strengthening of forces that stabilize the cubic KTO perovskite structure (#12). Most striking were X-ray pump, diffuse X-ray scattering probe measurements from STO and KTO (at LCLS) that revealed large-amplitude longitudinal acoustic phonon responses with wavevectors in every direction in the BZ (#30). The results (See Fig. 2a) suggest ~ 10 -nm point-like sources of localized stress associated with an unusual type of polaron formation that could be viewed as a unique manifestation of electron-phonon coupling.

2. X-ray transient grating excitation. In recent developments, transient grating (TG) experiments have been conducted with crossed pulses in the extreme UV (EUV) spectral range that have formed interference patterns with periods Λ as small as 20 nm. These have been used to generate sample responses at the corresponding TG wavevectors \mathbf{q} , with $|\mathbf{q}| = q = 2\pi/\Lambda$. In these measurements we have initiated acoustic waves, thermal transport, coherent optical phonons, and magnetization dynamics at the selected wavevectors. Preliminary TG measurements have also been conducted using hard X-ray excitation, achieved through Talbot imaging of a phase mask pattern to produce TG interference periods that were sufficiently large to permit probing by diffraction of optical wavelengths (#3). Illustrative results are shown in Figs. 2b-d including an example (d) of resonant pumping that is selective for both energy and wavevector.

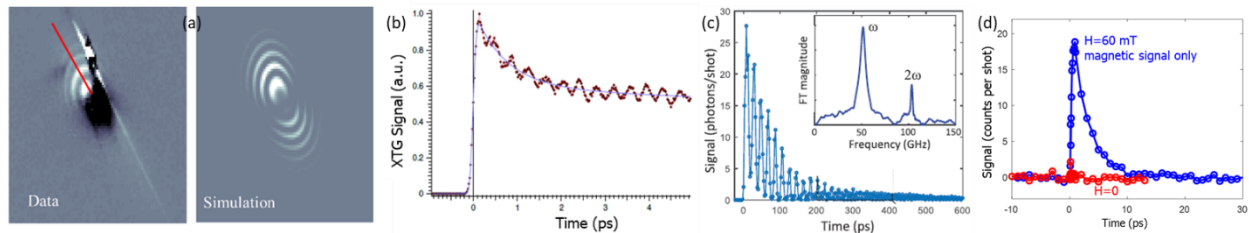


Figure 2. X-ray excitation data. (a) X-ray diffuse scattering from $SrTiO_3$ showing strong longitudinal acoustic signals induced by a 9.88 keV excitation pulse. The data are consistent with a roughly 10-nm strain source (simulation) around each absorption site. (#30) (b) Hard X-ray (7.1 keV) TG excitation of with a TG period of 770 nm generated coherent optical phonons in bismuth germanate that were observed through diffraction of 400-nm probe pulses (#3). (c) EUV TG data from 51.7 GHz surface acoustic waves in $SrTiO_3$ generated by crossed 39.9-nm excitation pulses that formed a TG period of 83.6 nm and probed by diffraction of 13.3-nm probe pulses (#1). (d) Depolarized EUV TG signal (incident probe beam V-polarized, diffracted signal H-polarized) from a magnetization transient grating in a CoNi multilayer sample. Excitation and probe wavelengths were 20.8 nm (Co M-edge) and the TG period was 44 nm. (#4).

During the new project, we will use hard and soft X-ray and EUV excitation pulses to generate electronic, spin, and phonon responses with experimentally specified TG wavevectors. X-ray TG

experiments will be used for both study and control of high-wavevector excitations and nanoscale features in quantum materials. A current methodological effort is directed toward achieving high wavevectors in TG experiments with hard X-ray excitation and probe wavelengths, with 0.1-10 nm TG periods comparable to those of crystal lattices, to the modulation periods of charge and spin-density waves, striped phases, and incommensurate structural phases, and to other nanoscale features of quantum materials.

3. Methodological advances and associated scientific insights

a. Optical generation of large-amplitude acoustic waves without optical damage. A control variable of great importance in quantum materials is strain. In many cases extensive efforts are devoted to growth of quantum materials by deposition over substrates with different lattice parameters, in order to explore the effects of strain on quantum phase stability. We have developed a method through which successive optical pulses irradiate successive substrate regions, with the excitation pulses progressing across the substrate surface at a speed that matches a selected acoustic velocity (#23). Thermoelastic responses at each irradiated region generate an acoustic wave that builds up to substantial amplitude. In-plane strains up to 3% were demonstrated through surface acoustic wave (SAW) excitation in SrTiO₃, an important substrate material for quantum phases. Optical damage is avoided because the excitation light is spread out across the successively irradiated regions, with the fluence of any one pulse below the optical damage threshold. The approach permits repeated generation of strains that can propagate to a deposited sample in a region that has not been irradiated. Pump-probe measurements can then be conducted on the strained sample using separate optical, IR, or THz excitation pulses and probe pulses in these or X-ray spectral regions. The acoustic pulse duration of > 1 ns allows ultrafast measurements on samples under quasi-static strain, with the strain magnitude controlled by the fluence of the successive excitation pulses. The approach is now being used for multimodal acoustic + optical/IR/THz excitation of quantum materials. The method also permits study of cumulative material damage due to repeated shock loading, which was measured in SrTiO₃. Longitudinal acoustic waves as well as SAWs can be generated, allowing suppression of shear-induced damage.

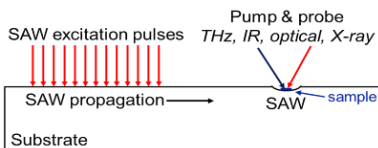


Figure 3. Large-amplitude SAW generation. The SAW builds up through a succession of excitation pulses. SrTiO₃ doped with 0.7% Nb to absorb 800-nm excitation light has been used to generate in-plane longitudinal strain exceeding 3% at the substrate surface. The strain duration is ~ 2 ns.

b. Single-shot measurements of photoinduced transitions into persistent metastable states, measurements of 2D spectroscopy signals, and (in design stage) X-ray measurements. We extended a single-shot optical measurement method that we had developed earlier to the THz spectral range (#11) and applied the approach to measurement of an ultrafast photoinduced quantum phase transition through which the transition metal dichalcogenide TaS₂ (#10) enters a metastable hidden “H” phase that persists indefinitely at low temperatures. Signals are measured at several hundred time points in a single shot, providing a complete time-dependent measurement

that covers a 10 ps temporal range. We determined that the persistent low-temperature H phase is similar to a transient phase that is photoinduced at temperatures above 80 K, and that the phase transition occurs through nonthermal melting of pre-existing CDW ordering followed by fluctuation-assisted relaxation into a new CDW configuration. We also applied the method to 2D THz spectroscopy in which two time variables, the time interval between a pair of THz excitation pulses and the time at which the nonlinear THz signal field is measured, must be varied. Measurement of the complete time-dependent signal field in each shot of a 1-kHz repetition rate laser system reduced the data acquisition time for a 2D THz spectrum from days to minutes. The reduction permitted systematic study of 2D magnon spectra in canted antiferromagnetic materials ErFeO_3 and YFeO_3 , revealing magnon-magnon coupling that had never been observed previously (#24, #25). We have also conducted 2D THz spectroscopy of multiferroics, with preliminary results showing mode-mode interactions involving electromagnon modes. A current methodological development is aimed at single-shot time-resolved measurements of X-ray diffraction, scattering, and absorption. This will permit incisive X-ray measurements of transitions into persistent metastable states, revealing the evolution of nanoscale features such as charge-density waves that cannot be resolved using optical or THz wavelengths. Even for measurements of reversible photoinduced phenomena, the method will permit extreme reductions of data acquisition times. This will enable complete XFEL studies to be conducted parasitically in some cases, using intermittent X-ray pulses while a primary user has a regular beamtime run. The total XFEL usage at any facility may increase substantially as a result. Another current methodological development is aimed at 2D THz spectroscopy in which excitation by a THz pulse pair is not followed by measurement of a THz signal field but rather by a variably delayed X-ray probe pulse and measurement of the resulting X-ray diffraction, nonresonant or resonant scattering, or absorption. This will provide new insights into the coupling between THz-frequency excitations and nanoscale structural, electronic, and/or magnetic responses of charge and spin-density wave phases, multiferroics, and other quantum phases.

4. Theoretical advances.

a. Formulation of core-hole XPS/XAS ultrafast thermometry. We have found the proper way to use the integrated areas of peaks in core-hole XPS as an ultrafast thermometer in cases where the core-hole electron interaction is large enough that the peaks are well separated (#31). In current work we are extending this approach to X-ray absorption spectroscopy. Using a novel classical Monte Carlo approach, which is similar to a nonequilibrium ab-initio molecular dynamics algorithm, we are developing the technology to use this for X-ray-based probes (primarily core-hole XPS and XAS). The focus is on electron-phonon coupled systems, and the approach should be applicable to CDW systems, multiferroics, and ferroelectrics where the instabilities are driven by soft phonon modes. Our results can then be compared to upcoming XFEL XPS and XAS measurements. Going further, we have presented a unified description of the calculation of time-resolved response functions for X-ray based probes (RIXS, XPS and XAS) of quantum materials. (#32) We anticipate wide applicability of these developments to X-ray based ultrafast experiments.

b. Driven nonequilibrium responses. A major theoretical challenge is to be able to calculate nonequilibrium phenomena to long times, especially for situations with THz drives. Using a semiclassical approach (electrons treated exactly with quantum mechanics, ion motion treated classically via Ehrenfest forces), which is accurate for low-frequency phonons in a strongly excited system, we are able to reach times out to tens of picoseconds. This enables theoretical input over both short timescales of the electrons and longer timescales of the phonons. The theoretical methods allow for modeling direct coupling of light to both phonons and electrons. This theoretical approach is uniquely capable of describing transient grating experiments because of the large-size systems studied which can include multiple TG spatial periods. The calculations will guide experimental parameter choices aimed at TG excitation and control over nanoscale features such as CDW period, orientation, and dimensionality.

Future Plans

Our team project is aimed at dramatic advances in ultrafast X-ray science applied to quantum materials. Our methodological developments are directed mainly toward two material classes: (1) multiferroics (MFs) and (2) correlated electron materials, primarily CDW and superconducting (SC) phases. Multimodal experimental control over collective spin, lattice vibrational, and strain degrees of freedom and 2D spectroscopic measurements on tabletops and especially with X-ray probing will be used for elucidation of the mode-mode interactions that underlie multiferroic phases. Our initial MF targets are the prototype TbMnO_3 and the magnetochiral NiI_2 , for which resonant X-ray scattering at the cycloid wavevector will reveal collective, coupled dipolar and spin responses to THz fields whose electric and magnetic field components will both play key roles that can be distinguished through the use of field enhancement structures for one or the other. 2D THz/X-ray measurements will be particularly incisive for study of the coupling among phonon, magnon, and electromagnon modes. For NiI_2 , which we determined to remain multiferroic all the way down to the monolayer limit (9), we will use circularly polarized THz fields to switch domain helicity. Our initial CDW systems will be the rare earth tritellurides RTe_3 , whose CDW orientations and dimensionalities are exquisitely sensitive to strain. We will exert multimodal control through strain and THz excitation of phase and amplitude modes (driven to first and second order respectively in the THz field). We will aim for X-ray TG excitation with periods near the CDW periods, and explore possibilities for CDW control with theoretical guidance. Finally, we will conduct THz excitation of CDW and Josephson plasmon resonance modes in superconducting cuprates. In 2D THz/X-ray measurements, we will use resonant X-ray scattering to discern the induced changes in CDW coherence and the associated competition between CDW and SC phases.

References

1. X. Li, T. Qiu, J. Zhang, E. Baldini, J. Lu, A. M. Rappe, and K. A. Nelson, *Terahertz field-induced ferroelectricity in quantum paraelectric SrTiO₃*, *Science* **364**, 1079 (2019).

Publications

Published or accepted in refereed journals

1. A. A. Maznev, R. Mincigrucchi, F. Bencivenga, V. Unikandanunni, F. Capotondi, G. Chen, Z. Ding, R. A. Duncan, L. Foglia, M. G. Izzo, C. Masciovecchio, A. Martinelli, G. Monaco, E. Pedersoli, S. Bonetti, and K. A. Nelson, *Generation and detection of 50 GHz surface acoustic waves by extreme ultraviolet pulses*, *Appl. Phys. Lett.* **119**, 044102 (2021).

2. N. Sirica, P. P. Orth, M. S. Scheurer, Y. M. Dai, M.-C. Lee, P. Padmanabhan, L. T. Mix, S. W. Teitelbaum, M. Trigo, L. X. Zhao, G. F. Chen, B. Xu, R. Yang, B. Shen, C. Hu, C.-C. Lee, H. Lin, T. A. Cochran, S. A. Trugman, J.-X. Zhu, M. Z. Hasan, N. Ni, X. G. Qiu, A. J. Taylor, D. A. Yarotski, and R. P. Prasankumar, *Photocurrent-driven transient symmetry breaking in the Weyl semimetal TaAs*, *Nature Materials* **21**, 62 (2021).

3. J. R. Rouxel, D. Fainozzi, R. Mankowsky, B. Rösner, G. Seniutinas, R. Mincigrucchi, S. Catalini, L. Foglia, R. Cucini, F. Döring, A. Kubec, F. Koch, F. Bencivenga, A. Al Haddad, A. Gessini, A. A. Maznev, C. Cirelli, S. Gerber, B. F. Pedrini, G. F. Mancini, E. Razzoli, M. Burian, H. Ueda, G. Pamfilidis, E. Ferrari, D. Yunpei, A. Mozzanica, D. Ozerov, M. Grazia Izzo, C. Bottari, C. Arrell, E. J. Divall, S. Zerdane, M. Sander, G. Knopp, P. Beaud, H. T. Lemke, C. David, R. Torre, M. Chergui, K. A. Nelson, C. Masciovecchio, U. Staub, L. Patthey, and C. Svetina, *Hard X-ray transient grating spectroscopy on bismuth germanate oxide*, *Nature Photonics* **15**, 499 (2021).

4. D. Ksenzov, A. A. Maznev, V. Unikandanunni, F. Bencivenga, F. Capotondi, A. Caretta, L. Foglia, M. Malvestuto, C. Masciovecchio, R. Mincigrucchi, K. A. Nelson, M. Pancaldi, E. Pedersoli, L. Randolph, H. Rahmann, S. Urazhdin, S. Bonetti, and C. Gutt, *Nanoscale transient magnetization gratings created and probed by femtosecond extreme ultraviolet pulses*, *Nano Letters* **21**, 2905 (2021).

5. R. D. Nesselrodt, J. K. Freericks, *Exact solution of two simple non-equilibrium electron-phonon and electron-electron coupled systems: The atomic limit of the Holstein-Hubbard model and the generalized Hatsugai-Komoto model*, *Phys. Rev. B* **104**, 155104 (2021).

6. M.-C. Lee, N. Sirica, S. W. Teitelbaum, A. A. Maznev, T. Pezeril, R. Tutchton, V. Krapivin, G. A. de la Pena Munoz, Y. Huang, L. X. Zhao, G. F. Chen, B. Xu, R. Yang, J. Shi, J.-X. Zhu, D. A. Yarotski, X. G. Qiu, K. A. Nelson, M. Trigo, D. A. Reis, and R. P. Prasankumar, *Direct observation of coherent longitudinal and shear acoustic phonons in the Weyl semimetal TaAs using ultrafast X-ray diffraction*, *Phys. Rev. Lett.* **128**, 155301 (2022).

7. P. Padmanabhan, F. L. Buessen, R. Tutchton, K. W. C. Kwock, S. Gilinsky, M.-C. Lee, M. A. McGuire, S. R. Singamaneni, D. A. Yarotski, A. Paramekanti, J.-X. Zhu, and R. P. Prasankumar, *Coherent helicity-dependent spin-phonon oscillations in the ferromagnetic van der Waals crystal CrI₃*, Nature Commun. **13**, 4473 (2022).
8. M.-C. Lee, C. Occhialini, J. Li, Z. Zhu, N. S. Sirica, L. T. Mix, D. A. Yarotski, R. Comin, and R. P. Prasankumar, *Ultrafast signatures of spin and orbital order in antiferromagnetic Sr₂CrO₄*, Commun. Physics **5**, 335 (2022).
9. Q. Song, C. A. Occhialini, E. Ergeçen, B. Ilyas, D. Amoroso, P. Barone, J. Kapteghian, K. Watanabe, T. Taniguchi, A. S. Botana, S. Picozzi, N. Gedik, and R. Comin, *Evidence for a single-layer van der Waals multiferroic*, Nature **602**, 601 (2022).
10. F. Y. Gao, Z. Zhang, Z. Sun, L. Ye, Y.-H. Cheng, Z.-J. Liu, J. G. Checkelsky, E. Baldini, and K. A. Nelson, *Snapshots of a light-induced metastable hidden phase driven by the collapse of charge order*, Sci. Adv. **8**, eabp9076 (2022).
11. F. Y. Gao, Z. Zhang, Z.-J. Liu, and K. A. Nelson, *High-speed two-dimensional terahertz spectroscopy with echelon-based shot-to-shot balanced detection*, Opt. Lett. **47**, 3479 (2022).
12. V. Krapivin, M. Gu, D. Hickox-Young, S. W. Teitelbaum, Y. Huang, G. de la Peña, D. Zhu, N. Sirica, M.-C. Lee, R. P. Prasankumar, A. A. Maznev, K. A. Nelson, M. Chollet, J. M. Rondinelli, D. A. Reis, and M. Trigo, *Ultrafast Suppression of the Ferroelectric Instability in KTaO₃*, Phys. Rev. Lett. **129**, 127601 (2022).
13. B. S. Dastrup, E. R. Sung, F. Wulf, C. J. Saraceno, and K. A. Nelson, *Enhancement of THz generation in LiNbO₃ waveguides via multi-bounce velocity matching*, Light: Science & Applications **11**, 335 (2022).
14. M. Herzog, A. von Reppert, J.-E. Pudell, M. Kronseder, C. Back, A. A. Maznev, and M. Bargheer, *Phonon-dominated transport in purely metallic heterostructures*, Advanced Functional Materials **32**, 2206179 (2022).
15. K. Keskinbora, A. Levitan, G. Schuetz, and R. Comin, *Maskless off-axis X-ray holography*, Optics Express **30**, 403 (2022).
16. A. A. Maznev and B. Song, *Comment on 'Theoretical paradigm for thermal rectification via phonon filtering and spectral confinement'*, Phys. Rev. Lett. **128**, 129601 (2022).
17. Khadijeh Najafi, J. Alexander Jacoby, R. D. Nesselrodt, and J. K. Freericks, *Nonequilibrium spectral moment sum rules of the Holstein-Hubbard model*, J. Phys. A: Math. Theor. Phys., to appear.

Ph.D. Theses

18. J. Shi, *Strong-field Phenomena in Low-dimensional Materials at Terahertz Frequencies*, May 2021.

19. Y. Gao, *Photoinduced Dynamics Studied via Single-Shot Optical and Terahertz Spectroscopy*, May 2021.

Submitted to refereed journals

20. Z. H. Zhu, W. Hu, C. A. Occhialini, J. Li, J. Pelliciani, C. S. Nelson, M. R. Norman, Q. Si, and R. Comin, *Neel and stripe ordering from spin-orbital entanglement in α - Sr_2CrO_4* , under review, npj Quantum Materials. arXiv:1906.04194 (v. 2, 2021)

21. J. Shi, Y.-Q. Bie, A. Zong, S. Fang, W. Chen, J. Han, Z. Cao, Y. Zhang, T. Taniguchi, K. Watanabe, V. Bulović, E. Kaxiras, E. Baldini, P. Jarillo-Herrero, and K. A. Nelson, *Intrinsic IT' phase induced in atomically thin 2H-MoTe₂ by a single terahertz pulse*, under review, Nature Materials. arXiv:1910.13609 (v. 2, 2022)

22. L. Foglia, R. Mincigrucci, A. A. Maznev, G. Baldi, F. Capotondi, F. Caporaletti, R. Comin, D. De Angelis, R. A. Duncan, D. Fainozzi, G. Kurdi, J. Li, A. Martinelli, C. Masciovecchio, G. Monaco, A. Milloch, K. A. Nelson, C. A. Occhialini, M. Pancaldi, E. Pedersoli, J. S. Pelli-Cresi, A. Simoncig, F. Travasso, B. Wehinger, M. Zanatta, and F. Bencivenga, *Extreme ultraviolet transient gratings: A tool for nanoscale photoacoustics*, under review, Photoacoustics.

23. J. Deschamps, Y. Kai, J. Lem, I. Chaban, A. Lomonosov, A. Anane, S. E. Kooi, K. A. Nelson, and T. Pezeril, *Additive laser excitation of multiple surface acoustic waves up to the nonlinear shock regime*, under review, Phys. Rev. Lett. arXiv:2209.13897 (2022).

24. Z. Zhang, F. Y. Gao, Y.-C. Chien, Z.-J. Liu, J. B. Curtis, E. Sung, X. Ma, W. Ren, S. Cao, P. Narang, A. von Hoegen, E. Baldini, and K. A. Nelson, *Nonlinear coupled magnonics: Terahertz field-driven magnon upconversion*, under review, Nature. arXiv:2207.07103 (2022).

25. Z. Zhang, F. Y. Gao, J. B. Curtis, Z.-J. Liu, Y.-C. Chien, A. von Hoegen, T. Kurihara, T. Suemoto, P. Narang, E. Baldini, and K. A. Nelson, *Three-wave mixing of anharmonically coupled magnons*, submitted, Nature.

26. Z. Zhang, J. Zhang, Z.-J. Liu, N. S. Dahodl, W. Paritmongkol, N. Brown, Y.-C. Chien, Z. Dai, K. A. Nelson, W. A. Tisdale, A. M. Rappe, and E. Baldini, *Discovery of enhanced lattice dynamics in a single-layered hybrid perovskite*, under review, Sci. Adv.

27. N. C. Golota, Z. P. Fredin, D. P. Banks, D. Preiss, S. Bahri, P. Patil, W. K. Langford, C. L. Blackburn, E. Strand, B. Dastrup, K. A. Nelson, N. Gershenfeld, and R. Griffin, *Diamond rotors*, under review, Sci. Adv.

28. P. H. Otsuka, R. Chinbe, M. Tomoda, O. Matsuda, Y. Tanaka, D. M. Profunser, S. Kim, H. Jeon, I. A. Veres, A. A. Maznev, and O. B. Wright, *Imaging gigahertz phonon eigenstates and elucidating the energy storage characteristics of a honeycomb-lattice phononic crystal cavity*, under review, Nature Commun.

In preparation (only includes drafts in advanced stages)

29. M. Först, M. Fechner, A.S. Disa, M. Buzzi, A. von Hoegen, V. Krapivin, Y. Huang, G. Orenstein, G. de la Peña, Q. Nguyen, R. Duncan, D. Reis, A. Cavalleri, and M. Trigo, *Control of lattice fluctuations in SrTiO₃ by nonlinear phononics*, in preparation.

30. S. W. Teitelbaum, P. Sun, Y. Sun, N. Wang, T. Osaka, R. A. Duncan, H. Y. Shin, A. A. Maznev, J. Haber, S. Nelson, S. Song, K. A. Nelson, J. B. Hastings, M. Trigo, D. Zhu, M. Yabashi, and D. A. Reis, *Excitation of high wavevector lattice vibrations with hard X-rays*, in preparation.

31. O. Matveev, A. Shvaika, and J. K. Freericks, *Ultrafast thermometry of electrons with X-ray probes*, Sci. Adv., in preparation.

32. Y. Wang, T. P. Devereaux, and J. K. Freericks, *Theory of X-ray pump-probe photon spectroscopies*, Rev. Mod. Phys, in preparation.

33. A. A. Maznev, S. Huberman, F. Bencivenga, A. Cannizzo, F. Capotondi, R. Cucini, R. A. Duncan, T. Feurer, T. D. Frazer, L. Foglia, H.-M. Frey, H. Kapteyn, J. Knobloch, G. Knopp, C. Masciovecchio, R. Mincigrucci, G. Monaco, M. Murnane, I. Nikolov, E. Pedersoli, A. Simoncig, A. Vega-Flick, G. Chen, and K. A. Nelson, *Thermal transport near ballistic limit in silicon and diamond investigated with extreme ultraviolet transient gratings*, in preparation.

34. X. Li, P. J. Taylor, E. Baldini, Y. Zhang, N. Gedik, L. Fu, and K. A. Nelson, *Ferroelectric phase transition and terahertz-field-induced nonlinearities in topological crystalline insulator Pb_{1-x}Sn_xTe*, in preparation.

35. M.-C. Lee, T. Sato, B. Paudel, B. Fauseweh, V. Krapivin, N. S. Sirica, Y. Kubota, O. Taito, O. Shigeki, A. A. Maznev, T. Pezeril, M. Trigo, D. A. Reis, J.-X. Zhu, A. Chen, K. A. Nelson, and R. P. Prasankumar, *Ultrafast strain modulation of superconductivity in a cuprate heterostructure*, in preparation.

36. E. R. Sung, Y. Kai, T. Pezeril, and K. A. Nelson, *Enhanced generation of terahertz fields in LiTaO₃ waveguides using a conical tilted pulse front*, in preparation.

Lattice instabilities, emergent electronic phases and collective behavior rooted in the quantum world (DE-SC0021973)

Prof. V. Petkov, Dept. of Physics, Central Michigan University, Mt. Pleasant, MI 48858

Keywords: quantum materials, broken local symmetry, high-energy x-ray diffraction, differential atomic pair distribution, structure modeling

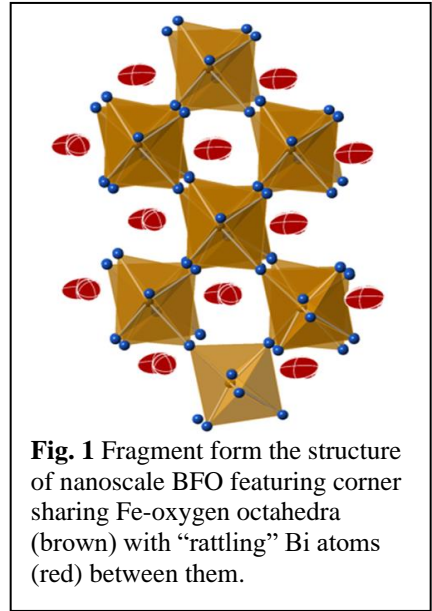
Research Scope

Using advanced x-ray scattering techniques and structure modeling, we study the interaction between lattice instabilities, electronic and magnetic degrees of freedom leading to the emergence of electronic phases and material's behavior rooted in the quantum world. The interaction is studied as important physical parameters, including system's dimensionally, chemical composition, temperature and magnetic field are varied in a systematic manner. We also push forward resonant total x-ray scattering as a technique to study complex materials with chemical specificity.

Recent Progress

1. Emergent magnetoelectric coupling in multiferroic BiFeO₃ (BFO) as a function of system's physical size

Rhombohedral/polar BiFeO₃ (BFO) is a unique multiferroic because it exhibits coexisting ferroelectric ($T_c = 1033$ K) and antiferromagnetic ($T_N = 643$ K) orders over a broad temperature range, including room temperature. The presence of a cycloid of Fe spins leading to a zero net magnetization negates any coupling present between electrical polarization and magnetization, hampering practical applications. We studied the emergence of magnetoelectric coupling as the physical size of BFO is reduced to nanoscale dimensions. We find that ferromagnetism and, hence, magnetoelectric coupling emerges when BFO particles become smaller than 60 nm, which is the cycloid's period. The coupling is maximized at a particle's size of ~ 20 nm. When the size is reduced further, BFO particles suddenly expand at atomic level the (unit cell volume increases), become superparamagnetic and adopt a non-polar cubic structure, which is inconsistent with ferroelectricity. As a result, BiFeO₃ loses both ferroic orders. This happens largely because, at the nanoscale, Bi atoms in BFO experience dramatically increased displacements (see Fig. 1). Another major finding is that, counterintuitively, the crystal symmetry of ionic perovskites appears to increase with diminishing crystallite's size due to an increased atomic structural disorder, which plays the role of an effectively "increased temperature"/"reduced pressure". For reference, metallic nanoparticles shrink with diminishing size. Our results are published in ref. [1].



2. Emergent magnetoelectric coupling in multiferroic BiFeO₃ (BFO) as a function of chemical composition and development of resonant total x-ray scattering

To induce magnetoelectric coupling, BiFeO₃ (Bi site) is often doped with rare earth elements. Doping with non-magnetic La creates atomic level stress which induces ferromagnetism without diminishing the ferroelectric order. We studied La substituted (La/Bi)FeO₃, where La is 10, 20, 30 and 40 at. %. Experimental data showed that the coupling is maximized at about 40 % La and likely due to the combined effect of an increased both i) local lattice strain (La is a bit smaller than Bi) and ii) Fe-O-Fe bond angles leading to an increase in the super-exchange Fe spin-Fe spin coupling. The local lattice strain, however, is difficult to assess because of the increased number of atomic correlations in rare earth substituted BFO (when n=4 atomic species we have $n(n+1)/2 = 10$ distinct atomic correlations). To achieve chemical specificity, we did resonant XRD experiment at the K edge of Bi (Z=83). The experiment was done at Sector 1, APS (Argonne). We used a single photon counting & large area Pilatus detector. Results are given in Fig. 2. The unwanted fluorescent radiation was largely removed by properly setting the gain and voltage threshold of the detector. Structure modeling based on the data is under way. Future Bi edge resonant XRD on BFO doped with Nd and Eu are planned for March 2023. We also studied lattice distortions in BaTiO₃ ferroelectric where Ba is partially replaced by Ce. Results are summarized in our paper (2).

3. Spin-lattice coupling in magnetocaloric Gd₅(Si,Ge)₄

Magnetocaloric effect allows to achieve magnetic refrigeration by harnessing concurrent changes in the magnetic and lattice entropy. The exemplary magnetocaloric Gd₅(Si,Ge)₄ alloys are built of Gd-(Ge/Si) slabs that are ferromagnetic but may be coupled either ferro- or antiferromagnetically. We studied it by total scattering over a wide range of temperatures (10-350 K) and magnetic fields (up to 5 T) at NSLS II. We showed that, regardless of whether induced by decreasing temperature in zero field

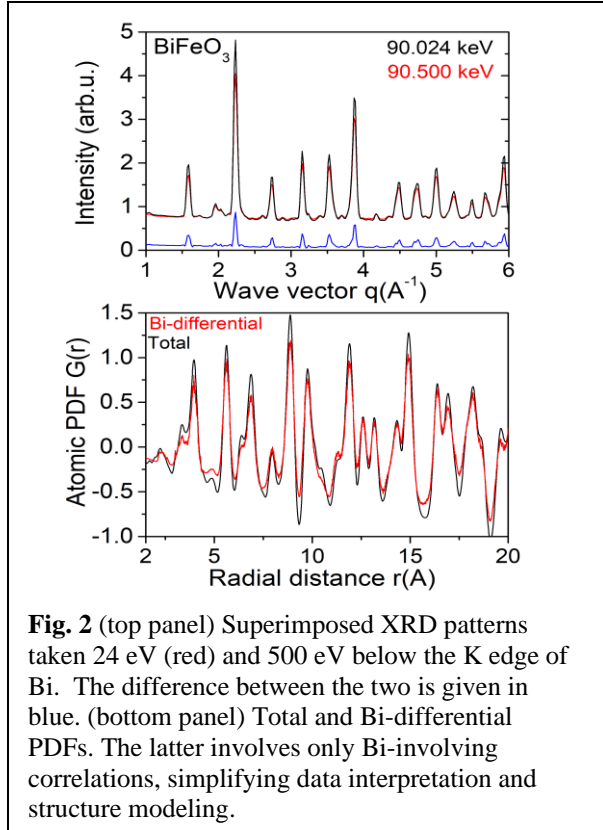


Fig. 2 (top panel) Superimposed XRD patterns taken 24 eV (red) and 500 eV below the K edge of Bi. The difference between the two is given in blue. (bottom panel) Total and Bi-differential PDFs. The latter involves only Bi-involving correlations, simplifying data interpretation and structure modeling.

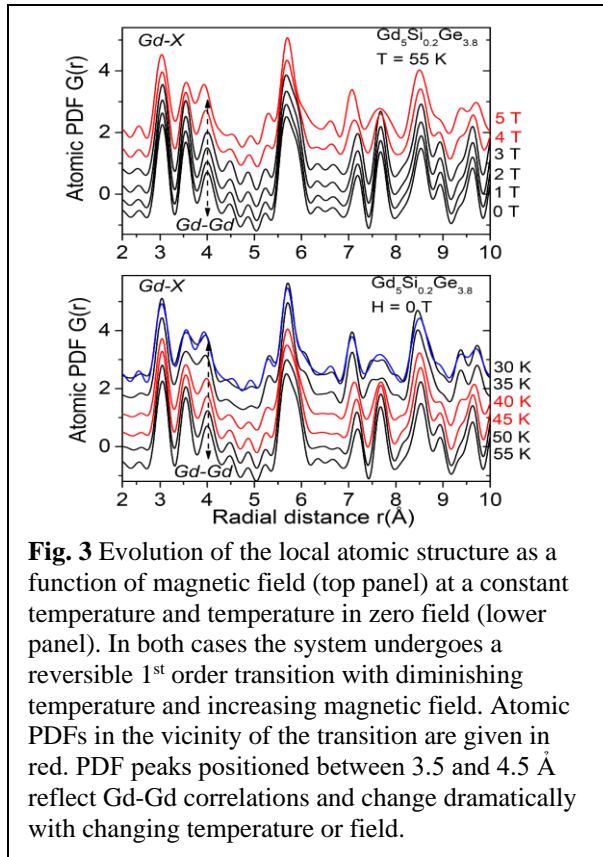


Fig. 3 Evolution of the local atomic structure as a function of magnetic field (top panel) at a constant temperature and temperature in zero field (lower panel). In both cases the system undergoes a reversible 1st order transition with diminishing temperature and increasing magnetic field. Atomic PDFs in the vicinity of the transition are given in red. PDF peaks positioned between 3.5 and 4.5 Å reflect Gd-Gd correlations and change dramatically with changing temperature or field.

or applying magnetic field isothermally, the transition dramatically modifies the mutual arrangement of Gd atoms from adjacent slabs, thus modifying the character of slab-slab coupling, and it is likely this repositioning that strongly couples the spin and lattice degrees of freedom in this system. We also show that the system exhibits considerable lattice distortions, which can be considered as “lattice degrees of freedom” bridging their different magnetic phases and giving rise to a giant magnetocaloric and magnetostriction effects. Remarkably, the distortions appear dependent on whether the magnetic phase boundary is crossed by decreasing temperature or increasing magnetic field, providing evidence that temperature and magnetic field are coupled but not necessarily equivalent control variables for triggering phase transitions in strongly correlated systems such as $\text{Gd}_5(\text{Si,Ge})_4$ alloys. Results from this study are published in ref. (3). Up to our knowledge, this is the first published total x-ray scattering study in magnetic field. The advantage over traditional XRD is that changes in interatomic correlations with changes in magnetic field can be directly observed (Fig. 3, top panel), and often interpreted, without structure modeling. In addition, magnetic systems not amenable to neutron scattering studies, such as Gd involving systems (nasty Gd resonance), can be easily studied under magnetic field at synchrotron facilities. We also did variable temperature and magnetic fields study on strongly correlated $\text{Ca}_3\text{Ru}_2\text{O}_7$. Results are published in ref. (4). We just summarized results from a temperature and magnetic field study on strongly correlated MnAs in a paper, which is under review (ref. 5).

4. Charge density waves (CDWs) in transition metal di-chalcogenides and large-scale structure modeling

CDWs are understood as a long-range modulation of the electron density coupled to a periodic distortion of the crystal lattice, usually appearing as a superstructure, and opening of a gap at the Fermi level. Often, CDW systems exhibit metal-insulator (M-I) transitions, hidden order and/or superconductivity. However, typically, it is difficult to define a CDW unit cell suitable for DFT calculations because either the CDW period of repetition is very long, e.g., tens of nanometers, and/or CDWs appear incommensurate with the underlying crystal lattice. 1T-TaS_2 has a remarkable phase diagram, exhibiting several distinct CDW phases and phase transitions. The material is built of layers of Ta–S trigonal prisms with a weak van-der-Waals bonding between the

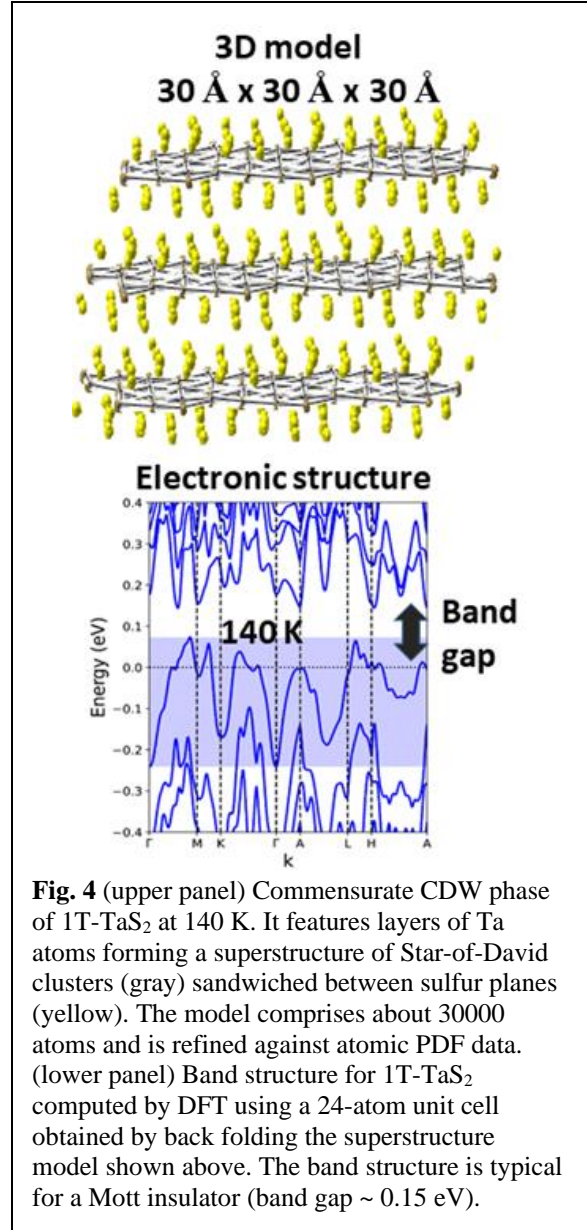


Fig. 4 (upper panel) Commensurate CDW phase of 1T-TaS_2 at 140 K. It features layers of Ta atoms forming a superstructure of Star-of-David clusters (gray) sandwiched between sulfur planes (yellow). The model comprises about 30000 atoms and is refined against atomic PDF data. (lower panel) Band structure for 1T-TaS_2 computed by DFT using a 24-atom unit cell obtained by back folding the superstructure model shown above. The band structure is typical for a Mott insulator (band gap ~ 0.15 eV).

layers. 1T-TaS₂ exhibits a metallic incommensurate (IC)-CDW phase below 550 K, a metallic nearly commensurate (NC)-CDW phase below 350 K and an insulating commensurate (C)-CDW phase below 180 K. The MI transition between the NC-CDW and C-CDW phases is first order and, upon cooling, accompanied by a large jump in resistivity that can be reversed by an application of intense electrical current or light pulse. Regardless of the extensive research effort over nearly four decades, there is still an ongoing debate about the nature of the insulating C-CDW phase. We did variable temperature total scattering experiments at APS, Argonne coupled to large scale computer modeling, which helped us capture the periodic lattice distortion (12 nm) in good detail (Fig. 4, upper panel). The large-scale model was back folded into a 24-atom unit cell (top-down approach) amenable to DFT calculations. The calculations showed that 1T-TaS₂ is a Mott and not trivial band insulator, i.e., the emergent band gap is due to strong electron-electron correlations. Prior studies produced controversial results because unrealistic assumptions were used to define a CDW “unit cell”. Our results are published in ref. (6). We also studied the Weyl semiconductor 1T-MoTe₂ (7) and layered TMPS₃ (TM=Mn, Co, Ni) showing 2D magnetism (8). In addition, we continued our prior DOE funded effort on materials for energy-related applications. Results are published in papers (9-11).

Future Plans

Systems: In the remaining 1.5 years of our project, we will continue studying physical systems showing interacting lattice, electronic and magnetic degrees of freedom leading to complex electronic phases. In particular, we will study i) heavy fermion systems LaPt₂Si₂ and UPt₂Si₂ showing coexisting Kondo lattices and 3D CDWs, ii) frustrated triangular/Kagome magnets TMTiO₃ (TM=Ni, Fe, Co), iii) CDW systems NdSe₂, TiS₂, VSe₂, NbTe₄ and HoTe₃. The systems will be studied as a function of temperature and/or magnetic field, which are “clean” control parameter. Experiments will be done at NSLS-II, Brookhaven. Indeed, a part of the experiments are already done (Fig. 5).

Methodological development: We will continue developing resonant total scattering. For a long time, we used cryogenically cooled, single point Ge detectors, which have an excellent x-ray energy resolution. A disadvantage is the limited dynamic range and long experimental time (10-16 h per sample). We started exploring single photon counting, 2D CdTe detectors. They are inferior in comparison to Ge detectors in terms of energy resolution but offer a larger dynamic range, reduced experimental time (4-6 h per sample) and, as a new technology and contrary to Ge detectors, are being improved constantly. We are planning to conduct experiments at the K edge of Bi species in Nd and Eu substituted BiFeO₃. We also plan to conduct an experiment at the K

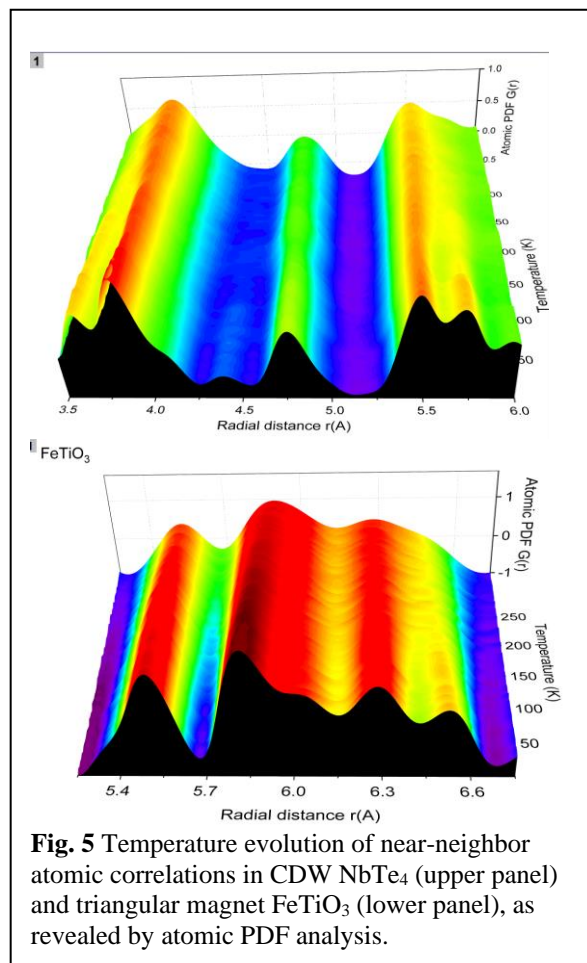


Fig. 5 Temperature evolution of near-neighbor atomic correlations in CDW NbTe₄ (upper panel) and triangular magnet FeTiO₃ (lower panel), as revealed by atomic PDF analysis.

edge of Bi species in Nd and Eu substituted BiFeO₃. We also plan to conduct an experiment at the K

edge of U (our USi_2Pt_2 sample). The experiments will be done at Sector 1, APS in March 2023, just before the facility is closed for an upgrade. We are planning more experiments, this time at the K edge of Te (our NbTe_4 and HoTe_3 samples where Te atoms form a superstructure). These experiments will be done at the beamline ID-22 at ESRF using a set of crystal analyzers.

Publications in years 2021 and 2022

1. V. Petkov, and S. Shastri “*Lattice symmetry breaking transition and critical size limit for ferroic orders in nanophase*” *BiFeO₃* Phys. Rev. B **104**, 054121-10 (2021).
2. V. Petkov and V. Buscaglia “*Rhombohedral distortion and percolation phenomena in B-site substituted perovskite ferroelectrics with enhanced piezoelectric response.*” Phys. Rev. Materials **5**, 044410 (2021).
3. V. Petkov, T. D. Rao, AM Milinda Abeykoon, Jorge R. Galeano-Cabral, and K. Wei “*Spin-lattice coupling in magnetocaloric $Gd_5(\text{Ge},\text{Si})_4$ alloys by in-situ x-ray pair distribution analysis in magnetic field*”. Phys. Rev. Mater. **6**, 104407 (2022).
4. V. Petkov, T. Durga Rao, A Zafar, AM M. Abeykoon, E Fletcher, J Peng, Z Q Mao and X Ke “*Lattice distortions and the metal–insulator transition in pure and Ti-substituted $\text{Ca}_3\text{Ru}_2\text{O}_7$* ” J. Phys.: Condens. Matter **51**, 015402 (2023).
5. V. Petkov, A. Zafar, D. R. Tadiseti and M. AM Abeykoon “*Lattice instability and magnetic phase transitions in strongly correlated MnAs*”, Phys. Rev. Lett. (under review).
6. V. Petkov, J. E. Peralta, B. Aoun and Y. Ren “*Atomic structure and Mott nature of the insulating charge density wave phase of $1T\text{-TaS}_2$* ” J. Phys.: Condens. Matter **34**, 345401-9 (2022).
7. V. Petkov and Y. Ren, “*Local structure memory effects in the polar and nonpolar phases of MoTe_2* ”, Phys. Rev. B **103**, 094101 (2021).
8. V. Petkov and Y. Ren “*Critical cation–anion radius ratio and two-dimensional antiferromagnetism in van der Waals magnets TMPS_3 ($\text{TM} = \text{Mn}, \text{Fe}, \text{Ni}$)*” J. Phys.: Condens. Matter **34**, 175404 (2022).
9. E. Lee, K. A. Kuttiyiel, K.-H. Kim, J. Jang, H. J. Lee, J. M. Lee, M. H. Seo, T.-H. Yang, S.-D. Yim, J. A. Vargas, V. Petkov, K. Sasaki, R. R. Adzic and G.-G. Park “*High Pressure Nitrogen-Infused Ultrastable Fuel Cell Catalyst for Oxygen Reduction Reaction*” ACS Catal. **11**, 5525 (2021.)
10. H. Kareem, Y. Maswadeh, Zhi-Peng Wu, A. C. Leff, Han-Wen Cheng, S. Shan, S. Wang, R. Robinson, D. Caracciolo, A. Langrock, D. M. Mackie, D. T. Tran, V. Petkov, and C.-J. Zhong “*Lattice Strain and Surface Activity of Ternary Nanoalloys under the Propane Oxidation Condition*” ACS Appl. Mat. & Interfaces **14**, 11435 (2022).
11. L. Ma, J. Vatamanu, N. T. Hahn, T. P. Pollard, O. Borodina, **V. Petkov**, M. A. Schroeder, Y. Ren, M. S. Ding, C. Luo, J. L. Allen, C. Wang, and K. Xua “*Highly reversible Zn metal anode enabled by sustainable hydroxyl chemistry*” PNAS **119**, e2121138119 (2022).

Coherent x-ray scattering investigations of nanoscale magnetic fluctuations in frustrated magnets

Kemp Plumb, Brown University, Department of Physics, Providence, RI 0290

Program Scope: In frustrated magnets, competing magnetic interactions prevent the formation of semi-classical magnetically ordered ground states and can give rise to phases of matter exhibiting non-trivial entanglement. However, frustrated magnets are also sensitive to chemical or structural disorder and the physical effects of this very minute disorder can mimic experimental signatures of a quantum state. Distinguishing disorder driven from intrinsic phenomena in quantum magnets is a major experimental challenge. The focus of this program is to utilize coherent x-ray scattering as a probe of spontaneous magnetization fluctuations in model frustrated magnets to elucidate signatures of disorder-induced from those of intrinsic quantum phenomena. There is a particular emphasis on studying materials where we have a degree of control over structure and chemical disorder introduced during synthesis. Through these studies, we aim to achieve a systematic empirical understanding of the roles of disorder in controlling the lowest energy magnetic fluctuations in quantum materials, with an eye towards realizing magnetic materials exhibiting quantum entangled ground states.

Recent Progress: *Correlated states and excitations in intercalated honeycomb iridates.* We have completed a series of resonant x-ray investigations of the intercalated honeycomb iridates $\text{Ag}_3\text{LiIr}_2\text{O}_6$ and $\text{H}_3\text{LiIr}_2\text{O}_3$. These compounds are derived from $\alpha\text{-Li}_2\text{IrO}_3$ but with interlayer Li atoms replaced with Ag or H in an attempt to bring the material closer to the Kitaev spin liquid limit [1]. $\text{H}_3\text{LiIr}_2\text{O}_3$ is currently considered a possible quantum spin liquid [2]. However, the specific role of intercalates to affect magnetic interactions and influence of disorder was not understood and a measurement of the dynamic correlations that can confirm the existence of a spin liquid has not been carried out.

In $\text{Ag}_3\text{LiIr}_2\text{O}_6$ we find deviations from cubic symmetry in the Ir local environment that diffraction measurements could not detect. By comparing *ab-initio* electronic structure calculations with our data, we have found that the replacement of Li with Ag in $\text{Ag}_3\text{Li}_2\text{IrO}_6$ generates a chemical pressure that drives this compound closer to an itinerant limit. Our results show how

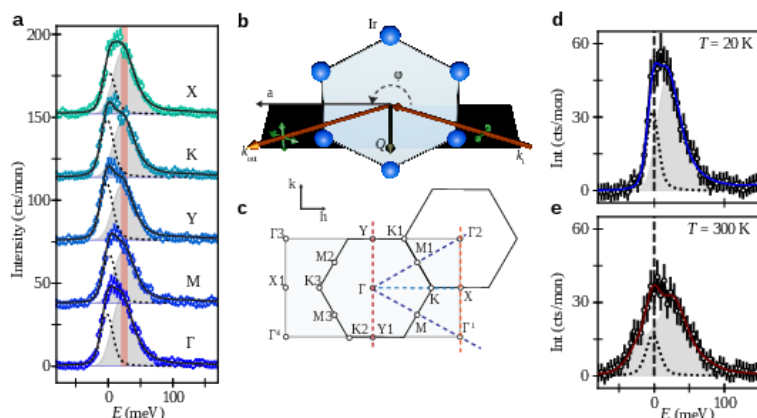


Figure 6. High-resolution low-energy Ir L_3 resonant inelastic X-ray spectra of $\text{H}_3\text{LiIr}_2\text{O}_3$. (a) Scans at high symmetry points of the Brillouin zone showing a damped harmonic oscillator entered at 28 meV. (b) Sketch of the scattering geometry and (c), Schematic of the extended BZ. (d) Gamma point temperature dependent RIXS spectra.

chemical pressure can influence the single ion state of transition metal magnets. We are currently preparing a publication describing these results.

In $\text{H}_3\text{LiIr}_2\text{O}_3$ we have measured the low energy magnetic excitation spectra and find collective excitations that are strikingly absent any momentum dependence [Fig. 1]. The data indicate dynamic spin-spin correlations with a vanishing correlation length, and are consistent with a ferromagnetic Kitaev model. Disorder evidently acts to limit correlation lengths in $\text{H}_3\text{LiIr}_2\text{O}_3$, but the excitations we observe demonstrate that the ground state is not glassy or a disordered dimer singlet, and quantum fluctuations of a spin liquid phase survive in a bond-disordered Kitaev spin liquid.

Excitonic magnetism, band vs correlated insulators in $J=0$ iridates. Pentavalent 4d/5d compounds with the octahedrally coordinated transition metal ions can realize a unique spin-orbit driven non-magnetic $J = 0$ Mott insulating singlet ground state. When exchange interactions are comparable to the gap between the orbital singlet and first excited triplet, novel excitonic magnetic phases can condense [3]. We used resonant inelastic x-ray scattering to elucidate the electronic configuration of two newly synthesized pentavalent iridates NaIrO_3 and $\text{Sr}_3\text{CaIr}_2\text{O}_9$, and show that they respectively realize distinct insulating states. $\text{Sr}_3\text{CaIr}_2\text{O}_9$ is a $J = 0$ Mott insulator, while NaIrO_3 is a band insulator. Our work provides concrete microscopic details about how two distinct insulating states: band vs Mott insulators, can be realized in nominally very similar materials and demonstrates how x-ray spectroscopy combined with detailed modeling can be used to distinguish between the two insulating limits when such a distinction is not possible through any bulk characterization.

Electron-Phonon Coupling in Frustrated Magnets. NiRh_2O_4 is the only known material with $S=1$ degrees of freedom on a frustrated diamond lattice, potentially supporting a unique topological paramagnetic state. Previous works had identified a possible valence bond solid ground state in this material, but progress was stymied because of uncertainty over the crystal field configuration and electronic structure. We used a broad suite of spectroscopic probes, including inelastic neutron scattering, resonant inelastic x-ray scattering, and x-ray absorption to elucidate the crystal field and electronic structure of NiRh_2O_4 . We showed explicitly how both metal-metal hybridization and electron-phonon couplings enter as essential energy scales. We expect that metal-metal hybridization and electron-phonon coupling are more broadly important across the family of A-site spinels. Thus, the implications of our work extend beyond NiRh_2O_4 and will inform research on a broad class of frustrated magnets. Our results suggest avenues for future experiments that seek to control magnetism through ultrafast resonant pumping of crystal field or phonon excitations.

Future Plans: We continue to investigate Ni and Fe based frustrated triangular lattice magnets that have been shown to exhibit anomalously slow dynamics. Using resonant scattering, we have uncovered a more complex magnetic ordering for NiGa₂S₄ that was not apparent in much coarser resolution neutron measurements. We are continuing to push for lower temperature (sub 10 K) sample environments for XPCS experiments in order to reach the regimes of slow and glassy dynamics in this compound and other frustrated magnets.

We have recently completed a series of resonant x-ray diffraction investigations on transition metal intercalated TMNb₃S₆ (TM = Ni, Co). The transition metal ions form a basal plane triangular lattice antiferromagnet between NbS₂ layers. In both compounds we found that nominally commensurate magnetic structures have long wavelength incommensurate modulations. In CoNb₃S₆, we found a 2Q scalar chiral stripe phase that may be responsible for the large anomalous Hall response in this compound. In NiNb₃S₆, we found a one dimensional chiral helimagnetic structure that is consistent with a zero-field antiferromagnetic soliton lattice. Both compounds exhibit slow dynamics in the AC magnetic response, and we aim to elucidate the nature of the dynamic response using resonant XPCS. Given the observation of a scalar chiral strip phase in the Co compound, this class of materials has potential to host more exotic, topologically non-trivial magnetic states, if the magnetic interactions can be suitably tuned. We are planning additional experiments to manipulate the magnetic states in the Co and Ni samples using applied fields and strain coupled with resonant x-ray experiments. We are also expanding the family of materials including different transition metals and intercalated TaS₂.

References

1. Faranak Bahrami, William Lafargue-Dit-Hauret, Oleg I. Lebedev, Roman Movshovich, Hung-Yu Yang, David Broido, Xavier Rocquefelte, and Fazel Tafti. “Thermodynamic Evidence of Proximity to a Kitaev Spin Liquid in Ag₃LiIr₂O₆”. *Phys. Rev. Lett.* **123**, 237203 (2019).
2. Kitagawa, K., Takayama, T., Matsumoto, Y. *et al.* “A spin–orbital-entangled quantum liquid on a honeycomb lattice.” *Nature* **554**, 341–345 (2018).
3. G. Khaliullin, Excitonic Magnetism in Van Vleck–type d4 Mott Insulators”. *Phys. Rev. Lett.* **111**, 197201 (2013).

Publications

1. A. de la Torre, B. Zager, F. Bahrami, G. Fabbris, M. H. Upton, J.-H. Kim, F. Tafti, K. W. Plumb, Magnetic excitations in the quantum spin liquid candidate H₃LiIr₂O₆, In Preparation (2023).
2. B. Zager, R. Fan, P. Steadman, K. W. Plumb, Observation of a chiral stripe phase in the anomalous Hall triangular antiferromagnet CoNb₃S₆, In preparation (2023).
3. A. de la Torre, B. Zager, J. R. Chamorro, M. H. Upton, G. Fabbris, D. Haskel, D. Casa, T. M. McQueen, and K. W. Plumb, On the electronic ground state of two non-magnetic honeycomb iridates. *Phys. Rev. Matter.* **6**, 084406 (2022).

4. B. Zager, J. R. Chamorro, T. M. McQueen, Valentina Bisogni, J. Li, G. Fabbri, M. Mourigal, K. W. Plumb Electronic structure of the frustrated diamond lattice antiferromagnet NiRh_2O_4 , *Phys. Rev. B* **106**, 045134 (2022).
5. A. de la Torre, B. Zager, F. Bahrami, M. DiScala, J. R. Chamorro, M. H. Upton, G. Fabbri, D. Haskel, D. Casa, T. M. McQueen, F. Tafti, K. W. Plumb, Enhanced hybridization in the electronic ground state of the intercalated honeycomb iridate $\text{Ag}_3\text{LiIr}_2\text{O}_6$, *Phys. Rev. B* **104** L100416 (2021).

Creating New Quantum States of Matter in Time and Space Through Engineering Artificial Interfaces and Structures

PIs: Andrej Singer, Nicole Benedek, Ankit Disa, Darrell Schlom, Kyle Shen (Cornell)

Keywords: X-ray Free-Electron Lasers, non-equilibrium states, ultrafast materials science, strained crystalline membranes, phonon dynamics.

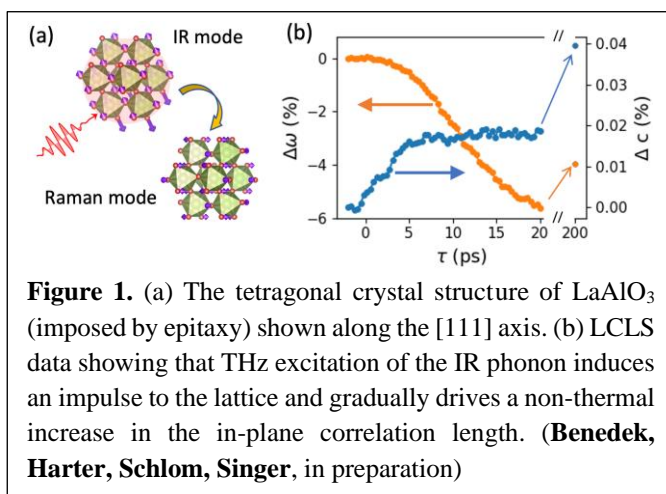
Research Scope

This proposal aims to combine ultrafast excitations with thin films and heterostructures, specifically tailored to enable the realization and control of new transient states of quantum matter that are not achievable in conventional bulk single crystals. The project integrates theory and computational methods of non-equilibrium dynamics, synthesis of structures with the desired blueprint, and characterization using optical lasers, ultrafast electron diffraction, and high-repetition x-ray free-electron lasers. The unique characteristics of x-ray lasers are crucial in establishing a synthesis-characterization feedback loop for engineering artificial quantum materials out of equilibrium.

Recent Progress

1. Achieving new transient states with light

Light-induced strain and domain switching in LaAlO₃: In recent years, the development of high-intensity THz light sources has enabled new forms of structural control based on optically driving the crystal lattice. Strong, resonant excitation of optical phonons creates extreme atomic displacements—up to several percent of the equilibrium bond distance—pushing the response of the lattice into a highly nonlinear regime, which can lead to new crystal structures and functional properties. Our theoretical exploration of the nonlinear phononics effect led **Benedek**, under the support of the current award, to design new strategies for coherent structural control, while unifying several concepts in the nonlinear phononics field with established perspectives from dynamical systems. Specifically, we derived a figure of merit for the nonlinear phononics mechanism to identify materials that may exhibit a particularly large or novel response based on microscopic material features [3]. We showed that among accessible modes, very few have the requisite characteristics for a significant response. Using the developed theory, we predicted optical control of ferroelastic domain switching in LaAlO₃, an idea that formed the basis of a successful proposal for LCLS beamtime. To access the excitation mechanism, we needed to biaxially strain LaAlO₃, which we (**Schlom**) accomplished by synthesizing 10-20 nm thin LaAlO₃ films on NSAT substrates. In the LCLS experiment (**PIs: Singer, Benedek, Schlom**), we used THz resonant excitation for driving an IR mode in LaAlO₃, which through nonlinear phonon-coupling excites a giant response in the lowest frequency Raman phonon. We observed an impulsive mechanism driving a lattice expansion and a delayed lateral increase of the correlation length (**Fig. 1**). The



combination of the lattice expansion, correlation length, and their timescales suggest a non-thermal structural phase induced by selectively driving IR modes.

Picosecond volume expansion followed by a later metal-insulator transition in a nano-textured Mott insulator:

Manipulating properties at THz rates requires accessing the intrinsic timescales of electrons (femtoseconds) and associated phonons (10s of femtoseconds to few picoseconds), possible with short-pulse photoexcitation. Yet in many Mott insulators, the electronic transition is accompanied by the nucleation and growth of percolating domains of the changed lattice structure, which lead to slow coarsening dynamics. Using time-resolved X-ray diffraction and reflectivity measurements, we (**Benedek, Harter, Schlom, Shen, Singer**, in collaboration with Averitt, Freeland, Millis, Shpyrko) investigated the photoinduced insulator-to-metal transition in an epitaxially strained Mott insulator Ca_2RuO_4 . The dynamical transition occurred without observable domain formation and coarsening effects, allowing the study of the intrinsic electronic and lattice dynamics.

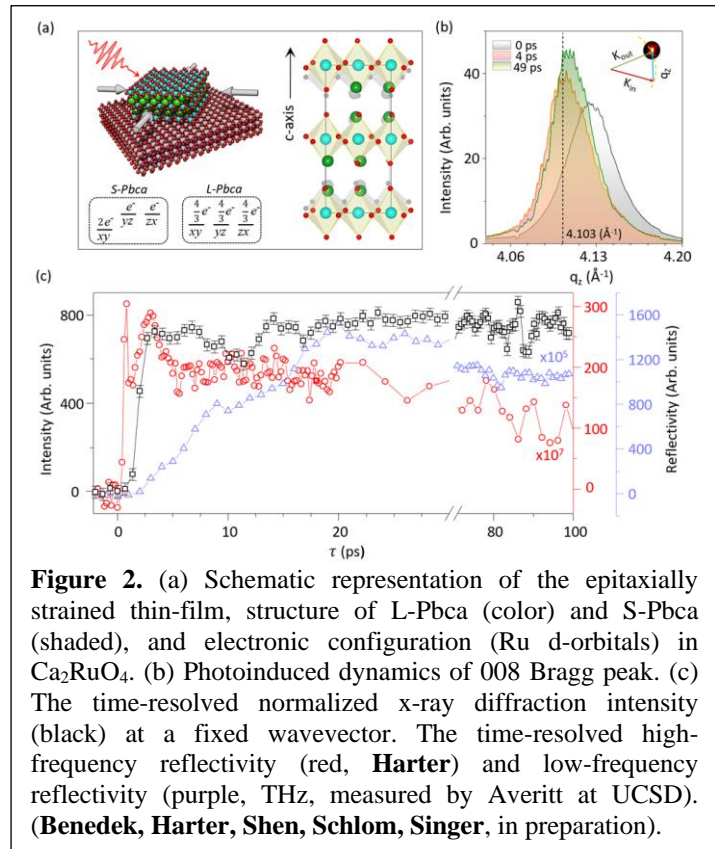


Figure 2. (a) Schematic representation of the epitaxially strained thin-film, structure of L-Pbca (color) and S-Pbca (shaded), and electronic configuration (Ru d-orbitals) in Ca_2RuO_4 . (b) Photoinduced dynamics of 008 Bragg peak. (c) The time-resolved normalized x-ray diffraction intensity (black) at a fixed wavevector. The time-resolved high-frequency reflectivity (red, **Harter**) and low-frequency reflectivity (purple, THz, measured by Averitt at UCSD). (**Benedek, Harter, Shen, Schlom, Singer**, in preparation).

A new imaging modality we developed (see below) revealed a strain-stabilized nano-texture, which we interpret as the origin for the ultrafast lattice expansion: the phase transformation nucleates at inclusions of the incipient high-temperature phase stabilized through epitaxial strain. Above a fluence threshold, a sufficiently large initial electronic excitation drove a fast lattice rearrangement, followed by a slower electronic phase transition into a metastable nonequilibrium state (**Fig. 2**). The structure-factor analysis supported by calculating symmetry-allowed atomic rearrangements (**Benedek**) elucidated the atomic arrangement in the nonequilibrium structure.

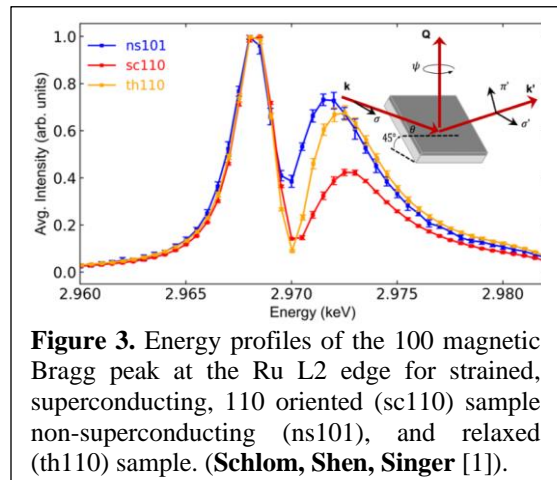


Figure 3. Energy profiles of the 100 magnetic Bragg peak at the Ru L2 edge for strained, superconducting, 110 oriented (sc110) sample, non-superconducting (ns101), and relaxed (th110) sample. (**Schlom, Shen, Singer** [1]).

2. Understanding electronic, magnetic, and structural properties in strained quantum materials

Strain-induced orbital energy shift in antiferromagnetic RuO₂:

In its ground state, RuO_2 was long thought to be an ordinary metallic paramagnet. Recent neutron and x-ray diffraction revealed that bulk RuO_2 is an antiferromagnet (AFM) with T_N above 300 K. Furthermore, we (**Schlom, Shen**) showed how epitaxial strain induces

superconductivity in thin films of RuO₂ below 2 K [4]. In the past funding period, we (**Schlom, Shen, Singer**) conducted a resonant elastic x-ray scattering (REXS) study at the Ru L2 edge of the strained RuO₂ films exhibiting strain-induced superconductivity. We observed an azimuthal modulation of the 100 Bragg peak consistent with canted AFM found in bulk. Most notably, in the strained films displaying novel superconductivity, we observed a ~1 eV shift of the Ru *e_g* orbitals to a higher energy [1]. The energy shift is smaller in thicker, relaxed films and films with a different strain direction (**Fig. 3**). Our future goal is to elucidate if the orbital shift is connected to superconductivity and how to exploit it to drive new states with light.

Real-space imaging of elastic nano-textures in thin films via inversion of diffraction data: Exploiting the emerging nanoscale periodicities in epitaxial, single-crystal thin films is an exciting direction in quantum materials science: confinement and periodic distortions induce novel properties. A critical step towards heterostructure engineering is understanding their nanoscale structure, best achieved through real-space imaging. We (**Schlom, Shen, Singer**) developed real-space imaging of periodic lattice distortions by combining an iterative phase retrieval algorithm with unsupervised machine learning to invert the diffuse scattering in conventional x-ray reciprocal-space mapping into real-space images of elastic textures in thin epitaxial films. We visualized strain-induced nano-texture emerging during the metal-insulator transition in Ca₂RuO₄ thin films. Instead of homogeneously transforming into a low-temperature structure (like in bulk), the strained Mott insulator splits into a nano-texture of regions with alternating lattice constants, as confirmed by cryogenic scanning transmission electron microscopy [2] (**Fig. 4**).

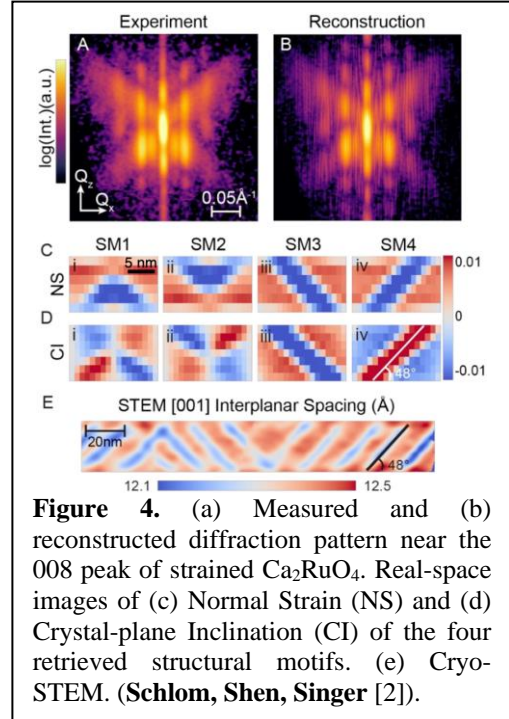


Figure 4. (a) Measured and (b) reconstructed diffraction pattern near the 008 peak of strained Ca₂RuO₄. Real-space images of (c) Normal Strain (NS) and (d) Crystal-plane Inclination (CI) of the four retrieved structural motifs. (e) Cryo-STEM. (**Schlom, Shen, Singer** [2]).

Instead of homogeneously transforming into a low-temperature structure (like in bulk), the strained Mott insulator splits into a nano-texture of regions with alternating lattice constants, as confirmed by cryogenic scanning transmission electron microscopy [2] (**Fig. 4**).

Future Plans

Tuning properties by driving zone-boundary phonons: In the complex oxide family of ABO₃ perovskites, the rotations of the BO₆ octahedra are decisive for a multitude of electronic, magnetic, and other functional properties and are associated with zone-boundary phonons of the prototypical cubic perovskite structure. In theoretical work by **Benedek** funded by this award, we have found that coupling between pumped IR modes and zone-edge octahedral rotations and, more generally, nonzero wavevector phonons is always allowed and can dominate the dynamics, giving ultrafast optical access to phases previously inaccessible in the equilibrium phase diagram. We will exploit this coherent optical manipulation mechanism for accessing new states in quantum materials and interrogate these states with XFEL experiments and UED.

Establishing a THz source at LCLS: The experimental access to the non-thermal structural phases predicted above requires selectively driving IR-active phonons, which in the proposed materials have frequencies in the ~1–18 THz range. Until recently, the lack of laser sources in this frequency band has made exploring nonlinear phononics experimentally unfeasible. Specifically, the critical range spanning the “THz gap” between different generation schemes has been challenging to access with tabletop sources and is unavailable at most XFEL sources. **Disa** and co-workers have

developed a new type of THz source, which greatly enhances the range and selectivity of generated pulses. We plan to expand the excitation capability of LCLS into the THz gap by developing such a source at LCLS.

Driving new properties in free-standing, strained crystalline membranes: Conventional epitaxial growth is limited to fixed values of strain and anisotropy dictated by the underlying substrate, severely restricting access to strain states. Bulk single crystals can be mechanically strained in a continuous fashion, yet the amount of strain that can be applied to a thick bulk crystal of a brittle material is modest (typically on the order of 0.1% in tension), which often prevents reaching a phase boundary before the crystal shatters. We will take advantage of a new synthesis technique called “remote epitaxy” to synthesize ultra-thin, free-standing films of quantum materials and heterostructures where extremely large strains can be applied continuously far beyond what is possible in bulk or even epitaxial thin films (**Fig. 5**). We will use diffraction and imaging at XFELs and UED to interrogate these states.

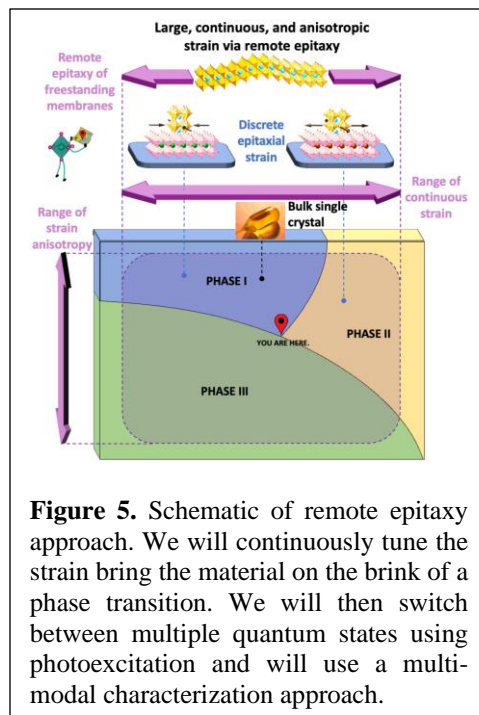


Figure 5. Schematic of remote epitaxy approach. We will continuously tune the strain bring the material on the brink of a phase transition. We will then switch between multiple quantum states using photoexcitation and will use a multi-modal characterization approach.

Inversion of ultrafast diffraction data: Understanding nano-texture at ultrafast and ultrasmall scales is a challenge of x-ray science and ultrafast materials science. We will expand the imaging modality we developed on static data (**Fig. 4**) to ultrafast diffraction data (**Fig. 2**). By collecting time-dependent high-quality reciprocal space maps and applying phase retrieval supported by machine learning, we will record snapshots of the local nanotexture after photoexcitation. We expect the superb resolution (few nm) will allow us to track changes in the nano-texture and potentially elucidate the interfaces between the different parts of the nanotexture at sub-ps times.

Ultrafast electron diffraction (UED): We will leverage a new, in-house UED system developed at Cornell, named MEDUSA (Micro Electron Diffraction for Ultrafast Structural Analysis), by our collaborator Jared Maxson [5]. The introduction of UED to our proposal will enable two key capabilities, including 1) the ability to employ **multi-modal** ultrafast studies of the dynamics of quantum materials through a combination of XFEL experiments, UED, and optical measurements, and 2) the ability to probe the dynamics of entirely new classes of systems (e.g., extremely strained, free-standing membranes placed on the brink of a phase transition).

References

1. B.Z. Gregory, J. Stempfer, D. Weinstock, J.P. Ruf, Y. Sun, H. Nair, N.J. Schreiber, D.G. Schlom, K.M. Shen, and A. Singer, *Strain-induced orbital-energy shift in antiferromagnetic RuO₂ revealed by resonant elastic x-ray scattering*, Physical Review B **106**, 195135 (2022).
2. Z. Shao, N. Schnitzer, J. Ruf, O.Y. Gorobtsov, C. Dai, B.H. Goodge, T. Yang, H. Nair, V.A. Stoica, J.W. Freeland, J. Ruff, L.-Q. Chen, D.G. Schlom, K.M. Shen, L.F. Kourkoutis, and A. Singer, *Real-space imaging of polar and elastic nano-textures in thin films via inversion of diffraction data*, arXiv **2211.01506**, (2022).
3. J.Z. Kaaret, G. Khalsa, and N.A. Benedek, *A strategy to identify materials exhibiting a large nonlinear phononics response: tuning the ultrafast structural response of LaAlO₃ with pressure*, J Phys Condens Matter **34**, 035402 (2021).

4. J.P. Ruf, H. Paik, N.J. Schreiber, H.P. Nair, L. Miao, J.K. Kawasaki, J.N. Nelson, B.D. Faeth, Y. Lee, B.H. Goodge, B. Pamuk, C.J. Fennie, L.F. Kourkoutis, D.G. Schlom, and K.M. Shen, *Strain-stabilized superconductivity*, Nat Commun **12**, 59 (2021).
5. W.H. Li, C.J.R. Duncan, M.B. Andorf, A.C. Bartnik, E. Bianco, L. Cultrera, A. Galdi, M. Gordon, M. Kaemingk, C.A. Pennington, L.F. Kourkoutis, I.V. Bazarov, and J.M. Maxson, *A kiloelectron-volt ultrafast electron micro-diffraction apparatus using low emittance semiconductor photocathodes*, Struct Dyn **9**, 024302 (2022).

Publications from past two years for DE- SC0019414

1. O. Gorobtsov, L. Ponet, S. K. K. Patel, N. Hua, A. G. Shabalin, S. Hrkac, J. Wingert, D. Cela, J. M. Glownia, D. Zhu, R. Medapalli, M. Chollet, S. Artyukhin, E. E. Fullerton, O. G. Shpyrko, and A. Singer, *Ultrafast control of a vibrational state near the spin density wave critical point*, Nature Communications **12**, 2865 (2021).
2. S. Salmani-Rezaie, L. Galletti, T. Schumann, R. Russell, H. Jeong, Y. Li, J.W. Harter, and S. Stemmer, *Superconductivity in magnetically doped SrTiO₃*, Applied Physics Letters **118**, 202602 (2021).
3. J.P. Ruf, H. Paik, N.J. Schreiber, H.P. Nair, L. Miao, J.K. Kawasaki, J.N. Nelson, B.D. Faeth, Y. Lee, B.H. Goodge, B. Pamuk, C.J. Fennie, L.F. Kourkoutis, D.G. Schlom, and K.M. Shen, *Strain-stabilized superconductivity*, Nature Communications **12**, 59 (2021).
4. S. Mallick, G. Khalsa, J. Z. Kaaret, W. Zhang, M. Batuk, A. S. Gibbs, J. Hadermann, P. S. Halasyamani, N. A. Benedek, and M. A. Hayward, *The influence of the 6s² configuration of Bi³⁺ on the structures of A'BiNb₂O₇ (A' = Rb, Na, Li) layered perovskite oxides*, Dalton Trans. **50**, 15359 (2021).
5. Salva Salmani-Rezaie, Hanbyeol Jeong, Ryan Russell, John W. Harter, and Susanne Stemmer, *Role of locally polar regions in the superconductivity of SrTiO₃*, Phys. Rev. Materials **5**, 104801 (2021).
6. J. Z. Kaaret, G. Khalsa, and N. A. Benedek, *A strategy to identify materials exhibiting a large nonlinear phononics response: tuning the ultrafast structural response of LaAlO₃ with pressure*, J. Phys.: Condens. Matter **34** 035402 (2022).
7. Jiaruo Li, Oleg Yu Gorobtsov, Sheena KK Patel, Nelson Hua, Benjamin Gregory, Anatoly G Shabalin, Stjepan Hrkac, James Wingert, Devin Cela, James M Glownia, Matthieu Chollet, Diling Zhu, Rajasekhar Medapalli, Eric E Fullerton, Oleg G Shpyrko, Andrej Singer, *Phonon-assisted formation of an itinerant electronic density wave*, Communications Physics **5**, 125 (2022).
8. B. Gregory, J. Stremper, D. Weinstock, J. Ruf, Y. Sun, H. Nair, N. J. Schreiber, D. G. Schlom, K. M. Shen, and A. Singer, *Strain-induced orbital energy shift in antiferromagnetic RuO₂ revealed by resonant elastic x-ray scattering*, Physical Review B **106**, 195135 (2022).
9. Hyeon Jun Lee, Youngjun Ahn, Samuel D. Marks, Deepankar Sri Gyan, Eric C. Landahl, Jun Young Lee, Tae Yeon Kim, Sanjith Unithrattil, Sae Hwan Chun, Sunam Kim, Sang-Youn Park, Intae Eom, Carolina Adamo, Darrell G. Schlom, Haidan Wen, Soohyeong Lee, Ji Young Jo, and Paul G. Evans, *Subpicosecond Optical Stress Generation in Multiferroic BiFeO₃*, Nano Letters **22**, 4294 (2022).

10. Hanbyeol Jeong, Ryan Russell, Nicholas G. Combs, Tyler N. Pardue, John W. Harter, and Susanne Stemmera, *Similarity in the critical thicknesses for superconductivity and ferroelectricity in strained SrTiO₃ films*, Applied Physics Letters **121**, 012601 (2022).
11. Ziming Shao, Noah Schnitzer, Jacob Ruf, Oleg Y Gorobtsov, Cheng Dai, Berit H Goodge, Tiannan Yang, Hari Nair, Vlad A Stoica, John W Freeland, Jacob Ruff, Long-Qing Chen, Darrell G Schlom, Kyle M Shen, Lena F Kourkoutis, and Andrej Singer, *Real-space imaging of polar and elastic nano-textures in thin films via inversion of diffraction data*, arXiv:2211.01506 (2022).

Quantum Engineering Exciton Dynamics in 2D-Heterostructures

Xiaodong Xu, Department of Physics and Department of Materials Science and Engineering, University of Washington, Seattle, WA 98195

Research Scope

The recent emergence of two-dimensional (2D) quantum materials, such as 2D semiconductors and magnetic insulators, have provided new platforms for studying light matter interactions with external controls. Access to high quality heterostructures formed by different 2D materials further enabled the exploration of emergent phenomena which were not otherwise. The objective of this program is to create, investigate, and understand these phenomena associated with excitons via advanced heterostructure engineering. During the last couple of years, we have made progress in two directions. *Direction 1:* Excitons in van der Waals magnets and heterostructures. We uncovered highly anisotropic excitons and multiple phonon bound states in antiferromagnetic insulator NiPS₃,¹ exciton-interlayer magnetism coupling in antiferromagnetic semiconductor CrSBr,² reversible strain induced AFM/FM phase transition probed by exciton,³ and direct visualization of magnetic domains and moiré magnetism in twisted 2D magnet CrI₃.⁴ *Direction 2:* Excitons and correlation effects in moiré superlattices. We realized Moiré trions in MoSe₂/WSe₂ heterobilayers,⁵ light induced ferromagnetism in moiré superlattices WS₂/WSe₂,⁶ and intercell moiré exciton complexes in electronic lattices.⁷ Selected progress is described below.

Self-identify keywords to describe your project: exciton, magnetism, moiré, strain.

Recent Progress

Direction 1: Excitons in van der Waals magnets and heterostructures

Highly Anisotropic Excitons and Multiple Phonon Bound States in NiPS₃: As powerful as semiconducting quantum wells are for studying fundamental light-matter interactions and developing modern solid-state devices, atomically thin quantum wells with intrinsic magnetic order remain rare. In this project, we demonstrate that atomically thin NiPS₃ is a quantum well platform with *intrinsic* magnetic order for investigating excitons with strong correlations. We found excitonic photoluminescence with a linewidth as narrow as 350 μeV (Fig. 1a), much narrower than the best reported 2D transition metal dichalcogenides. Using time resolved photoluminescence measurements with a streak camera, we measured an exciton lifetime of about 11 ps. We also found that the exciton is highly anisotropic due to strong coupling to the material's

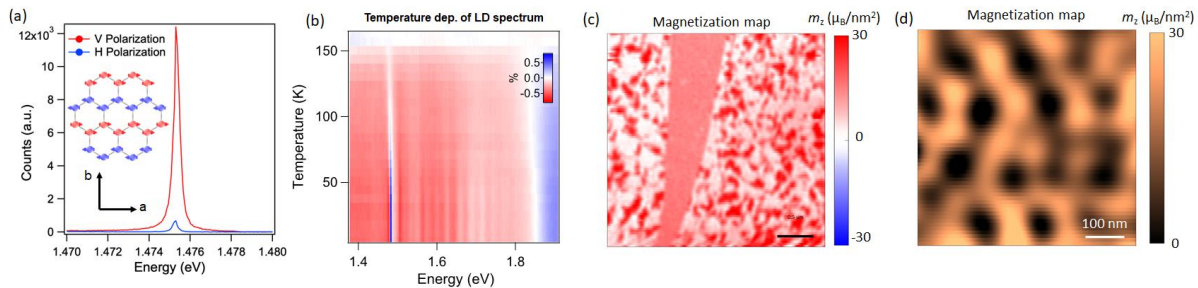


Figure 1. Excitons in 2D magnets and moiré magnetism. **a**, Observation of near-unity linearly polarized exciton emission from NiPS₃ with the polarization axis locked to the zigzag spin chain (inset). **b**, Linear dichroism intensity plot as a function of temperature and photon energy. The oscillation features are resulted from exciton-phonon bound states. **e-f**, Magnetization map by single-spin quantum magnetometry of small angle twisted CrI₃. **c**, A twisted bilayer with a crack in the middle. Disordered ferromagnetic (red) and antiferromagnetic (white) domain patterns are observed. **d**, Distorted triangular lattice magnetic domain pattern is observed in twisted trilayer/trilayer CrI₃ sample, evidence of moiré magnetism.

zigzag magnetic order. It shows near unity linear polarization in photoluminescence and strong linear dichroism in optical reflection, with the optical anisotropic axis determined by the zigzag antiferromagnetic order. Linear dichroism spectroscopy reveals exciton-phonon bound states down to trilayers with an unprecedented number of replicas (over 10, Fig. 1b). This exceptionally strong exciton-phonon coupling arises from the strong modulation of charge transfer energy between the Ni-S bonds by the A_{1g} phonon.

moiré magnetism in twisted 2D magnets: Although moiré superlattices formed by non-magnetic 2D materials have been widely studied, moiré superlattices of 2D magnets were challenging to realize due to the difficulty in both fabrication and detection. In this project, we explore emerging magnetic textures in small-angle twisted 2D magnet chromium triiodide (CrI_3). In collaboration with Jorg Wrachtrup's group at University of Stuttgart, we employed scanning single NV center spin in a diamond tip with a spatial resolution of ~ 50 nm to visualize the magnetic domains and provide quantitative information about the domain magnetization. In the twisted bilayer, both antiferromagnetic (AFM) and ferromagnetic (FM) domains are identified (Fig. 1c). The emergence of the FM and AFM magnetic domains originates from the spatial variation of local stacking-dependent interlayer coupling. The lack of a periodic FM/AFM pattern reflects local structural distortion, common for small angle twisted heterostructures. By using stiffer trilayers, we constructed small-angle twisted trilayer on trilayer superlattices. The reconstructed magnetization map indeed confirms the coexistence of AFM and FM domains. Distinct from the disorder-like AFM/FM patterns in twisted bilayer, the magnetization map shows a hexagonal periodic pattern (Fig. 1d). This work represents a breakthrough in the realization of moiré magnetism.

Reversible strain-induced magnetic phase transition in CrSBr: Strain is a powerful experimental control knob for tuning fundamental properties of bulk quantum materials. Recent attempts to apply in-situ strain to 2D materials at cryogenic temperatures tend to rely on bendable substrates⁸. As a result, these studies are hampered by the limited flexibility of the substrate at low temperatures. Consequently, most experiments are not tunable *in situ* at cryogenic temperatures, and have failed to apply beyond 1% strain despite expectations that some of these materials may be strained up to a few percent before yielding⁹. During the award period, we developed a cryogenic strain system to realize in-situ control over 2D materials with over 2% uniaxial strain (Figs. 2a-b). Using this new capability, we realized drastic and continuous tuning of the magnetic properties of in layered A-type antiferromagnetic semiconductor CrSBr (Figs. 2c&d). We first

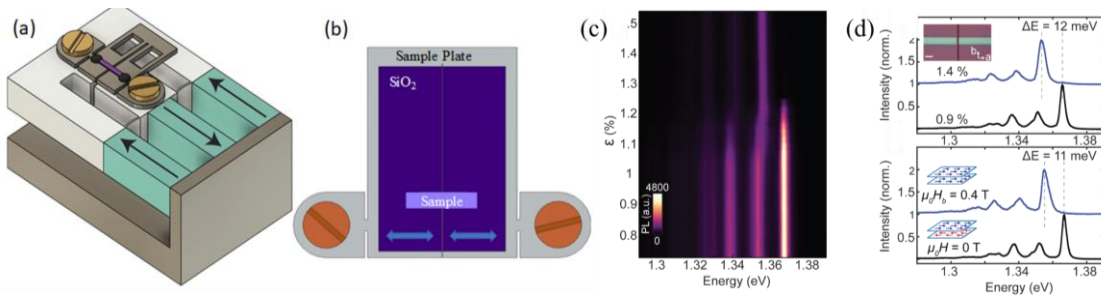


Fig. 2. Cryo-strain design and reversible strain-induced magnetic phase transition. **a**, Piezoelectric-based Hicks strain tuning setup adapted from *RSI* **85**, 065003 (2014). **b**, A zoomed-in view of the sample plate with a gapped silicon. **c**, Strain dependent photoluminescence (PL) intensity plot of a 20 nm CrSBr flake with the strain applied along the a axis. **d**, Top: PL spectra at 0.9 % (black) and 1.4 % strain (blue). Inset: optical micrograph of the sample. Scale bar: 30 μm . Bottom: PL spectra at 0 T (black) and 0.4 T magnetic field applied along the b (easy) axis. Insets depict the zero field A-type AFM and high field FM states.

established unique exciton-interlayer magnetism coupling effects. We found that the exciton peak energy and intensity are drastically changed when the magnetic order is switched from A-type AFM to the field-induced FM states (Figs. 2d, bottom panel). This effect arises from the tuning of interlayer exciton wavefunction hybridization. Using exciton to probe the interlayer magnetism, we demonstrate a reversible strain-induced AFM to FM phase transition at *zero* magnetic field (Fig. 2c). We show that increasing strain decreases the saturating field by nearly 50%, a dramatic control of magnetic anisotropy.

Direction 2: Excitons and correlation effects in moiré superlattices

Light induced ferromagnetism in moiré superlattices: Optical excitation of strongly correlated quantum materials can have profound effects on the many-body electronic states, such as light induced superconductivity, hidden charge density wave order, etc. Recently, two-dimensional moiré superlattices have emerged as a promising platform for quantum engineering strongly correlated phenomena. In this project, we discover that optical excitation can drastically tune the spin-spin interactions between moiré trapped carriers and thus result in long-range ferromagnetic order in WS_2/WSe_2 moiré superlattices, which is otherwise absent in the dark condition. We fabricated dual gated WS_2/WSe_2 heterostructures. Figure 3a is a piezoresponse force microscopy image showing homogeneous triangular moiré superlattices with a moiré wavelength of about 7.5 nm. We perform reflective magnetic circular dichroism measurements (RMCD) to probe the magnetic response as a function of filling factor ν . For the filling factor ν ranging from $-2/3$ to $1/3$, RMCD signal at zero magnetic field emerges with the increase of optical excitation power. More importantly, above the threshold power, the hysteresis loops are clearly resolved in RMCD signal vs magnetic field $\mu_0 H$, key evidence of a spontaneous long-range ferromagnetic order (Fig. 3b). Our temperature dependent RMCD measurements show enhanced critical temperature T_C at formation of correlated charge orders (e.g. $\nu=-1/2$ and $-1/7$ shown in Fig. 3c). This suggests that ferromagnetic order is stabilized with the formation of correlated insulating states at fractional fillings, where the spin fluctuations among moiré spins are minimized. In collaboration with Prof. Wang Yao at Hong Kong University, our theoretical model finds that the spin-spin exchange interaction between moiré trapped holes can be greatly enhanced by optically excited excitons. We

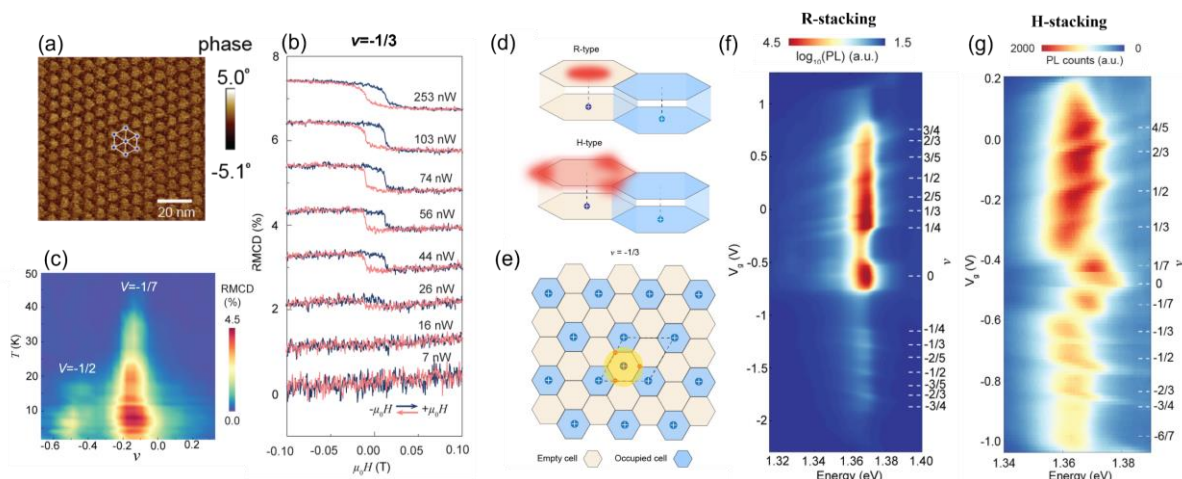


Fig. 3. Excitons and correlation effects in moiré superlattices. a-c, Light induced magnetism in WS_2/WSe_2 moiré superlattices. a, Piezoresponse force microscopy image of a heterobilayer. Scale bar: 20 nm. b, Power dependent RMCD vs out-of-plane magnetic field. c, Extracted RMCD signal amplitude vs temperature and filling factor, showing the enhanced magnetic response at correlated insulating states at fractional fillings ($-1/2$, $-1/7$). d-g, Intercell moiré excitons. See text for details.

envision several immediate exciting possibilities as described in the proposed project “light induced magnetism”.

Intercell moiré exciton complexes in electronic lattices: It has been well established that TMD moiré superlattice can host generalized Wigner crystal states. On the other hand, we and others have shown excitons can be trapped in the moiré potential to form moiré excitons. Thus, TMD moiré superlattices provides a unique platform to study the interactions between excitons and electron crystals. In this project, we discovered a new type of excitonic many-body ground states, which is formed by moiré excitons bound to correlated charge lattice in H-stacked WS₂/WSe₂ moiré superlattices. In collaboration with Ting Cao (UW), Di Xiao (UW), and Wang Yao (Hongkong University), we find distinct charge distributions between R- and H-stacked heterobilayers using first principles calculations. In the former, the ground state moiré exciton only has a vertical dipole (Fig. 3d top), which does not allow the binding of the exciton to the charges in the adjacent moiré cell. However, in the H-stacked heterobilayer, the hole in the WSe₂ layer is surrounded by its partner electron’s wavefunction spread among three adjacent moiré traps in the WS₂ layer (Fig. 3d bottom). Thus, this new type of interlayer moiré exciton possesses both vertical dipole and in-plane electric quadrupole moments. The electric quadrupole enables the binding of interlayer exciton with correlated electron lattices to form the intercell charged exciton complex. We obtained experimental evidence by comparing PL spectra of interlayer moiré excitons in both R- and H-stacked heterobilayers (Figs. 3e-g). Both heterobilayers exhibit a plethora of integer and fractionally filled correlated charge states, evident by the enhancement of photoluminescence intensity when charge orders form. The key distinction between the two stackings manifests in the photoluminescence peak energies. For R-stacking, there is little peak energy difference between charge neutral and fractionally filled states (Fig. 3f), where the electron lattice behaves as an inert background to the exciton. In contrast, for H-stacking, the electric-quadrupole moment enables binding of the moiré exciton with the charges in the adjacent moiré traps (Fig. 3g). The binding to individual nearest-neighbors at $|\nu|=1/7$ filling, and to the entire electron lattice at $|\nu|=1/3$ can be distinguished with ~ 7 meV, and ~ 14 meV red shifts respectively, consistent with our theoretical estimation.

Future Plans

We will continue to investigate emergent many-body electronic states, excitonic states, their interaction effects, and associated dynamics in moiré superlattices and magnetic heterostructures with external control, including twist angle, electrical field, doping, strain, hydrostatic pressure, and exchange field effects.

References

1. Hwangbo, K. et al., Highly Anisotropic Excitons and Multiple Phonon Bound States in a Van der Waals Antiferromagnetic Insulator, *Nature Nanotechnology* doi.org/10.1038/s41565-021-00873-9 (2021);
2. Wilson, N. P. et al. Interlayer electronic coupling on demand in a 2D magnetic semiconductor. *Nat Mater* **20**, 1657–1662 (2021).
3. Cenker, J. et al. Reversible strain-induced magnetic phase transition in a van der Waals magnet. *Nat Nanotechnol* **17**, 256–261 (2022).
4. Song, T. et al. Direct visualization of magnetic domains and moiré magnetism in twisted 2D magnets. *Science* (1979) **374**, 1140–1144 (2021).
5. Wang, X et al., Moiré trions in MoSe₂/WSe₂ heterobilayers, *Nature Nanotechnology*, <https://doi.org/10.1038/s41565-021-00969-2> (2021).

6. Wang, X. *et al.* Light-induced ferromagnetism in moiré superlattices. *Nature* **604**, 468–473 (2022).
7. Wang, Xi. Et al., Intercell moiré exciton complexes in electronic lattices, *Nature Materials*, accepted (2022); preprint: arxiv.org/abs/2206.08424.
8. Mohiuddin, T. M. G. et al. Uniaxial strain in graphene by Raman spectroscopy: G peak splitting, Grüneisen parameters, and sample orientation. *Phys. Rev. B* **79**, (2009).
9. S., B., Brivio, J. & Kis, A. Stretching and breaking of ultrathin MoS₂. *ACS Nano* **5**, (2011).

Publications

1. Wang, X. *et al.* Light-induced ferromagnetism in moiré superlattices. *Nature* **604**, 468–473 (2022).
2. Wang, Xi. Et al., Intercell moiré exciton complexes in electronic lattices, *Nature Materials*, accepted (2022); preprint: arxiv.org/abs/2206.08424.
3. Cenker, J. *et al.* Reversible strain-induced magnetic phase transition in a van der Waals magnet. *Nat Nanotechnol* **17**, 256–261 (2022).
4. Cai, J. *et al.* Electric control of a canted-antiferromagnetic Chern insulator. *Nature Communications* **2022 13:1** **13**, 1–7 (2022).
5. Ovchinnikov, D. *et al.* Topological current divider in a Chern insulator junction. *Nature Communications* **2022 13:1** **13**, 1–6 (2022).
6. van Tuan, D., Shi, S.-F., Xu, X., Crooker, S. A. & Dery, H. Six-Body and Eight-Body Exciton States in Monolayer WSe₂. *Phys. Rev. Lett.* **129**, 076801 (2022).
7. Wilson, N. P., Yao, W., Shan, J. & Xu, X. Excitons and emergent quantum phenomena in stacked 2D semiconductors. *Nature* vol. 599 383–392 Preprint at <https://doi.org/10.1038/s41586-021-03979-1> (2021).
8. Wang, X et al., Moiré trions in MoSe₂/WSe₂ heterobilayers, *Nature Nanotechnology*, <https://doi.org/10.1038/s41565-021-00969-2> (2021).
9. Song, T. *et al.* Direct visualization of magnetic domains and moiré magnetism in twisted 2D magnets. *Science* (1979) **374**, 1140–1144 (2021).
10. Song, T. *et al.* Spin photovoltaic effect in magnetic van der Waals heterostructures. *Sci Adv* **7**, eabg8094 (2021).
11. Wilson, N. P. *et al.* Interlayer electronic coupling on demand in a 2D magnetic semiconductor. *Nat Mater* **20**, 1657–1662 (2021).
12. Rivera, P. *et al.* Intrinsic donor-bound excitons in ultraclean monolayer semiconductors. *Nature Communications* **2021 12:1** **12**, 1–8 (2021).
13. Lin, Z. *et al.* Magnetism and Its Structural Coupling Effects in 2D Ising Ferromagnetic Insulator VI₃. *Nano Lett* **21**, 9180–9186 (2021).
14. He, M. *et al.* Competing correlated states and abundant orbital magnetism in twisted monolayer-bilayer graphene. *Nature Communications* **2021 12:1** **12**, 1–8 (2021).
15. Zhang, Q. *et al.* Observation of Giant Optical Linear Dichroism in a Zigzag Antiferromagnet FePS₃. *Nano Lett* **21**, 6938–6945 (2021).
16. Ovchinnikov, D. *et al.* Intertwined Topological and Magnetic Orders in Atomically Thin Chern Insulator MnBi₂Te₄. *Nano Lett* **21**, 2544–2550 (2021).
17. Hwangbo, K. et al., Highly Anisotropic Excitons and Multiple Phonon Bound States in a Van der Waals Antiferromagnetic Insulator, *Nature Nanotechnology* doi.org/10.1038/s41565-021-00873-9 (2021);
18. Sun, Q. et al., Magnetic domains and domain wall pinning in two-dimensional ferromagnets revealed by nanoscale imaging, *Nature Communications*, **12**, Article number: 1989 (2021).

19. Liam P. McDonnell, et al, Superposition of intra- and inter-layer excitons in twistrionic MoSe₂/WSe₂ bilayers probed by resonant Raman scattering, *2D Materials* DOI: /10.1088/2053-1583/abe778 (2021); The work at UW is exclusively supported by DMSE.
20. Li, B et al, Van der Waals epitaxial growth of air-stable CrSe₂ nanosheets with thickness-tunable magnetic order, *Nature Materials*, <https://doi.org/10.1038/s41563-021-00927-2> (2021);

Ultrafast Control of Emerging Electronic Phenomena in 2D Quantum Materials

Principle Investigator: Prof. Xiaodong Xu (Department of Physics, Department of Material Science and Engineering, University of Washington)

Co-PI: Prof. Nuh Gedik (Department of Physics, MIT),

Dr. Haidan Wen (Materials Science Division, Argonne National Lab),

Prof. Di Xiao (Department of Material Science and Engineering, Department of Physics, University of Washington)

Research Scope

The objective of this collaborative program is to investigate emerging ultrafast phenomena arising from the interactions between spin, charge, and lattice degrees of freedom in two-dimensional (2D) quantum materials and their heterostructures through theory-guided experimental efforts. We employ a suite of multimodal approaches using ultrafast technologies involving terahertz, (magneto) optical, x-ray, and electron pulses. Large-scale x-ray user facilities such as the Advanced Photon Source (APS) and the Linac Coherent Light Source (LCLS) play crucial roles for advancing this research program.

Self-identify keywords to describe your project: 2D materials, ultrafast, correlated physics, user facility

Recent Progress

1. Ultrafast spin-lattice coupling: Mechanism

The interplay between a multitude of electronic, spin, and lattice degrees of freedom underlies the complex phase diagrams of quantum materials. Layer stacking in van der Waals (vdW) heterostructures is responsible for exotic electronic and magnetic properties¹. Beyond the interplay between stacking order and interlayer magnetism, we discover a spin-shear coupling mechanism in which a subtle shear of the atomic layers can have a profound effect on the intralayer magnetic order in a family of vdW antiferromagnets². Our studies focus on a family of isostructural vdW antiferromagnets prepared by the **Xu** group. MPS_3 (M : Fe, Ni, Mn), exhibits monoclinic structures (Fig. 1a). Below the Néel temperature (T_N), bulk FePS₃ and NiPS₃ exhibit the zigzag AFM order along the a axis, while MnPS₃ is a Neel-type AFM. Employing optical linear dichroism measurements, **Xu** and **Wen** found critical slowing down behavior near the Neel temperature. Using time-resolved x-ray diffraction measurements, **Wen** and **Gedik** identified the interlayer shear as the primary structural degree of freedom that couples with the magnetic order. As shown in the schematic of the reciprocal space (Fig. 1b), the opposite shifts of 002 and $\bar{2}02$ peak corresponds to a decrease in the monoclinic angle β (Fig. 1c), i.e., there is an interlayer shear along

the a axis after laser excitation. The recovery times of interlayer shear and the magnetic order significantly slow down near T_N . The time-dependent Ginzburg-Landau theory developed by **Xiao** shows that this concurrent critical slowing down arises from a linear coupling of the interlayer shear to the magnetic order, which is dictated by the broken mirror symmetry intrinsic to the monoclinic stacking. Our results highlight the importance of interlayer shear in ultrafast control of magnetic order via spin-mechanical coupling.

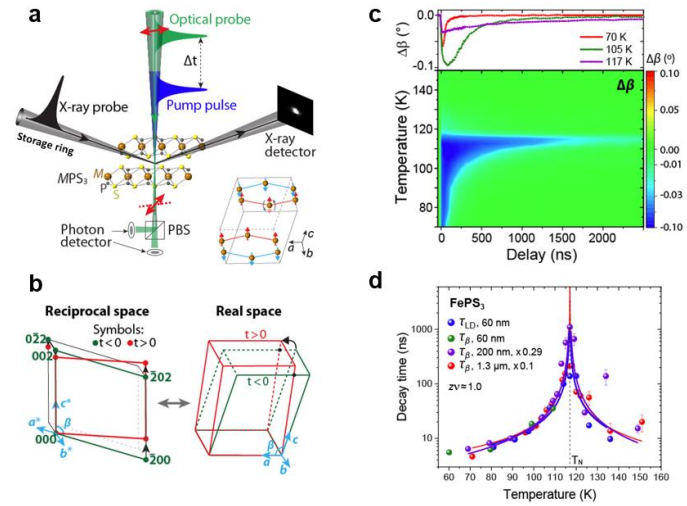


Figure 7. **a**, Time-resolved multimodal measurements of optically excited vdW antiferromagnets. **b**, Schematics of the reciprocal and real space unit cell before (green dots and lines) and after (red dots and lines) laser excitation. **c**, Dynamics of β change ($\Delta\beta$) as a function of the temperature. **d**, Relaxation time of OLD and monoclinic angle β in FePS_3 .

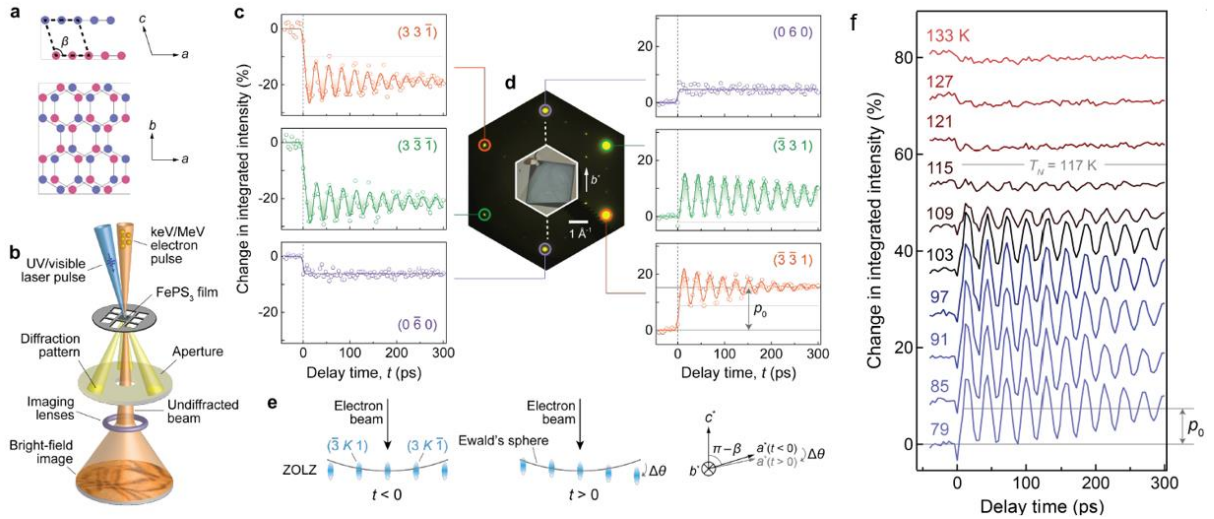


Figure 8. Coherent seesaw oscillation of reciprocal lattice induced by a femtosecond laser pulse. **a**, Schematic crystal structure of FePS_3 . Red (or blue) color denotes spin orientations on Fe site parallel (or anti-parallel) to the c^* axis in the antiferromagnetic state. **b**, Schematic of the ultrafast electron diffraction and bright-field microscopy setups. **c**, Time evolution of integrated intensities of six selected peaks in the electron diffraction pattern in **d**. Data were taken at 79 K with a 260-nm pump pulse at 0.5 mJ/cm^2 incident fluence. **d**, Electron diffraction pattern taken with 26 keV kinetic energy in the $[1\ 0\ 3]$ zone axis. The inset shows an optical image of the sample. The white dashed line indicates the axis of rotation during the seesaw motion of the diffraction peaks, which is approximately parallel to the b^* axis. **e**, Schematic snapshots of the seesaw rotation around the b^* axis in momentum space, which leads to time-varying intersections between the Ewald's sphere and rel-rods. Drawings are exaggerated for visual clarity. ZOLZ, zeroth-order Laue zone. **f**, Evolution of integrated intensity of Bragg peak $(-3\ 3\ 1)$ at different temperatures across T_N .

2. Ultrafast spin-lattice coupling: Application

A fundamental but challenging question in magnetic materials is how their microscopic spin configuration ties to properties manifested at the macroscopic length scale. In ferromagnets, the Einstein–de Haas effect provides one such bridge, where the angular momentum of individual spins can be converted into mechanical rotation of an entire object. However, for antiferromagnets that possess zero net magnetic moment, suppressing the spin order is not expected to yield any rotation of the crystal. Inspired by the discovery of interlayer shear and intralayer magnetic order as reported above, **Wen, Gedik, and Xu** explored how the melting of antiferromagnetic order in FePS_3 can couple to mechanical motion on ps time scales using a suite of ultrafast diffraction and microscopy techniques³ (Figure 8a,b). Upon above-band-gap ultrafast optical excitation and electron diffraction measurements, we observed a seesaw-like rotational motion in the reciprocal lattice (Figure 8c-e), which exhibits a thirty-fold amplification of its gigahertz structural resonance upon cooling below the Néel temperature (Figure 8f). Our systematic studies show that the rotation in reciprocal space manifests as an unusually large interlayer shear rather than a sample rotation in real space, where individual micro-patches of the film behave as synchronized shear oscillators with the same shear direction. Using time-resolved optical polarimetry, we further show that the enhanced mechanical response strongly correlates with ultrafast demagnetization, which releases elastic energy stored in local strain gradients to drive the oscillators. Our work not only offers the first microscopic view of spin-mediated mechanical motion of an antiferromagnet (by **Xiao**), but also identifies a new route towards realizing high-frequency resonators up to the millimeter band.

Our systematic studies show that the rotation in reciprocal space manifests as an unusually large interlayer shear rather than a sample rotation in real space, where individual micro-patches of the film behave as synchronized shear oscillators with the same shear direction. Using time-resolved optical polarimetry, we further show that the enhanced mechanical response strongly correlates with ultrafast demagnetization, which releases elastic energy stored in local strain gradients to drive the oscillators. Our work not only offers the first microscopic view of spin-mediated mechanical motion of an antiferromagnet (by **Xiao**), but also identifies a new route towards realizing high-frequency resonators up to the millimeter band.

3. Ultrafast spin-lattice coupling: Coherent detection

To understand the complex underlying mechanisms of interactions between multiple degrees of freedom in vdW magnets, novel experimental tools sensitive to subtle couplings among excitations are required. Conventional techniques are typically insensitive to phase. Therefore, novel methods

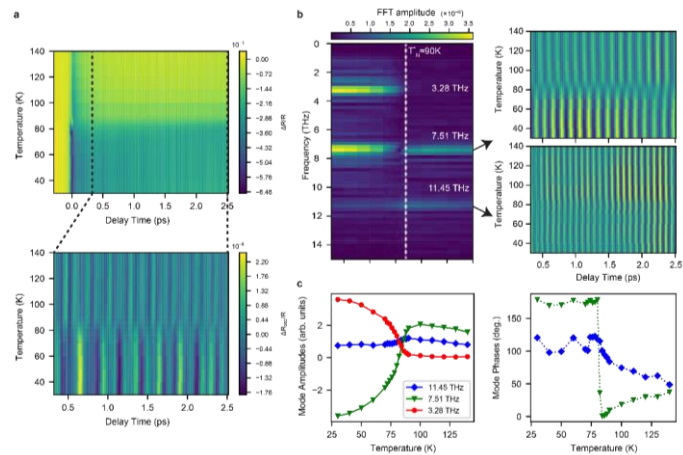


Fig. 3. The Néel order selectively couples to the 7.51 THz A_{1g} phonon mode. **a.** The temperature dependent coherent phonon spectroscopy on FePS_3 exhibits a pronounced change near $T_N \sim 90$ K (upper panel). Lower panel shows the oscillatory part of the traces. **b.** (Left panel) Below T_N , in temperature dependent Fourier spectra of oscillations, a new phonon emerges mode at 3.28 THz. Fourier filtered time traces of the 7.51 THz and 11.45 THz modes are shown on the right. **c.** Temperature dependent phase-corrected amplitudes and phases of phonons is shown on the left. The 3.28 THz mode displays an order parameter-like behavior, and its onset is concomitant with the magnetic order. Following the emergence of this mode, the 7.51 THz mode undergoes a π -phase shift and hence its phase-corrected amplitude changes sign. The 11.45 THz mode amplitude shows no discernable change.

with phase sensitivity are required to understand ground states with phase modulations⁴ and interactions that couple to the phase of collective modes. By performing phase-resolved coherent phonon spectroscopy (CPS), we reveal a hidden spin-lattice coupling in FePS₃ (Fig. 3a-c) that eluded other phase-insensitive conventional probes, such as Raman and X-ray scattering.⁵ With comparative analysis and analytical calculations, we directly show that the magnetic order selectively couples to the trigonal distortions through partially filled t_{2g} orbitals. This coupling is linear in magnetic order and lattice parameters, rendering these distortions inaccessible to inelastic scattering techniques. Our results not only capture the elusive spin-lattice coupling in FePS₃, but also establish phase-resolved CPS as a tool to investigate hidden interactions.

4. Ultrafast spin-charge coupling: exciton sensing magnon

The interactions between distinct excitations in solids are of both fundamental interest and technological importance. An example is an exciton coupled to collective spin excitations, i.e., magnons. Our previous work has shown strong coupling between the exciton resonance and interlayer spin alignment, which is the underlying mechanism for exciton-magnon coupling (Fig. 4a). In collaboration with Xiaoyang Zhu's group at Columbia, we first demonstrate exciton sensing of magnon dynamics by time-resolved optical pump and probe experiment down to bilayers⁶. Built on this result, we further demonstrate control over the coherent coupling between exciton and both bright and dark magnon modes in CrSBr via external magnetic fields and uniaxial strain (ϵ) (Figs. 4b-c)⁷. Our results demonstrate an unprecedented level of control in the opto-mechanical-magnonic coupling, a step towards the predictable and controllable implementation of hybrid quantum magnonics.

Future Plans

We will continue our efforts in studying coupled charge, spin, and lattice effects in layered vdW magnets while extending our investigation to the newly discovered physics of moiré magnetism. Our future plan focuses on three research topics: (1) nonlinear phonon-magnon interactions; (2) strain control of dynamic 2D magnetism; (3) dynamic exciton-magnon coupling and moiré effects. Driven by these topics, we will continue to develop and optimize a wide range of cutting-edge

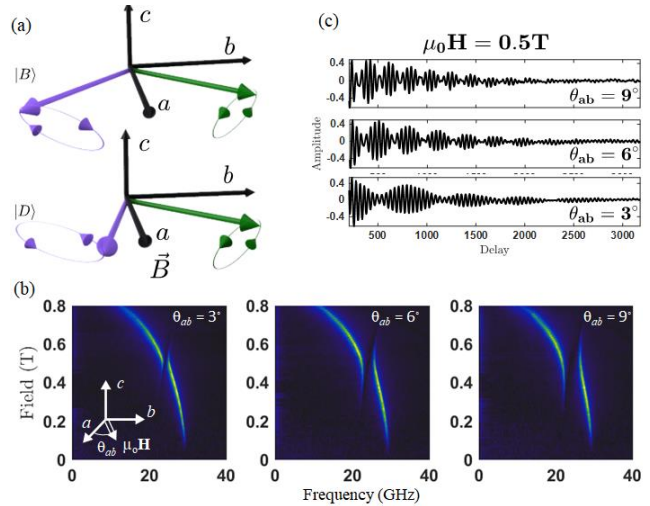


Figure 4. Tunable exciton-magnon coupling in layered magnetic semiconductor CrSBr. **a**, Cartoon of optically bright ($|B\rangle$) and dark ($|D\rangle$) modes. **b**, Magnon spectrum with magnetic field tilted from crystal **a** axis 3° (left), 6° (middle), and 9° (right). **c**, Transient optical reflectance as a function of pump-probe delay time at avoided crossing. The beating pattern is from the bright and dark magnon hybridization.

multimodal probes, including time- and energy-resolved photoluminescence (PL) spectroscopy, femtosecond optical pump-probe spectroscopy, time- and space- resolved magneto-optical Kerr microscopy, nonlinear THz spectroscopy, time- and angle-resolved photoemission spectroscopy (tr-ARPES), ultrafast electron diffraction (UED), ultrafast electron microscopy (UEM), and ultrafast X-ray diffraction and microscopy at DOE X-ray facilities. In particular, we will capitalize on new and enhanced ultrafast x-ray techniques that become available at the upgraded Advanced Photon Source (APS) and newly commissioned Linac Coherent Light Source (LCLSII).

References

- 1 B. Huang *et al.* "Emergent phenomena and proximity effects in two-dimensional magnets and heterostructures", *Nature Materials* **19**, 1276(2020).
- 2 F. Zhou *et al.* "Dynamical criticality of spin-shear coupling in van der Waals antiferromagnets", *Nature Communications* **13**, 6598(2022).
- 3 A. Zong, et al. "Direct imaging of synchronized shear oscillators in a van der Waals antiferromagnet", *Nature*, *under review* (2022).
- 4 M. H. Hamidian *et al.* "Detection of a Cooper-pair density wave in Bi₂Sr₂CaCu₂O_{8+x}", *Nature* **532**, 343(2016).
- 5 Emre Ergecen *et al.* "Coherent detection of hidden spin-lattice coupling in a van der Waals antiferromagnet", *PNAS* **in print**(2022).
- 6 Y. J. Bae *et al.* "Exciton-coupled coherent magnons in a 2D semiconductor", *Nature* **609**, 282(2022).
- 7 G. M. Diederich *et al.* "Tunable interaction between excitons and hybridized magnons in a layered semiconductor", *Nature Nanotechnology*(2022).

Publications (* indicate joint papers between PIs)

1. *G. M. Diederich, Di Xiao, Xiaodong Xu et al., Tunable Exciton-Hybridized Magnon Interactions in a Layered Semiconductor, *Nature Nanotechnology*, <https://doi.org/10.1038/s41565-022-01259-1> (2022).
2. *Faran Zhou, Nuh Gedik, Xiaodong Xu, Di Xiao, and Haidan Wen, et al. "Dynamical criticality of spin-shear coupling in van der Waals antiferromagnets", *Nature Communications* **13**, 6598 (2022)
3. *Emre Ergecen, Di Xiao, Nuh Gedik et al, Coherent detection of hidden spin-lattice coupling in a van der Waals antiferromagnet, in print, *PNAS* (2022).
4. *Anomalous Second Harmonic Generation from Atomically Thin MnBi₂Te₄, Jordan Fonseca, Di Xiao, and Xiaodong Xu et al., *Nano Letters* **24**, 10134 (2022).
5. Youn Jue Bae, Xiaodong Xu, Xiaoyang Zhu et al., Exciton-coupled coherent magnons in a 2D semiconductor, *Nature* **609**, 282–286 (2022).

6. *B. Q. Lv, Haidan Wen, Nuh Gedik et al., Unconventional hysteretic transition in a charge density wave, *Phys. Rev. Lett.* 128, 036401 (2022)
7. Emre Ergeçen, Nuh Gedik et al., Magnetically brightened dark electron-phonon bound states in a van der Waals antiferromagnet, *Nature Communications* 13, Article number: 98 (2022).
8. *T. Song D. Xiao, X. Xu et al., “Direct visualization of magnetic domains and moiré magnetism in twisted 2D magnets”, *Science*, DOI: 10.1126/science.abj7478 (2021).
9. Torben L. Purz, X. Xu, S. T. Cundiff et al, “Imaging dynamic exciton interactions and coupling in transition metal dichalcogenides”, *J. Chem. Phys.*, <https://doi.org/10.1063/5.0087544> (2022).
10. *Q. Zhang, H. Wen, D. Xiao, and X. Xu et al., “Observation of Giant Optical Linear Dichroism in a Zigzag Antiferromagnet FePS₃”, *Nano Letters* 21, 6938 (2021).
11. Carina A. Belvin, Nuh Gedik et al, Exciton-driven antiferromagnetic metal in a correlated van der Waals insulator, *Nature Communications*, 12, Article number: 4837 (2021).
12. Coherent Control of Asymmetric Spintronic Terahertz Emission from Two-Dimensional Hybrid Metal Halides, Kankan Cong, Haidan Wen et al., *Nature Comm.* 12, 5744 (2021)
13. Chiral Phonons in Moiré Superlattices, N. Suri, D. Xiao et al., *Nano Lett.* 21, 10026 (2021)
14. *K. Hwangbo, Di Xiao, Xiaodong Xu et al., Highly Anisotropic Excitons and Multiple Phonon Bound States in a Van der Waals Antiferromagnetic Insulator, *Nature Nanotechnology* doi.org/10.1038/s41565-021-00873-9 (2021)
15. *John Cenker, Di Xiao, Xiaodong Xu, Direct observation of 2D magnons in atomically thin CrI₃, *Nature Physics* 17, 29 (2021).

Layer-By-Layer Disentanglement of Electronic States in Quantum Materials*

Shuolong Yang, The University of Chicago

Layer-by-layer engineering, ultrafast spectroscopy, frequency-domain photoemission, magnetic topological materials, topological superconductors

*** Project started on July 1, 2022.**

Research Scope

Artificial heterostructural materials provide an enormous testbed for energy and quantum applications due to the tremendous flexibilities to engineer many-body interactions. In particular, layer-by-layer engineering has enabled us to create new materials with tunable electronic correlations, magnetism, superconductivity, and nontrivial topology. Yet, the understanding of the distribution of electronic wavefunctions across different layers, which is key to the realization of various topological and strongly correlated phases, has remained experimentally formidable. For this BES funded project in the Yang laboratory at the University of Chicago, we aim at developing new time-resolved spectroscopies to address this challenge. The objectives of this project are three-fold: 1) to establish and optimize the layer-encoded frequency-domain photoemission spectroscopy, where the layer origins of electronic wavefunctions are visualized through analysis of the electronic responses to layer-specific lattice modes; 2) to resolve outstanding mysteries in topological quantum materials such as magnetic topological insulators and topological superconductors, establishing the engineering principles for tuning topology in digital superlattices; 3) to connect layer-by-layer electron spectroscopy with layer-by-layer material engineering to fabricate heterostructural quantum materials with rational designs.

Recent Progress

1. Layer-by-layer disentanglement of Bloch states in $(\text{MnBi}_2\text{Te}_4)(\text{Bi}_2\text{Te}_3)$ superlattices

Manipulating electronic, magnetic, and lattice degrees of freedom layer-by-layer allows us to engineer materials' electronic properties at the level of single atomic sheets. This is profoundly demonstrated in magnetic topological insulators $(\text{MnBi}_2\text{Te}_4)(\text{Bi}_2\text{Te}_3)_n$, where magnetism breaks the time-reversal symmetry and enables exotic topological phases of matter such as the axion insulators and quantum anomalous Hall insulators [1,2]. Notably, significant controversies have arisen over the coupling between the topological surface state (TSS) and the broken-symmetry MnBi_2Te_4 layers, due to the observation of a negligible broken-symmetry gap using static ARPES. A surgical probe of electronic states with both a milli-eV energy resolution and a layer-wise spatial resolution is key to unveiling the layer origins of the critical electronic states.

Here we demonstrate a layer-encoded frequency-domain ARPES (FD-ARPES) experiment to disentangle electronic states layer-by-layer in $(\text{MnBi}_2\text{Te}_4)(\text{Bi}_2\text{Te}_3)$ superlattices [3]. Infrared pump pulses launch coherent phonon modulations. The induced electronic energy oscillations are

measured by time-resolved ARPES, and linked to different layers through a pixel-wise Fourier transform (Fig. 1). Our measurements yield predominant electronic coupling to the MnBi_2Te_4 A_{1g} mode at 1.2 THz and the Bi_2Te_3 A_{1g} mode at 1.8 THz. The FD-ARPES spectra taken at these two frequencies allow us to probe the layer origins of the TSS and the Rashba-split state (RS). Notably, the electronic couplings with the 1.8 and 1.2 THz mode are respectively dominant at or away from the zone center. These two momentum regions correspond to the band characters of the TSS and the RS, respectively. Therefore, the FD-ARPES measurements utilize the lattice perturbations to demonstrate that the TSS is relocated to the Bi_2Te_3 layer.

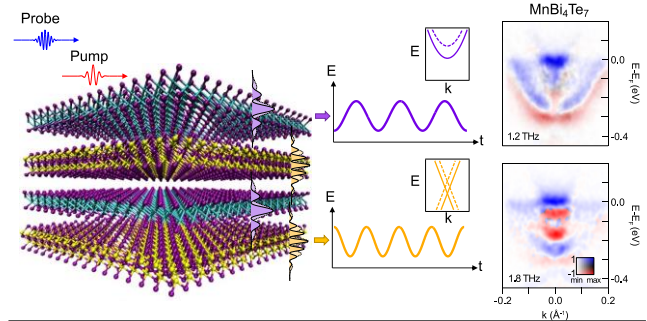


Figure 1. Layer-encoded FD-ARPES on $(\text{MnBi}_2\text{Te}_4)(\text{Bi}_2\text{Te}_3)$ superlattices. The left cartoon illustrates how different layer origins can be detected using layer-specific phonon frequencies. The experimental results on the right illustrate the disentanglement of electronic states using the 1.2 THz MnBi_2Te_4 A_{1g} mode, and the 1.8 THz Bi_2Te_3 A_{1g} mode.

This experiment not only demonstrates the proof-of-principle for layer-encoded FD-ARPES, but also reveals the surprising TSS wavefunction relocation in $(\text{MnBi}_2\text{Te}_4)(\text{Bi}_2\text{Te}_3)_n$ superlattices. The experimental finding explains the missing broken-symmetry gaps and provides the foundation to understand and control topology in a variety of van der Waals superlattices.

2. Layer-by-layer engineering and spectroscopy on topological heterostructures

The understanding from the layer-encoded FD-ARPES experiment on bulk-crystal $(\text{MnBi}_2\text{Te}_4)(\text{Bi}_2\text{Te}_3)$ [3] provides direct feedback for layer-by-layer engineering: the TSS can be migrated to nonmagnetic layers if the cleaving process leads to a 10% enlarged interlayer spacing at the top magnetic layer. Hence, layer-by-layer engineering using molecular beam epitaxy (MBE) will be key to tuning the topological quantum phases in magnetic topological insulators. We have recently fabricated $\text{MnBi}_2\text{Te}_4/(\text{Bi}_2\text{Te}_3)_n$ heterostructures through a two-step process [4]: first deposit $n+1$ layers of Bi_2Te_3 and 1 layer of MnTe , followed by annealing to form the top MnBi_2Te_4 monolayer. Static ARPES results clearly demonstrate the existence of the TSS, along with quantum well states due to quantum confinement. The electronic structure is distinct from the bulk $(\text{MnBi}_2\text{Te}_4)(\text{Bi}_2\text{Te}_3)_n$ superlattices [1,2]. Furthermore, we performed layer-encoded FD-ARPES to characterize the layer origins of electronic states. The MnBi_2Te_4 A_{1g} mode near

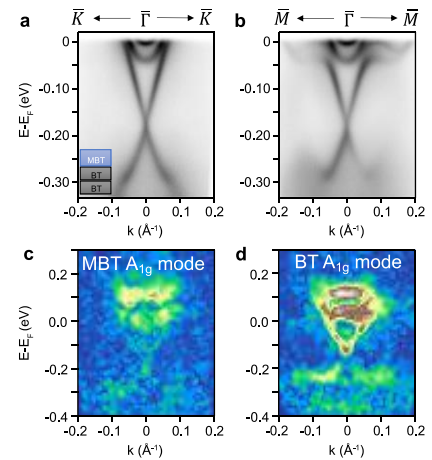


Figure 2. Fabrication of $\text{MnBi}_2\text{Te}_4/(\text{Bi}_2\text{Te}_3)_5$ using MBE and layer-encoded FD-ARPES. (a,b) Static high-resolution ARPES measurements. (c,d) FD-ARPES at the MBT and BT A_{1g} mode frequencies.

1.2 THz and the Bi_2Te_3 A_{1g} mode near 1.8 THz are identified. Decomposition of the FD-ARPES data at these two frequencies reveal that the TSS is still predominantly localized in the Bi_2Te_3 layer. This experiment demonstrates the feasibility to combine layer-by-layer engineering and layer-by-layer spectroscopy in a feedback loop. Even though we have not completely mitigated the wavefunction relocation issue, substantial tuning can be applied to this material system in the future utilizing the powerful technique of MBE.

3. Wafer-scale thin film liberation and re-assembly

A significant challenge for building programmable superlattices using MBE is the incompatible growth conditions for different material species, and the potential mutual contaminations due to inter-diffusion. A new tool is needed to integrate wafer-scale topological thin films in a programmable fashion. Traditional exfoliation and stacking are constrained to micrometer-sized flakes and hence do not apply to MBE-grown thin films. The Yang group has

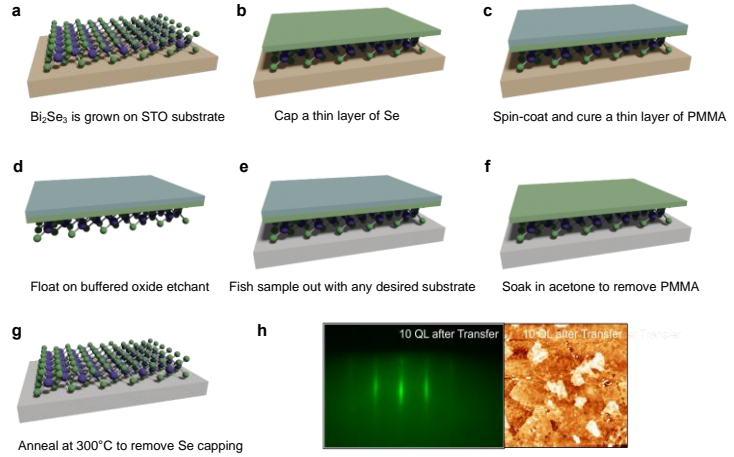


Figure 3. Wafer-scale liberation of ultrathin Bi_2Se_3 films. (a-g) The protocol of liberating Bi_2Se_3 thin films. (h) Electron diffraction and atomic force microscopy characterizations.

developed a unique protocol to leverage the Se-capping and oxide etching process [5] (Fig. 3), which enables them to liberate wafer-scale Bi_2Se_3 ultrathin films to be transferred to any other substrates. ARPES characterizations before and after the film transfer demonstrate that the surface quality is mostly preserved. This protocol will enable the Yang group to build complex wafer-scale superlattices with programmable stacking and twisting.

Future Plans

1. Layer-encoded FD-ARPES on tunable magnetic topological insulators

Recently it was shown by the Yang group that $\text{MnBi}_6\text{Te}_{10}$ [1] and Sb-doped MnBi_4Te_7 [2] exhibit tunable magnetism, where a change of the defect concentrations leads to a fundamental change of the magnetic ground state. Furthermore, ferromagnetic $\text{MnBi}_6\text{Te}_{10}$ exhibits a broken-symmetry gap in contrast to the antiferromagnetic counterpart [1]. Understanding the layer origins of the TSS in these tunable magnetic topological insulators will be key to revealing the mechanism for layer-by-layer engineering of $(\text{MnBi}_2\text{Te}_4)(\text{Bi}_2\text{Te}_3)_n$ superlattices. Hence, we will apply layer-encoded FD-ARPES on these materials and utilize the layer-specific vibration frequencies to disentangle electronic states layer-by-layer. Furthermore, we will also construct a coherent control experiment utilizing the pump-pump-probe configuration. By tuning the pump-pump delay, we

will selectively suppress or enhance particular modes. This experiment will be important in quantifying the weak mode coupling, which plays an important role in determining the wavefunction-layer overlap.

2. Layer-encoded FD-ARPES on ultrathin topological superconductors $\text{FeTe}_x\text{Se}_{1-x}$

Bulk $\text{FeTe}_x\text{Se}_{1-x}$ with $x > 0.5$ was predicted to host a topological superconducting phase due to the innate TSS and its coupling with the superconducting bulk. However, theory also predicted the existence of a bulk-originated topological Dirac semimetal state (TDSS). The surface and bulk nature for the TSS and TDSS, respectively, have not been experimentally revealed. Moreover, it remains to be explored how the TSS and TDSS evolve when pushing a 3D topological superconductor to the 2D limit. In this direction, we will apply layer-encoded FD-ARPES on MBE-fabricated topological superconductors $\text{FeTe}_x\text{Se}_{1-x}$, and utilize the bulk and surface A_{1g} modes to disentangle the TSS and TDSS in the frequency domain. To visualize the 3D-2D crossover, we will systematically perform measurements on a series of $\text{FeTe}_x\text{Se}_{1-x}$ thin films with varied Te:Se ratio, thickness, and temperature.

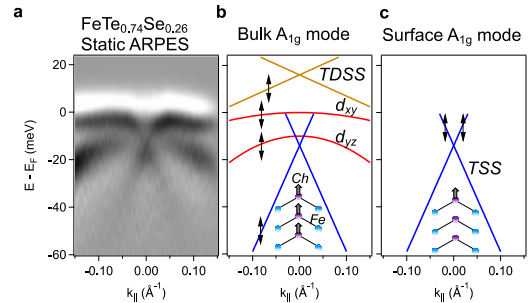


Figure 4. Layer-encoded FD-ARPES on $\text{FeTe}_x\text{Se}_{1-x}$ ultrathin films. (a) Static ARPES data on 10-unit-cell-thick $\text{FeTe}_{0.74}\text{Se}_{0.26}$. (b,c) Expected coherent phonon oscillations for (b) the bulk A_{1g} mode and (c) the surface A_{1g} mode.

References

1. C. Yan, Y. Zhu, L. Miao, S. Fernandez-Mulligan, E. Green, R. Mei, H. Tan, B. Yan, C.-X. Liu, N. Alem, Z. Mao, and S.-L. Yang, *Delicate ferromagnetism in $\text{MnBi}_6\text{Te}_{10}$* . *Nano Lett.* **22**, 9815-9822 (2022).
2. Y. D. Guan, C. H. Yan, S. H. Lee, X. Gui, W. Ning, J. L. Ning, Y. L. Zhu, M. Kothakonda, C. Q. Xu, X. L. Ke, J. W. Sun, W. W. Xie, S.-L. Yang, and Z. Q. Mao, *Ferromagnetic MnBi_4Te_7 obtained with low-concentration Sb doping: A promising platform for exploring topological quantum states*. *Phys. Rev. Materials* **6**, 054203 (2022).
3. W. Lee, S. Fernandez-Mulligan, H. Tan, C. Yan, Y. Guan, S. H. Lee, R. Mei, C. Liu, B. Yan, Z. Mao, and S.-L. Yang, *Layer-by-layer disentanglement of Bloch states via frequency-domain photoemission*, arXiv **2301.01094**. *In review with Nature Physics* (2023).
4. W. Lee, H. Lin, K. D. Nguyen, Y. Zhang, H. Tan, B. Yan, P. Y. Huang, and S.-L. Yang, *Resolving and controlling the layer origin of the topological electronic state in $\text{MnBi}_2\text{Te}_4/(\text{Bi}_2\text{Te}_3)_n$ ultrathin films*. *In preparation* (2023).

5. J. C. Ip, K. D. Nguyen, C. Yan, W. Lee, E. Hoenig, C. Liu, and S.-L. Yang, *Wafer-scale liberation of topological chalcogenide films grown by molecular beam epitaxy. In preparation (2023).*

Publications (project started on July 1, 2022)

1. W. Lee, S. Fernandez-Mulligan, H. Tan, C. Yan, Y. Guan, S. H. Lee, R. Mei, C. Liu, B. Yan, Z. Mao, and S.-L. Yang, *Layer-by-layer disentanglement of Bloch states via frequency-domain photoemission*, arXiv **2301.01094**. *In review with Nature Physics (2023).*

*Author
Index*

Anitescu, Mihai.....	39	Konik, Robert.....	5, 18, 22
Bao, Ning.....	18	Konik, Robert M.....	2
Bendek, Nicole.....	189	Kukreja, Roopali.....	159
Bostwick, Aaron.....	23	Lanzara, Alessandra.....	23
Bozin, Emil.....	45	Lee, W. S.....	8
Cao, Y.....	129	Limmer, David.....	124
Cao, Yue.....	12	Lin, Yu.....	34
Cha, Wonsuk.....	59	Lin, Yuewei.....	75
Chen, L. Q.....	129	Lindenberg, A. M.....	129
Chiang, Tai Chang.....	82	Lindenberg, A. R.....	8
Chueh, William.....	29	Lindenberg, Aaron.....	29
Collins, Brian A.....	88	Lu, D.H.....	63
Comin, Riccardo.....	93, 170	Ma, Jihong.....	98
Cotts, Benjamin.....	98	Mao, Wendy L.....	34
Cuk, T.....	8	Martin, L. W.....	129
Cundiff, Steven T.....	101	Mitrano, Matteo.....	2, 163
Dean, Mark.....	5, 6, 7, 18	Moritz, B.....	8, 63
Dean, Mark P M.....	2	Murnane, Margaret.....	166
Devereaux, T.P.....	8, 63	Nelson, Keith A.....	170
Disa, Ankit.....	189	Osborn, Raymond.....	39
Durbin, Stephen M.....	105	Pasupathy, Abhay.....	18
Evans, Paul G.....	107	Pateras, Anastasios.....	59
Fohtung, Edwin.....	113	Pellicciari, Johnathan.....	18
Freeland, J. W.....	129	Petkov, V.....	180
Freericks, James.....	170	Plumb, Kemp.....	185
Gedik, Nuh.....	119, 201	Reis, David.....	29, 170
Ginsburg, Naomi.....	124	Robinson, Ian.....	45, 75
Gopalan, V.....	129	Rollett, Anthony D.....	59
Gray, Alexander.....	138	Rosenkranz, Stephan.....	39
Gu, Genda.....	18	Roy, Ananda.....	18
Haley, Charlotte.....	39	Roy, Sujoy.....	54
Harder, Ross J.....	59	Sandberg, Richard L.....	59
Hasan, M. Zahid.....	143	Schlom, Darrell.....	189
Hashimoto, M.....	63	Shen, Kyle.....	189
Heinz, T. F.....	8	Shen, Z. X.....	8
Highland, Matthew J.....	12	Shen, Zhi-xun.....	63
Hormozi, Layla.....	18	Shi, Jian.....	113
Hruszkewycz, Stephan.....	59	Singer, Andrej.....	189
Hruszkewycz, Stephan O.....	12	Sirica, Nicholas.....	170
Hu, Wanzheng.....	150	Sobota, J.A.....	63
Jiang, H. C.....	8	Stoica, Vladimir.....	129
Jozwiak, Chris.....	23	Suter, Robert M.....	59
Kapteyn, Henry.....	166	Talapin, Dmitri.....	124
Karunadasa, Hemamala.....	34	Teitelbaum, Samuel.....	124
Katoch, Jyoti.....	154	Trigo, Mariano.....	29, 170
Kirchman, P.S.....	63	Turner, J. J.....	69

Wei, Tzu-Chieh.....	18	Xu, Xiaodong.....	195, 201
Weichselbaum, Andreas	18	Yang, Shuolong.....	207
Wen, H.	129	Yoo, Shinjae.....	75
Wen, Haidan	12, 201	You, Hoydoo.....	12
Wu, Longlong	75	Zaliznyak, Igor.....	18
Xiao, Di.....	201		

Participant List

Name

Abbamonte, Peter
Anitescu, Mihai
Benedek, Nicole
Bisogni, Valentina
Bostwick, Aaron
Bozin, Emil
Cao, Yue
Chen, Long-Qing
Chiang, Tai
Chueh, William
Collins, Brian
Comin, Riccardo
Cotts, Ben
Cuk, Tanja
Cundiff, Steven Thomas
Dean, Mark
Devereaux, Thomas
Disa, Ankit
Durbin, Steve
Evans, Paul
Fohtung, Edwin
Freeland, John
Freericks, James
Gavvalapalli, Mani
Gedik, Nuh
Ginsberg, Naomi
Gopalan, Venkatraman
Granite, Evan
Gray, Alexander
Hasan, M. Zahid
Hashimoto, Makoto
Hastings, Todd
Heinz, Tony
Highland, Matt
Hruszkewycz, Stephan
Hu, Wanzheng
Jiang, Hongchen
Jozwiak, Chris
Kapteyn, Henry
Karunadasa, Hemamala
Katoch, Jyoti
Kerch, Helen
Kevan, Steve

Organization

University of Illinois
Argonne National Laboratory
Cornell University
Brookhaven National Laboratory
Lawrence Berkeley National Laboratory
Brookhaven National Laboratory
Argonne National Laboratory
Pennsylvania State University
University of Illinois
SLAC National Accelerator Laboratory
Washington State University
Massachusetts Institute of Technology
Middlebury College
University of Colorado, Boulder
University of Michigan
Brookhaven National Laboratory
SLAC National Accelerator Laboratory
Cornell University
Purdue University
University of Wisconsin, Madison
Rensselaer Polytechnic Institute
Argonne National Laboratory
Georgetown University
Department of Energy
Massachusetts Institute of Technology
University of California, Berkeley
Pennsylvania State University
Department of Energy
Temple University
Princeton University
SLAC National Accelerator Laboratory
University of Kentucky
SLAC National Accelerator Laboratory
Argonne National Laboratory
Argonne National Laboratory
Boston University
SLAC National Accelerator Laboratory
Lawrence Berkeley National Laboratory
University of Colorado
SLAC National Accelerator Laboratory
Carnegie Mellon University
Department of Energy
Lawrence Berkeley National Laboratory

Kirchmann, Patrick	SLAC National Acceleratory Laboratory/SIMES
Kish, Lazar	Brookhaven National Laboratory
Konik, Robert	Brookhaven National Laboratory
Kukreja, Roopali	University of California, Davis
Lanzara, Alessandra	University of California, Berkeley/Lawrence Berkeley National Laboratory
Lee, Wei-Sheng	SLAC National Accelerator Laboratory
Lin, Yu	SLAC National Accelerator Laboratory
Lin, Yuewei	Brookhaven National Laboratory
Lindenberg, Aaron	Stanford University/SLAC National Accelerator Laboratory
Lu, Donghui	SLAC National Accelerator Laboratory
Ma, Jihong	University of Vermont
Mao, Wendy	Stanford University
Martin, Lane	University of California, Berkeley/Lawrence Berkeley National Laboratory
Mewes, Claudia	Department of Energy
Miranda, Raul	Department of Energy
Mitrano, Matteo	Harvard University
Moritz, Brian	SLAC National Accelerator Laboratory
Mullen, Jessica	National Energy Technology Laboratory
Murnane, Margaret	JILA/University of Colorado
Nelson, Keith	Massachusetts Institute of Technology
Osborn, Raymond	Argonne National Laboratory
Pelliciani, Johnathan	Brookhaven National Laboratory
Petkov, Valeri	Central Michigan University
Plumb, Kemp	Brown University
Reis, David	SLAC National Accelerator Laboratory
Robinson, Ian	Brookhaven National Laboratory
Rosenkranz, Stephan	Argonne National Laboratory
Roy, Sujoy	Lawrence Berkeley National Laboratory
Rustad, James	Department of Energy
Sandberg, Richard	Brigham Young University
Schlom, Darrell	Cornell University
Sefat, Athena	Department of Energy
Shen, Kyle	Cornell University
Shen, Zhi-Xun	Stanford University
Shi, Jian	Rensselaer Polytechnic Institute
Singer, Andrej	Cornell University
Sirica, Nicholas	Los Alamos National Laboratory
Smith, Rachele	Department of Energy
Sobota, Johnathan	SLAC National Accelerator Laboratory
Stoffa, Joseph	Department of Energy
Stoica, Vladimir	Pennsylvania State University
Talapin, Dmitri	University of Chicago

Teitelbaum, Samuel	Arizona State University
Thomas, Burt	National Energy Technology Laboratory
Trigo, Mariano	SLAC National Accelerator Laboratory
Turner, Joshua	Stanford University/SLAC National Accelerator Laboratory
Wen, Haidan	Argonne National Laboratory
Wilson, Lane	Department of Energy
Wu, Longlong	Brookhaven National Laboratory
Xiao, Di	University of Washington
Xu, Xiaodong	University of Washington
Yang, Shuolong	University of Chicago
You, Hoydoo	Argonne National Laboratory
Zaliznyak, Igor	Brookhaven National Laboratory
Zhernenkov, Mikhail	Department of Energy